Quaternary Research

Horváth Erzsébet
ELTE TTK FFI Természetföldrajzi Tanszék

Lektorálta: Mari László

A jegyzet megjelenését az ELTE jegyzettámogatási pályázata támogatta
2021

ELTE EÖTVÖS LORÁND TUDOMÁNYEGYETEM

QUATERNARY RESEARCH

- **Horváth Erzsébet**
- **erzsebet.horvath@ttk.elte.hu**

QUATERNARY RESEARCH

- **The main topics of the course:**
  - Boundary of the Quaternary
  - Climate of the Quaternary
  - Quaternary dating methods
    - Relative chronology
    - Absolute chronology
  - Quaternary in the Carpathian-Basin

Boundary of the Quaternary

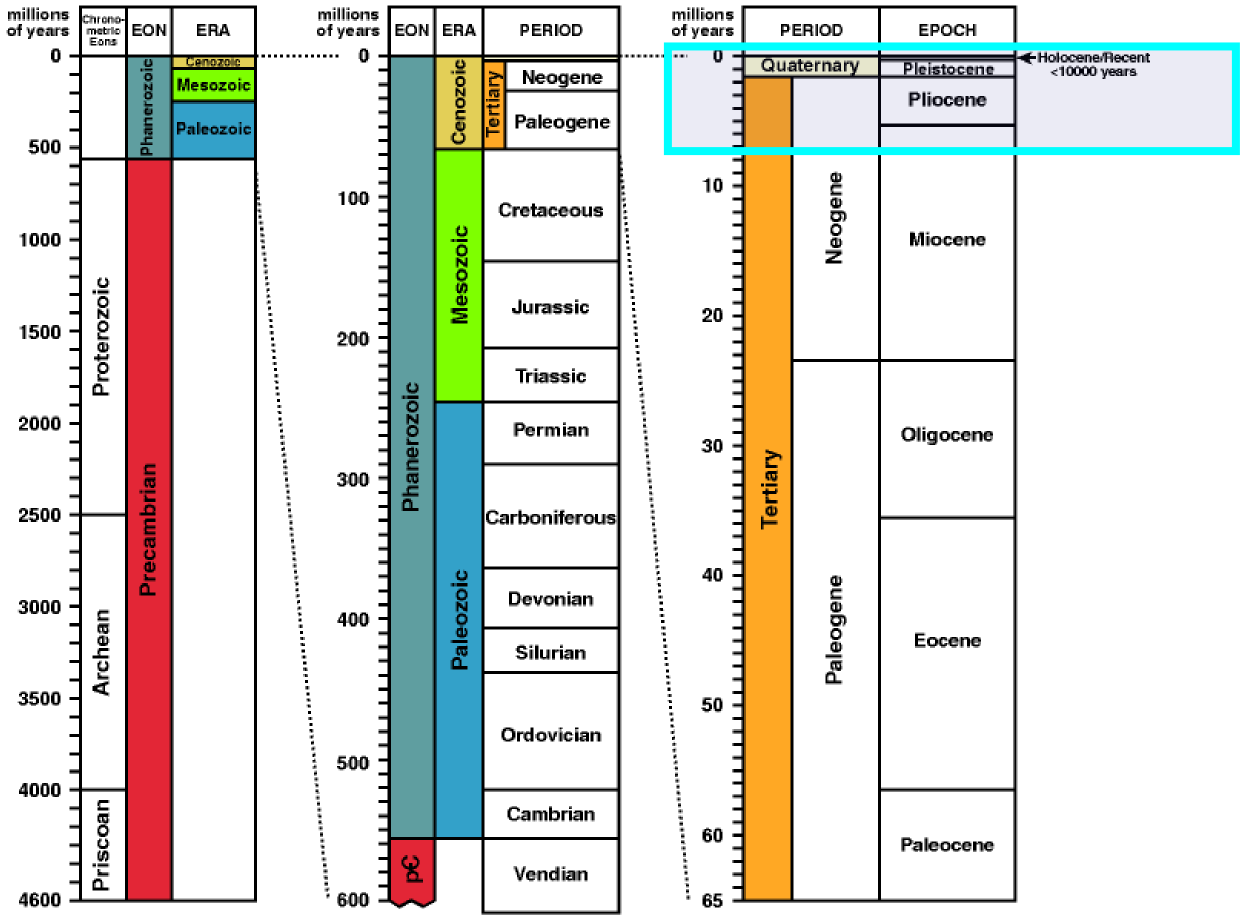

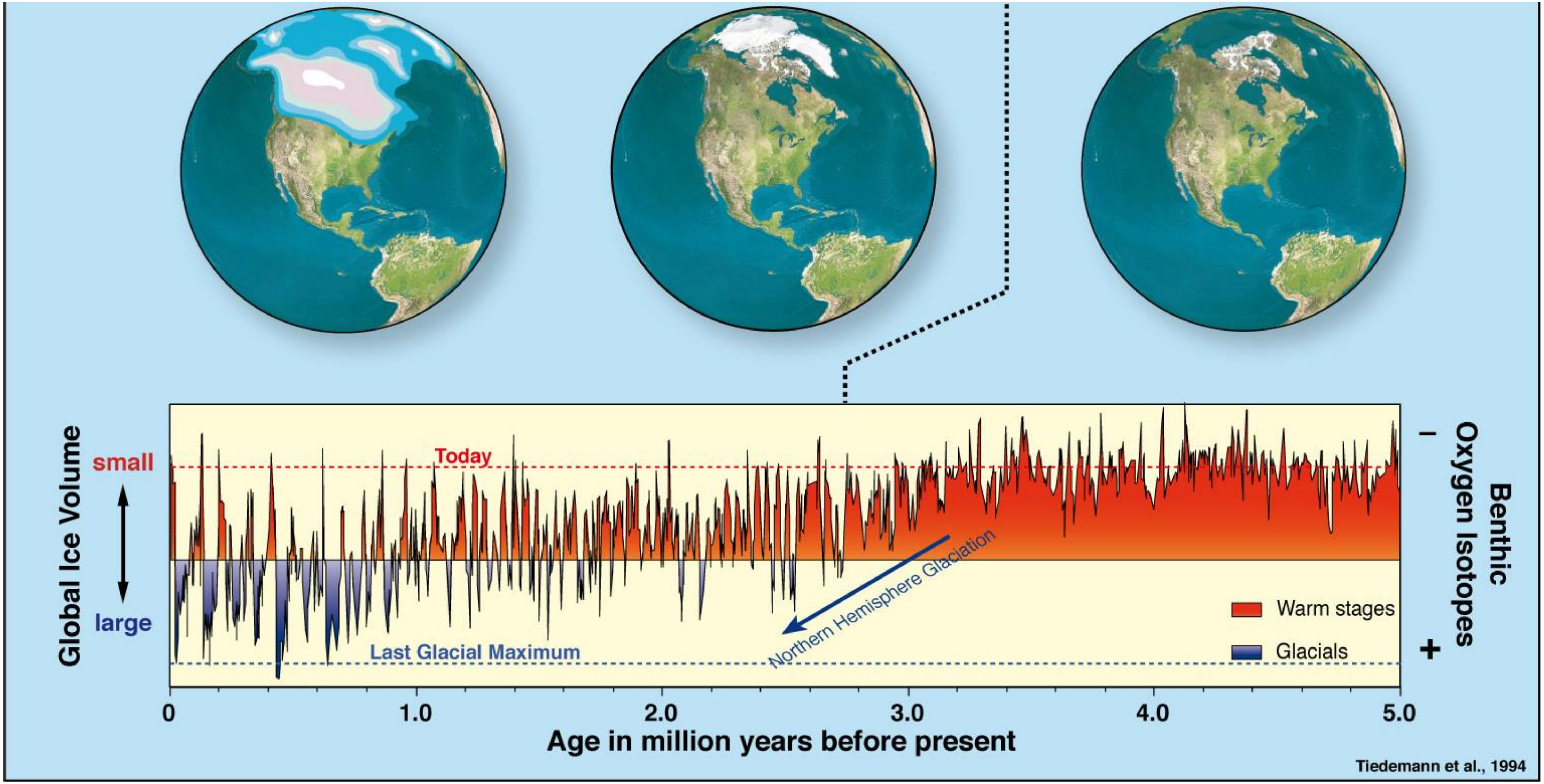
Global Ice Volume
small
large
Today
Last Glacial Maximum
Northern Hemisphere Glaciation
Warm stages
Glacials
Benthic Oxygen Isotopes
–
+
0
1.0
2.0
3.0
4.0
5.0
Age in million years before present
Tiedemann et al., 1994

- **Boundary of the Quaternary**

Quaternary Period with the Anthropocene Epoch

Eonothem/ Eon	Erathem/ Era	System/ Period	Series/ Epoch	Stage/ Age	millions of years ago
Phanerozoic	Cenozoic	Quaternary	Anthropocene[1]		1950 CE
			Holocene		0.0117
			Pleistocene	Upper	0.126
				Middle	0.781
				Calabrian	1.806
				Gelasian	2.588

[1] In August 2016 the Anthropocene Working Group (AWG), a special body created within the International Commission on Stratigraphy (ICS), recommended that the Anthropocene Epoch be made a formal interval within the International Chronostratigraphic Chart. The AWG recommended that the year 1950 be used as the starting point of the Anthropocene Epoch.

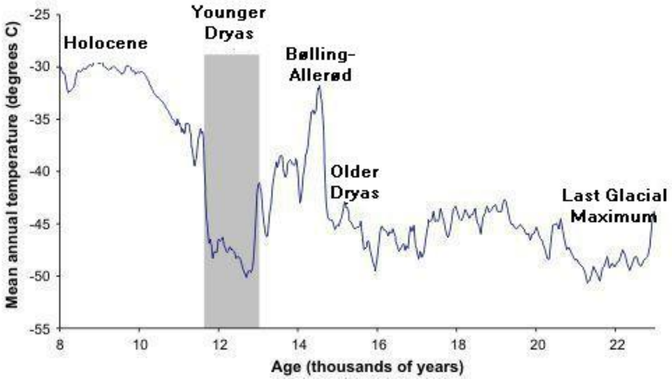

Surface temperature of the Greenland ice sheet

(„Last Glacial Maximum" (LGM), Older Dryas, Bølling-Allerød and Younger Dryas)
(http://www.dandebat.dk/eng-klima6.htm)

The actual distribution of the ice cover:

- 15.000.000 km²
  - Antartctica: 13.500.000 km² (max. thickness: 4270 m),
  - Greenland: 1.800.000 km² (max. thickness: 3240 m)

The ice of Antarctica and Greenland
97% of the Earth ice surface,
and 99% of the ice cover of the Earth

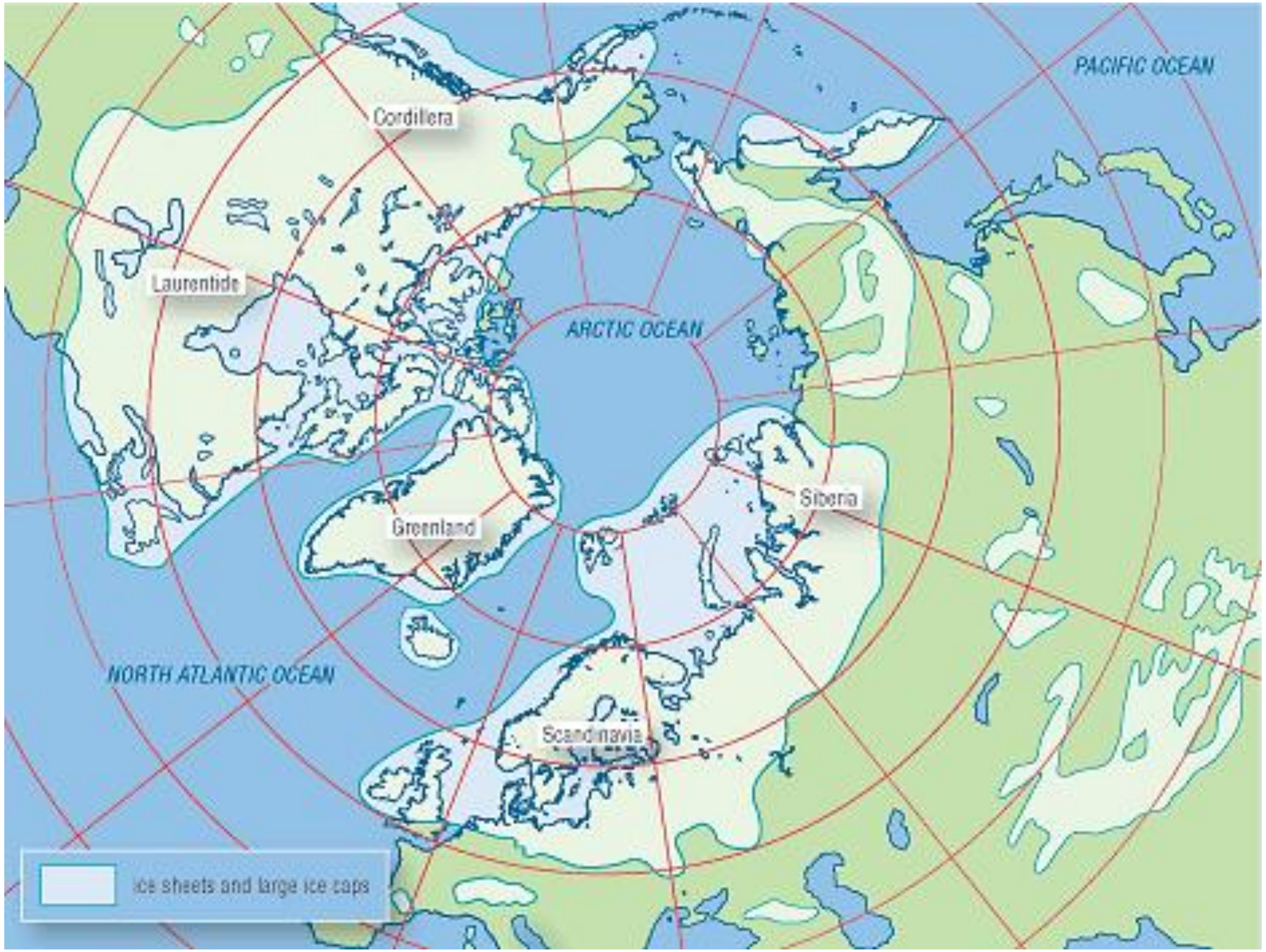

During the maximal distribution of the glacial: 35.000.000 km²

Extra:

- N-America: 12.000.000 km²
- Eurasia: 6.000.000 km²

Glacials and interglacials in the world

		Alps	Middle-Europe		Eastern-Europe	North-America
glacial		würm	wisztula		valdaj	wisconsin
interglacial		riss-würm	eem		mikulino	sangamon
glacial	stadial	riss II	sa	warta	moszkvai	iowa
	interstadial		a	trene	odinzovo	
	stadial	riss I	le	drente	dnyeper	illinois
interglacial		mindel-riss	holstein		lichvin	yarmouth
glacial		mindel	elster		oka	kansas
interglacial		günz-mindel	cromer		bjelovesz	afton
glacial		günz	menap		narev	nebraska
interglacial		duna-günz	waal			
glacial		duna	eburon			
interglacial		duna-biber	tegelen			
glacial		biber				

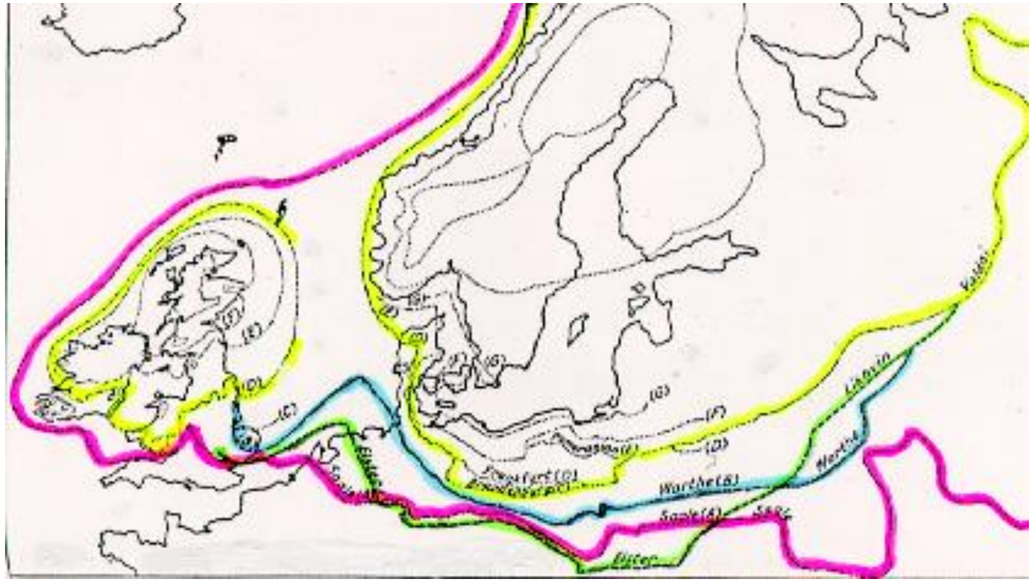

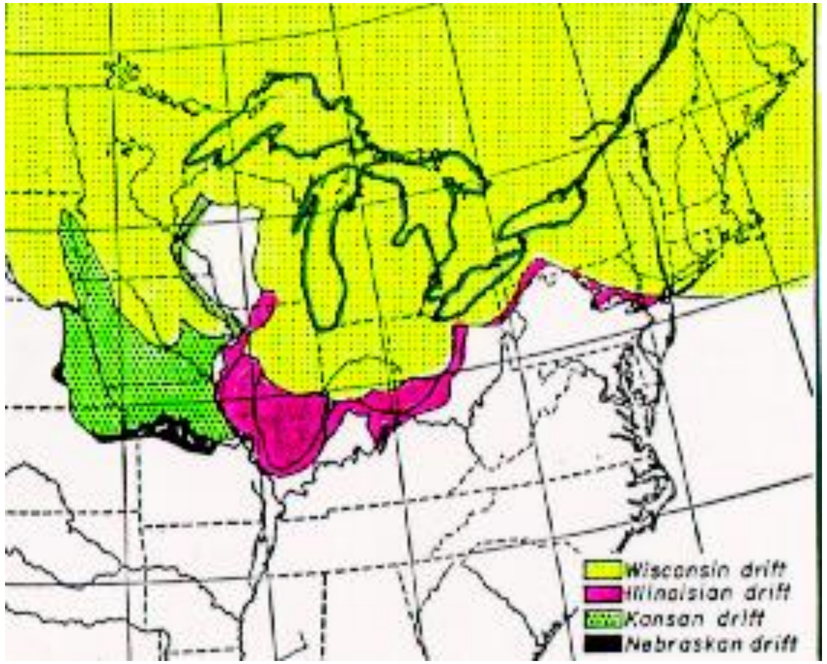

Ice cover in the Alps during the Pleistocene

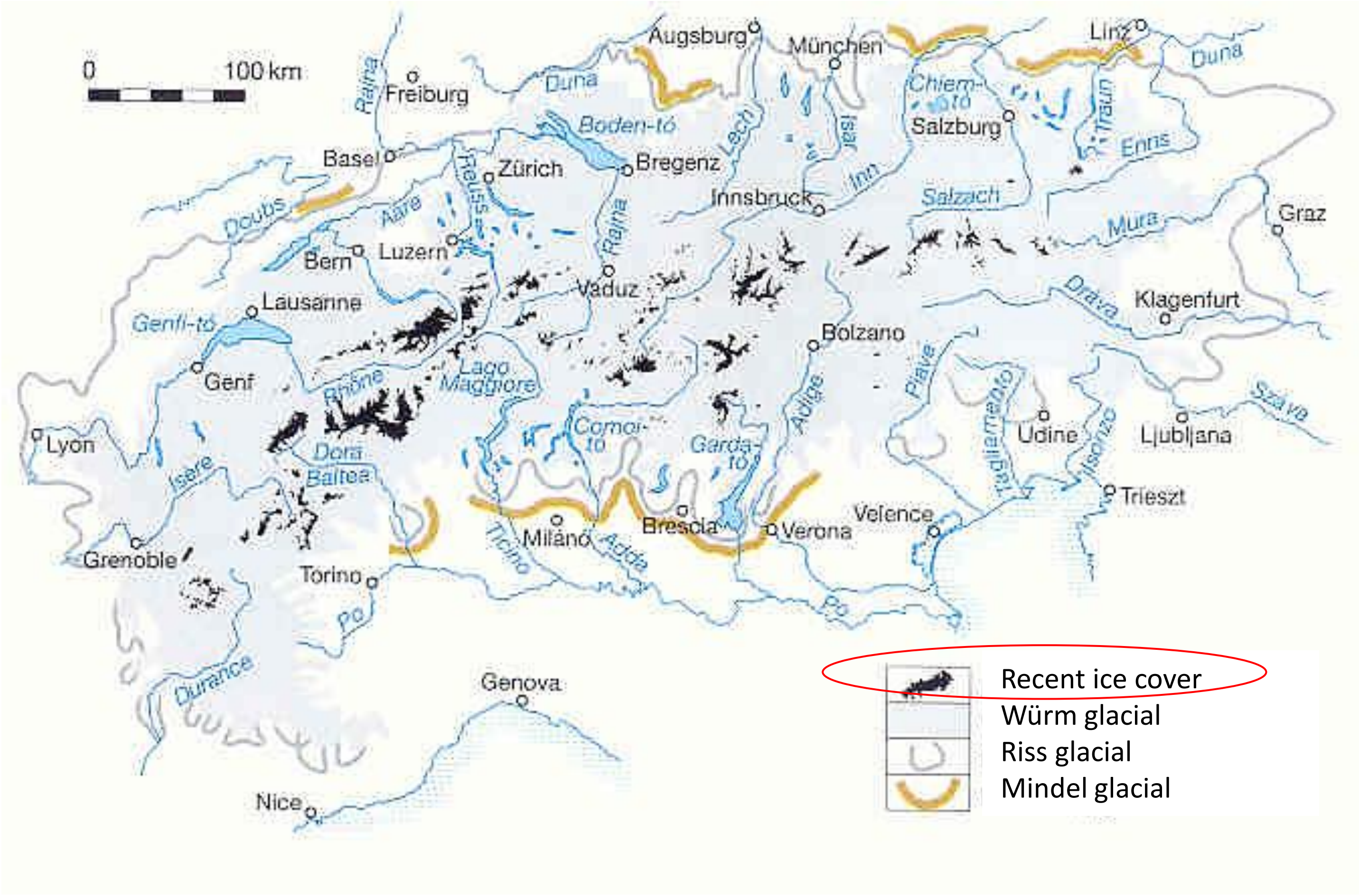

Climate changes in the Earth history

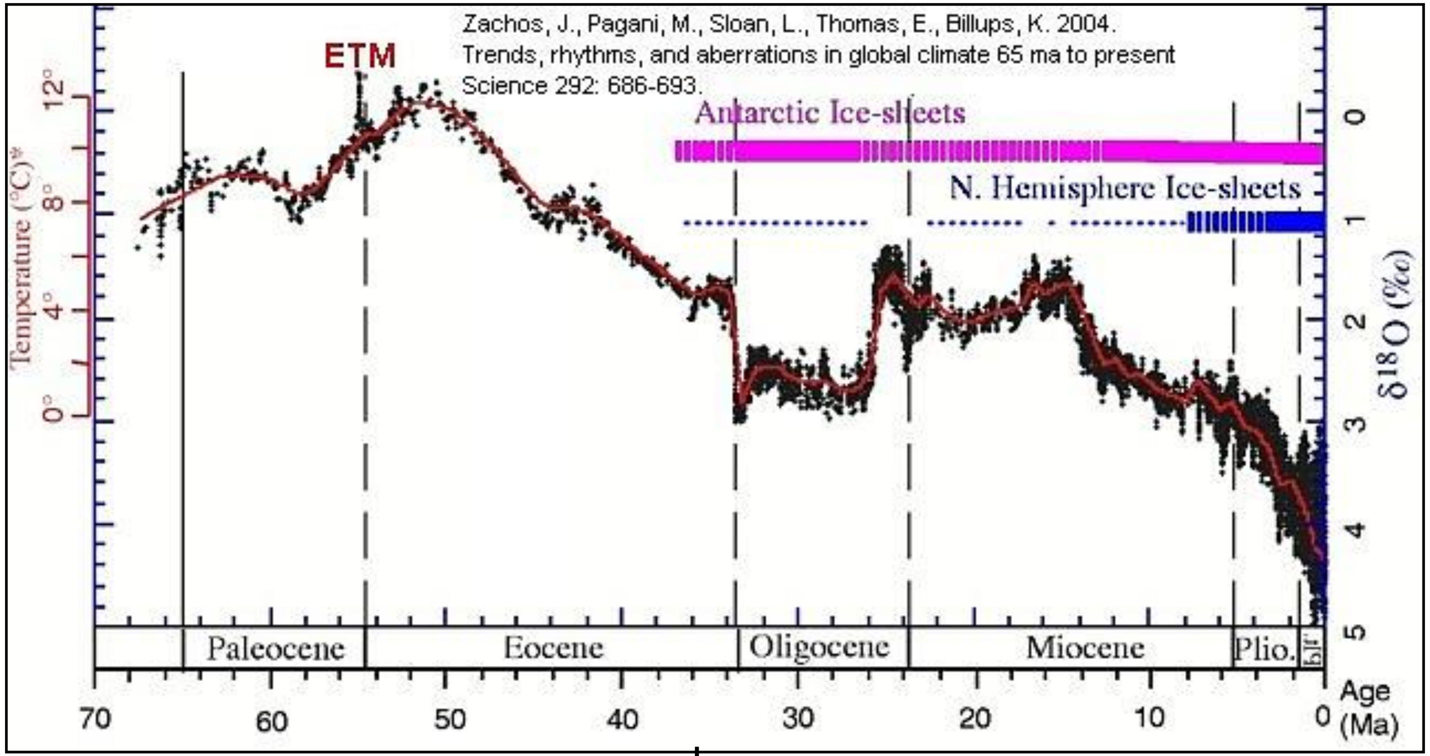

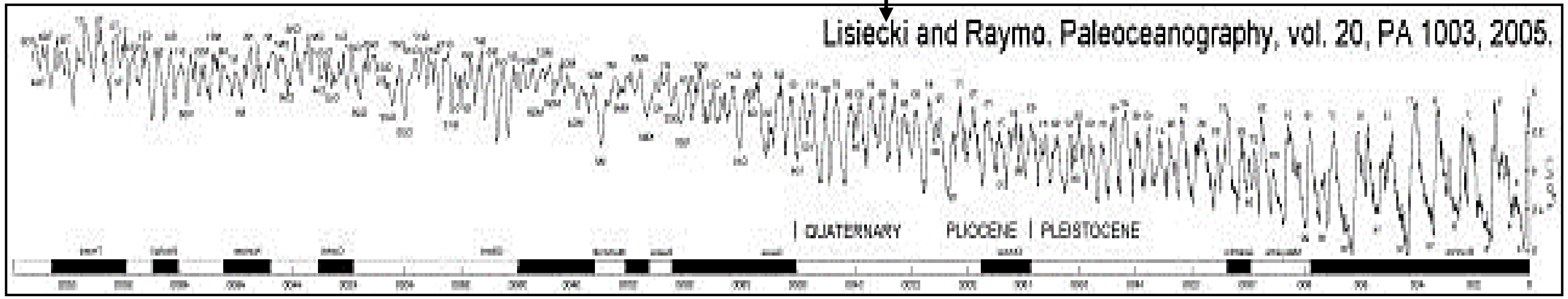

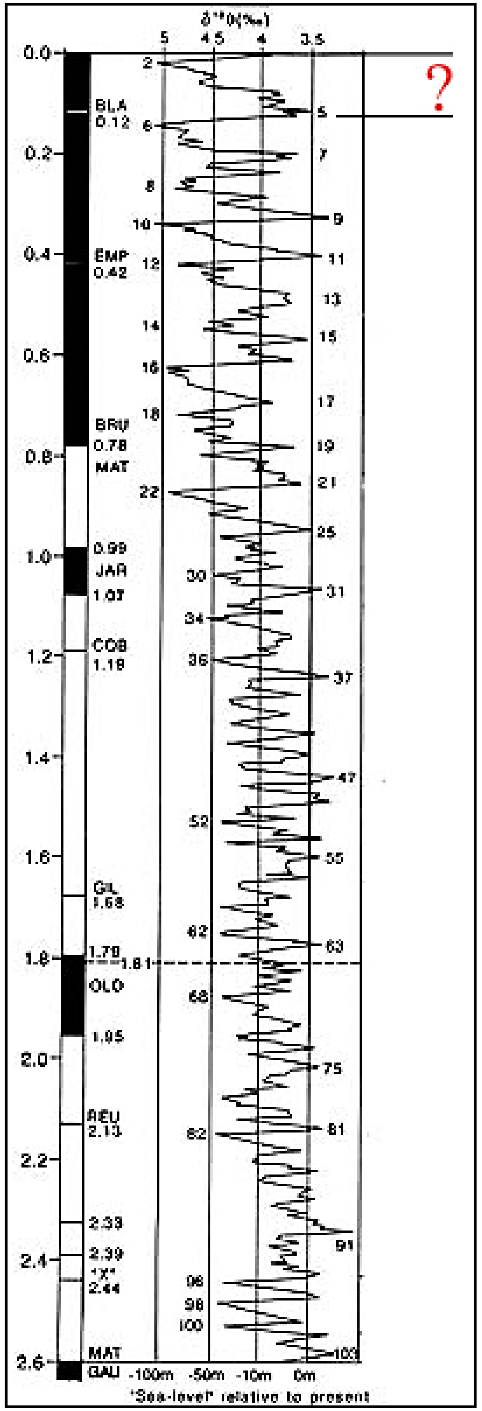

Boundary of the Quaternary:

Pleistocene/Holocene

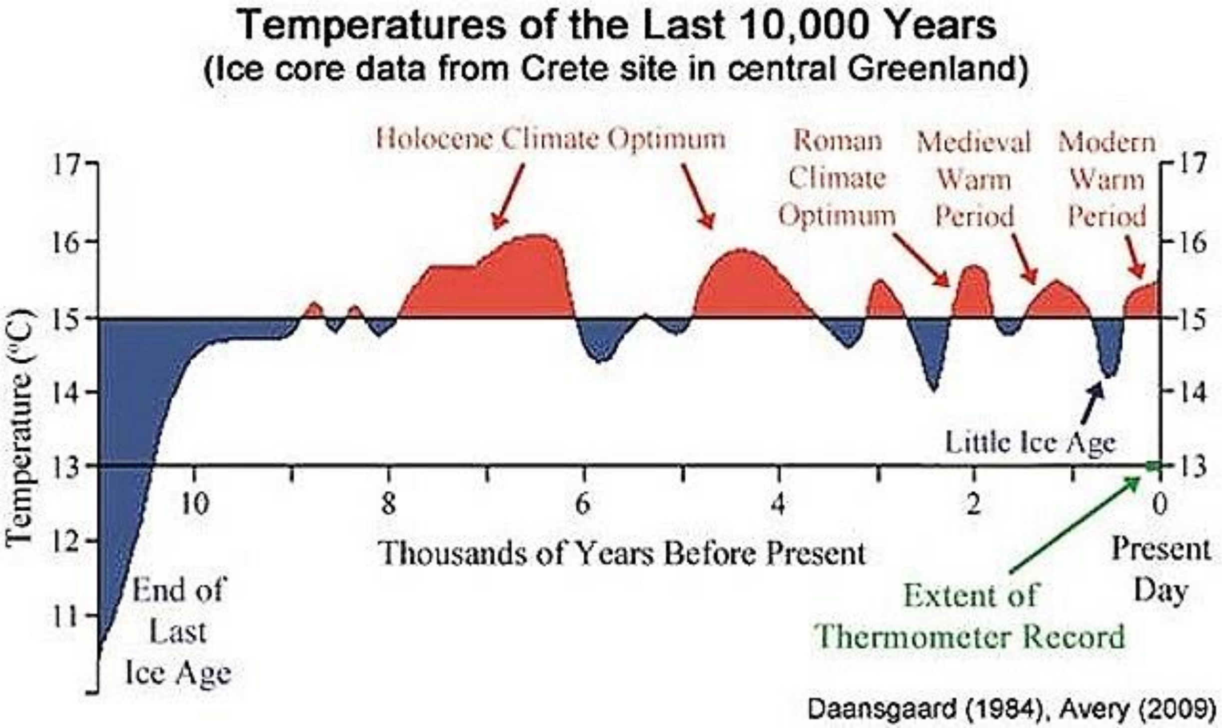

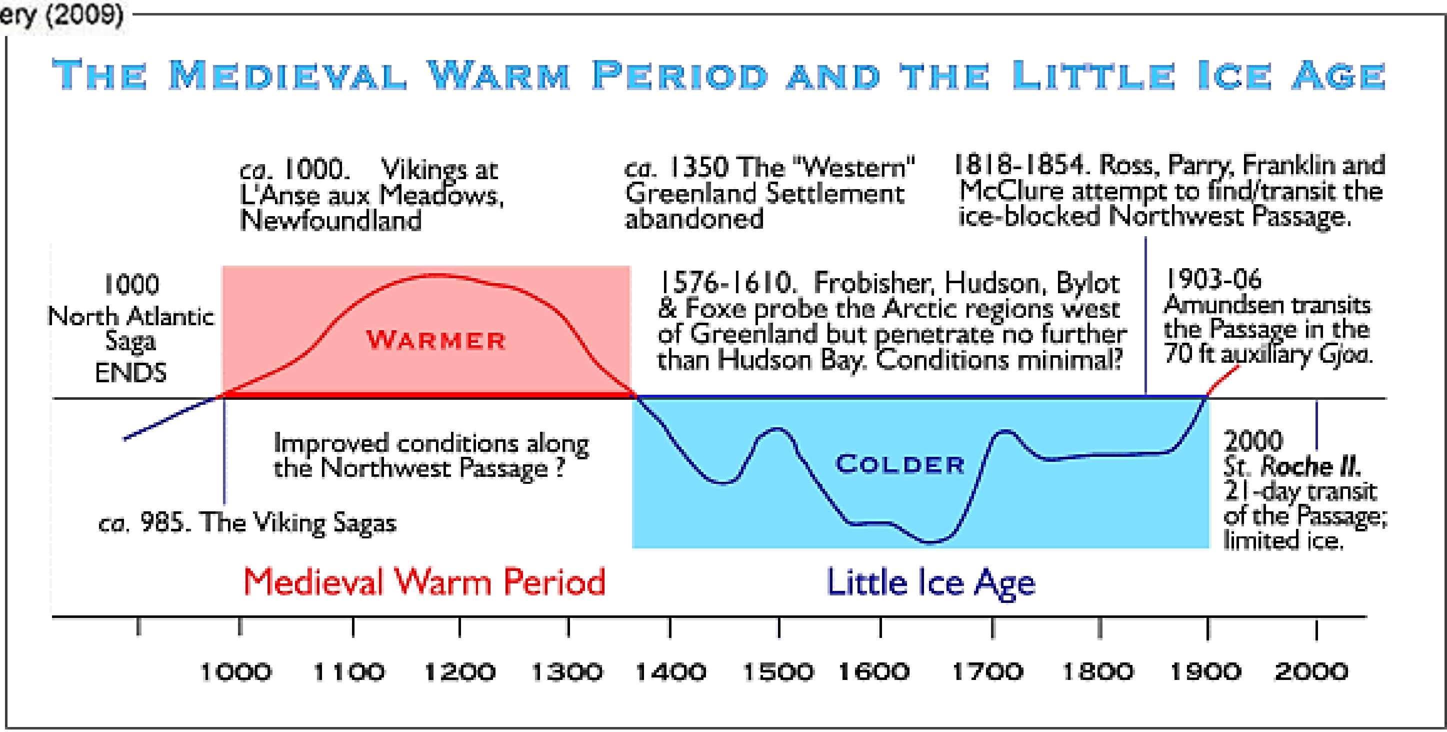

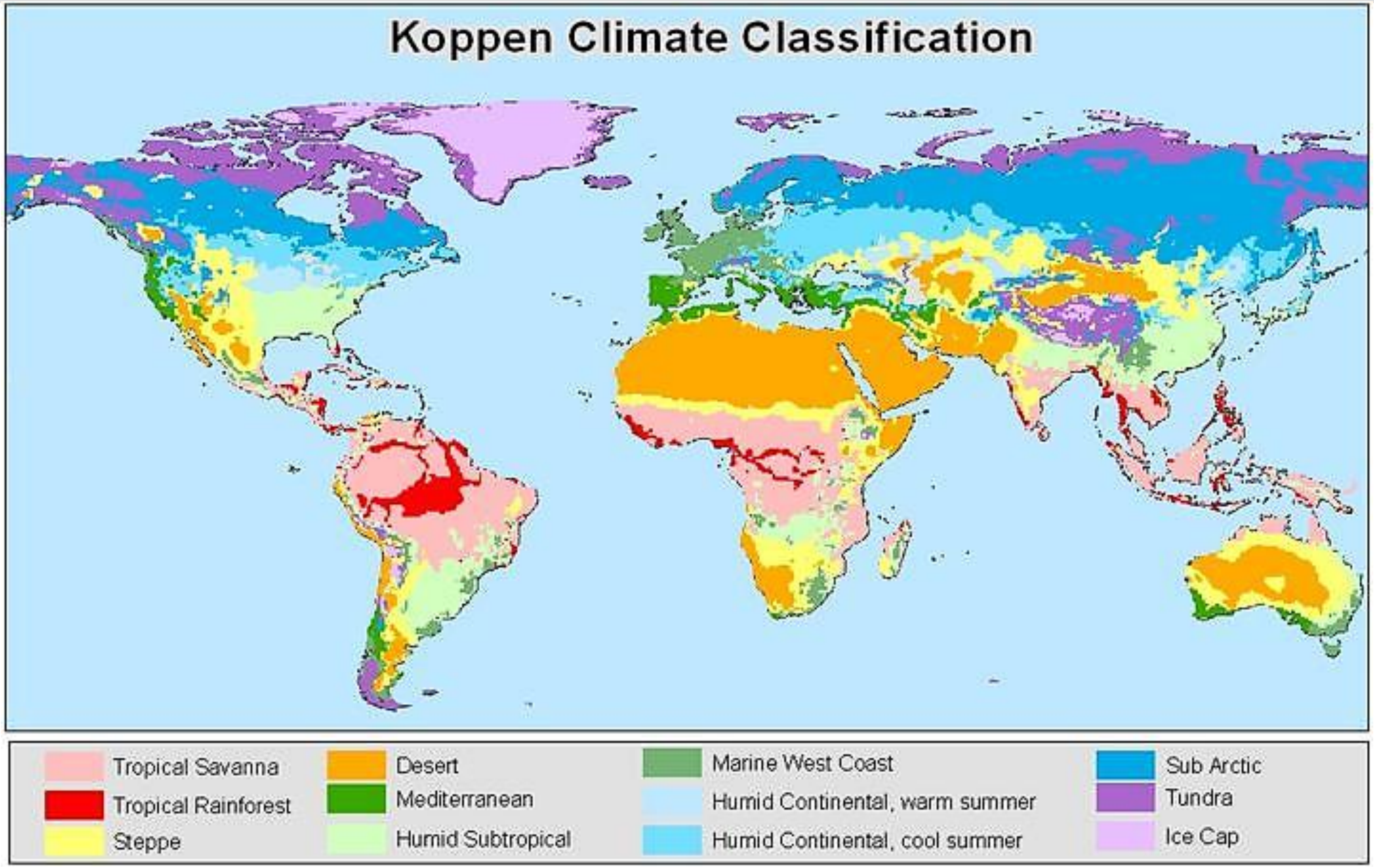

https://uwcm-geog.wikispaces.com/EXTREME+ENVIRONMENTS

Vegatation cover during the Last Glacial Maximum (LGM) 20000 years before present

- Comparison of the distribution of vegetation types and ice sheet extent between (A) modern and (B) Last Glacial Maximum (LGM) (13, 14). The LGM was marked by much wider distribution of dry vegetation biotopes, including those of deserts, grasslands and savanna, semidesert and dry steppe, polar desert, and southern steppe tundra compared with the present day. [Reproduced with permission from ref. 14 (Copyright 2003, American Geophysical Union)
- *https://www.semanticscholar.org/paper/Glacial-demise-and-methane's-rise-Behl/295890b12b8c07129b7b32c0e459ab9e16bb7e1c/figure/0*

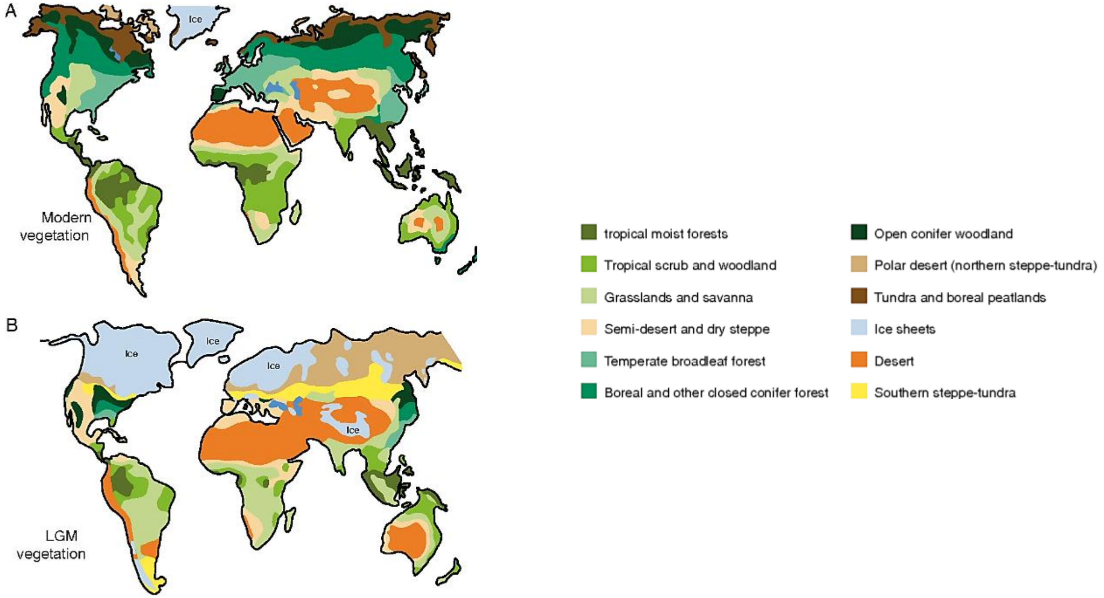

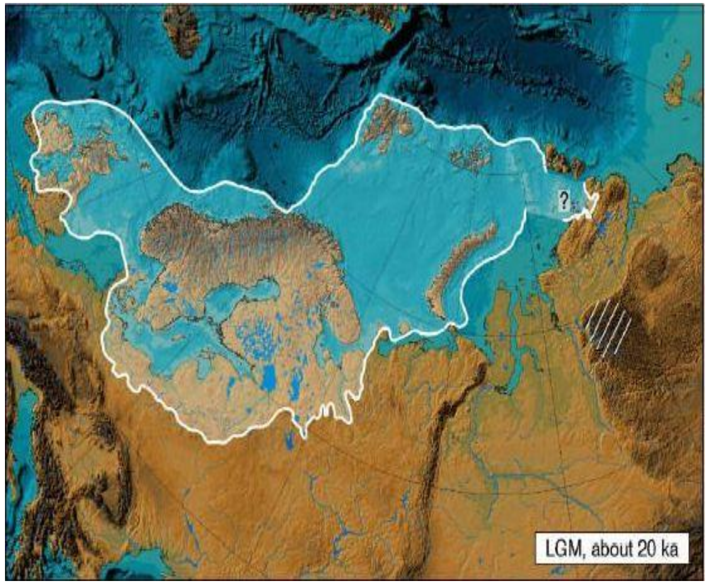

Factors influencing the climate

Ice

Ocean

Continents

aus: PAGES

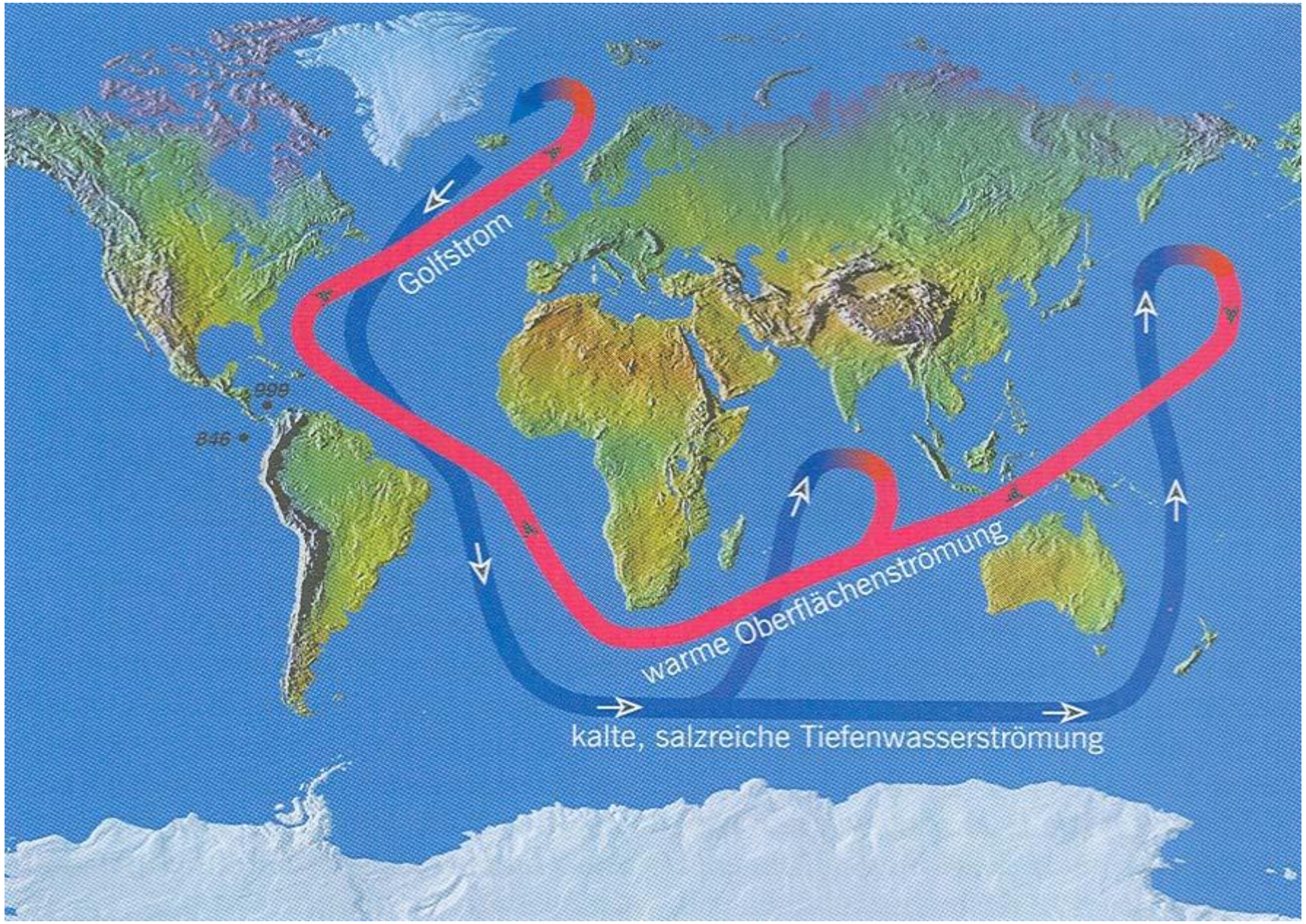
Golfstrom
998
846
warme Oberflächenströmung
kalte, salzreiche Tiefenwasserströmung

Pleistocene Glaciation

At maximum covered 1/3 of total land surface

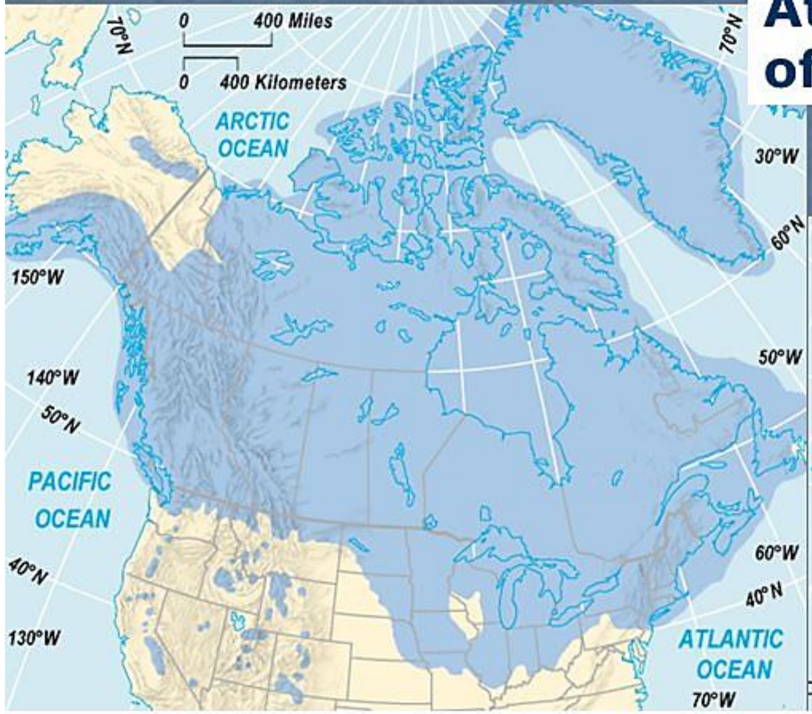

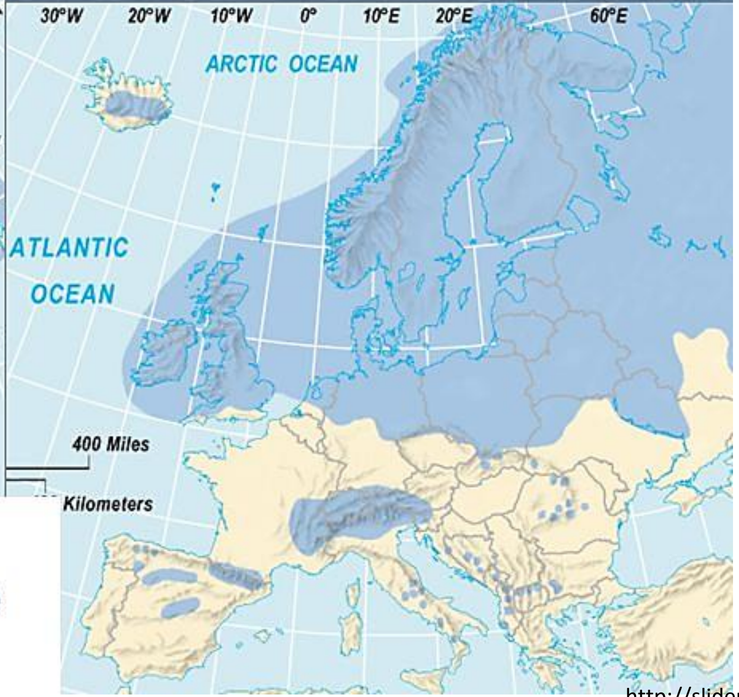

The Laurentide ice was the most extensive Pleistocene ice mass

http://slideplayer.com/slide/8652412/

The climate of the Quaternary

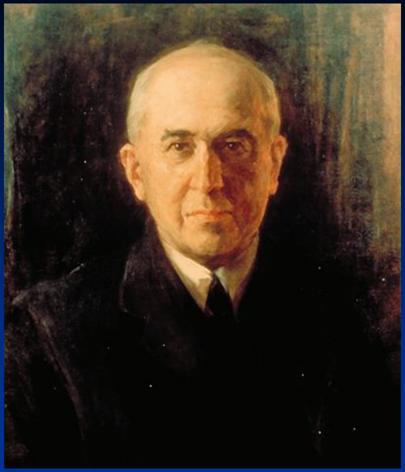

Milankovich theory and the climate changes

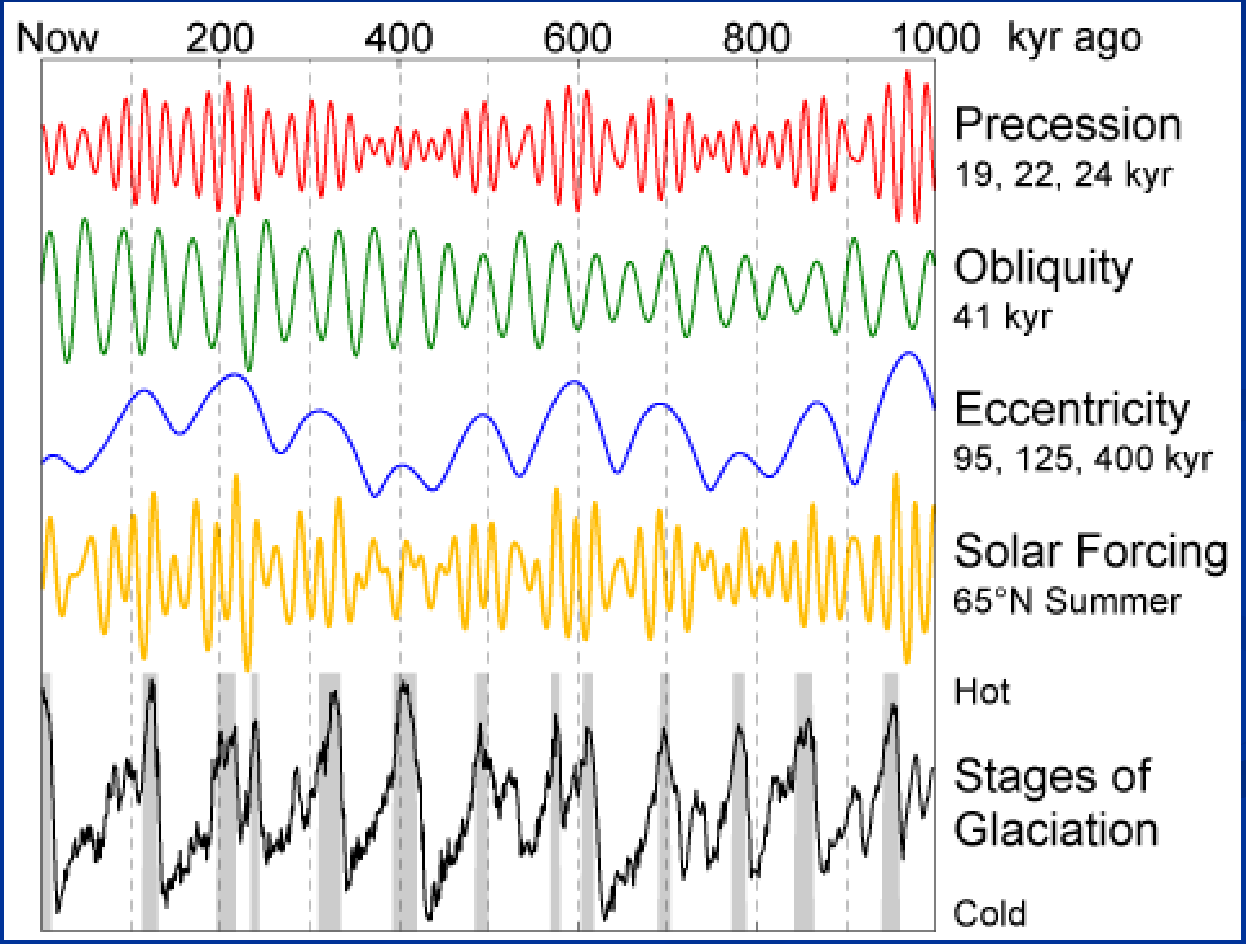

More details about Milankovitch theory:

https://climate.nasa.gov/news/2948/milankovitch-orbital-cycles-and-their-role-in-earths-climate/

The whole article:
https://climate.nasa.gov/news/2948/milankovitch-orbital-cycles-and-their-role-in-earths-climate/

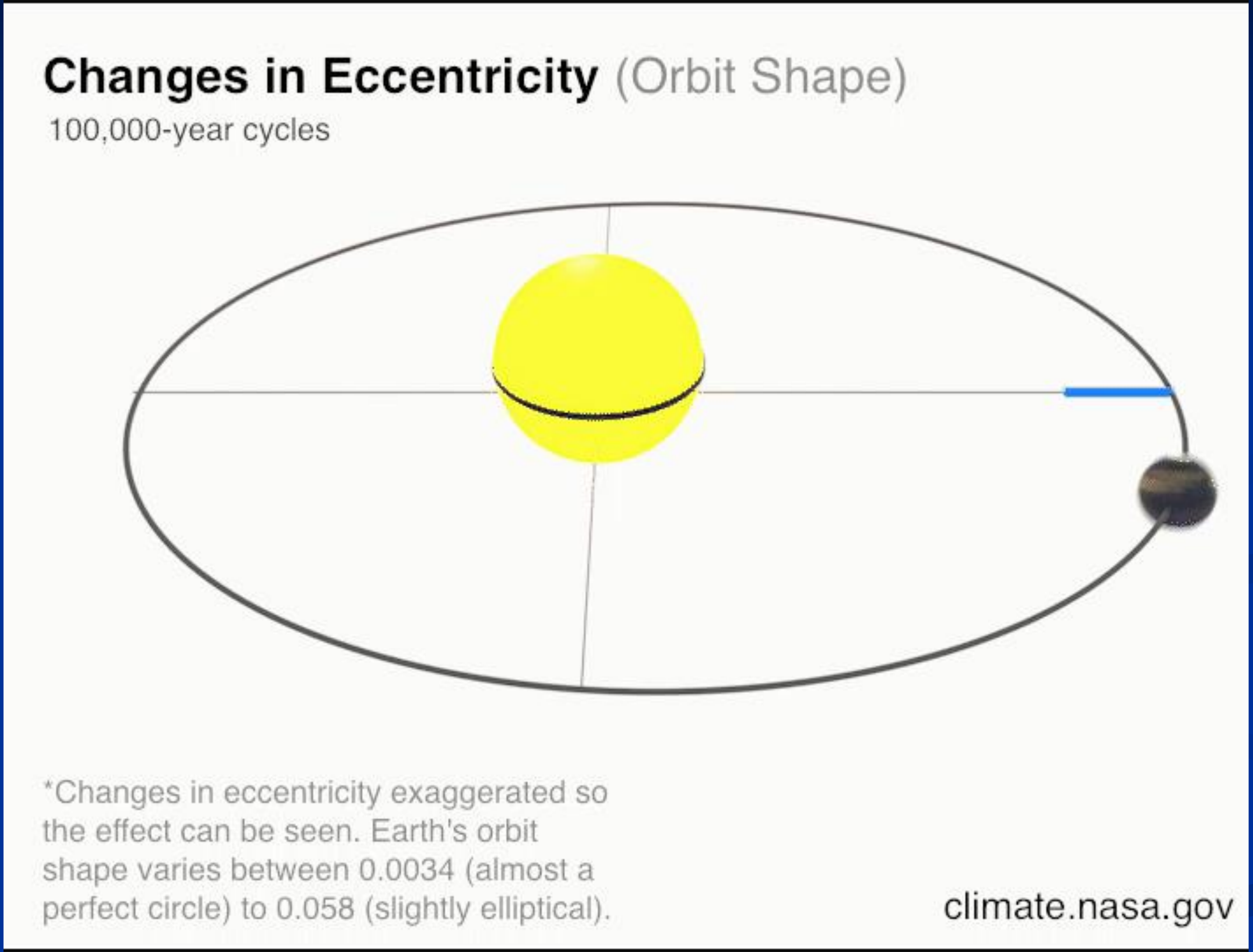

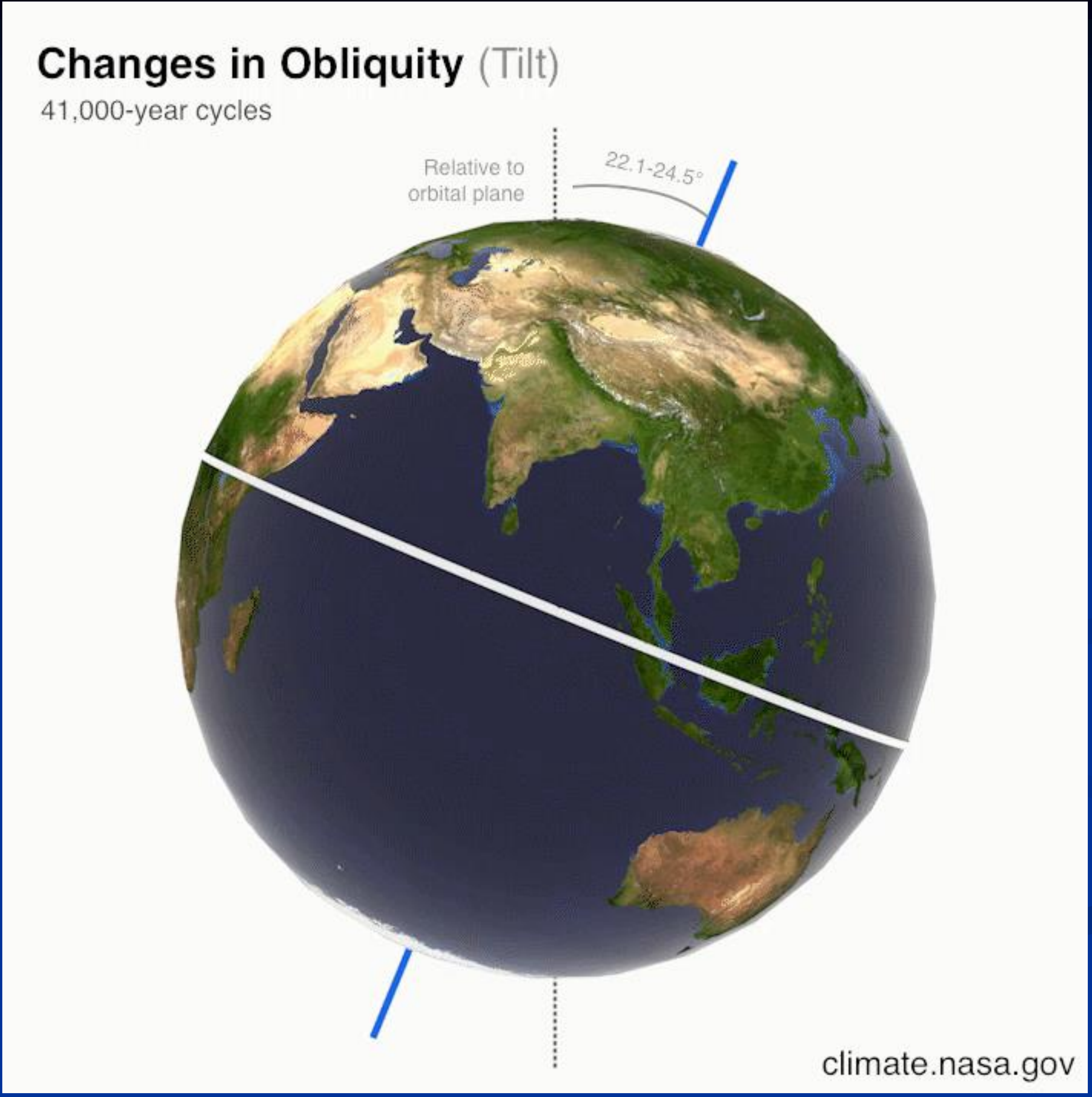
Changes in Obliquity (Tilt)
41,000-year cycles
Relative to
orbital plane
22.1-24.5°
climate.nasa.gov

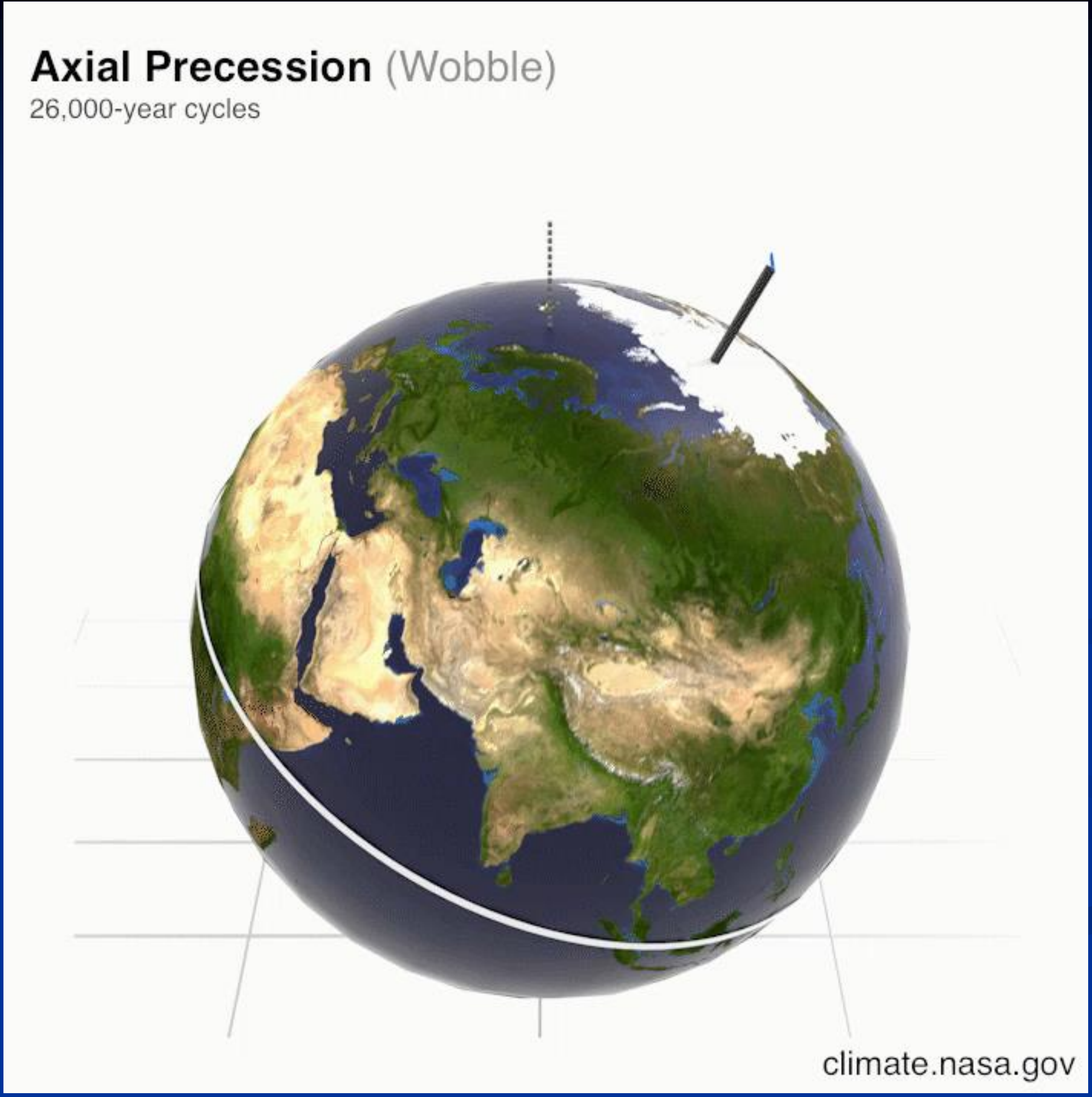
Axial Precession (Wobble)
26,000-year cycles
climate.nasa.gov

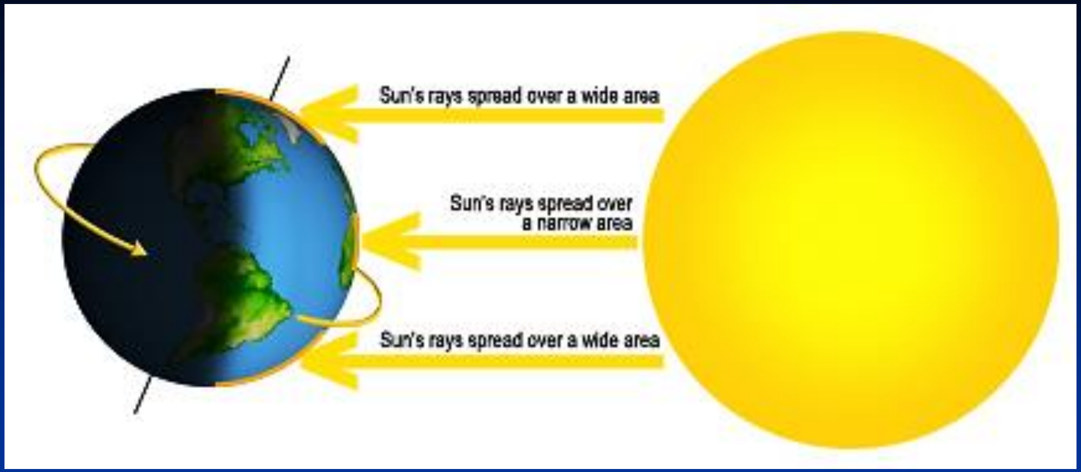

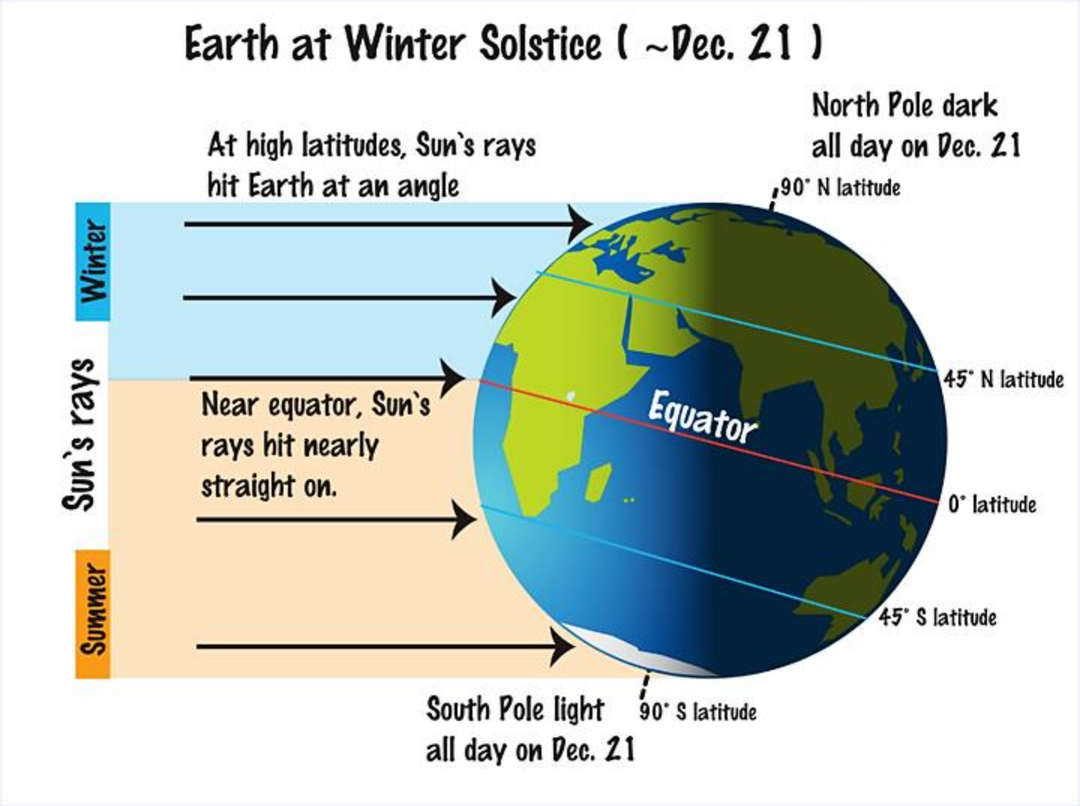

https://uwcm-geog.wikispaces.com/EXTREME+ENVIRONMENTS

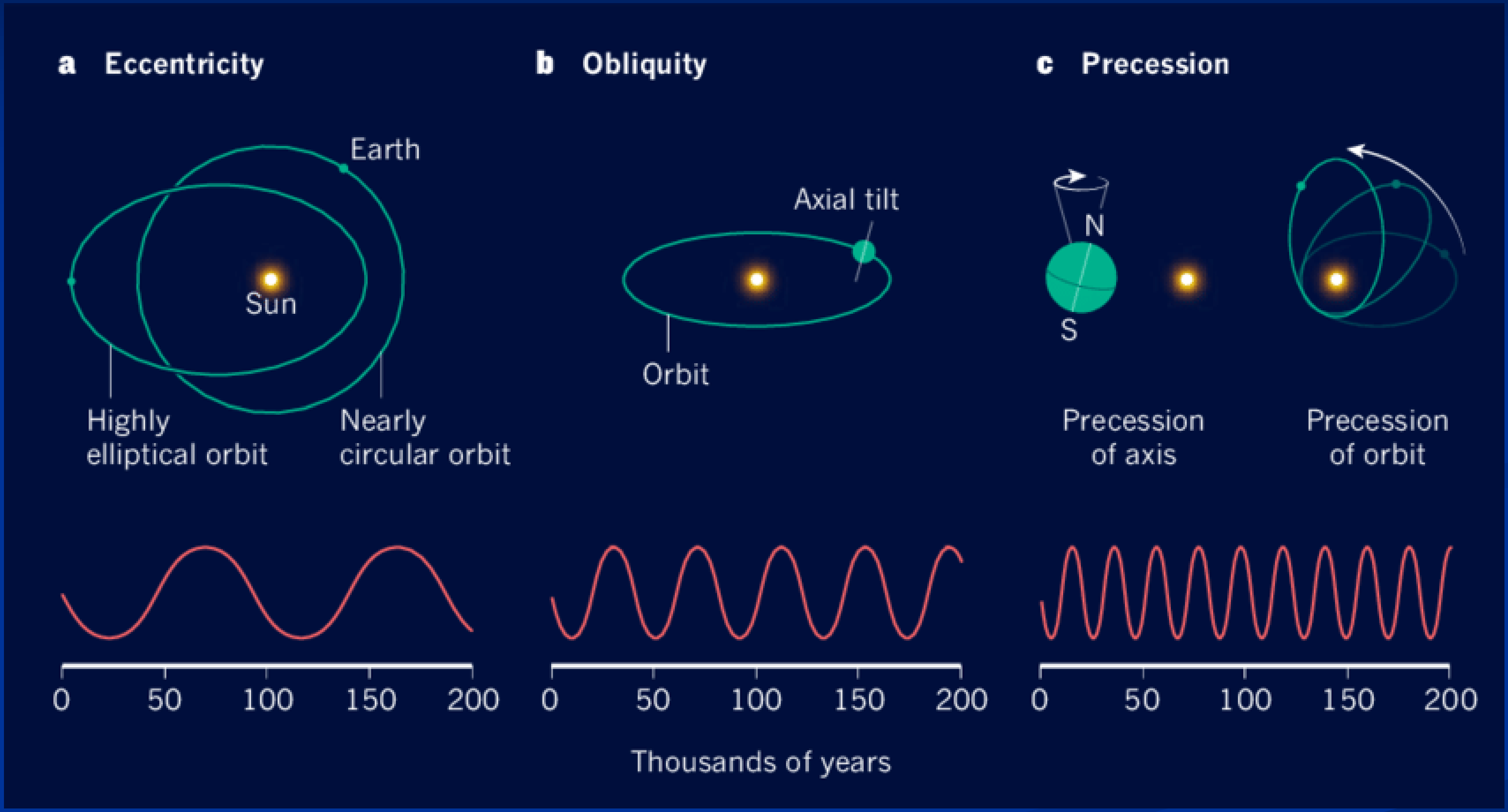

In: Maslin, NV. 2016

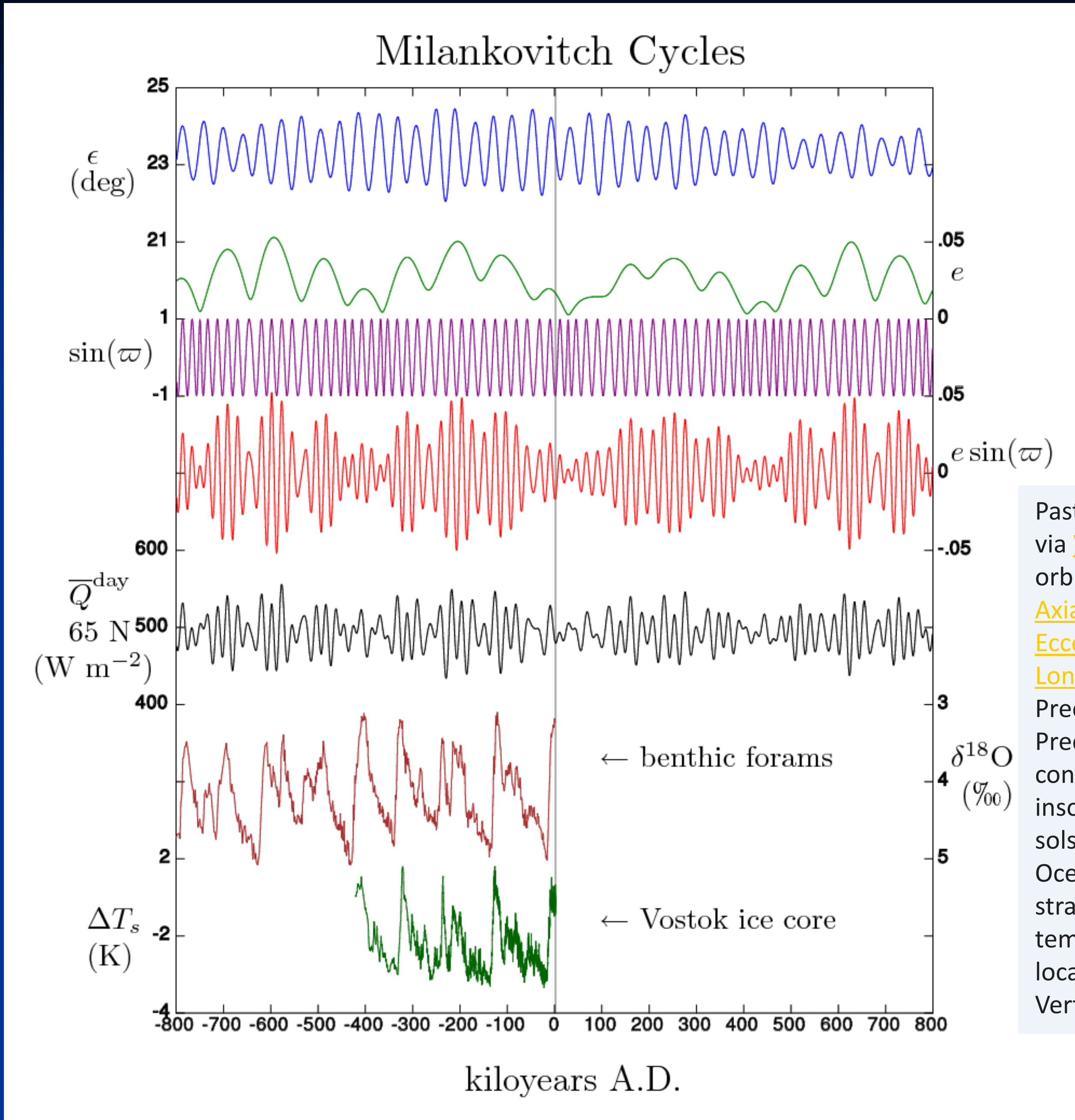

Past and future Milankovitch cycles via VSOP model • Graphic shows variations in five orbital elements:
Axial tilt or obliquity (ε).
Eccentricity (*e*).
Longitude of perihelion (sin(ϖ)).
Precession index (*e* sin(ϖ))
Precession index and obliquity control insolation at each latitude: Daily-average insolation at top of atmosphere on summer solstice () at 65° N
Ocean sediment and Antarctic ice strata record ancient sea levels and temperatures: Benthic forams (57 widespread locations) Vostok ice core (Antarctica)
Vertical gray line shows present (2000 CE)

https://upload.wikimedia.org/wikipedia/commons/5/53/MilankovitchCyclesOrbitandCores.png

Complex explanation of climate changes

Not only astronomical reasons!

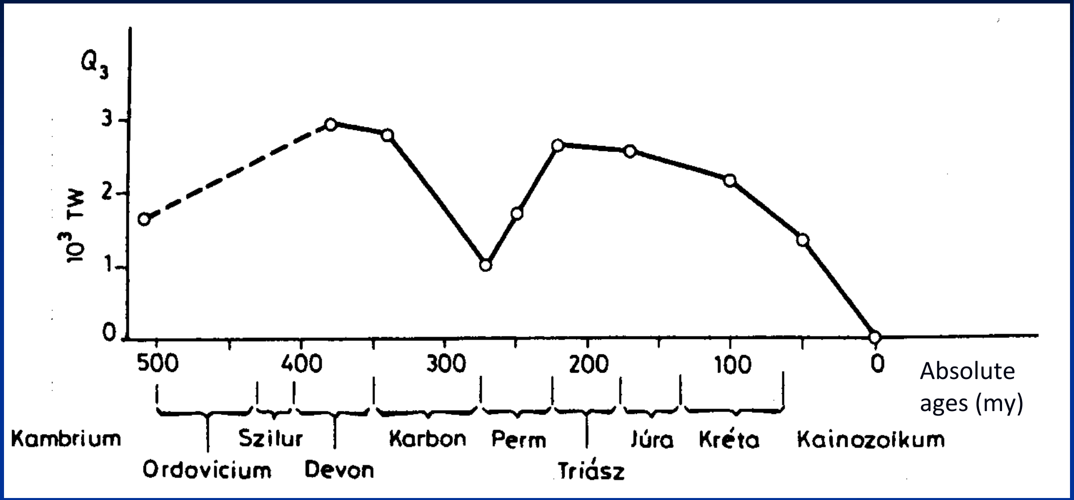

Other important factors:

- Oceanic currents
- Feedback of the ice sheets
- Volcanic activity

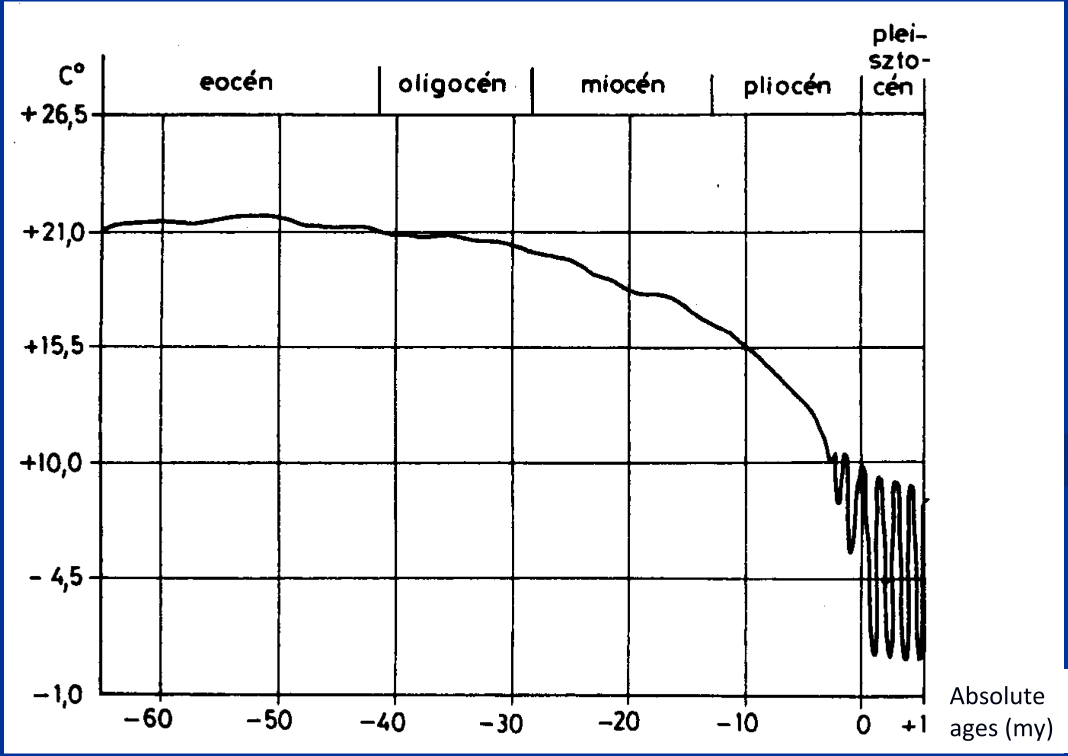

Cold and warm periods of the Earth history

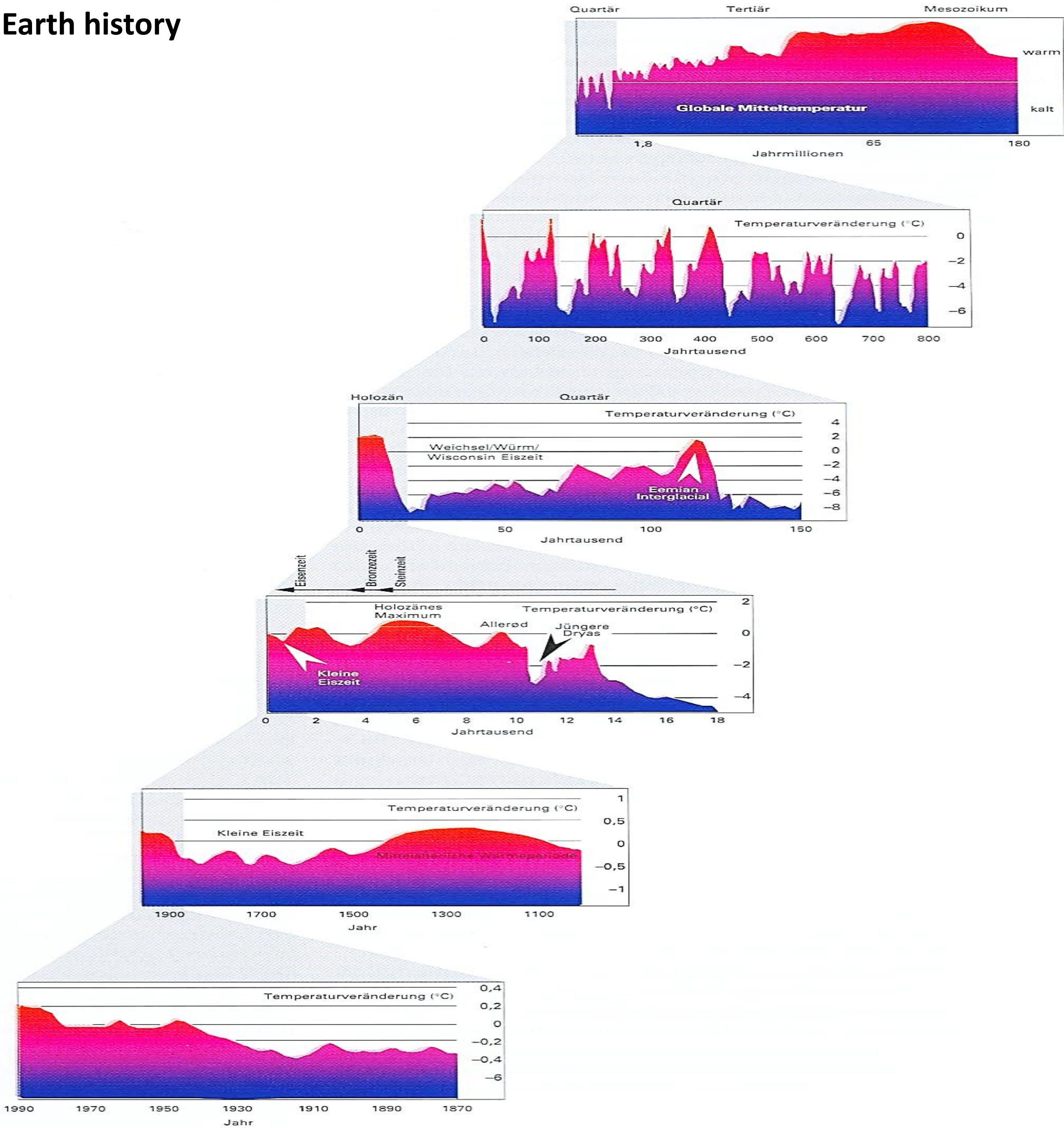

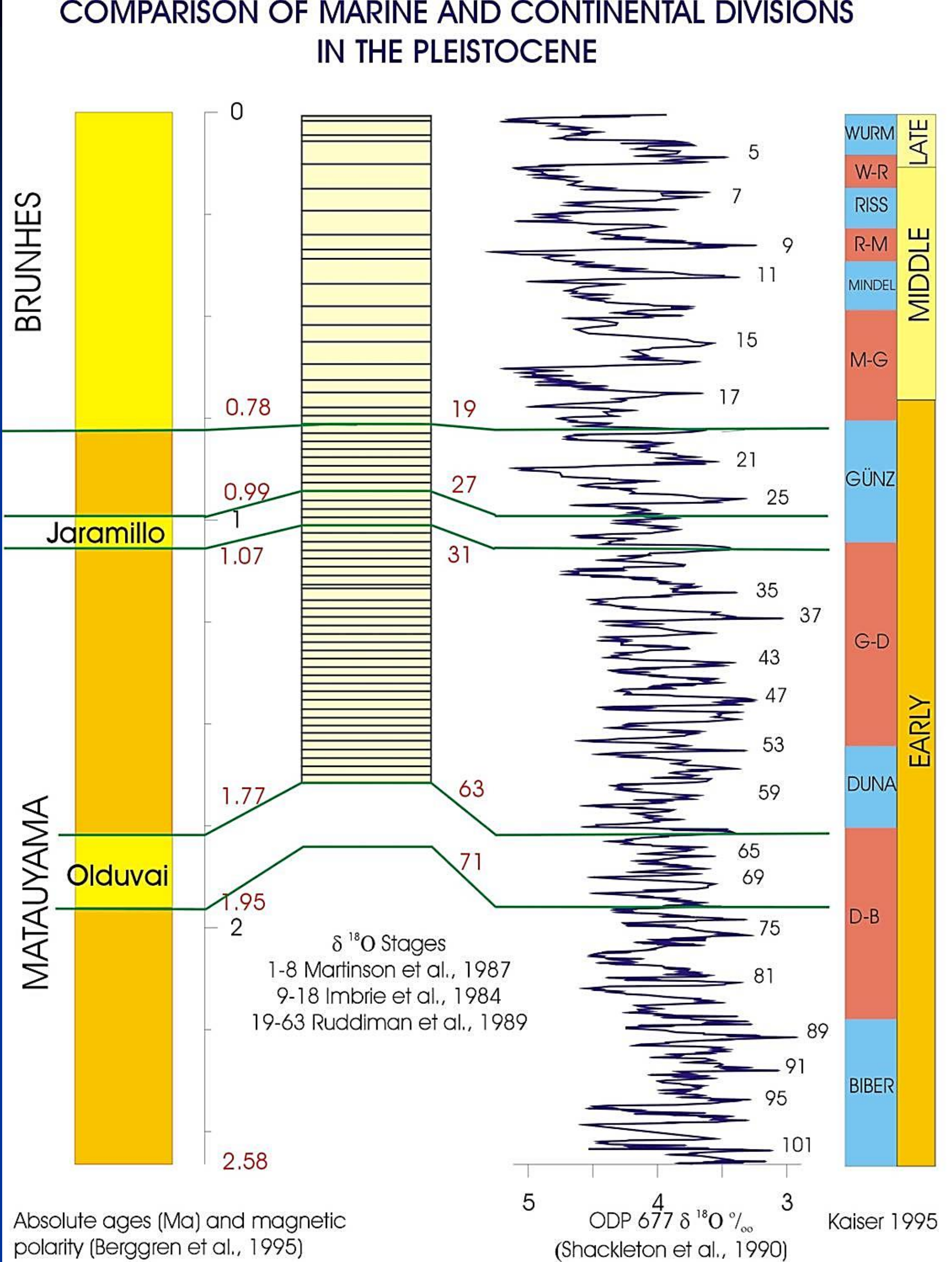

MIS 1 – Holocén

MIS 2-5d – Würm (Weischelian)

MIS 5e – RW interglac. (Eemian)

MIS 6 – Riss (Saalian)

MIS 11 – MR interglac. (Holstein)

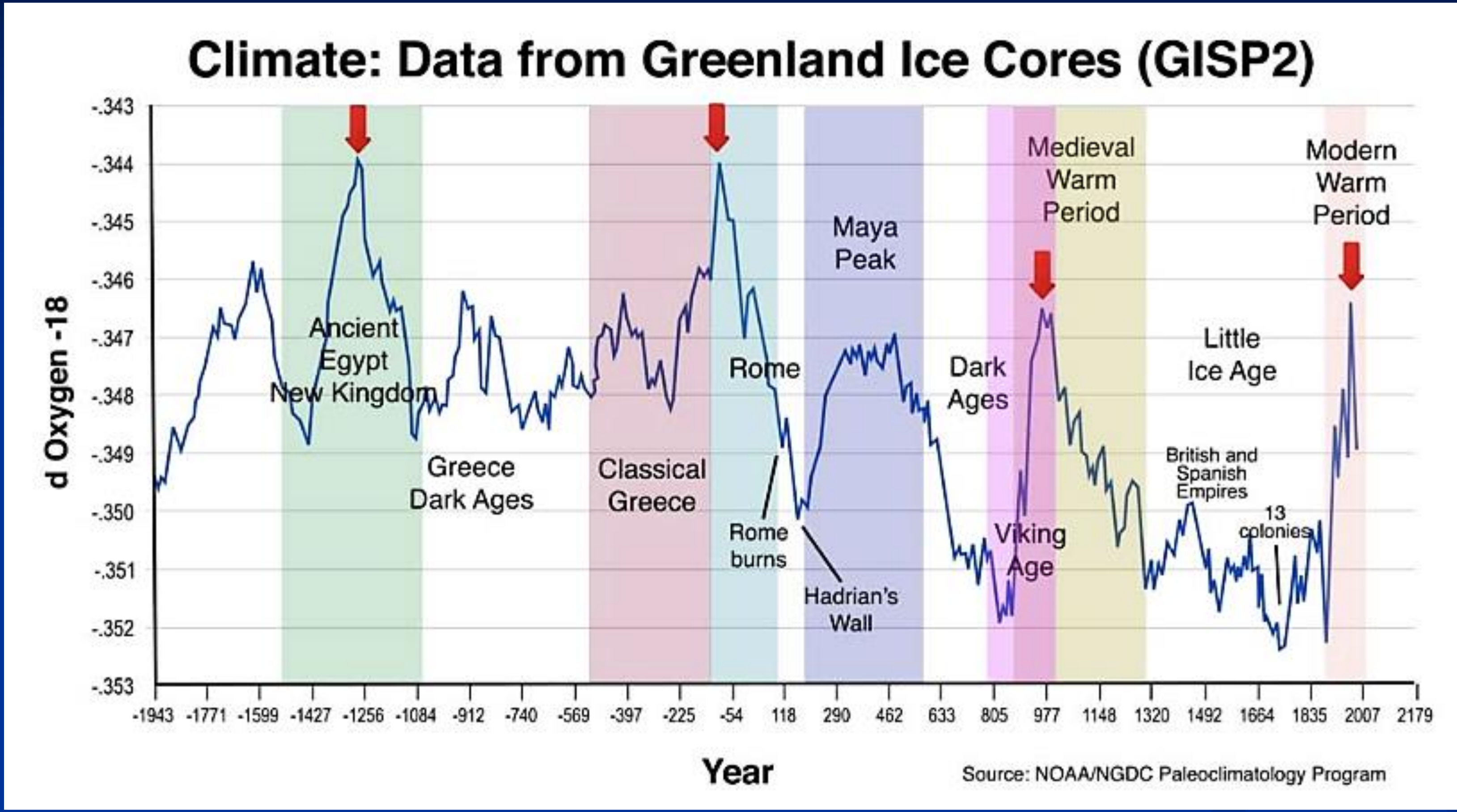

https://www.thegwpf.com/understanding-climate-cycles-or-how-to-avoid-climate-panics/

Temperature changes in the Bernese Alps in the last 500 years

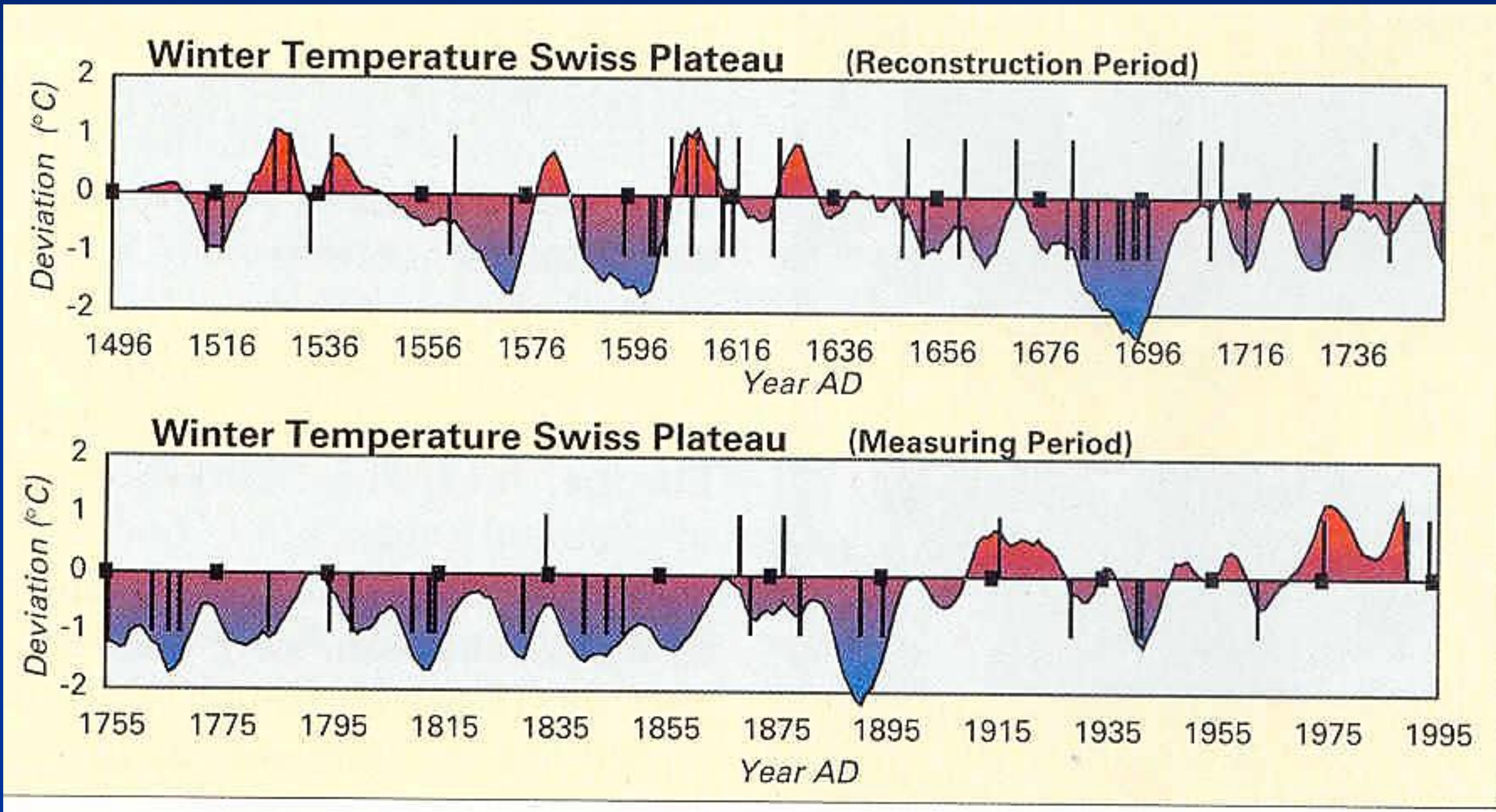

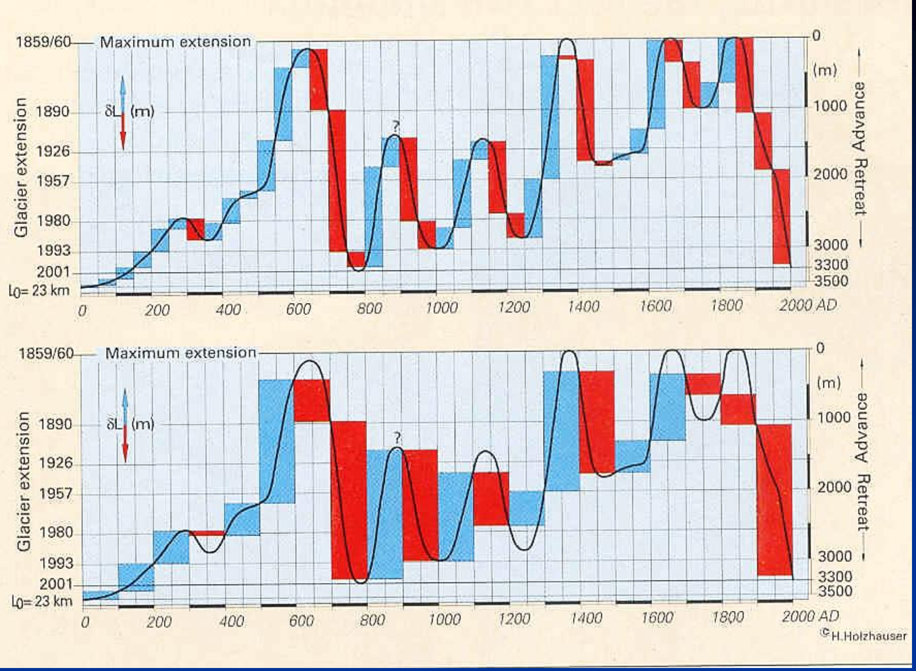

Changes of the ice mass of the Aletsch glacier (Western Alps, Switzerland) during the last 2000 years

1856

1987

2030

Aletsch glacier (CH)

- Lenght: 23 km
- Surface: 86 km^2
- Waterflow in summer: 80 m^3/sec
- Average retreat: 30m/year (sometimes: 90m/year)

Aletsch glacier from theEggishorn

1900

2001

Retreat of the Aletsch glacier

1979

1991

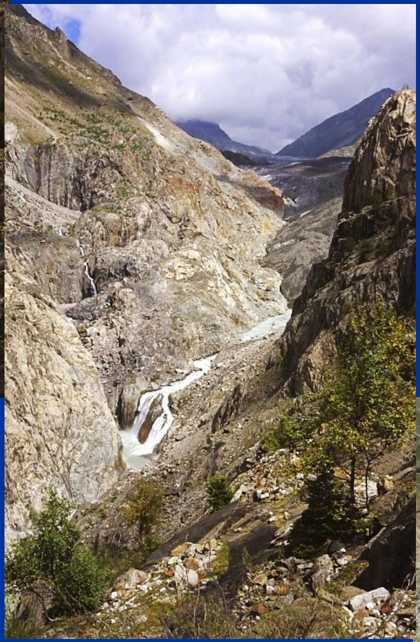

2002

2003

Aletschwald (330ha)

(Protected since 1933, Pro Natura site)

Retreat of the Pasterze glacier (Eastern-Alps, Austria)

2000

2003

DATING METHODS IN THE QUATERNARY STUDIES

RELATIVE DATING METHODS/RELATIVE STRATIGRAPHY

1. **Lithostratigraphy**
   - marker horizons:
     - tephrostratigraphy
     - buried soils (paleosols, fossil soils)
2. **Biostratigraphy**
   - Vertebrata
   - Molluscs
     - -Malacothermometer
     - -$\delta^{18}O$ of molluscs shells
   - Marine microfauna
   - Pollen
   - Biomarkers
3. **Magnetostratigraphy**
4. **Magnetic susceptibility (MS)**
5. **Amino Acid Racemisation (AAR)**
6. **Stable isotopes**
   - $\delta^{18}O$ ($^{16}O/^{18}O$)
     - (Milankovich theory)
   - $\delta^{13}C$ ($^{12}C/^{13}C$)
7. **Ice cores from the icesheets**
8. **Geomorphological horizons**
   - terraces: fluvial marine
   - correlative sediments

DATING METHODS IN THE QUATERNARY STUDIES

ABSOLUTE DATING METHODS

9. Varve-, and dendrochronology

“Absolute” methods or numerical age estimation

10. Non-stable (radioactive) isotopes
    - 10/a Potassium-argon series
        - $^{40}K/^{40}Ar$
        - $^{40}Ar/^{39}Ar$
        - laser fusion $^{40}Ar/^{39}Ar$
    - 10/b Uranium decay series
        - $^{238}U/^{230}Th$
        - $^{234}U/^{230}Th$
        - $^{230}Th/^{231}Pa$ (^{235}U)
    - 10/c Fission-track (^{238}U)
    - 10/d Radiocarbon dating (^{14}C)
11. Luminescence methods
    - -Thermoluminescence (TL)
    - -Optically stimulated luminescence (OSL)
        - InfraRed Stimulated Luminescence (IRSL)
12. Electron-spin resonance (ESR)
13. Cosmogenic isotopes

RELATIVE DATING METHODS/RELATIVE STRATIGRAPHY

1. **Lithostratigraphy**

marker horizons:

tephrostratigraphy

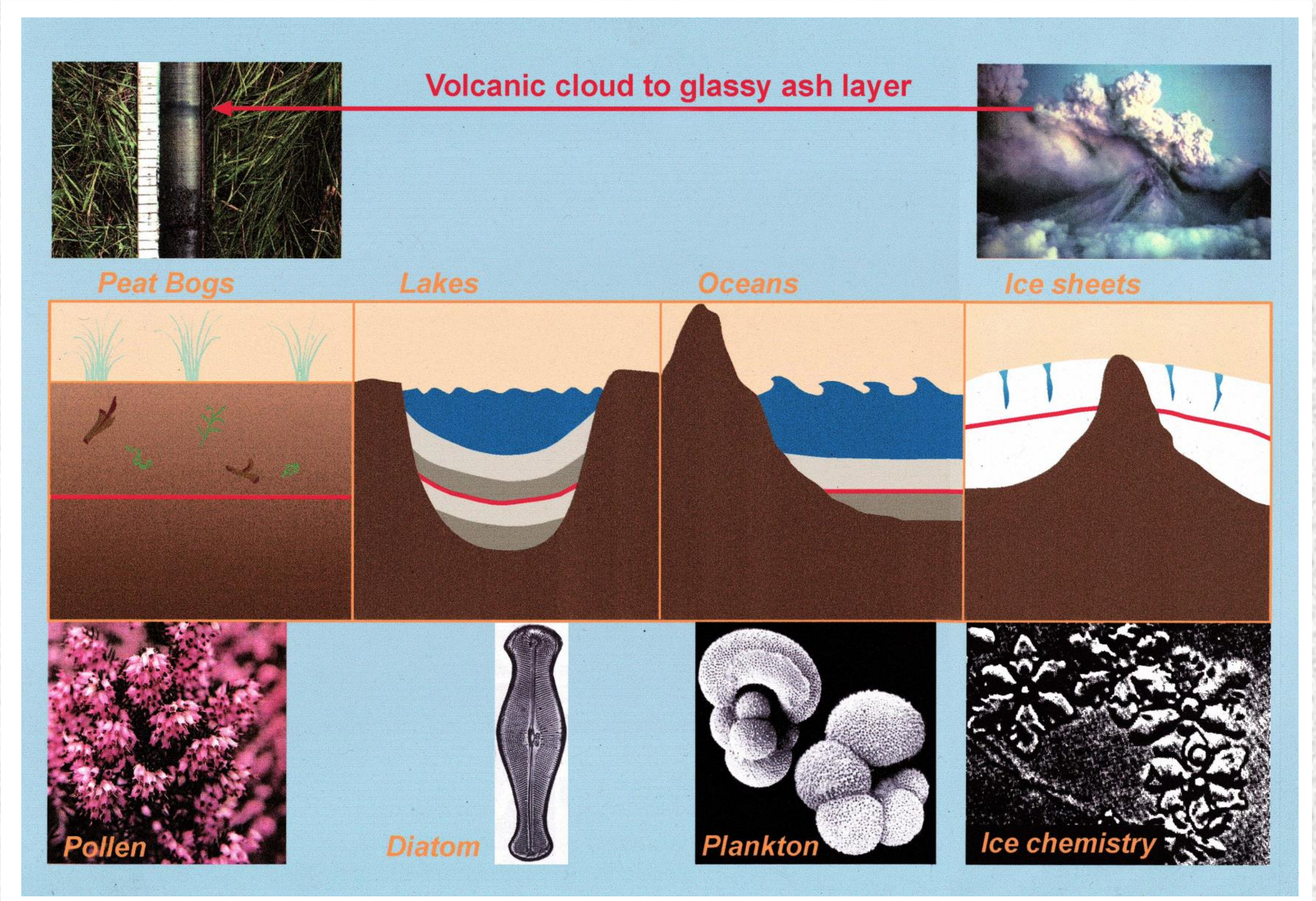

The importance of the marker horizons (in this case tephra layer) in Quaternary research in Hungary

• Projection of stratigraphical results from well investigated profiles to less known profiles
• Possibility of correlation with the stratigraphy of neighboring countries (eg. Bohemian, Slovakian, Croatian)
• Reconstruction of the paleosurface

Loess profiles with Bag Tephra layer in the Carpathian Basin

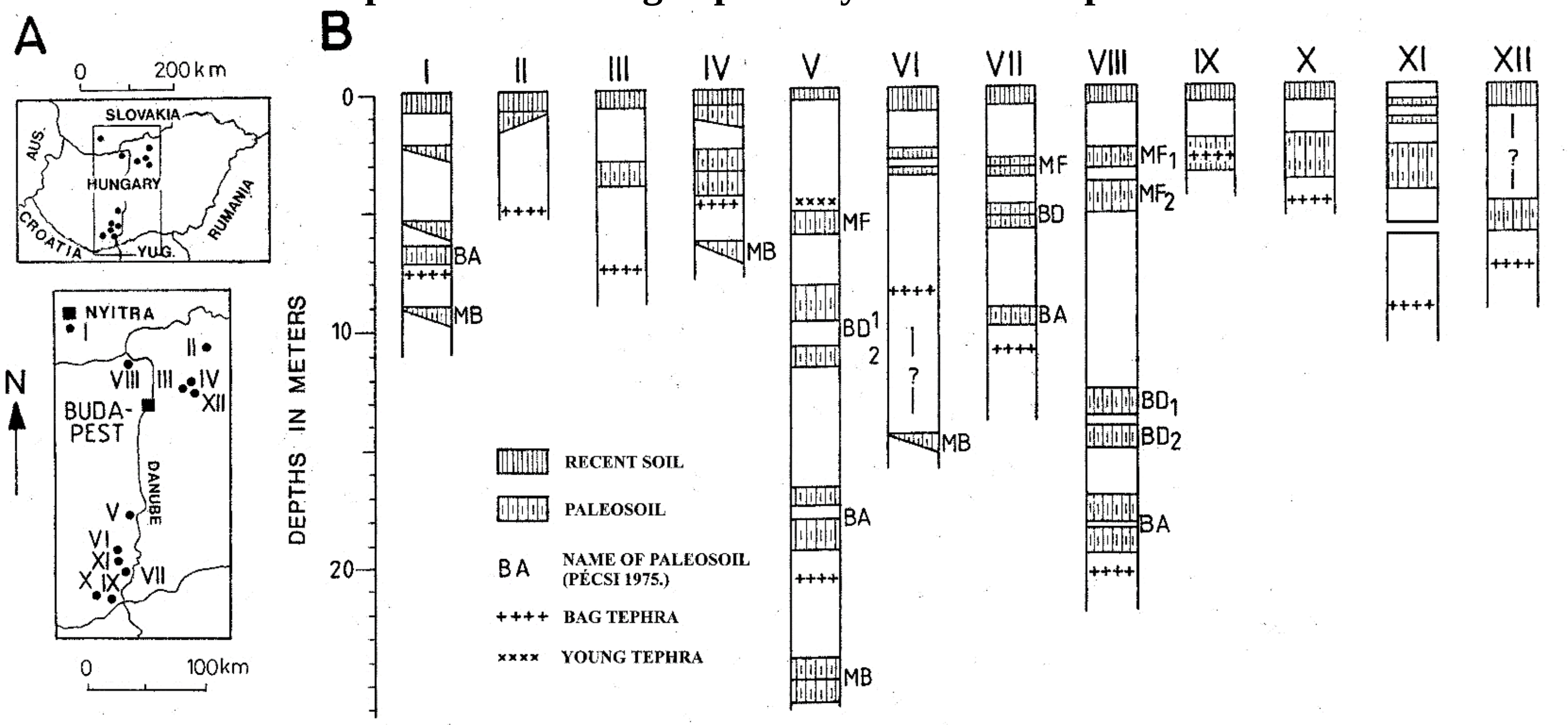

(see more in:Horváth 2001, Horváth et al. 2006)

Bag Tephra in the Carpathian Basin

Correlation based on:

-mineralogical investigations,
-grainsize distribution of clinopyroxenes,
-geochemical investigations

Most probable source area:

Appennines acidic (Rome)
semi acidic (Campania) lavas

Mte Vulture (Italy) high K-content

Active volcanoes in the time range 100-800ka:

Massif Central, Aegean island arch, East-Carpathians, West-Carpathians, Volcanic Eifel

1. **Lithostratigraphy**

1.2. buried soils (paleosols, fossil soils)

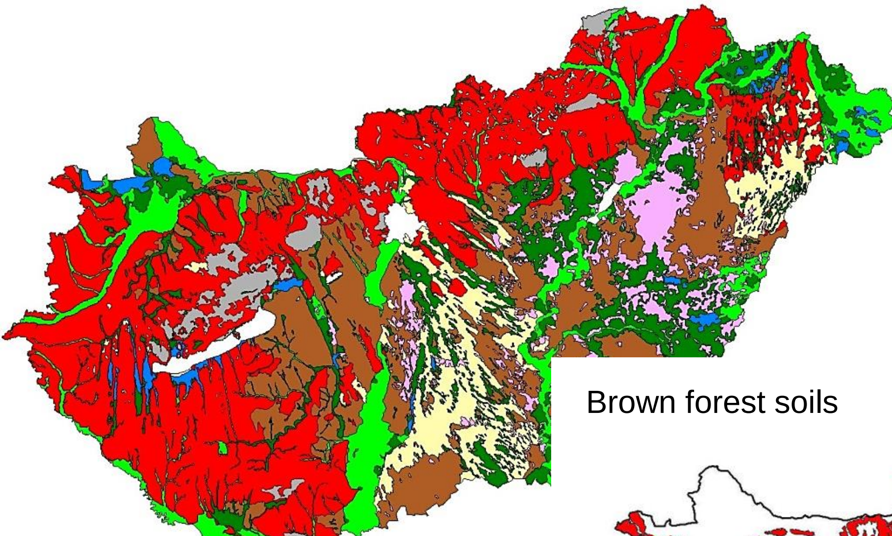

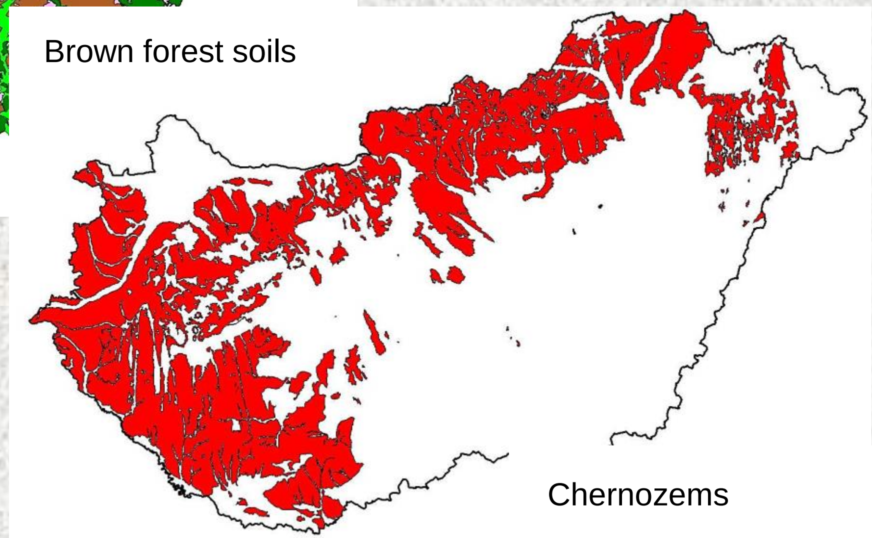

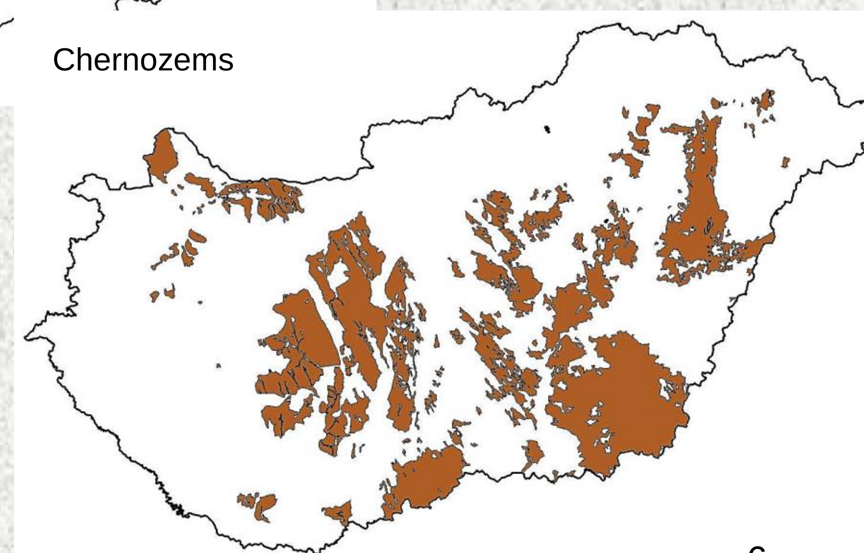

Recent soils of Hungary

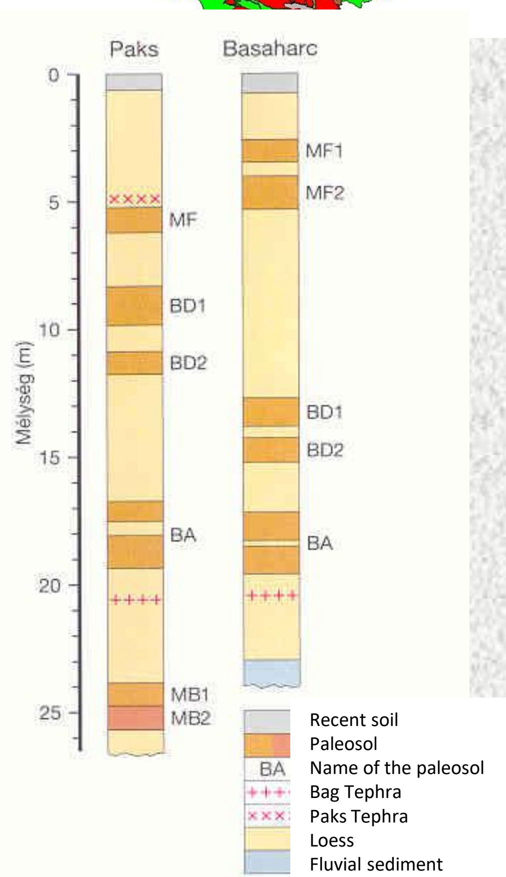

http://www.uni-miskolc.hu/~ecodobos/ktmcd1/huntalajok.htm

Palesols in different geomorphological position

(Süttő, Northern Hungary)

DATING METHODS IN THE QUATERNARY STUDIES

RELATIVE DATING METHODS/RELATIVE STRATIGRAPHY

1. **Lithostratigraphy**
   - marker horizons:
     - tephrostratigraphy
     - buried soils (paleosols, fossil soils)
2. **Biostratigraphy**
   - Vertebrata fauna
   - Molluscs
     - -Malacothermometer
     - -$\delta^{18}O$ of molluscs shells
   - Marine microfauna
   - Pollen
   - Biomarkers
3. **Magnetostratigraphy**
4. **Magnetic susceptibility (MS)**
5. **Amino Acid Racemisation (AAR)**
6. **Stable isotopes**
   - $\delta^{18}O$ ($^{16}O/^{18}O$)
     - (Milankovich theory)
   - $\delta^{13}C$ ($^{12}C/^{13}C$)
7. **Ice cores from the icesheets**
8. **Geomorphological horizons**
   - terraces: fluvial marine
   - correlative sediments

Vertebrata fauna in Hungary in Late-Pleistocene

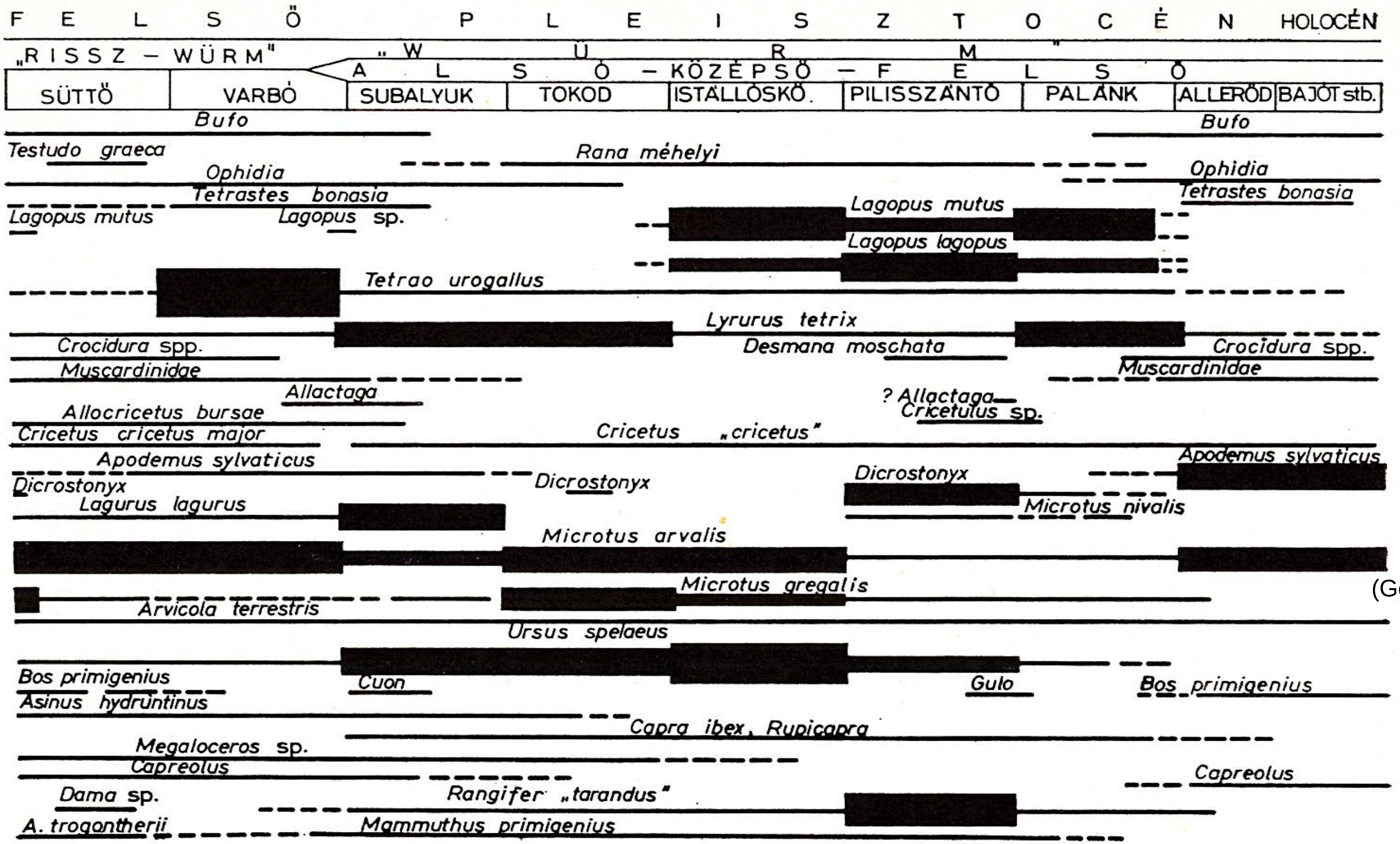

(Gopher)

Gophers, „the foraminiferans of the Quaternary"…

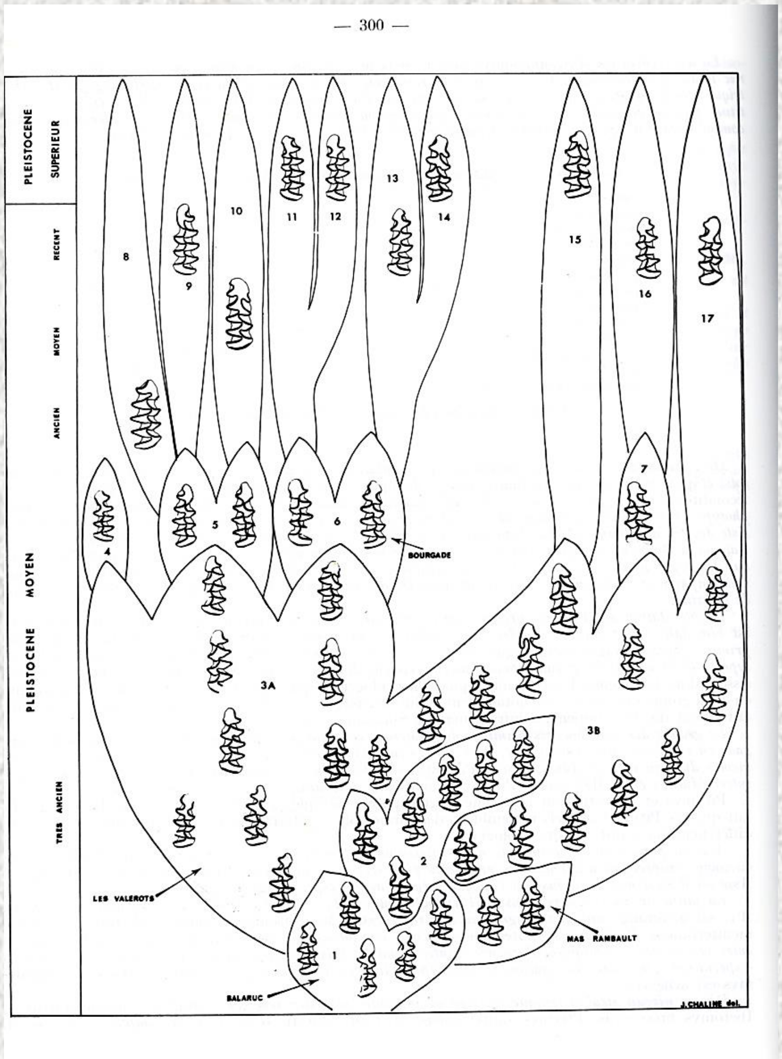

…and other rodents

Hey lemming (Dicrostonyx torquatus)

Hamster (Cricetus cricetus)

Alpine gopher(Microtus nivalis)

Siberian gopher(Microtus gregalis)

ground-squirrel (Citellus citellus)

Gophers in different environments

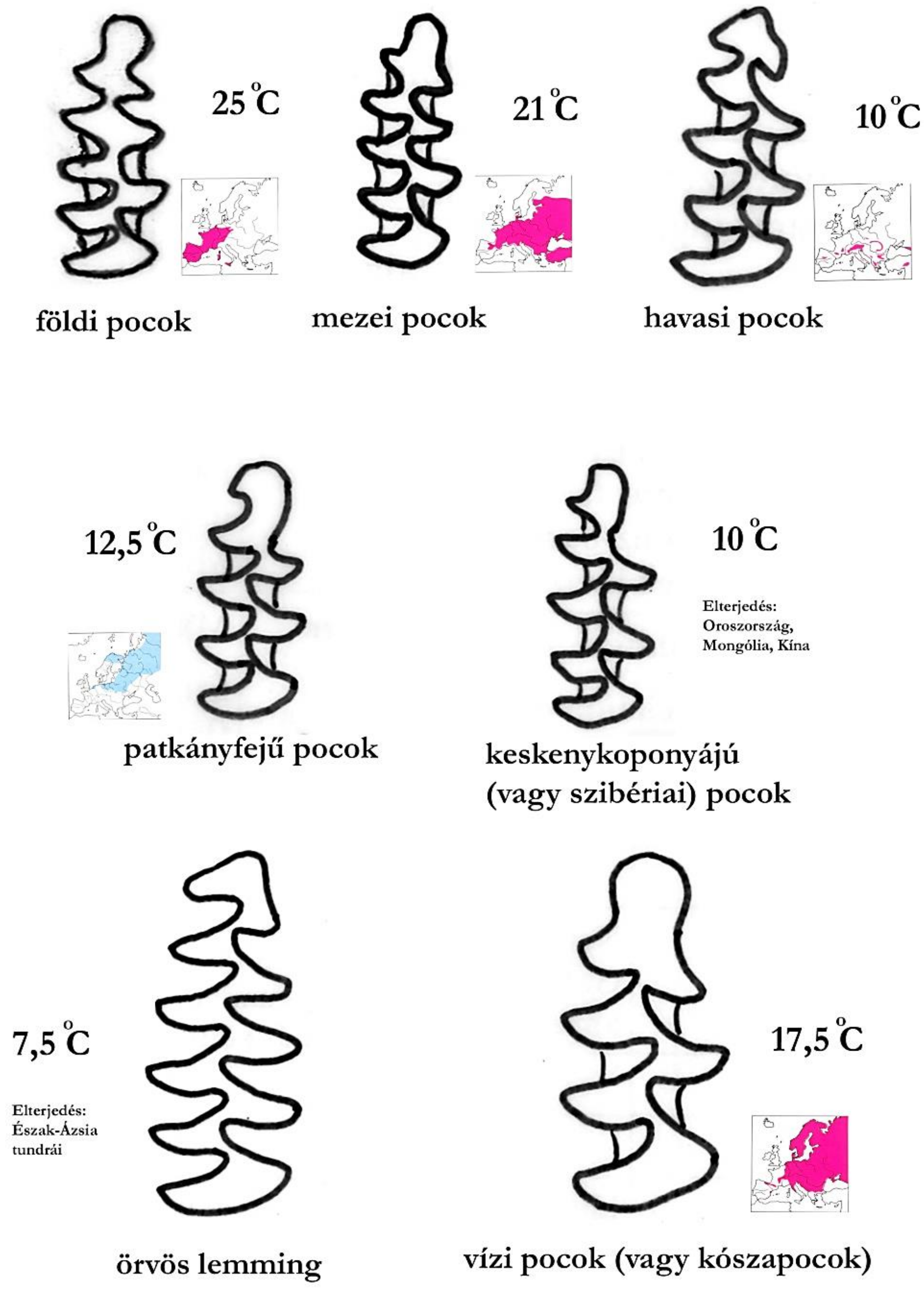

Mammoth-stratigraphy

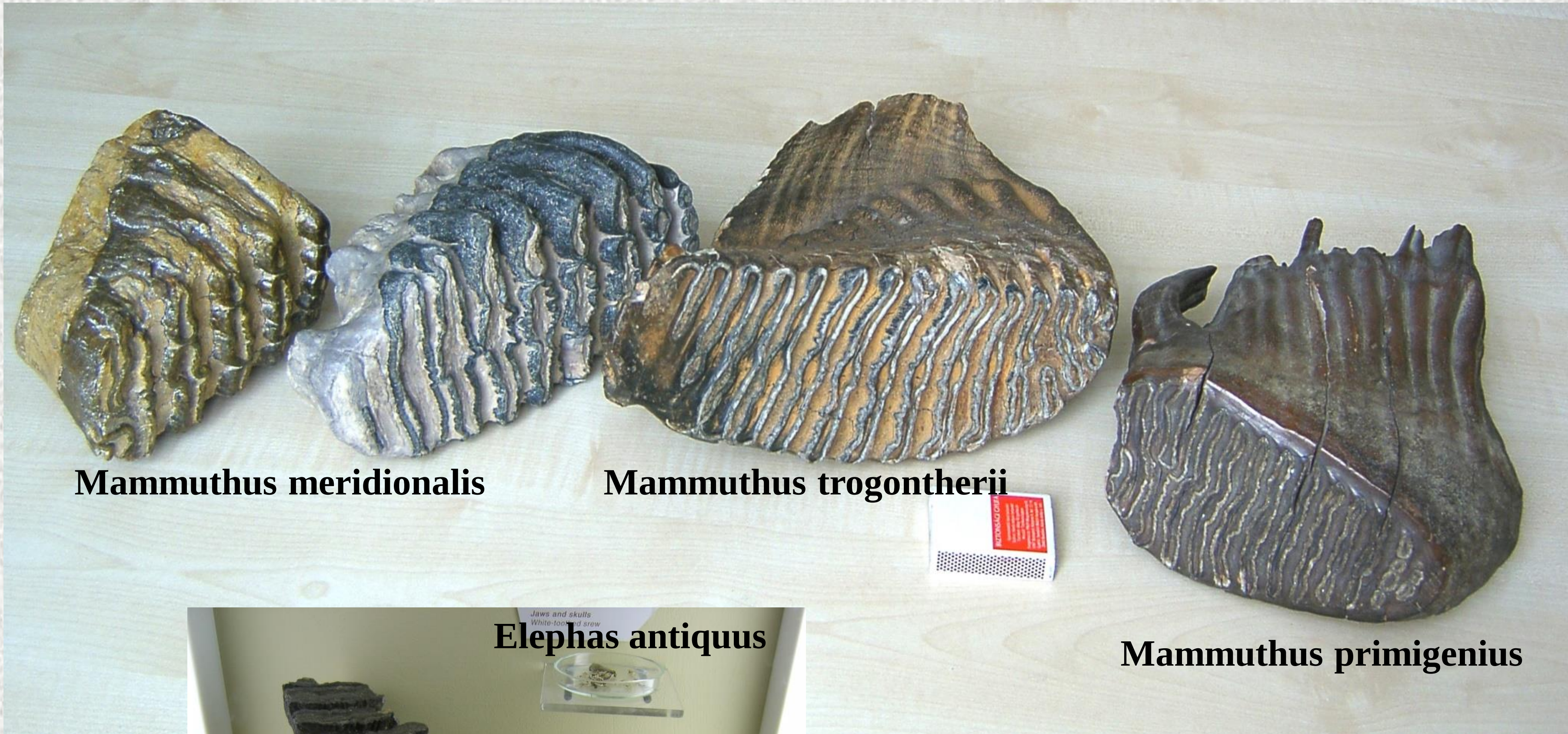

Distinction based on:

- Number of laminas
- Densitiy of laminas
- Thickness of enamel

DATING METHODS IN THE QUATERNARY STUDIES

RELATIVE DATING METHODS/RELATIVE STRATIGRAPHY

1. **Lithostratigraphy**
   - marker horizons:
     - tephrostratigraphy
     - buried soils (paleosols, fossil soils)
2. **Biostratigraphy**
   - Vertebrata fauna
   - Molluscs
     - -Malacothermometer
     - -$\delta^{18}O$ of molluscs shells
   - Marine microfauna
   - Pollen
   - Biomarkers
3. **Magnetostratigraphy**
4. **Magnetic susceptibility (MS)**
5. **Amino Acid Racemisation (AAR)**
6. **Stable isotopes**
   - $\delta^{18}O$ ($^{16}O/^{18}O$)
     - (Milankovich theory)
   - $\delta^{13}C$ ($^{12}C/^{13}C$)
7. **Ice cores from the icesheets**
8. **Geomorphological horizons**
   - terraces: fluvial marine
   - correlative sediments

Most common snails in the loess-paleosol sequences of the Carpathian Basin

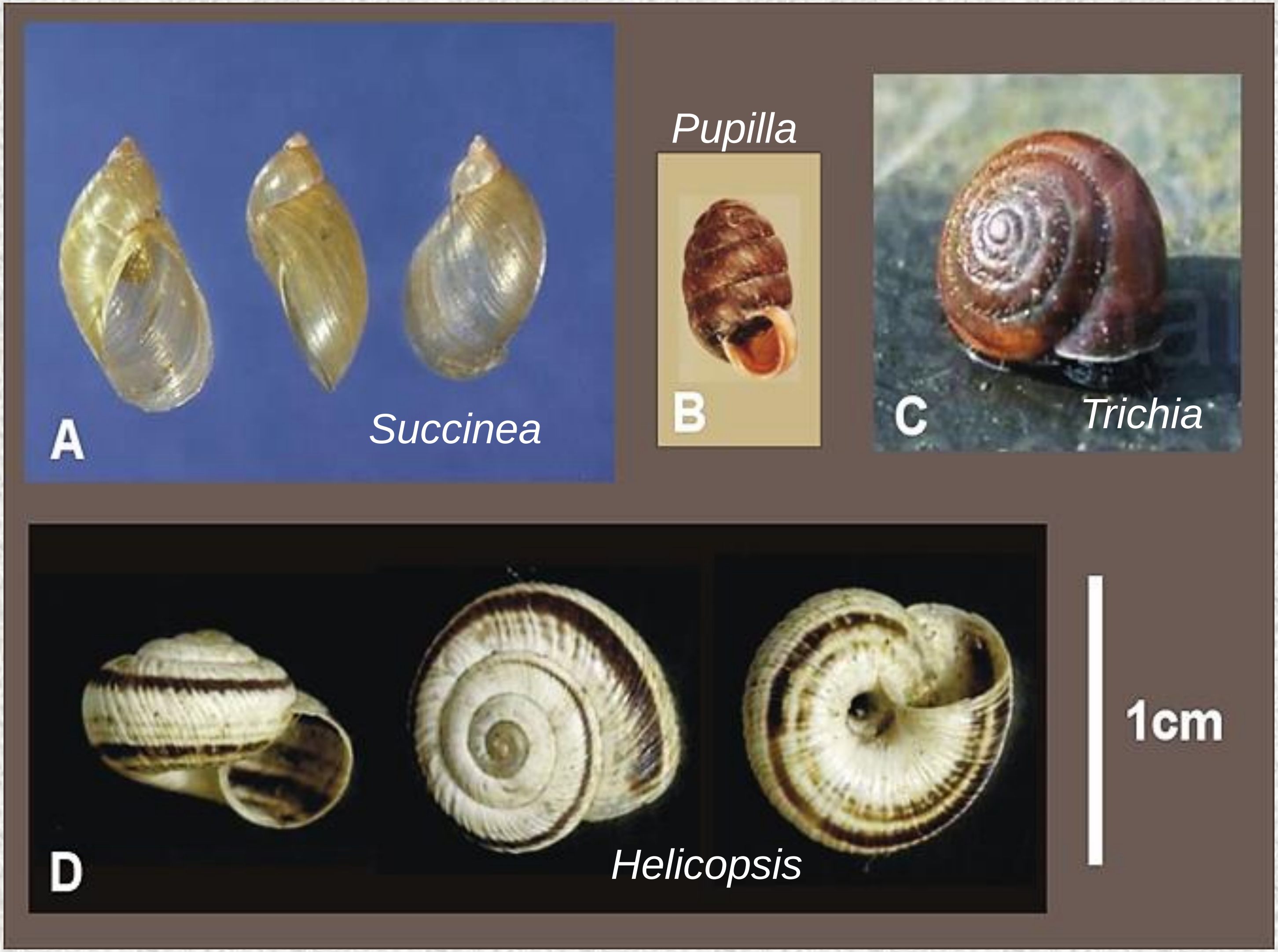

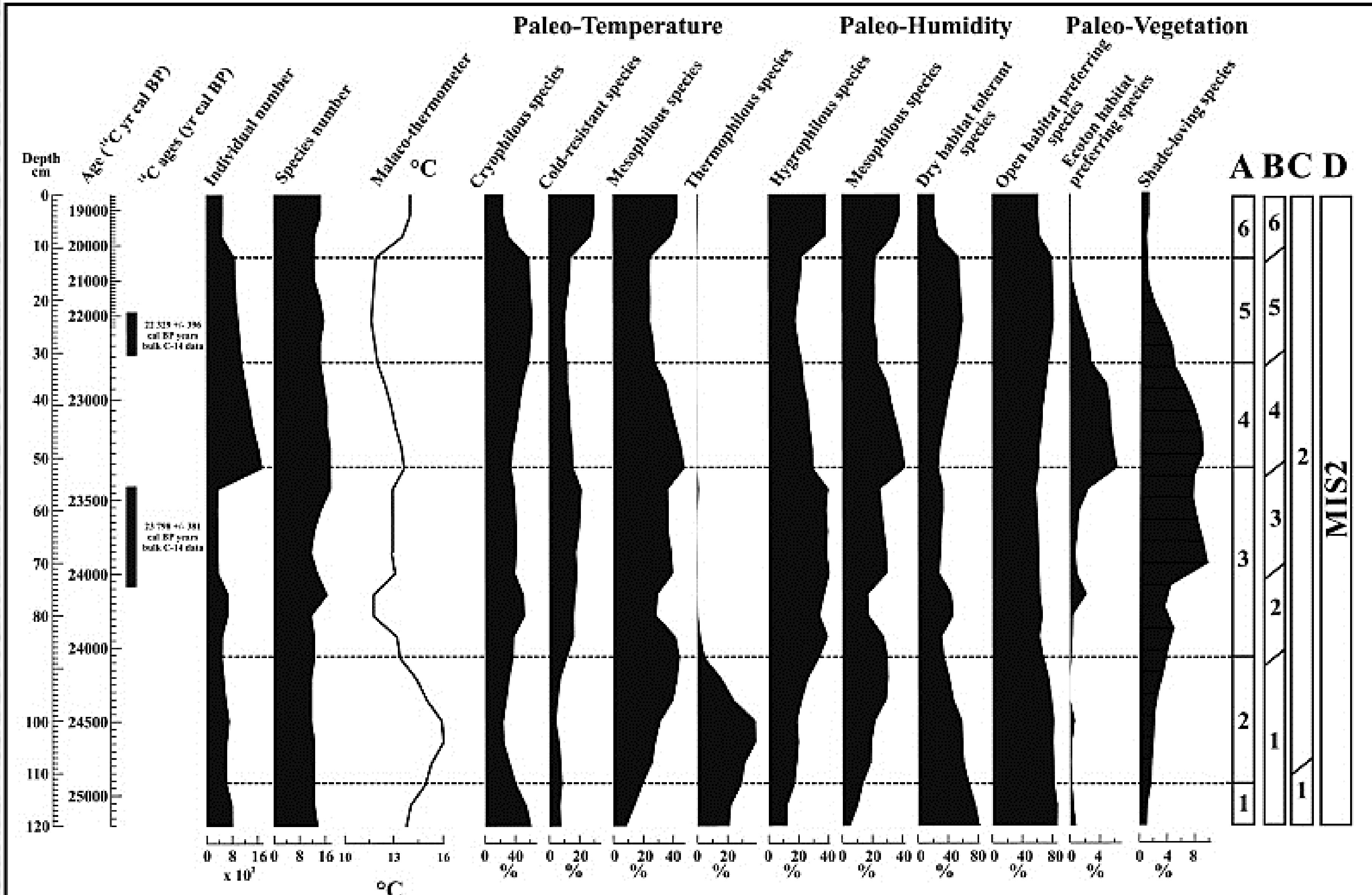

Bösken et al. 2017.

Malacothermometer

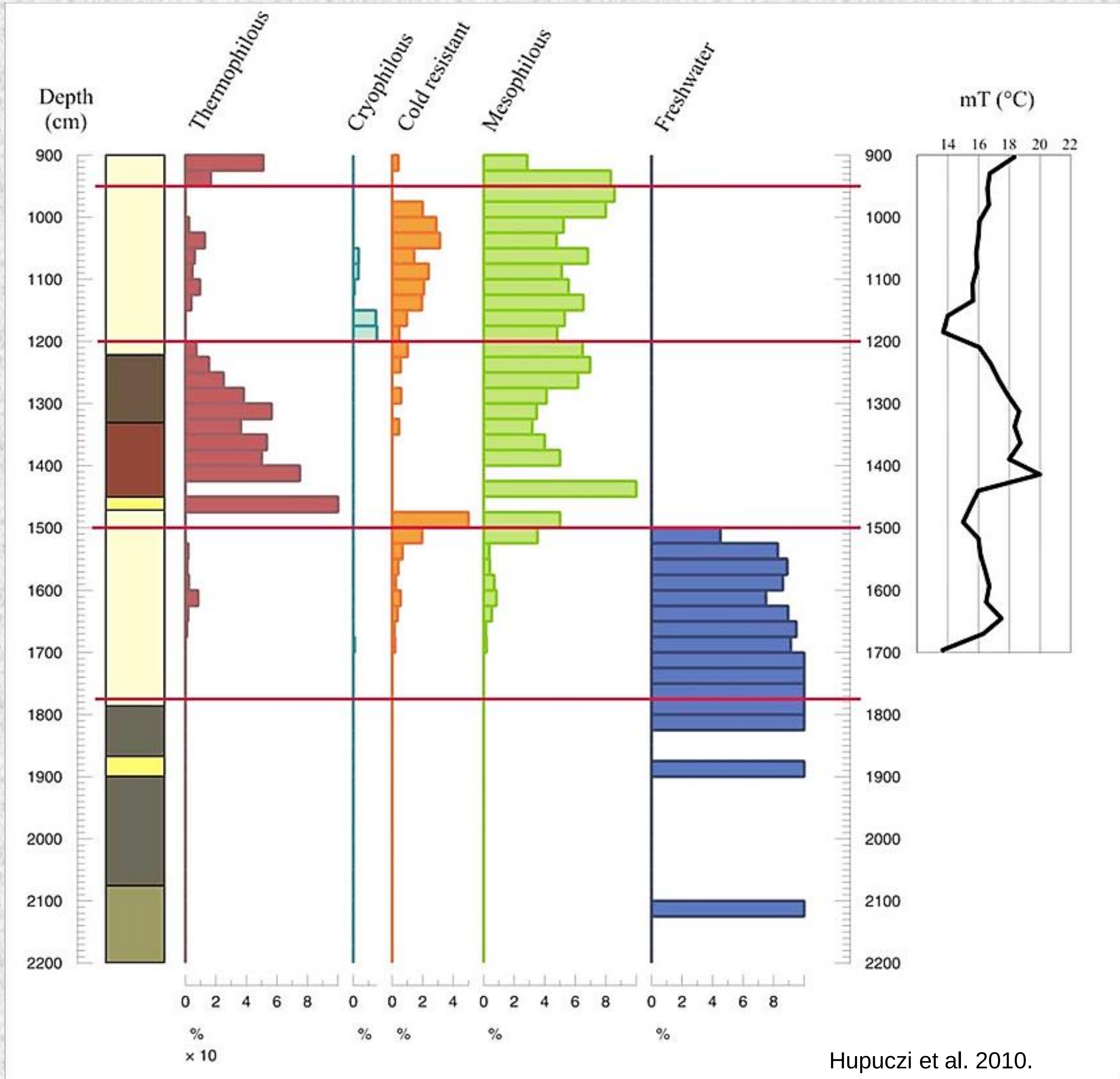

Hupuczi et al. 2010.

DATING METHODS IN THE QUATERNARY STUDIES

RELATIVE DATING METHODS/RELATIVE STRATIGRAPHY

1. **Lithostratigraphy**
   marker horizons:
      tephrostratigraphy
      buried soils (paleosols, fossil soils)
2. **Biostratigraphy**
   - Vertebrata
   - Molluscs
      -Malacothermometer
      -$\delta^{18}O$ of molluscs shells
   - Marine microfauna
   - Pollen
   - Biomarkers
3. **Magnetostratigraphy**
4. **Magnetic susceptibility (MS)**
5. **Amino Acid Racemisation (AAR)**
6. **Stable isotopes**
   - $\delta^{18}O$ ($^{16}O/^{18}O$)
      (Milankovich theory)
   - $\delta^{13}C$ ($^{12}C/^{13}C$)
7. **Ice cores from the icesheets**
8. **Geomorphological horizons**
   - terraces: fluvial marine
   - correlative sediments

Marine microfauna

Foraminiferans

https://paleonerdish.wordpress.com/2013/06/17/an-introduction-to-foraminifera/

DATING METHODS IN THE QUATERNARY STUDIES

RELATIVE DATING METHODS/RELATIVE STRATIGRAPHY

1. **Lithostratigraphy**
    - marker horizons:
        - tephrostratigraphy
        - buried soils (paleosols, fossil soils)
2. **Biostratigraphy**
    - Vertebrata
    - Molluscs
        - -Malacothermometer
        - -$\delta^{18}O$ of molluscs shells
    - Marine microfauna
    - Pollen
    - Biomarkers
3. **Magnetostratigraphy**
4. **Magnetic susceptibility (MS)**
5. **Amino Acid Racemisation (AAR)**
6. **Stable isotopes**
    - $\delta^{18}O$ ($^{16}O/^{18}O$)
        - (Milankovich theory)
    - $\delta^{13}C$ ($^{12}C/^{13}C$)
7. **Ice cores from the icesheets**
8. **Geomorphological horizons**
    - terraces: fluvial marine
    - correlative sediments

Pollens

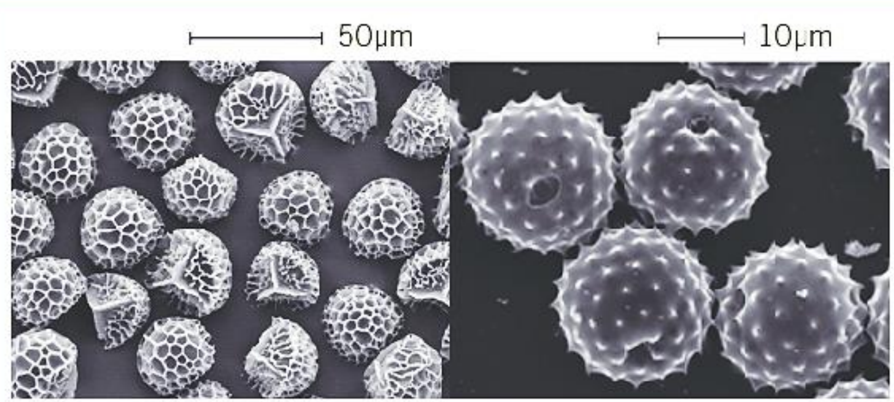

Source: Sporomex

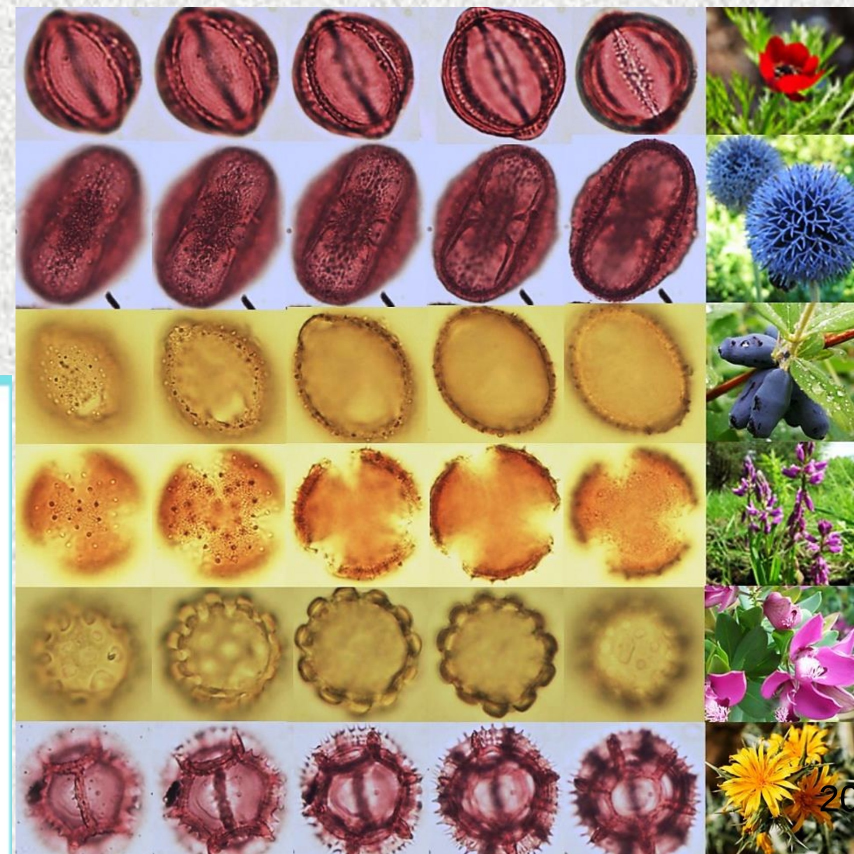

Pollen diagrams

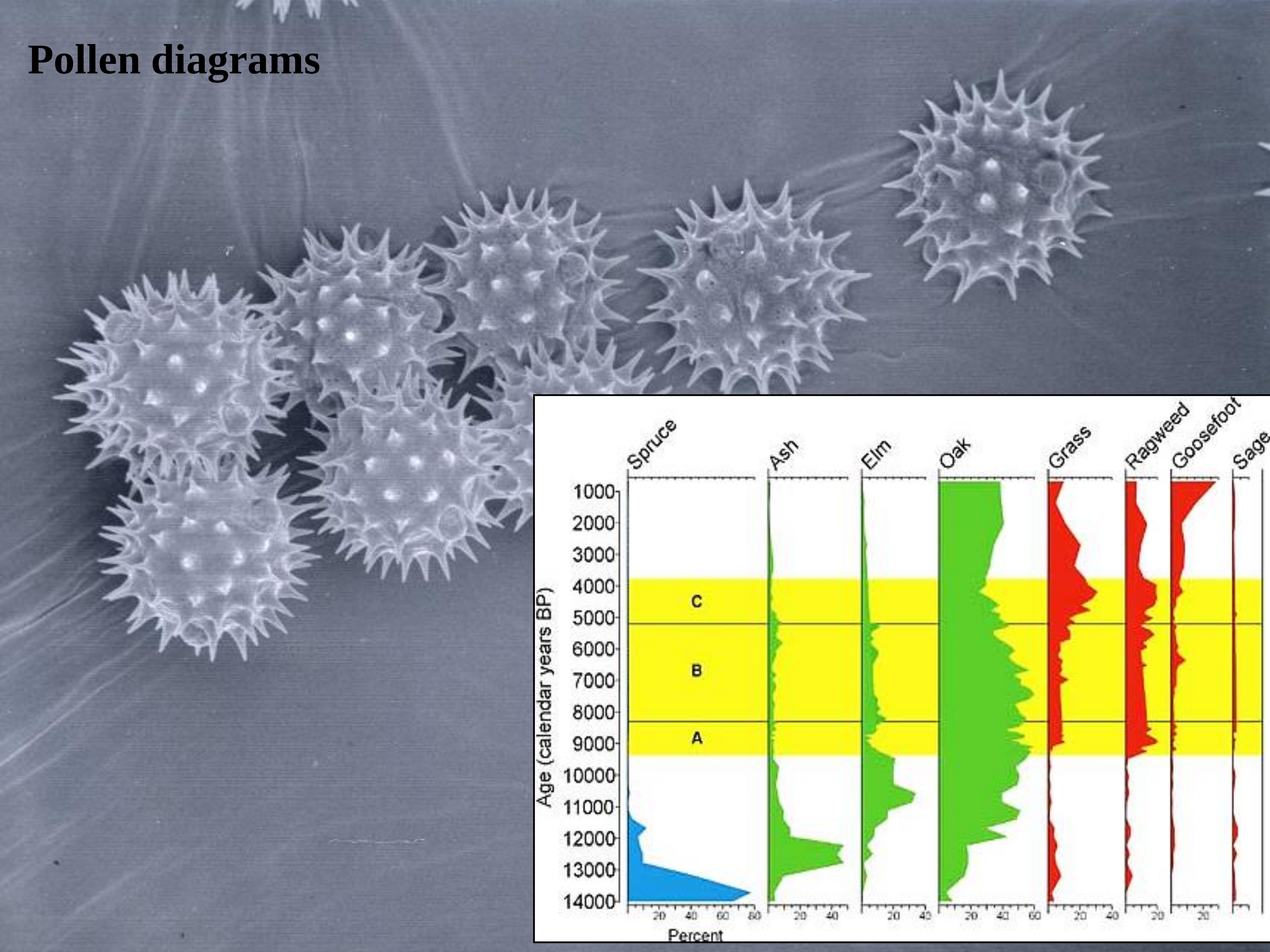

DATING METHODS IN THE QUATERNARY STUDIES

RELATIVE DATING METHODS/RELATIVE STRATIGRAPHY

1. **Lithostratigraphy**
   - marker horizons:
     - tephrostratigraphy
     - buried soils (paleosols, fossil soils)
2. **Biostratigraphy**
   - Vertebrata
   - Molluscs
     - -Malacothermometer
     - -$\delta^{18}O$ of molluscs shells
   - Marine microfauna
   - Pollen
   - Biomarkers
3. **Magnetostratigraphy**
4. **Magnetic susceptibility (MS)**
5. **Amino Acid Racemisation (AAR)**
6. **Stable isotopes**
   - $\delta^{18}O$ ($^{16}O/^{18}O$)
     - (Milankovich theory)
   - $\delta^{13}C$ ($^{12}C/^{13}C$)
7. **Ice cores from the icesheets**
8. **Geomorphological horizons**
   - terraces: fluvial marine
   - correlative sediments

Biomarkers

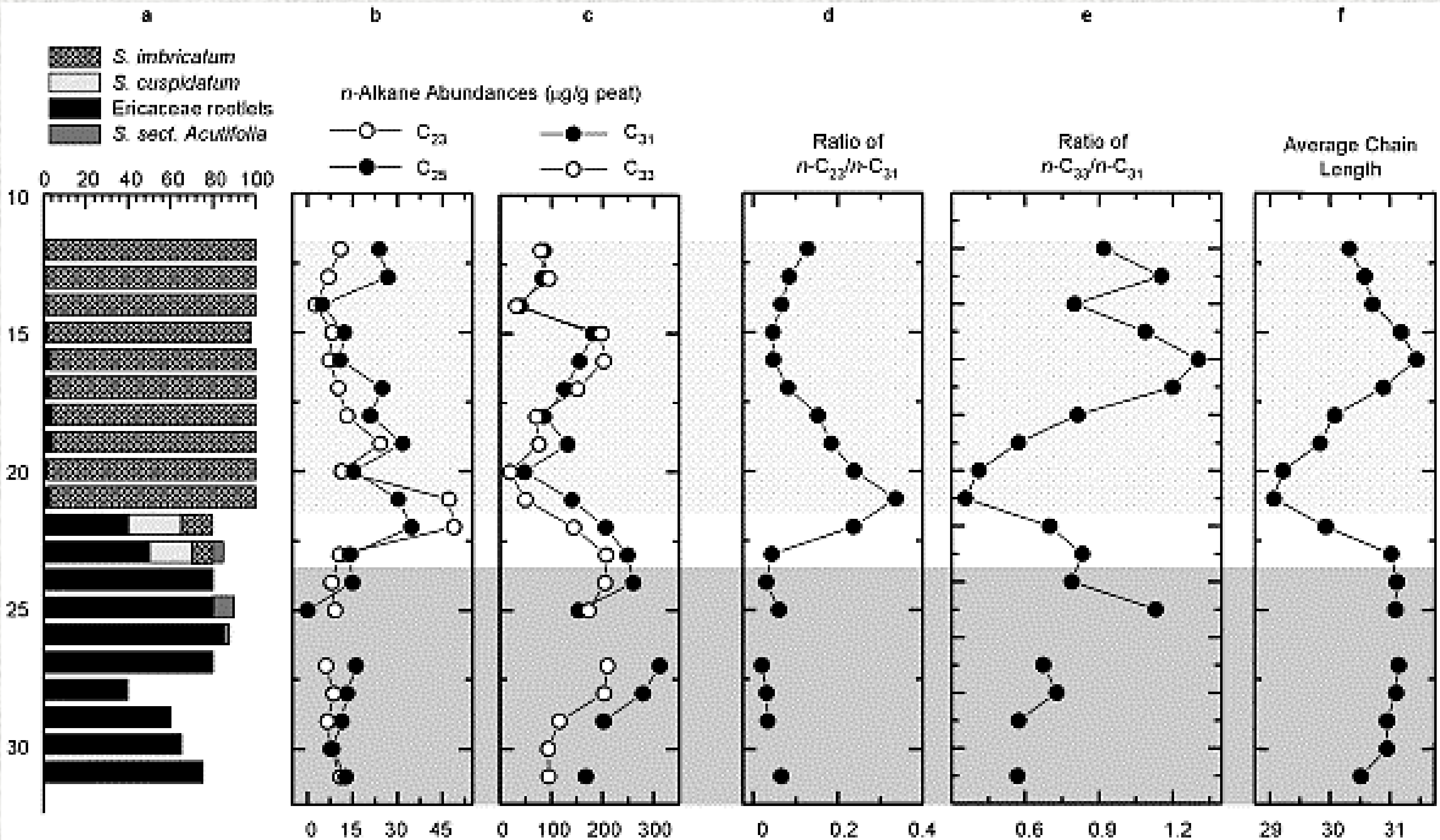

a
b
c
d
e
f
S. imbricatum
S. cuspidatum
Ericaceae rootlets
S. sect. Acutifolia
n-Alkane Abundances (µg/g peat)
C23
C25
C31
C33
Ratio of
n-C23/n-C31
Ratio of
n-C33/n-C31
Average Chain
Length
0 20 40 60 80 100
10
15
20
25
30
0 15 30 45
0 100 200 300
0 0.2 0.4
0.6 0.9 1.2
29 30 31

DATING METHODS IN THE QUATERNARY STUDIES

RELATIVE DATING METHODS/RELATIVE STRATIGRAPHY

1. **Lithostratigraphy**
   - marker horizons:
     - tephrostratigraphy
     - buried soils (paleosols, fossil soils)
2. **Biostratigraphy**
   - Vertebrata
   - Molluscs
     - -Malacothermometer
     - -$\delta^{18}O$ of molluscs shells
   - Marine microfauna
   - Pollen
   - Biomarkers
3. **Magnetostratigraphy**
4. **Magnetic susceptibility (MS)**
5. **Amino Acid Racemisation (AAR)**
6. **Stable isotopes**
   - $\delta^{18}O$ ($^{16}O/^{18}O$)
     - (Milankovich theory)
   - $\delta^{13}C$ ($^{12}C/^{13}C$)
7. **Ice cores from the icesheets**
8. **Geomorphological horizons**
   - terraces: fluvial marine
   - correlative sediments

3.1 Introduction

3. Magnetostratigraphy

Origin of the Earth's geomagnetic field

The geomagnetic field is generated in some poorly understood way by the motion of highly conducting nickel-iron (Ni-Fe) fluids in the outer part of Earth' core; this motion is assumed to be controlled by thermal convection and by the Coriolis force generated by Earth's rotation, constituting what is called a **self-exciting dynamo**.

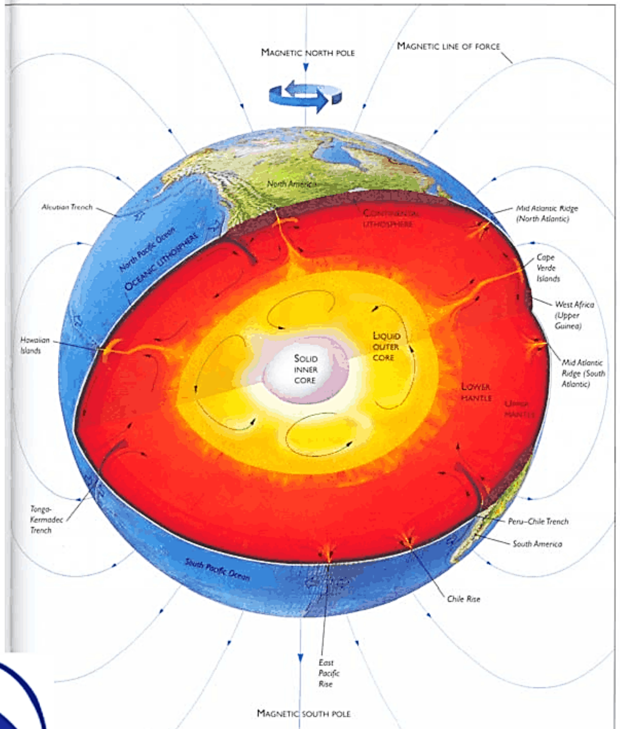

Lamb & Sington (1998)

The Earth's magnetic field

When Earth's magnetic field has the present orientation, it is said to have **normal polarity**. When this orientation changes 180°, it has **reversed polarity**. Studies of the remanent magnetism in igneous and sedimentary rocks show that the dipole (main) component of Earth's magnetic field has reversed its polarity at irregular intervals from Precambrian time onward, apparently owing to instabilities in outer-core convection.

Reversals of Earth's magnetic field are recorded in sediments and igneous rocks by patterns of normal and reversed remanent magnetism. These geomagnetic reversals are contemporaneous worldwide phenomena. Thus, they provide unique stratigraphic markers in igneous and sedimentary rocks. The reversal process is thought to take place over a period of 1,000 – 10,000 years.

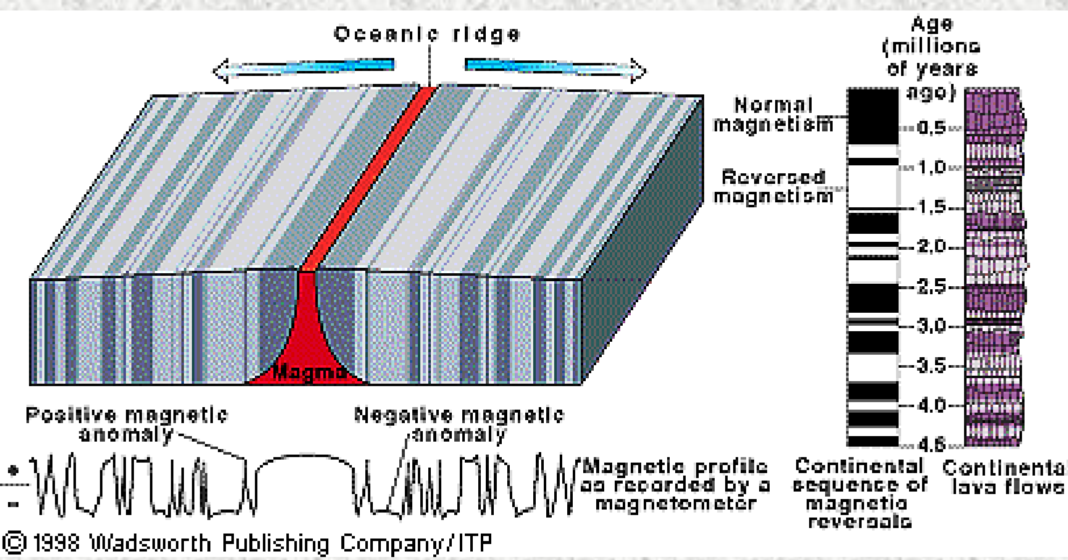

https://www.quora.com/Is-there-any-evidence-of-the-earth-ever-going-thru-a-magnetic-polar-shift

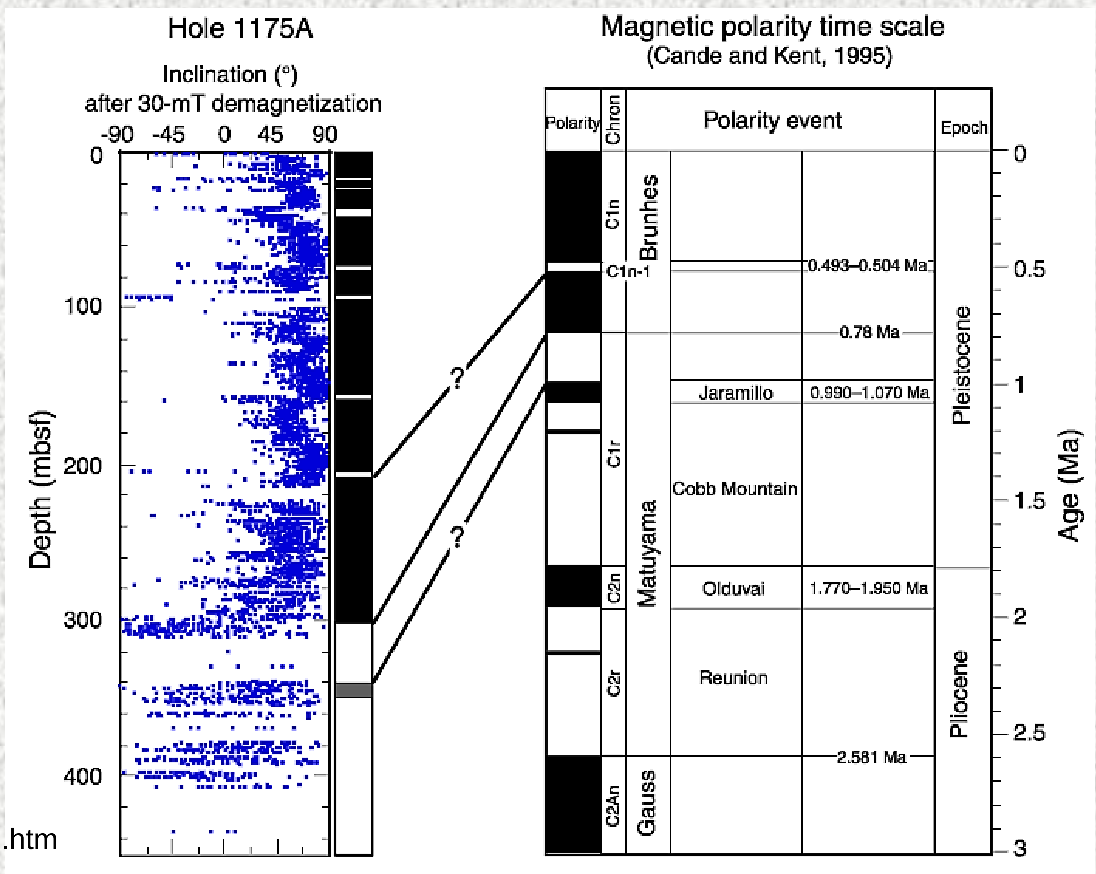

http://www-odp.tamu.edu/publications/190_IR/chap_06/c6_f16.htm

Magnetic susceptibility (MS)

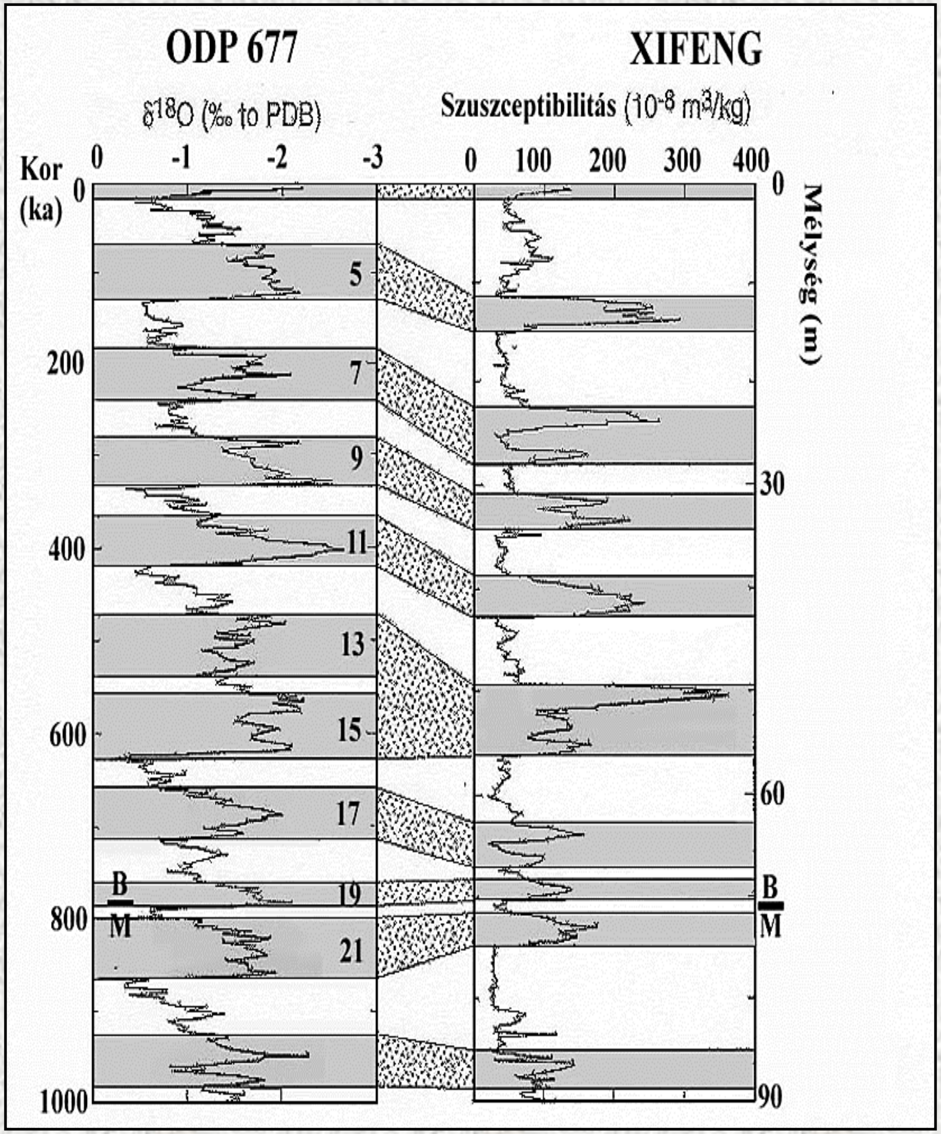

Magnetic susceptibility:

$$\mathbf{M} = \mu_0 \kappa \mathbf{H}$$

M-*magnetization, (magnetic dipole moment per unit volume)*; **H**-*magnetic field strength*; μ_0-*magnetic permeability*; κ-*Magnetic susceptibility , MS.*

Magnetic susceptibility is a dimensionless proportionality constant that indicates the degree of magnetization of a material in response to an applied magnetic field.

If the magnetic susceptibility is greater than zero, the substance is said to be "paramagnetic"; the magnetization of the substance is higher than that of empty space. If the magnetic susceptibility is less than zero, the substance is "diamagnetic"; it tends to exclude a magnetic field from its interior.
Mathematically it is the ratio of magnetization ***M*** (magnetic moment per unit volume) to the applied magnetizing field intensity ***H.***

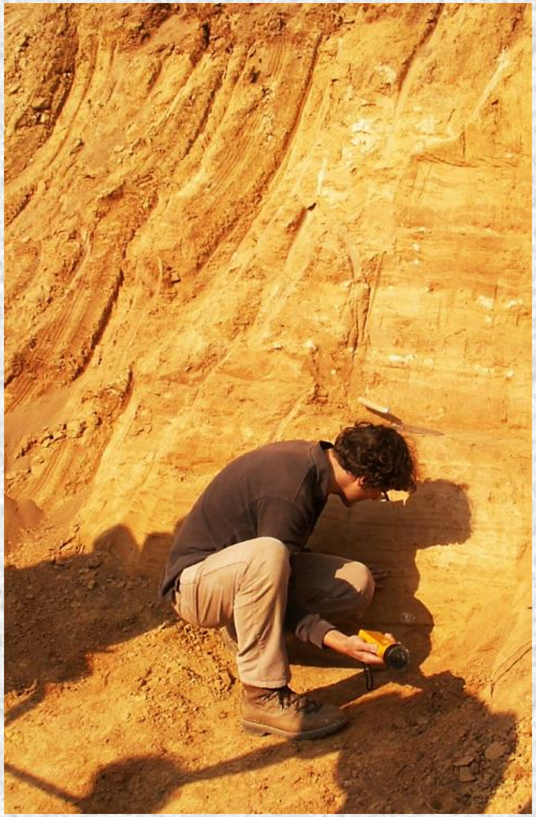

Forming and influencing factors of magnetization

•**Ferromagnetic minerals:** magnetite (Fe_3O_4), maghemite (γ-Fe_2O_3), hematite (Fe_2O_3) and goethite (α-FeO(OH));
•**Paramagnetic minerals:** clay minerals containing Fe^{2+}, Fe^{3+}, Mn^{2+} ions, carbonates (siderite, rhodochrosite).

paleosol ↔ loess: 2-3-fold difference!

„Dilution hypothesis" ***(Kukla, G. et al. 1988):***
Continuous sedimentation of the magnetic minerals (dust) on global scale (more or less independently from climate changes)
On local scale simultaneous sedimentation of coarser silt fraction from adjacent areas (the main volume of the loess), dilution of magnetic minerals.

„Soilformation hypothesis" ***(Heller, F. és Liu, T. S. 1986):*** formation of magnetic minerals due to soil forming processes.

Magnetic susceptibility in loess-paleosol series

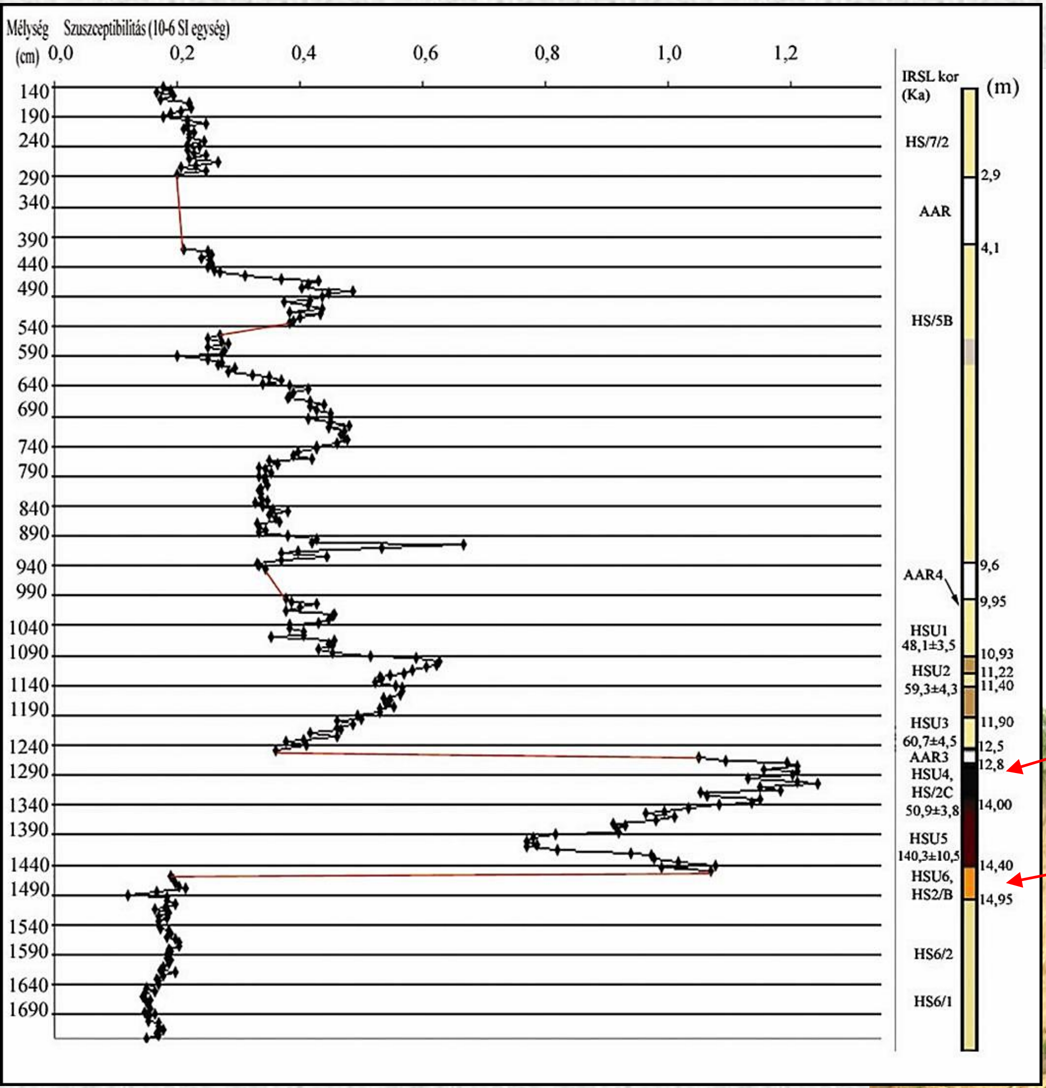

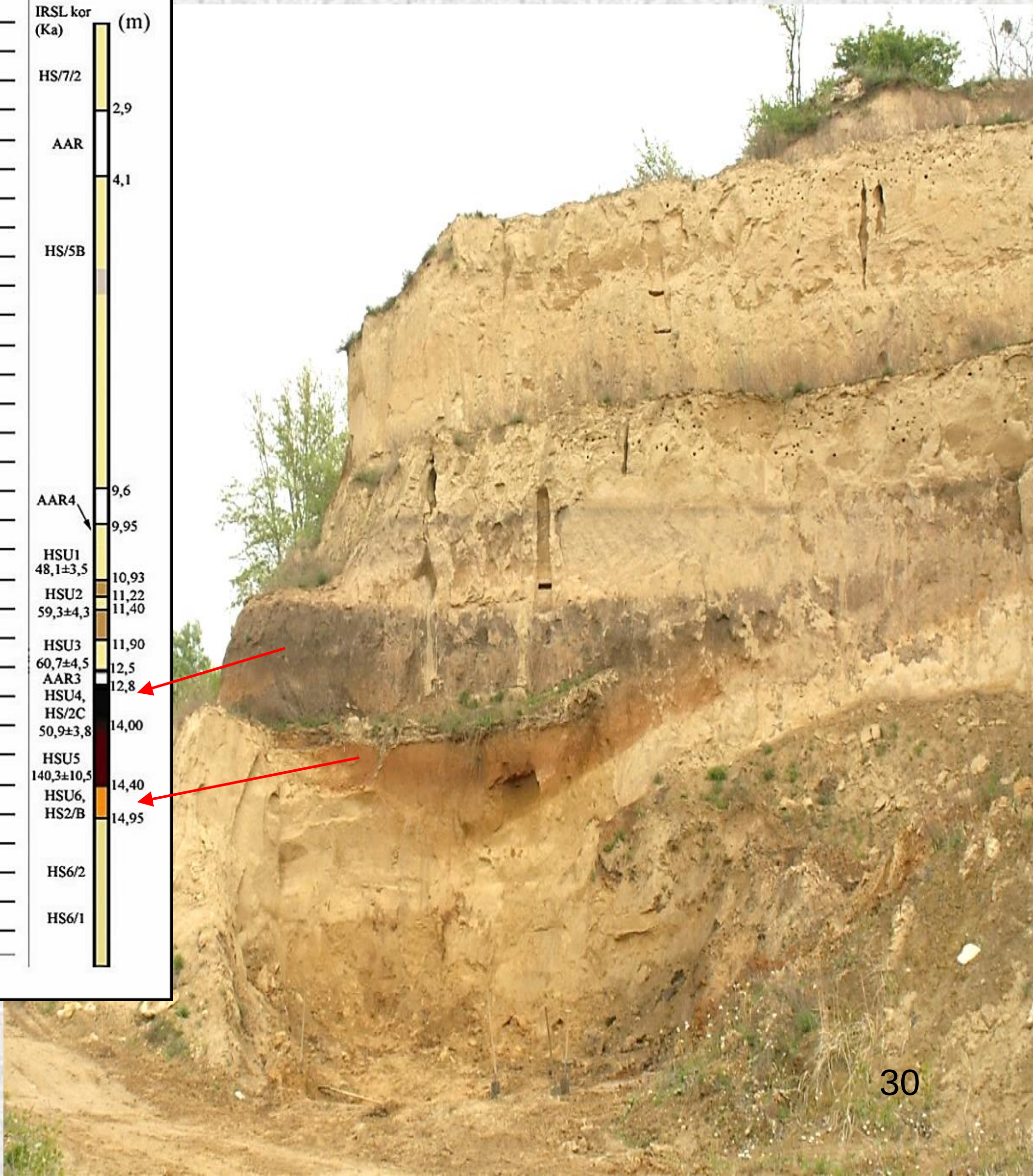

Discovery of tephra layers with MS investigations

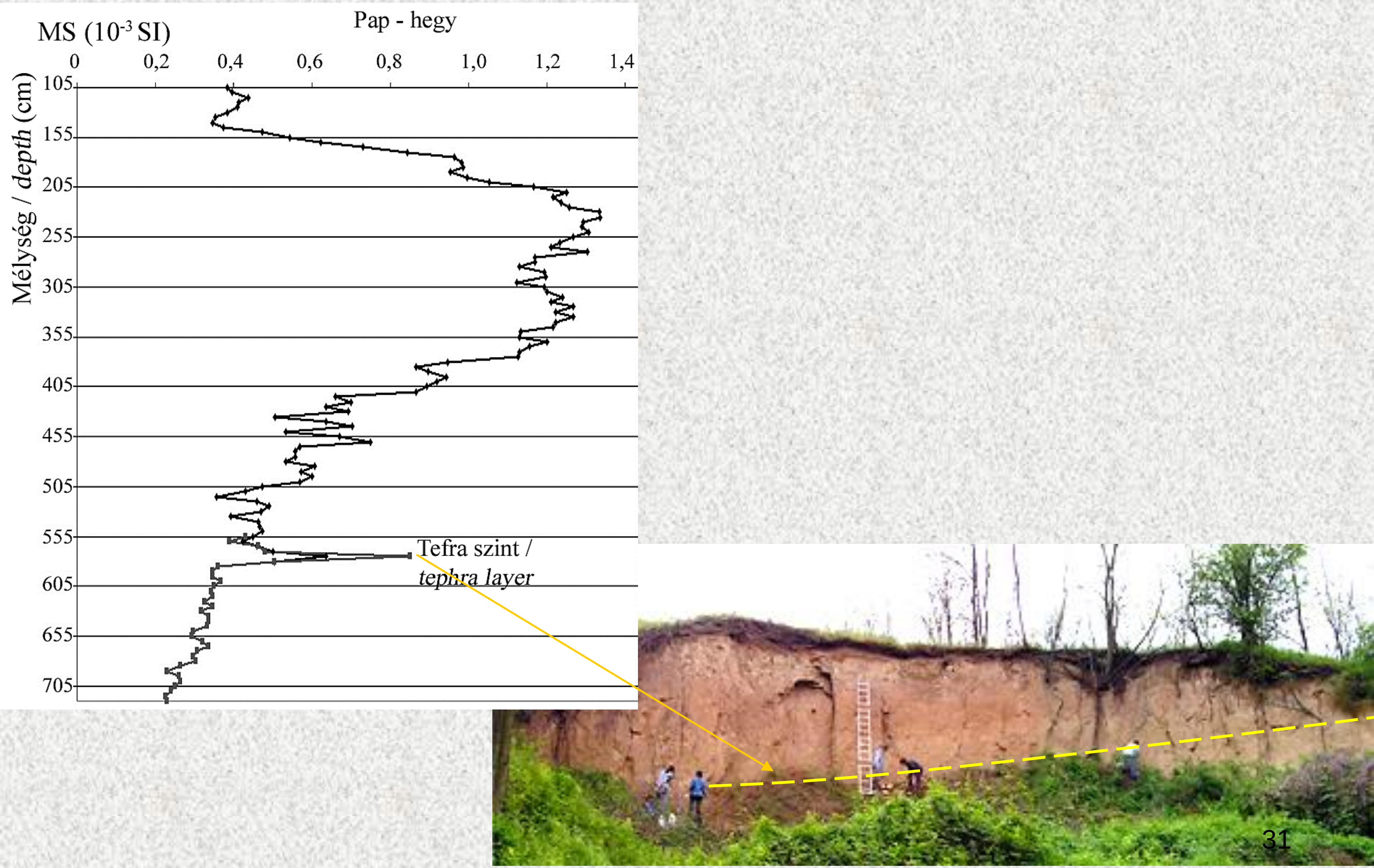

Correlation of MS curves

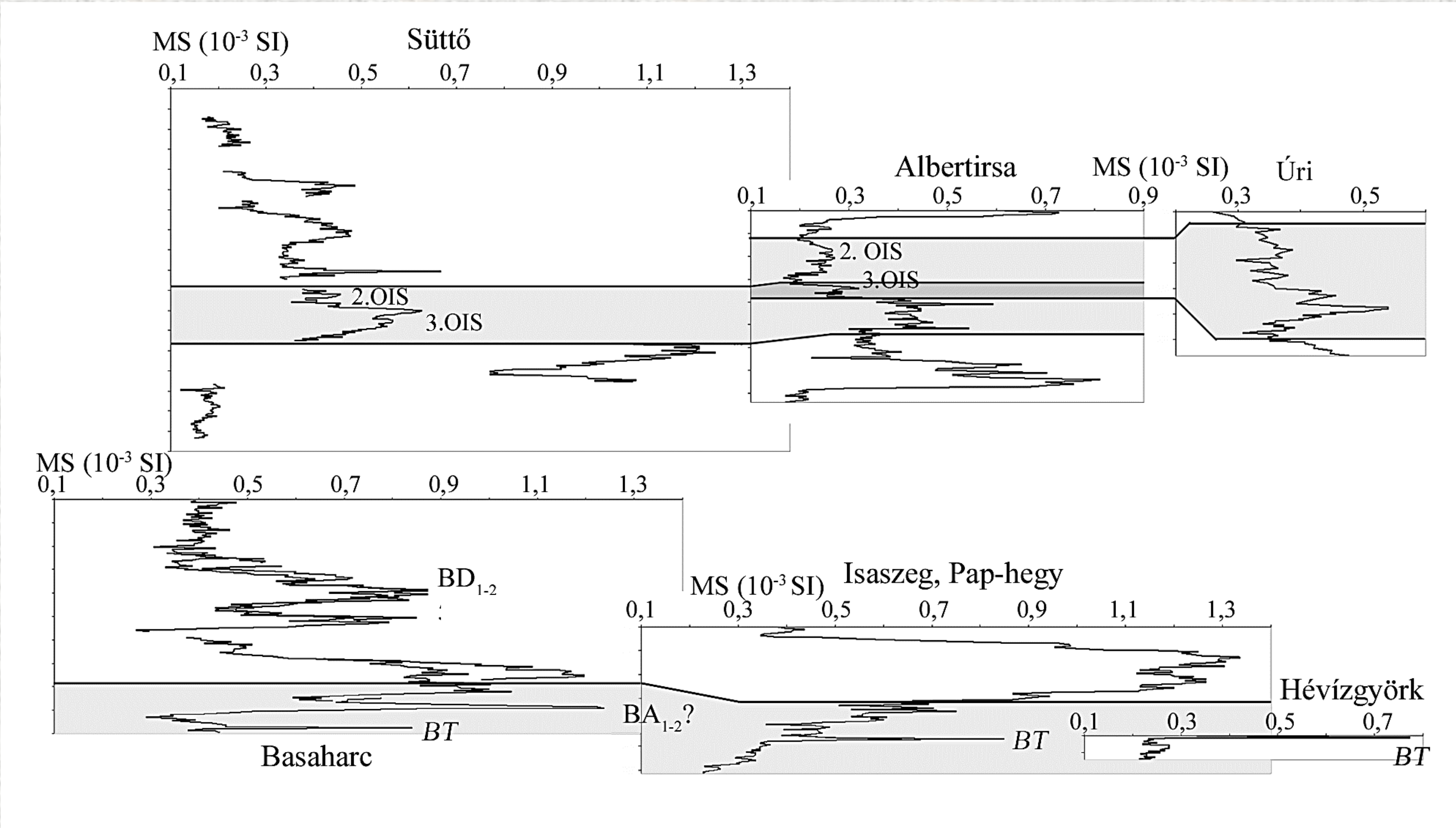

DATING METHODS IN THE QUATERNARY STUDIES

RELATIVE DATING METHODS/RELATIVE STRATIGRAPHY

1. **Lithostratigraphy**
   - marker horizons:
     - tephrostratigraphy
     - buried soils (paleosols, fossil soils)
2. **Biostratigraphy**
   - Vertebrata fauna
   - Molluscs
     - -Malacothermometer
     - -$\delta^{18}O$ of molluscs shells
   - Marine microfauna
   - Pollen
   - Biomarkers
3. **Magnetostratigraphy**
4. **Magnetic susceptibility (MS)**
5. **Amino Acid Racemisation (AAR)**
6. **Stable isotopes**
   - $\delta^{18}O$ ($^{16}O/^{18}O$)
     - (Milankovich theory)
   - $\delta^{13}C$ ($^{12}C/^{13}C$)
7. **Ice cores from the icesheets**
8. **Geomorphological horizons**
   - terraces: fluvial marine
   - correlative sediments

Amino Acid geochronology

Leucozonella cf. rufispira (Martens 1874)

Amino Acid geochronology

- relative age
- stratigraphical correlation

with calibration and/or the kinethic modell of racemization:

- numerical age estimation
- paleotemperature

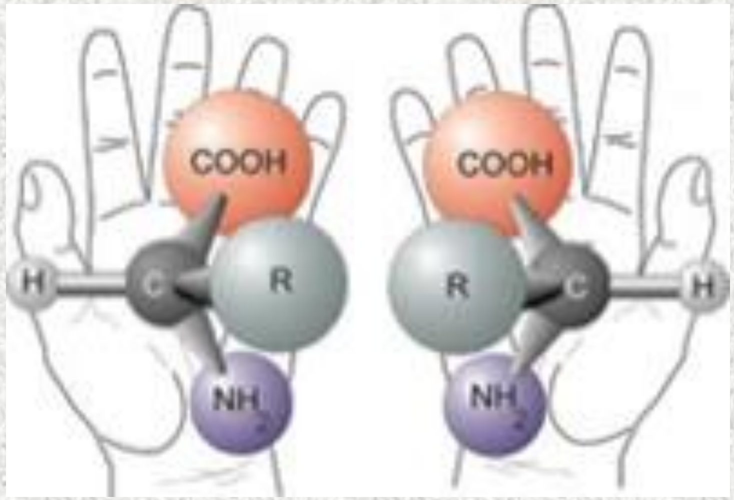

L-amino acid (living) ↔ D-amino acid (dead)

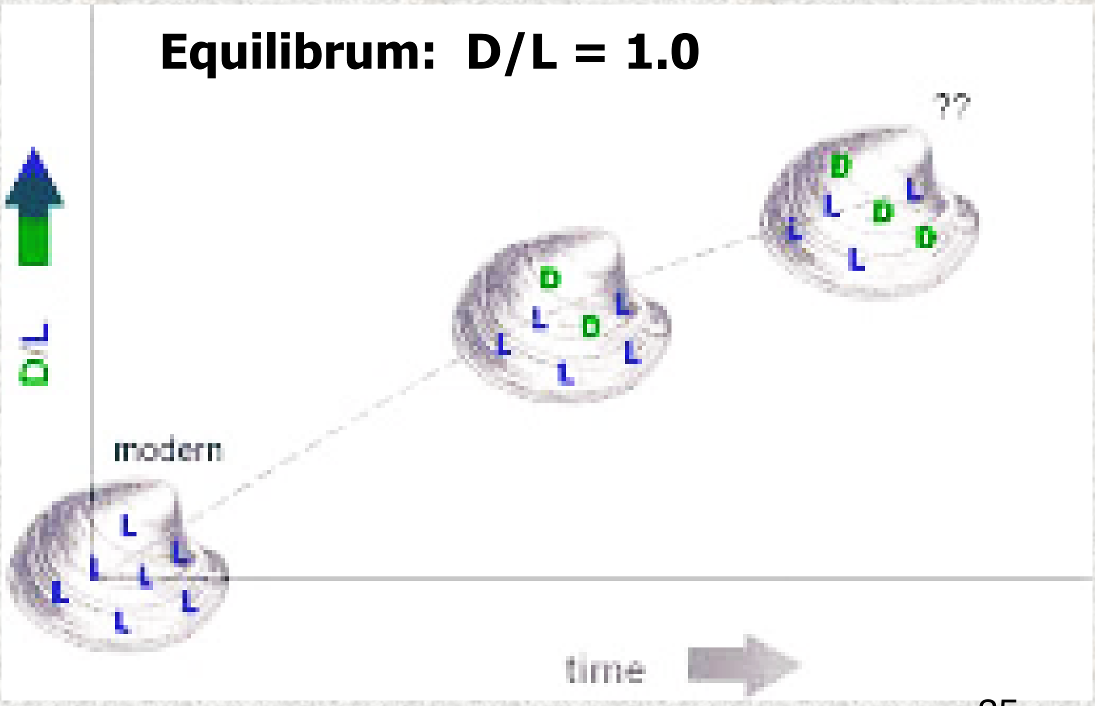

Influencing environmental factors of amino acid racemization

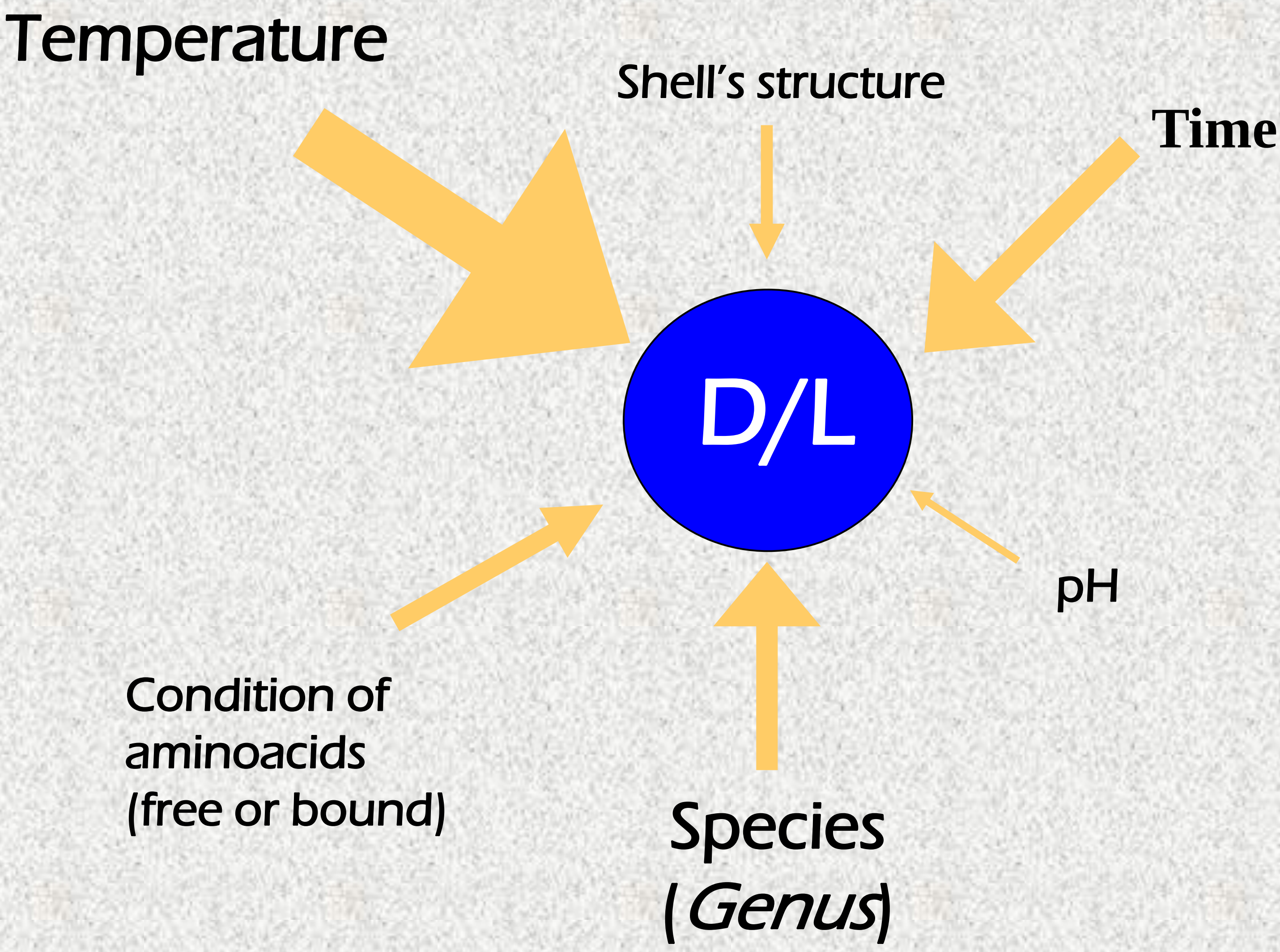

European loess-snails used in AAR studies

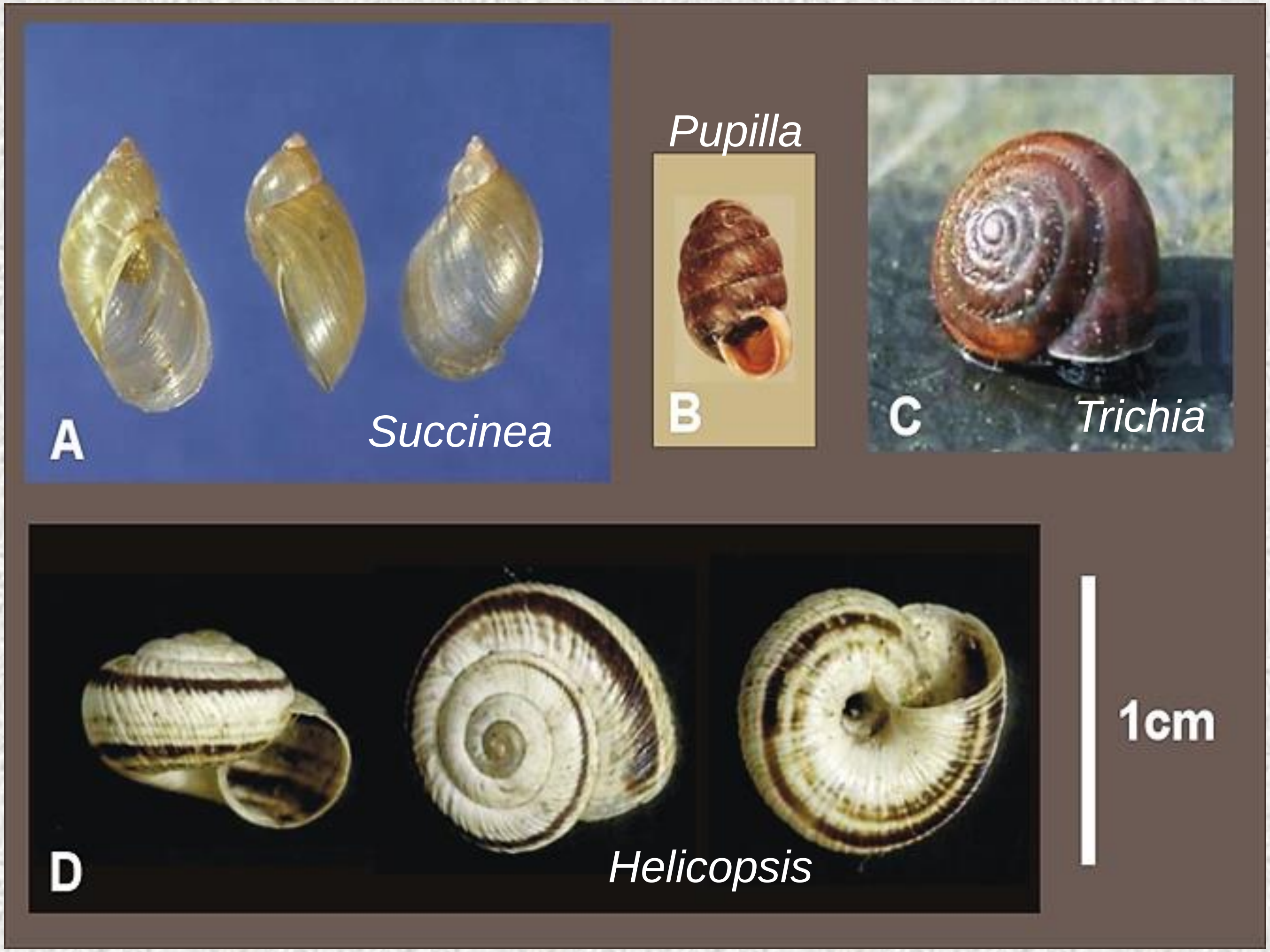

DATING METHODS IN THE QUATERNARY STUDIES

RELATIVE DATING METHODS/RELATIVE STRATIGRAPHY

1. **Lithostratigraphy**
   marker horizons:
      tephrostratigraphy
      buried soils (paleosols, fossil soils)
2. **Biostratigraphy**
   - Vertebrata
   - Molluscs
      -Malacothermometer
      -$\delta^{18}O$ of molluscs shells
   - Marine microfauna
   - Pollen
   - Biomarkers
3. **Magnetostratigraphy**
4. **Magnetic susceptibility (MS)**
5. **Amino Acid Racemisation (AAR)**
6. **Stable isotopes**
   - $\delta^{18}O$ ($^{16}O/^{18}O$)
      (Milankovich theory)
   - $\delta^{13}C$ ($^{12}C/^{13}C$)
7. **Ice cores from the icesheets**
8. **Geomorphological horizons**
   - terraces: fluvial marine
   - correlative sediments

Isotopes

- **Isotopes** are distinct nuclear species (or *nuclides*, as technical term) of the same element. They have the same atomic number (number of protons in their nuclei) and position in the periodic table (and hence belong to the same chemical element), but differ in nucleon numbers (mass numbers) due to different numbers of neutrons in their nuclei.
  - For example, carbon-12, carbon-13, and carbon-14 are three isotopes of the element carbon with mass numbers 12, 13, and 14, respectively. The atomic number of carbon is 6, which means that every carbon atom has 6 protons so that the neutron numbers of these isotopes are 6, 7, and 8 respectively.
  - A nuclide is a species of an atom with a specific number of protons and neutrons in the nucleus, for example carbon-13 with 6 protons and 7 neutrons. The *nuclide* concept (referring to individual nuclear species) emphasizes nuclear properties over chemical properties, whereas the *isotope* concept (grouping all atoms of each element) emphasizes chemical over nuclear.

- **Stable isotopes**
  - Their amount is constant in the earth's system
  - Their ratio variable in the subsystems – isotope fractionation (=the lighter isotope participate more likely in chemical, physical, biological processes than the heavier isotope of the same element)

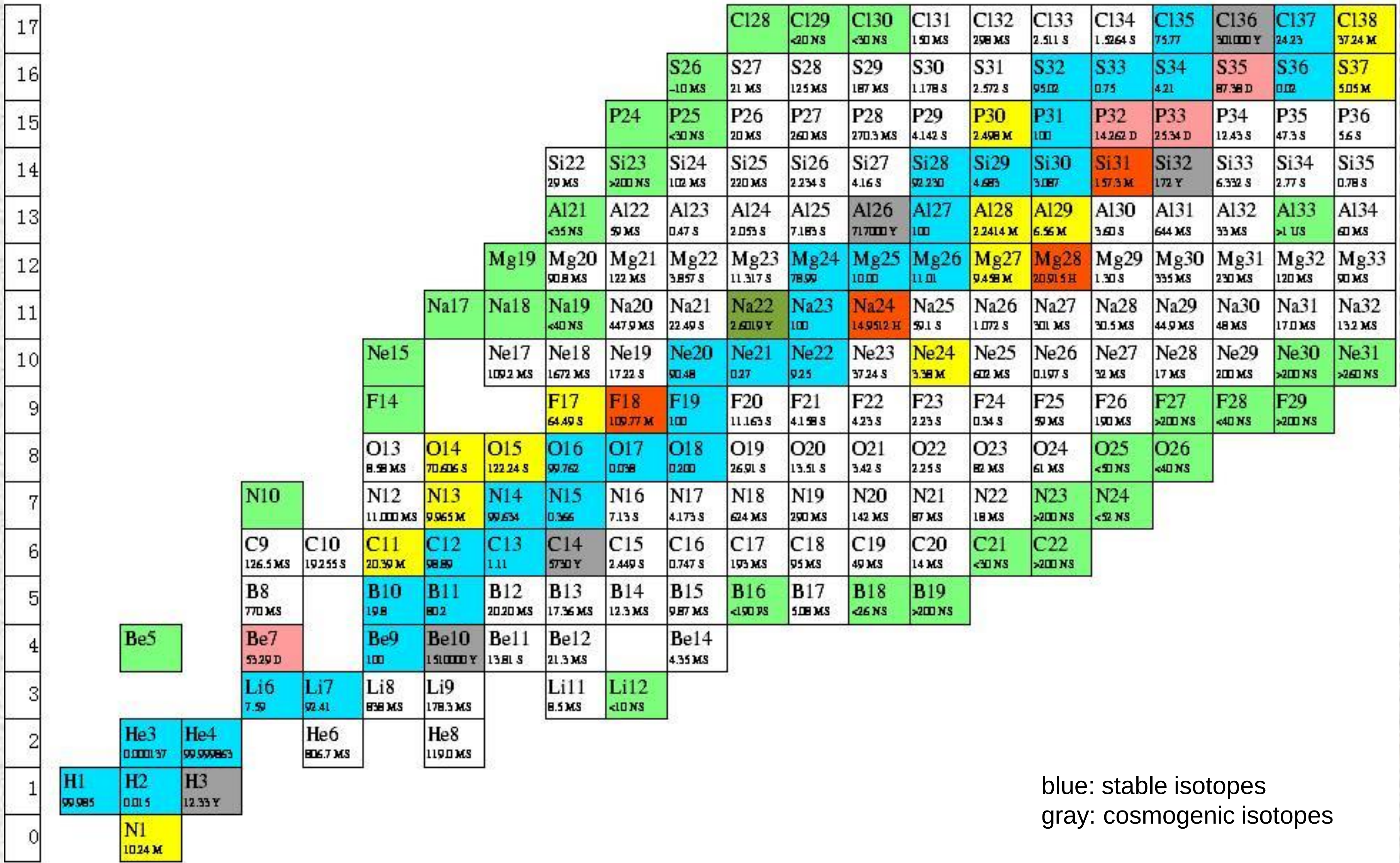

Stable isotopes

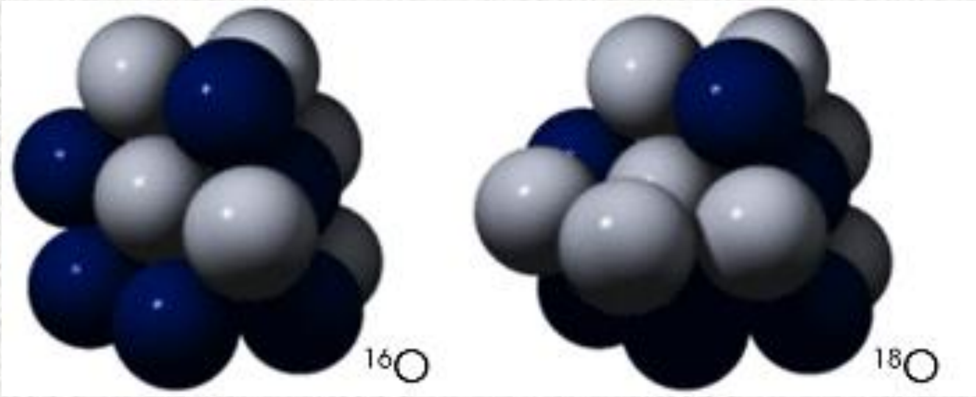

https://earthobservatory.nasa.gov/Features/Paleoclimatology_OxygenBalance/

The **Oxygen-18 isotope** has an extra two neutrons, for a total of 10 neutrons and 8 protons, compared to the 8 neutrons and 8 protons in a normal oxygen atom. The *slighty greater mass of ^{18}O—12.5 percent more than ^{16}O*—results in differentiation of the isotopes in the Earth's atmosphere and hydrosphere. Scientists measure differences in oxygen isotope concentrations to **reveal past climates**. [Roll mouse over nuclei to animate.]

(Illustration by Robert Simmon, NASA GSFC)

$$\delta^{13}C = \left(\frac{\left(\frac{13C}{12C}\right) sample}{\left(\frac{13C}{12C}\right) standard} - 1 \right) \times 1000$$

$$\delta^{18}O = \left(\frac{\left(\frac{18O}{16O}\right) sample}{\left(\frac{18O}{16O}\right) standard} - 1 \right) \times 1000$$

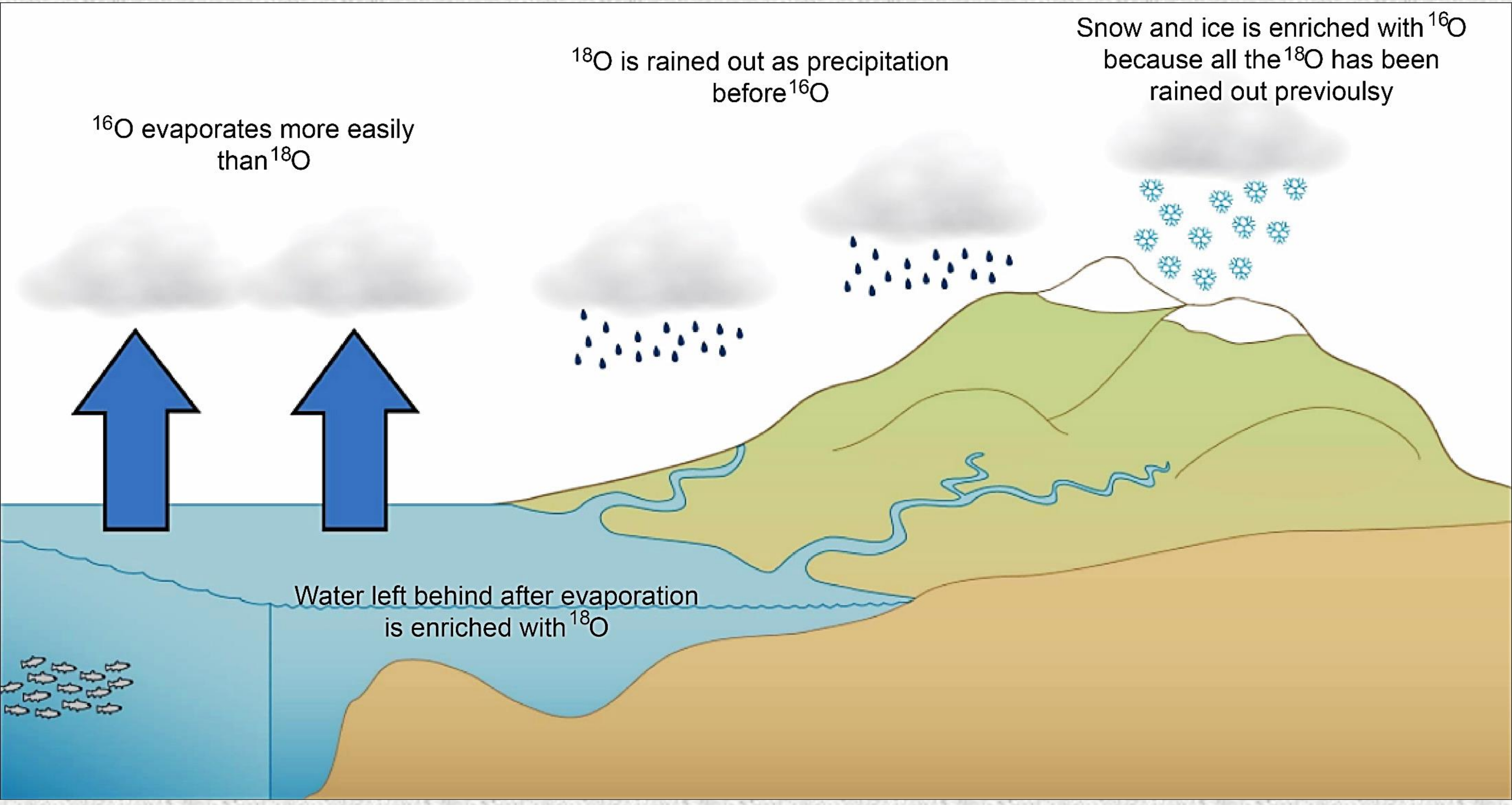
^{16}O evaporates more easily than ^{18}O
^{18}O is rained out as precipitation before ^{16}O
Snow and ice is enriched with ^{16}O because all the ^{18}O has been rained out previoulsy
Water left behind after evaporation is enriched with ^{18}O

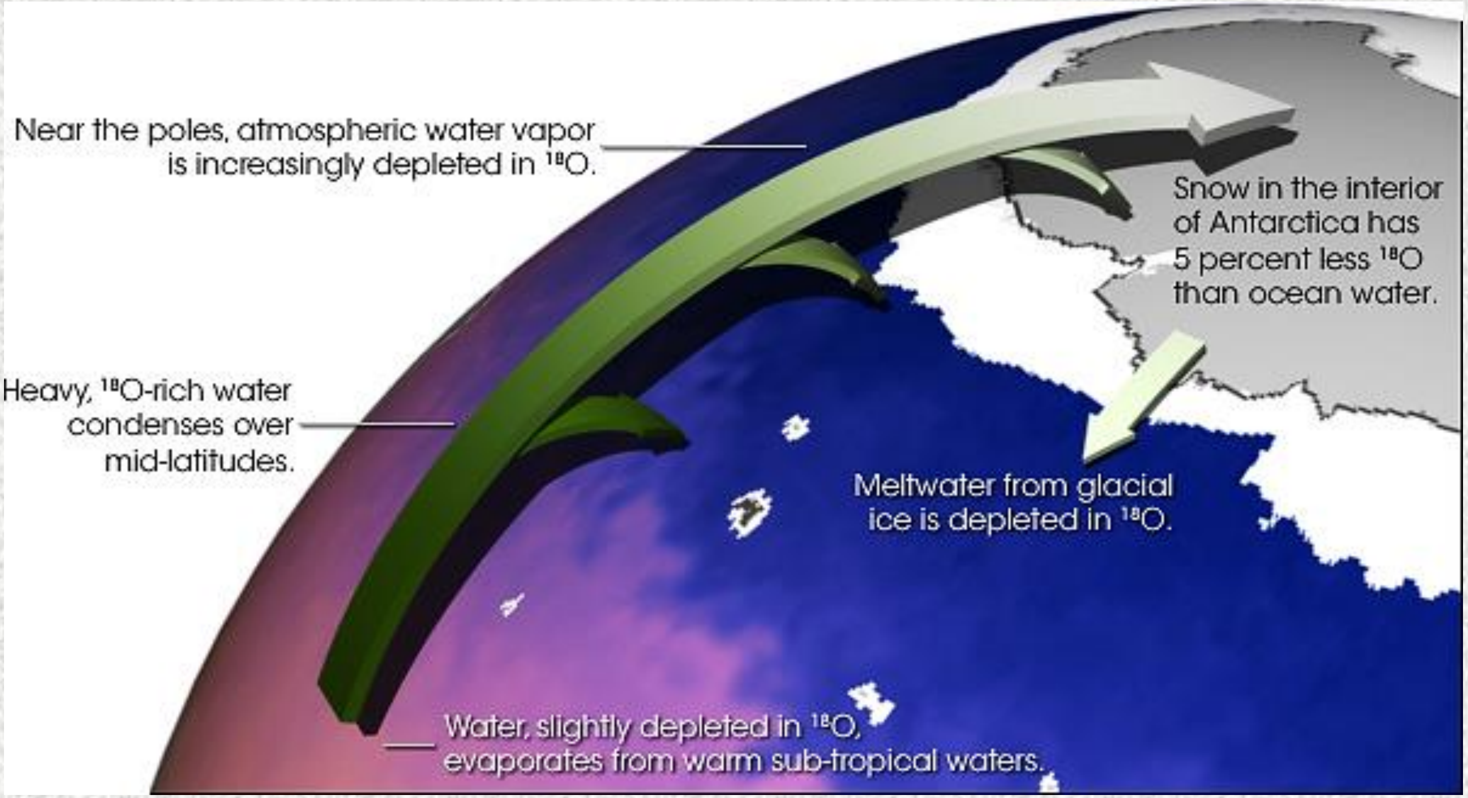

https://earthobservatory.nasa.gov/Features/Paleoclimatology_OxygenBalance/

Water vapor gradually loses ^{18}O as it travels from the equator to the poles. Because water molecules with heavy ^{18}O isotopes in them condense more easily than normal water molecules, air becomes progressively depleted in ^{18}O as it travels to high latitudes and becomes colder and drier. In turn, the snow that forms most glacial ice is also depleted in ^{18}O. As glacial ice melts, it returns ^{16}O-rich fresh water to the ocean. Therefore, oxygen isotopes preserved in ocean sediments provide evidence for past ice ages and records of salinity.

(Illustration by Robert Simmon, NASA GSFC)

Importance of the unicellulars:

Oxygene isotope stratigraphy ($\delta^{18}O$)

Globorotalia menardii

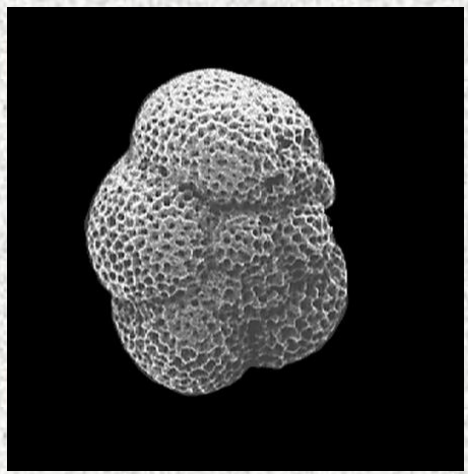

Neogloboquadrina pachyderma

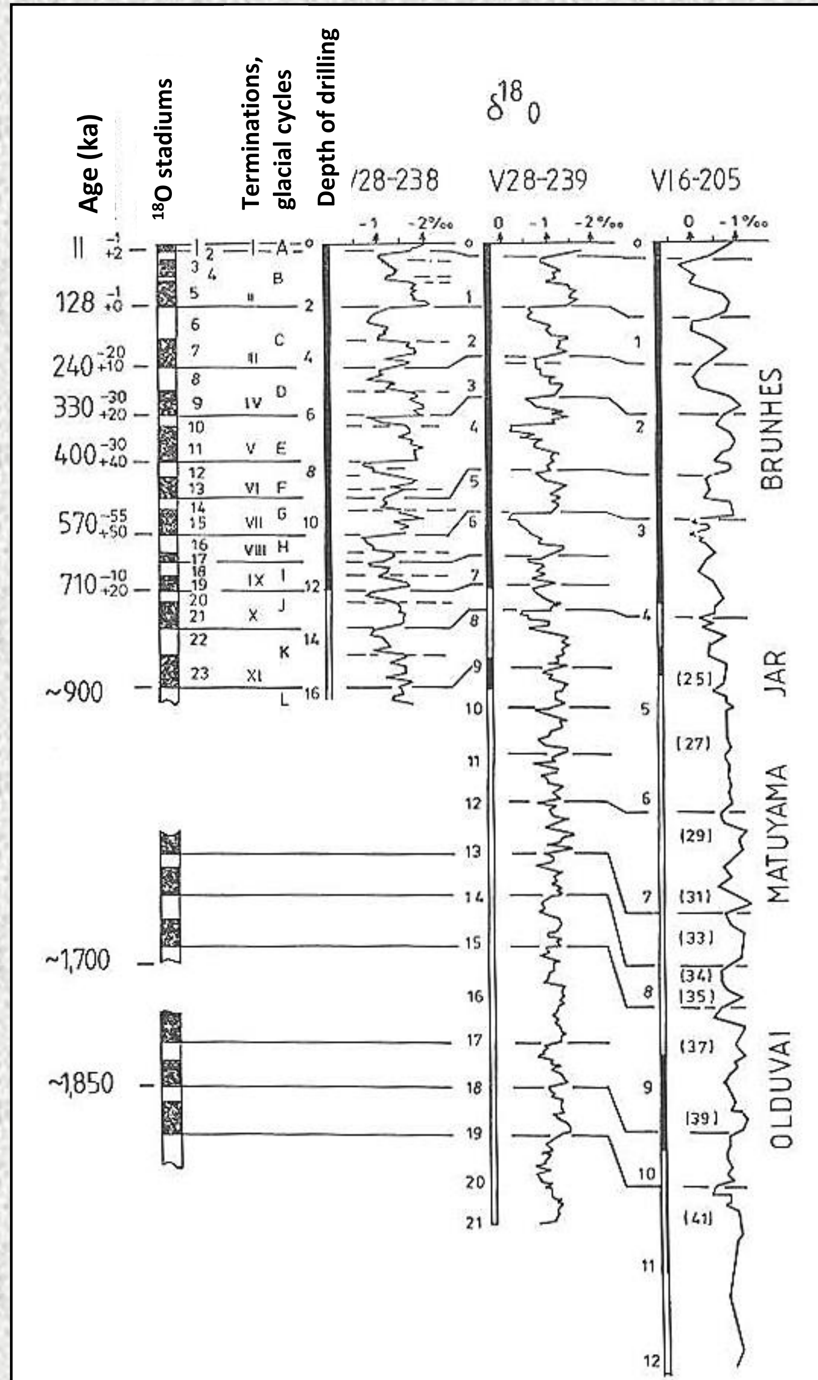

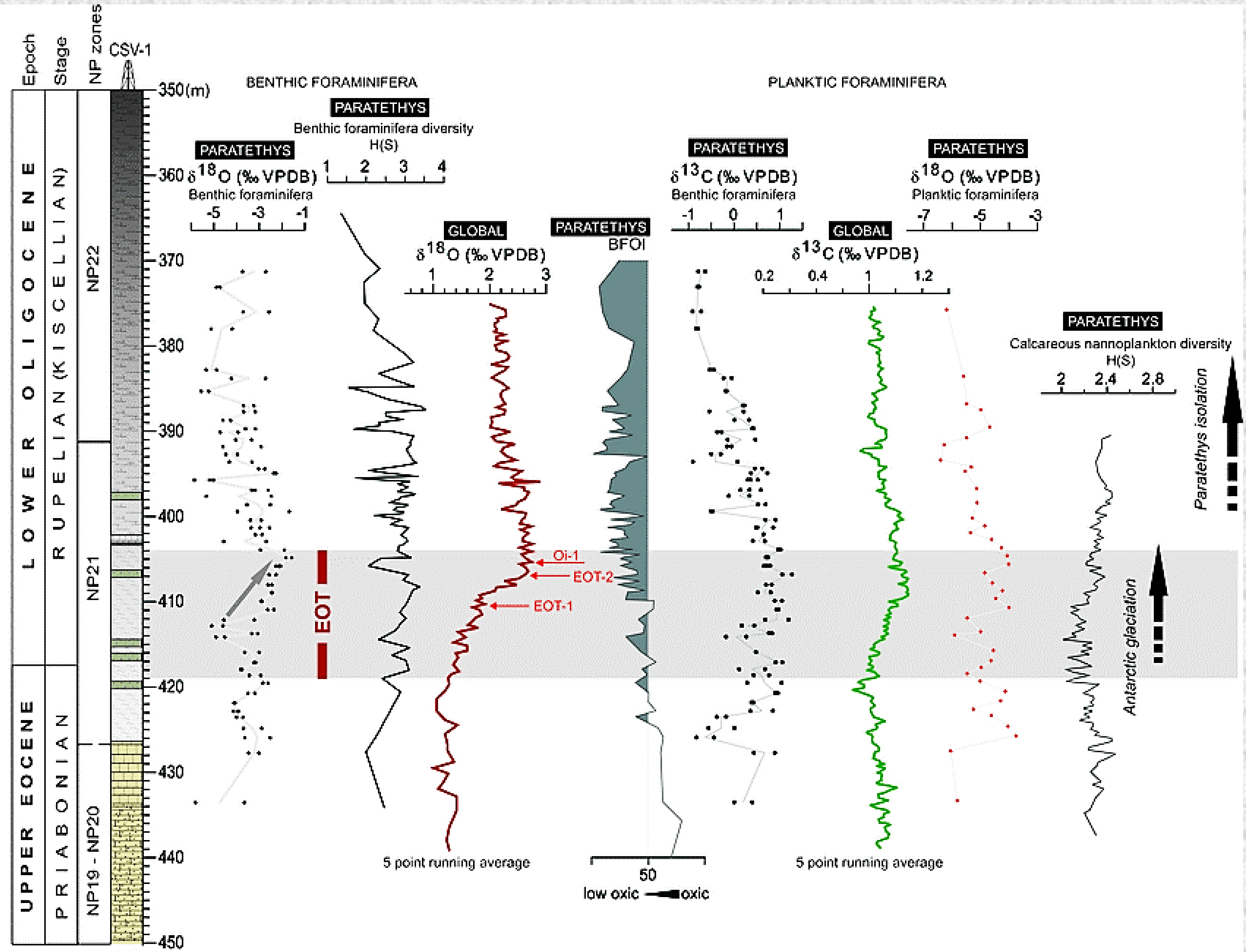

Oxygen isotope curves of benthic foraminifera from the CSV-1 and KL-1 boreholes and a composite global deep-sea oxygen isotope curve. Raw data for the global curve are based on benthic foraminifera from DSDP 77, DSDP 522, DSDP 529, DSDP 563, DSDP 574, ODP 689, ODP 744, ODP 748 and ODP 1218 sites (after Grossman, 2012).

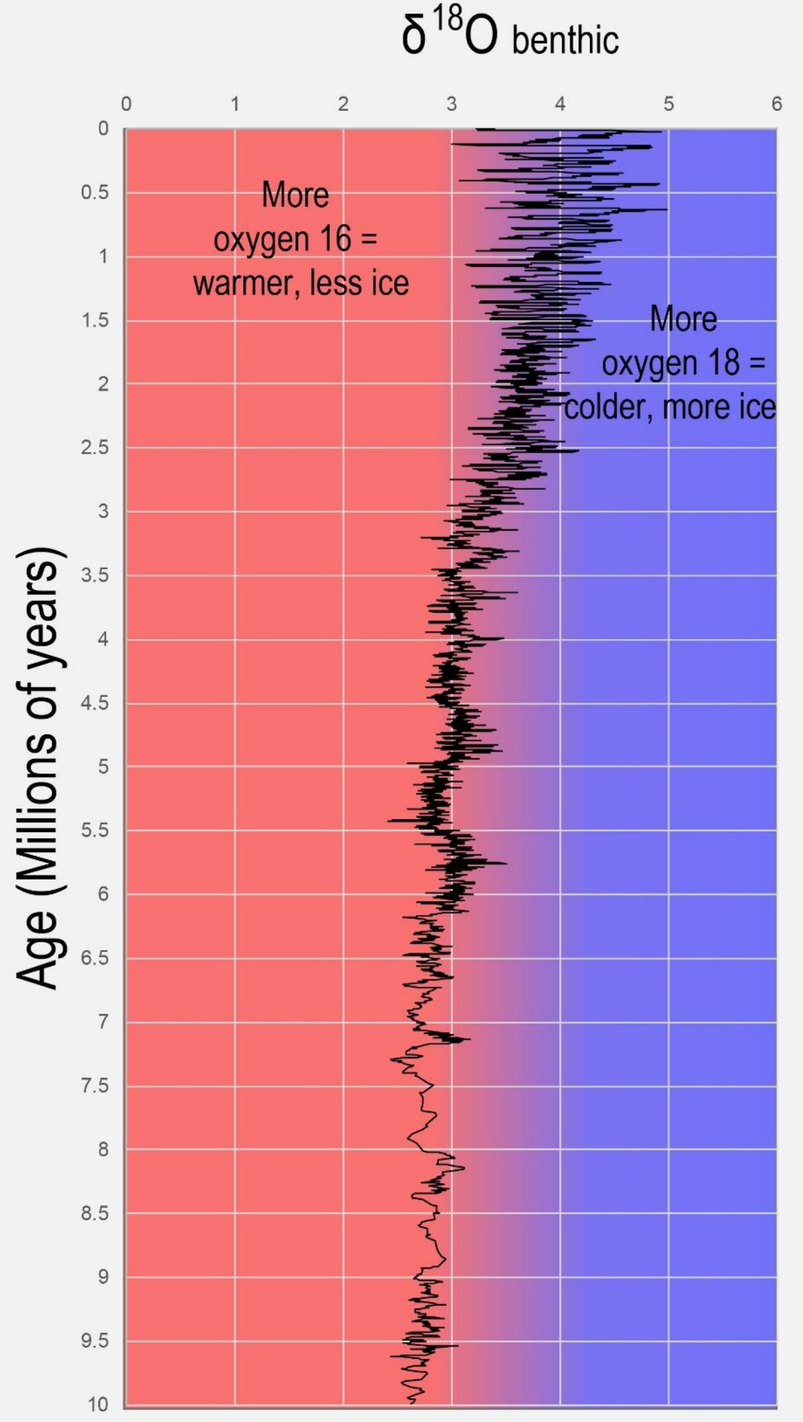

https://timescavengers.blog/introductory-material/what-is-paleoclimatology/proxy-data/carbon-oxygen-isotopes/

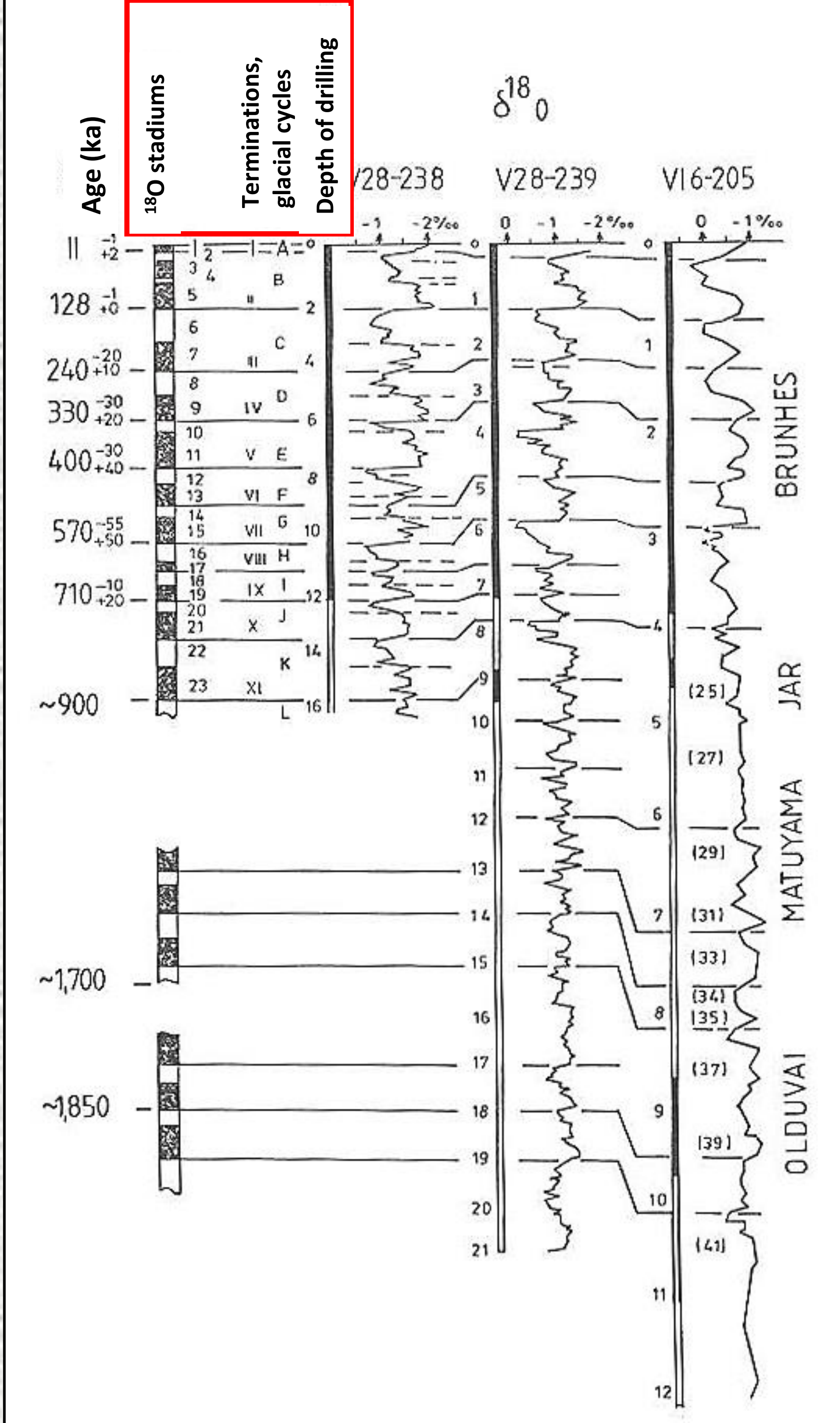
Age (ka)
18O stadiums
Terminations, glacial cycles
Depth of drilling
δ18O
V28-238
V28-239
V16-205
128
240
330
400
570
710
~900
~1,700
~1,850
BRUNHES
JAR
MATUYAMA
OLDUVAI

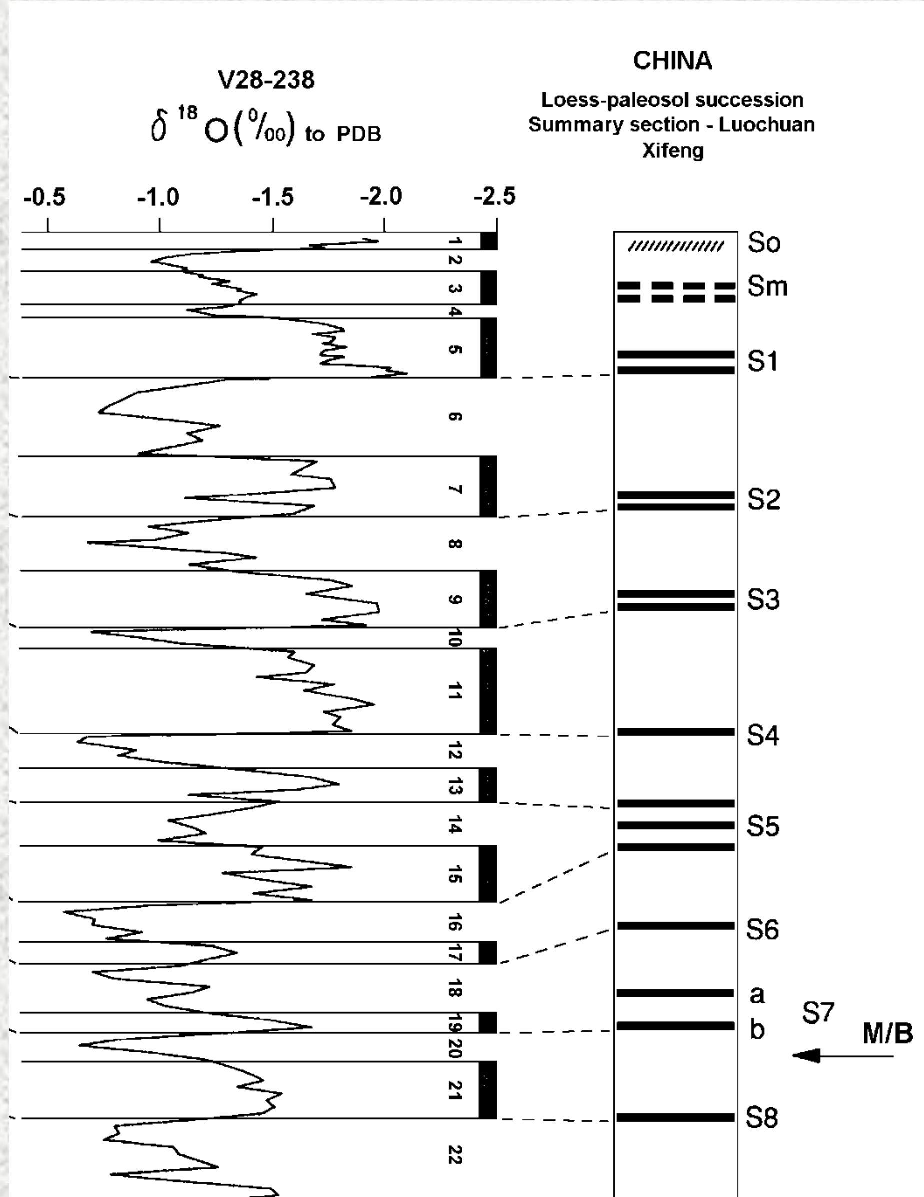
V28-238
δ 18 O(‰) to PDB
-0.5
-1.0
-1.5
-2.0
-2.5
CHINA
Loess-paleosol succession
Summary section - Luochuan
Xifeng
So
Sm
S1
S2
S3
S4
S5
S6
a
S7
b
M/B
S8

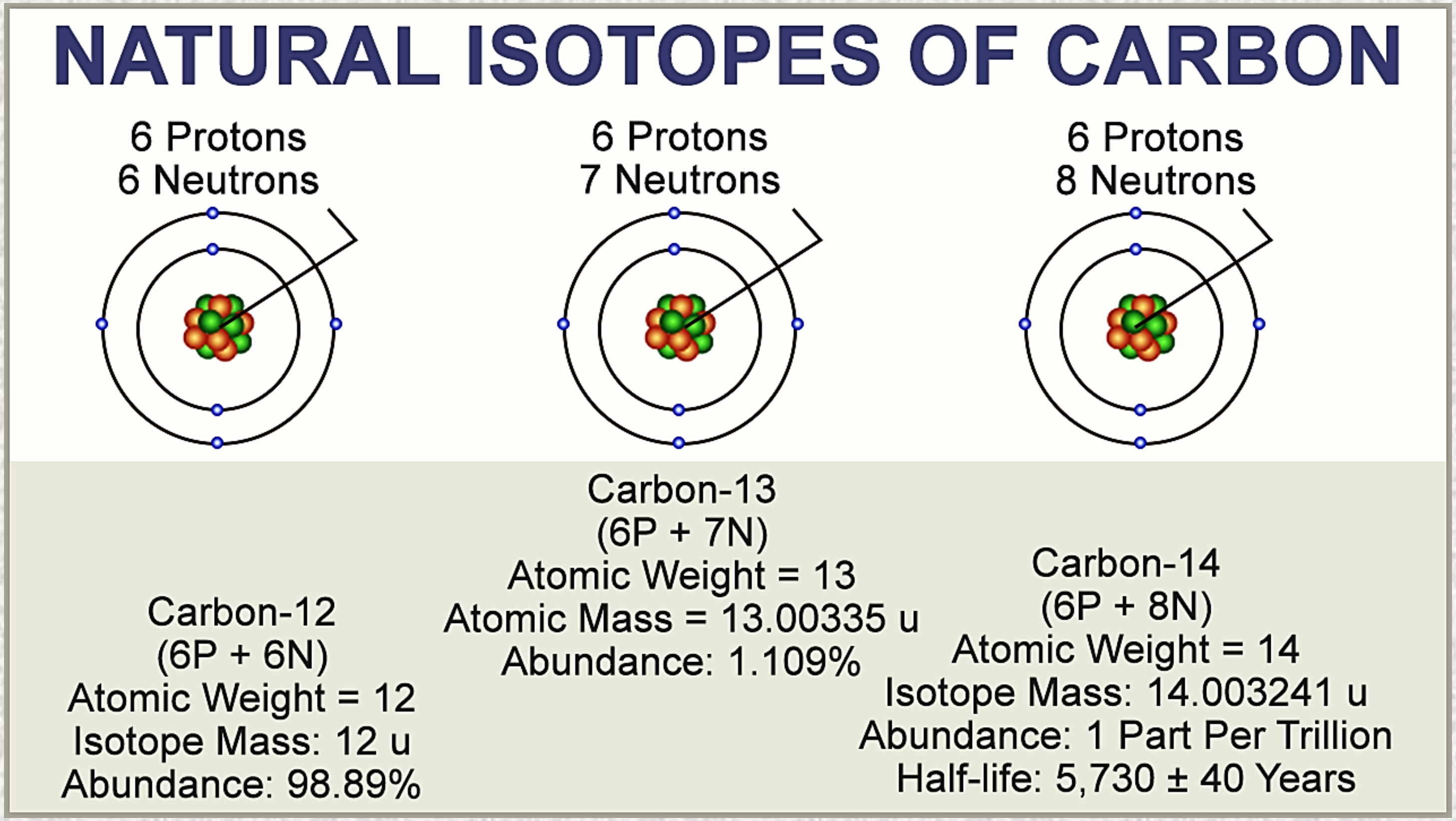

https://sciencestruck.com/isotopes-of-carbon

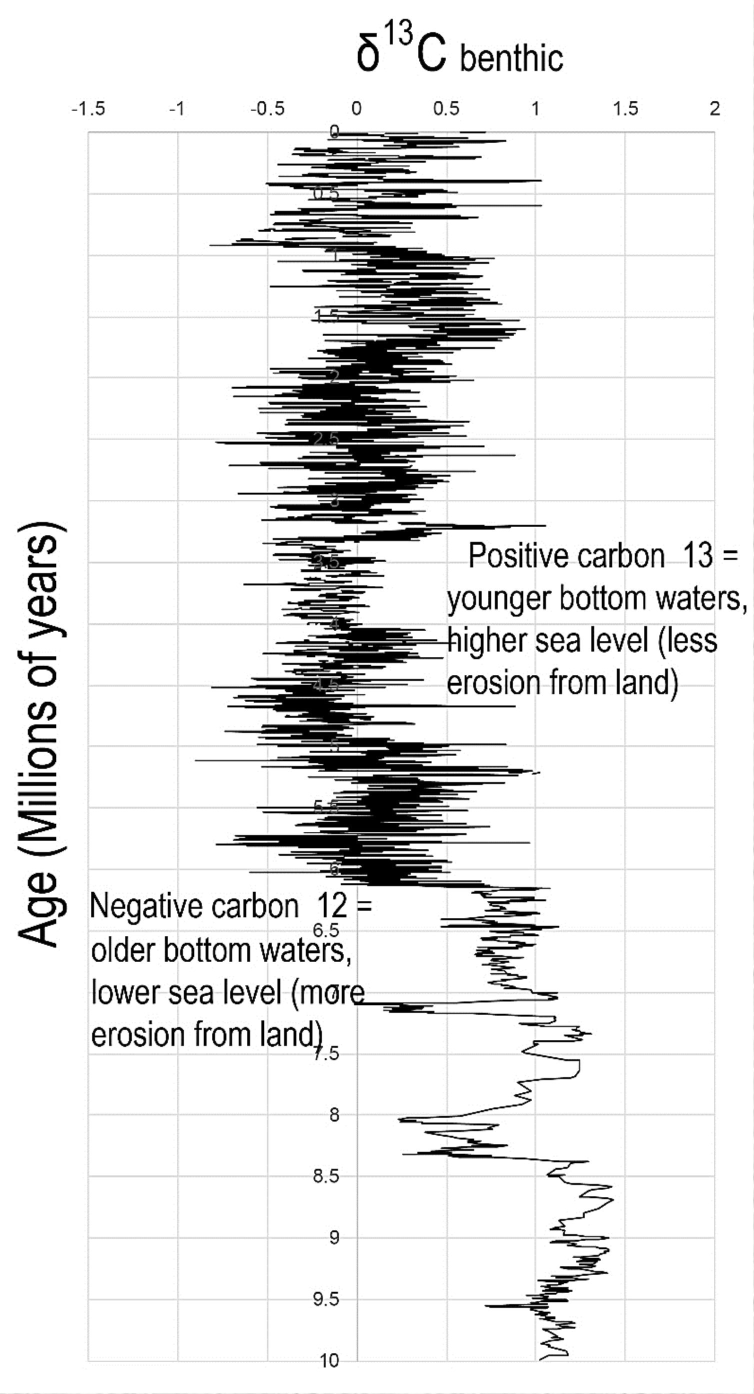

https://timescavengers.blog/introductory-material/what-is-paleoclimatology/proxy-data/carbon-oxygen-isotopes/

2 different type of plants based on different photosynthetic pathway:

- C_4 plants: mild or cold growing season
  - Grasses and forbs
- C_3 plants: warmer and more humid environments
  - Distinction: closed canopy, top of the canopy, or open environment

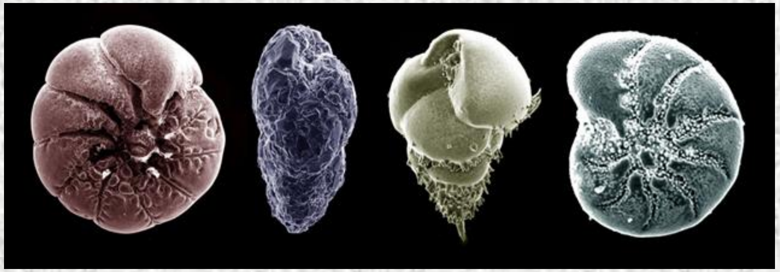

	$\delta^{18}O$ More Negative	$\delta^{18}O$ More Positive	$\delta^{13}C$ More Negative	$\delta^{13}C$ More Positive
Benthic Foraminifera	-Warmer global climate -Decreased ice volume	-Colder global climate -Increased ice volume	-Older bottom waters -Increased continental weathering	-Younger bottom waters -Decreased continental weathering
Planktic Foraminifera	-Warmer local temperatures -Decreased ice volume -Increased local precipitation	-Colder local temperatures -Increased ice volume -Increased local evaporation	-Decreased local productivity -Increased upwelling (increased local productivity)	-Increased local productivity -Decreased-no upwelling (low local productivity)

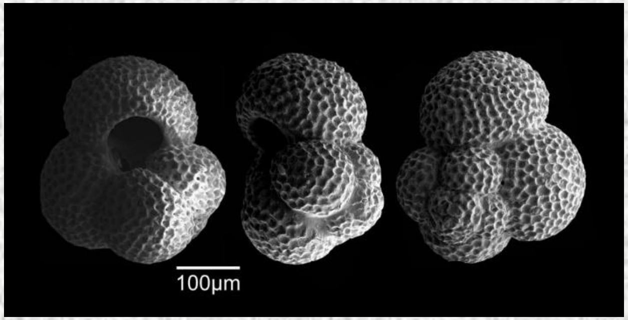

DATING METHODS IN THE QUATERNARY STUDIES

RELATIVE DATING METHODS/RELATIVE STRATIGRAPHY

1. **Lithostratigraphy**
   - marker horizons:
     - tephrostratigraphy
     - buried soils (paleosols, fossil soils)
2. **Biostratigraphy**
   - Vertebrata
   - Molluscs
     - -Malacothermometer
     - -$\delta^{18}O$ of molluscs shells
   - Marine microfauna
   - Pollen
   - Biomarkers
3. **Magnetostratigraphy**
4. **Magnetic susceptibility (MS)**
5. **Amino Acid Racemisation (AAR)**
6. **Stable isotopes**
   - $\delta^{18}O$ ($^{16}O/^{18}O$)
     - (Milankovich theory)
   - $\delta^{13}C$ ($^{12}C/^{13}C$)
7. **Ice cores from the icesheets**
8. **Geomorphological horizons**
   - terraces: fluvial marine
   - correlative sediments

7. Ice drillings

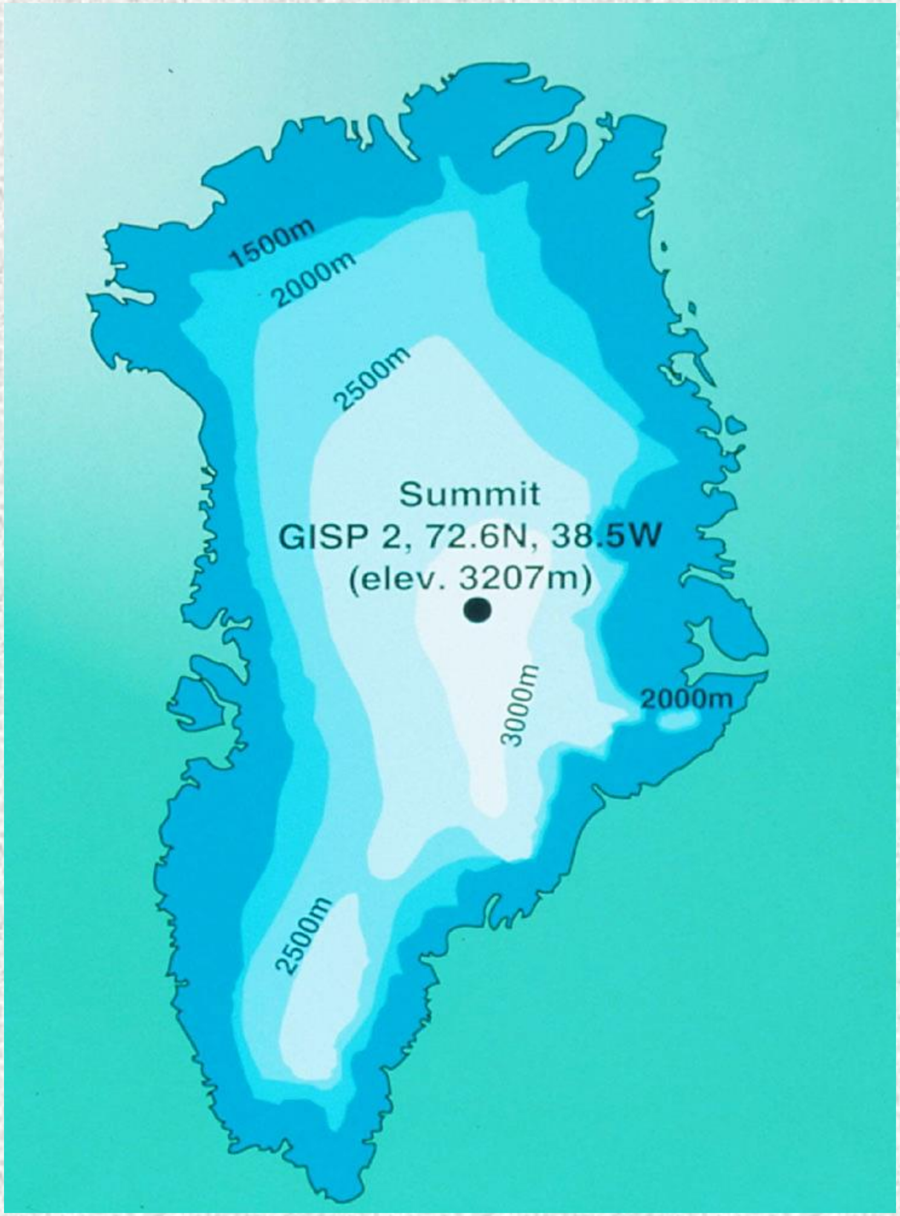

A three-dimensional view of the age and structure of the Greenland Ice Sheet:
https://www.nasa.gov/content/goddard/nasa-data-peers-into-greenlands-ice-sheet

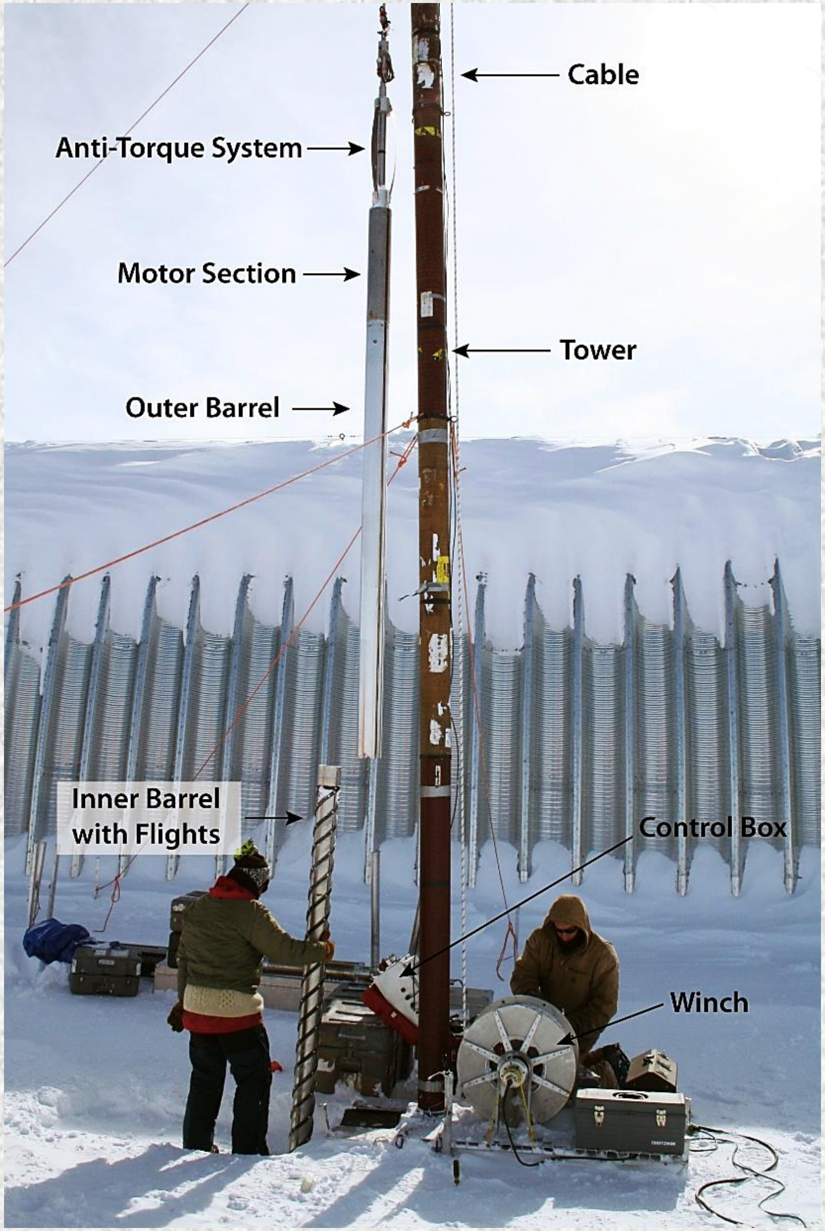

Joseph Souney, Univ. New Hampshire
(https://icecores.org/icecores/drilling.shtml)

A mechanical drill head showing the cutters used to shave an annulus around the ice to be cored.
—Credit: Steven Profaizer, NSF

A thermal drill head showing the absence of cutters. Thermal drills use a heating element to melt an annulus around the ice to be cored.
—Credit: Tony Wendricks, Univ. Wisconsin

Jay Johnson, Univ. Wisconsin
(https://icecores.org/icecores/drilling.shtml)

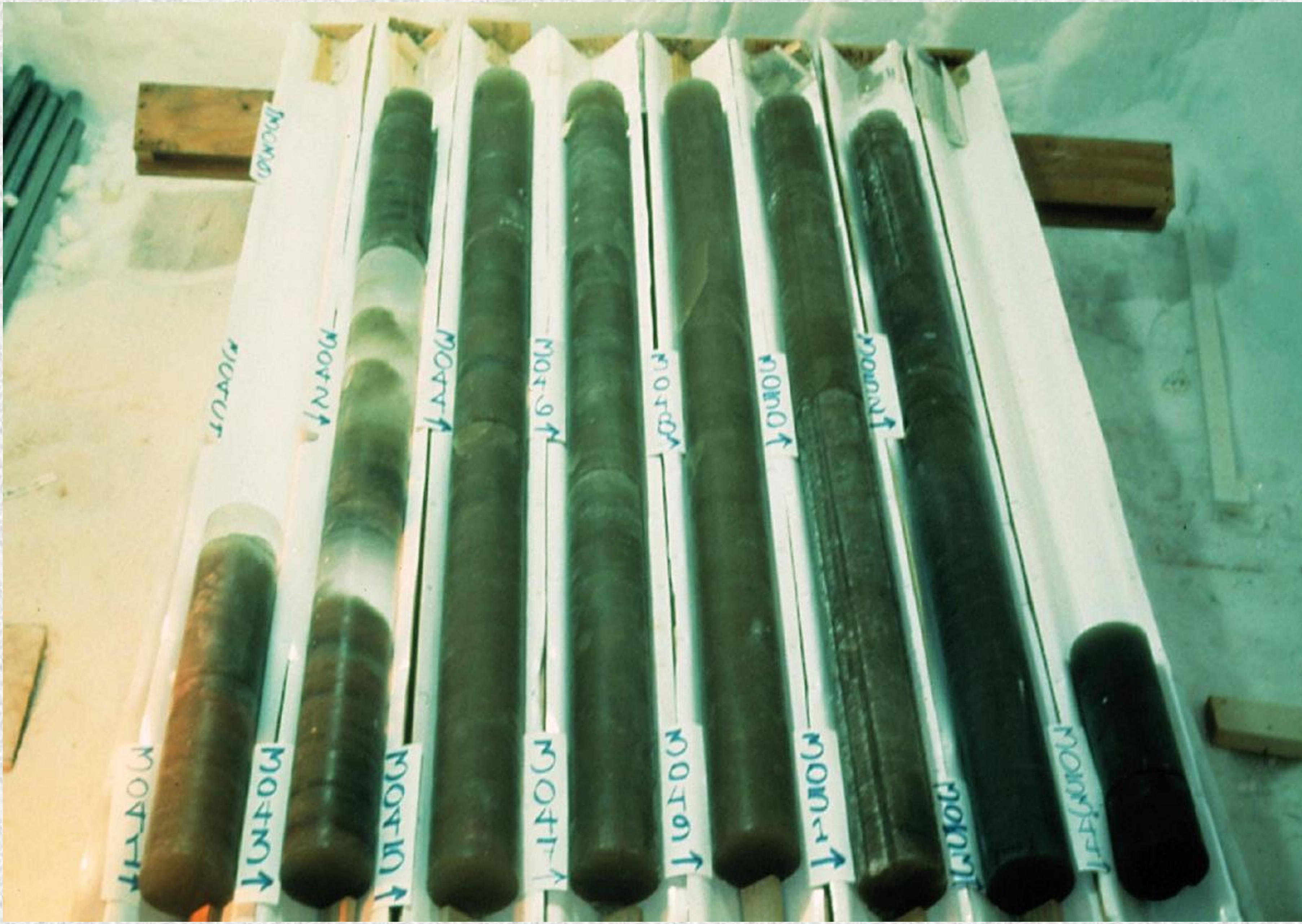

Investigation of ice cores

a. Melt Layers
 cores taken in cold areas where melting infrequent
 frequency of melting = index of summer temperature
b. Gas Bubbles
 gas composition set when ice forms from snow
 CO_2 content in bubbles 100 ppm lower during Last Glacial Maximum
c. Annual Layer Thickness
 Age determined by counting annual layers
 Climate determined by annual layer thickness
d. Dissolved and Particulate Matter
 Wind Blown Silt 3-20 times greater during isotope stage 2
 Volcanic Ash also more abundant in stage 2
 More dirt in Arctic cores = MELTED during Stage 5 (Koerner 1989)
 Nitrate Ion: produced by UV radiation of N_2 (solar)
 e. Oxygen (and Hydrogen) Isotope Analysis
  Mirror image of ocean core isotopes: when ocean cores enriched in 18O, ice cores are depleted. Raleigh Fractionation
  Modern temperature-isotope relationships determined

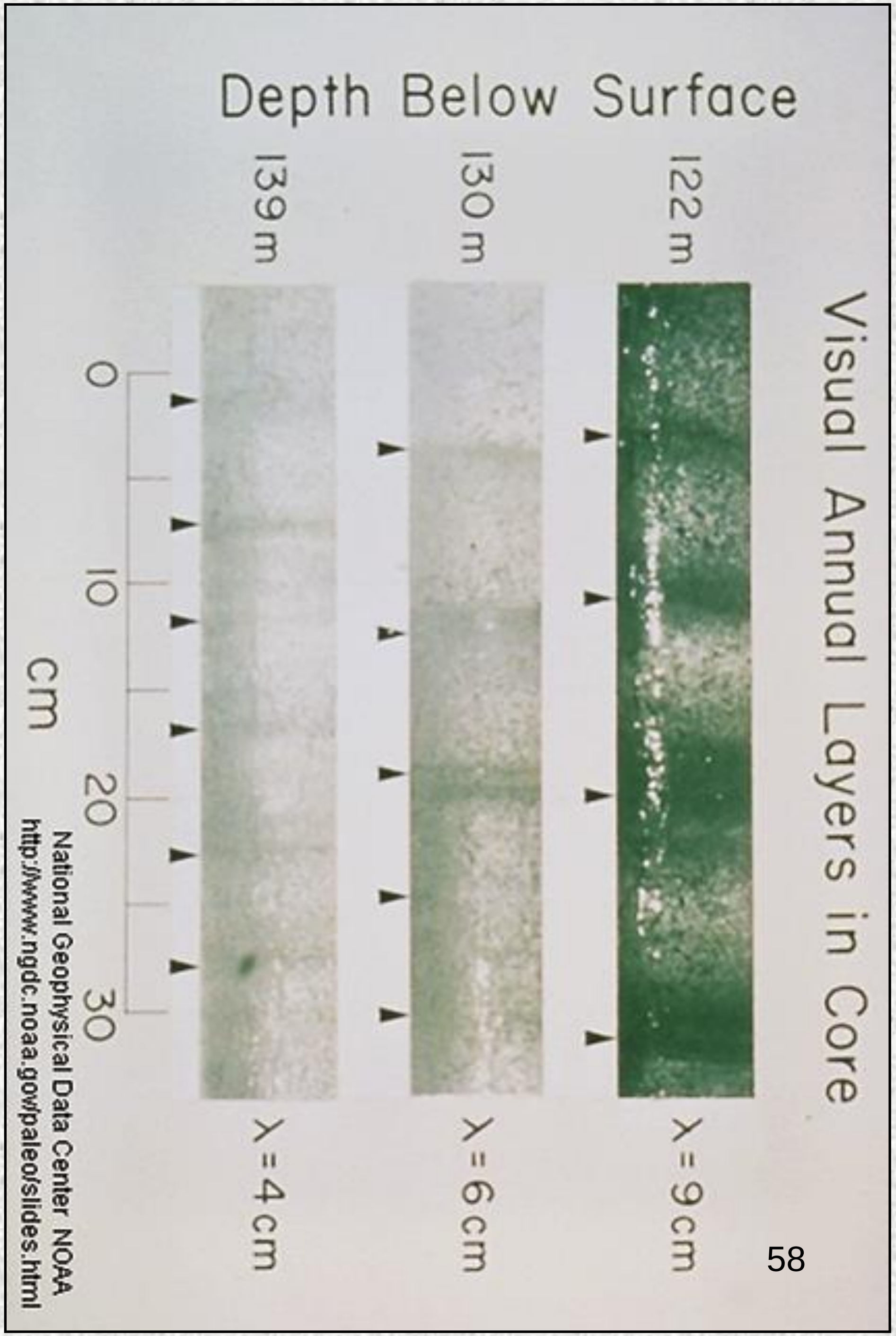

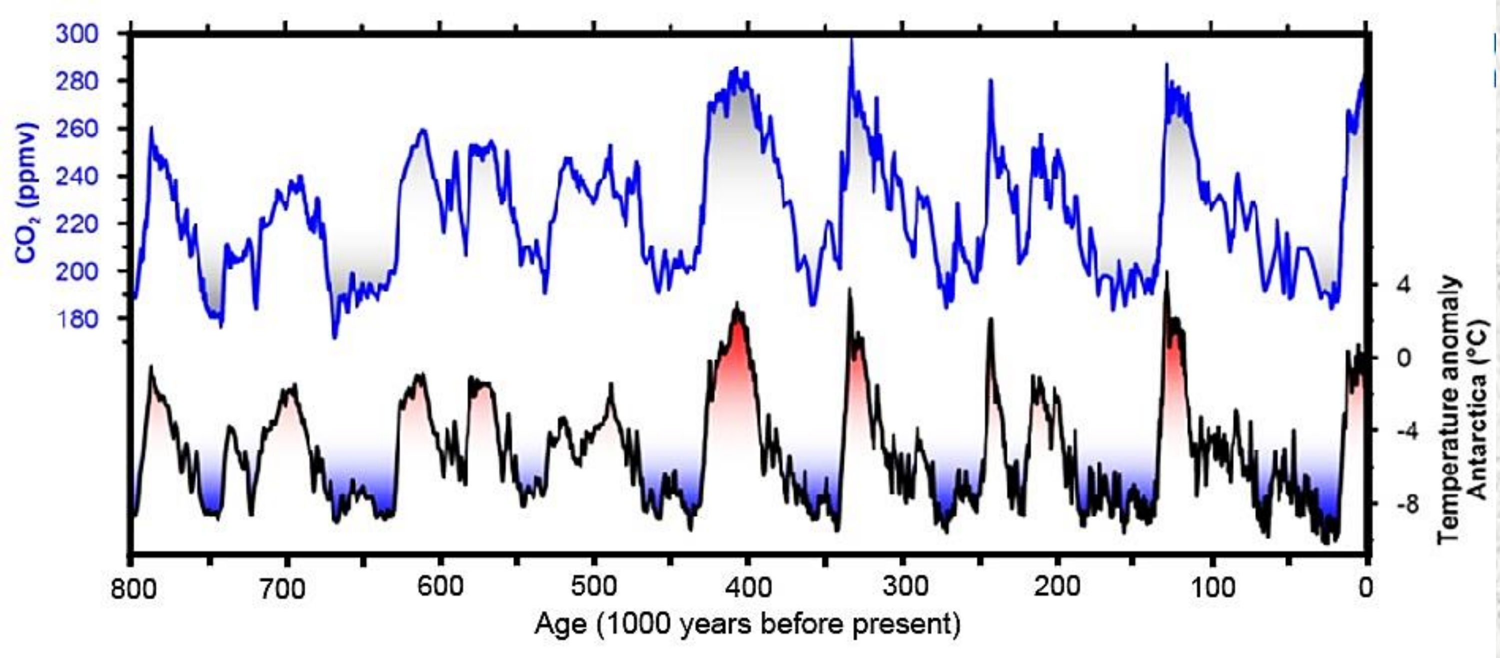

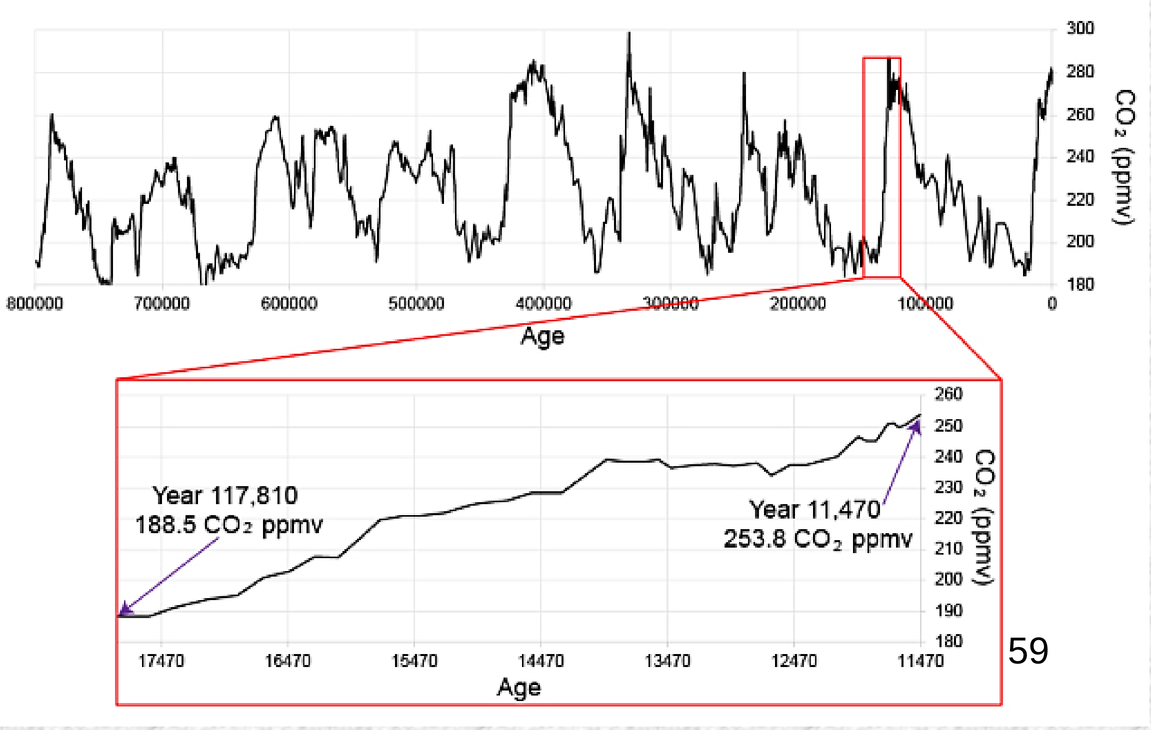

https://timescavengers.blog/climate-change/co2-past-present-future/

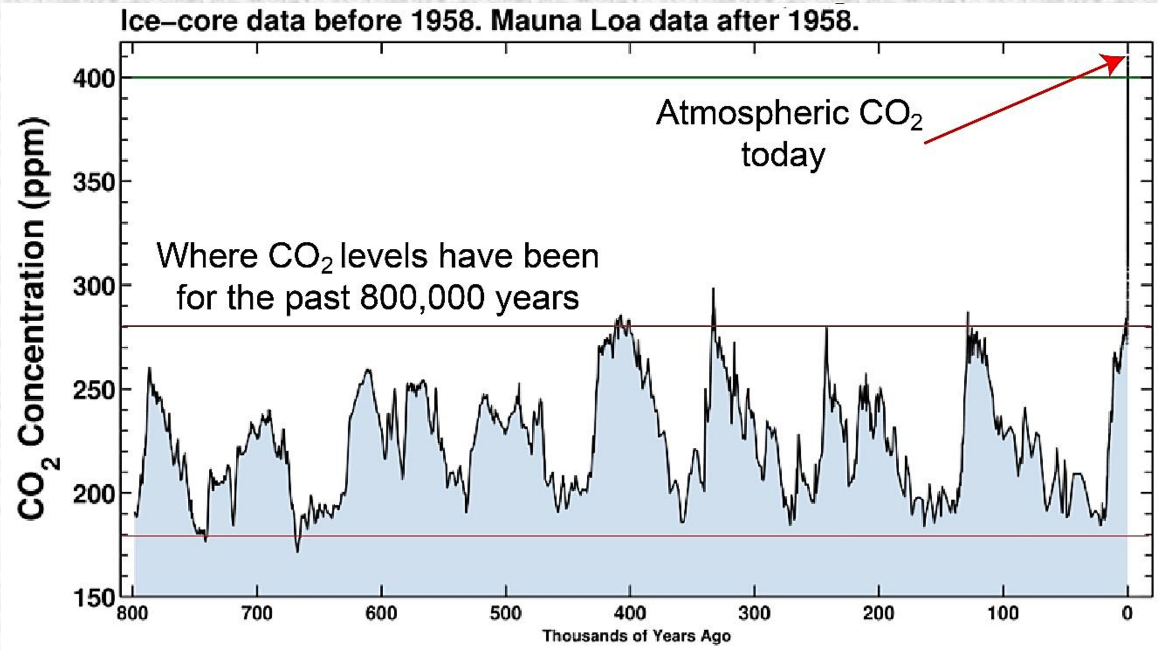

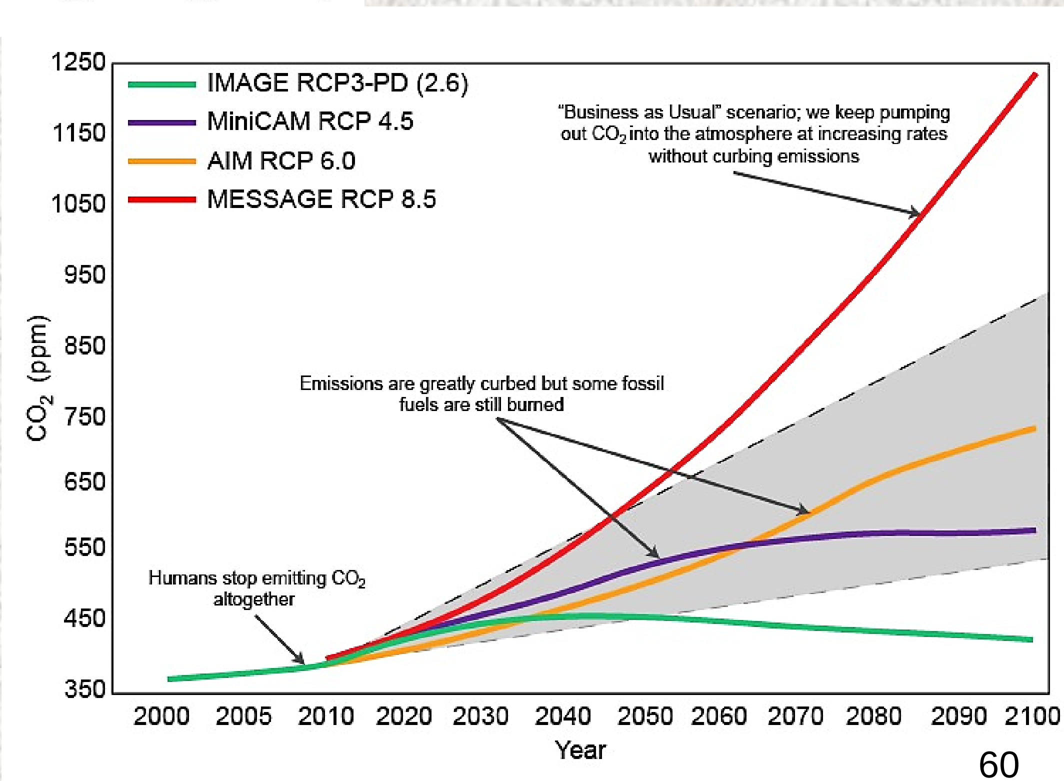

https://timescavengers.blog/introductory-material/what-is-paleoclimatology/proxy-data/carbon-oxygen-isotopes/

Cooler and dustier climatic periods such as the Younger Dryas and Wisconsin glacial are characterized by high calcium concentrations in the GISP2 ice record.

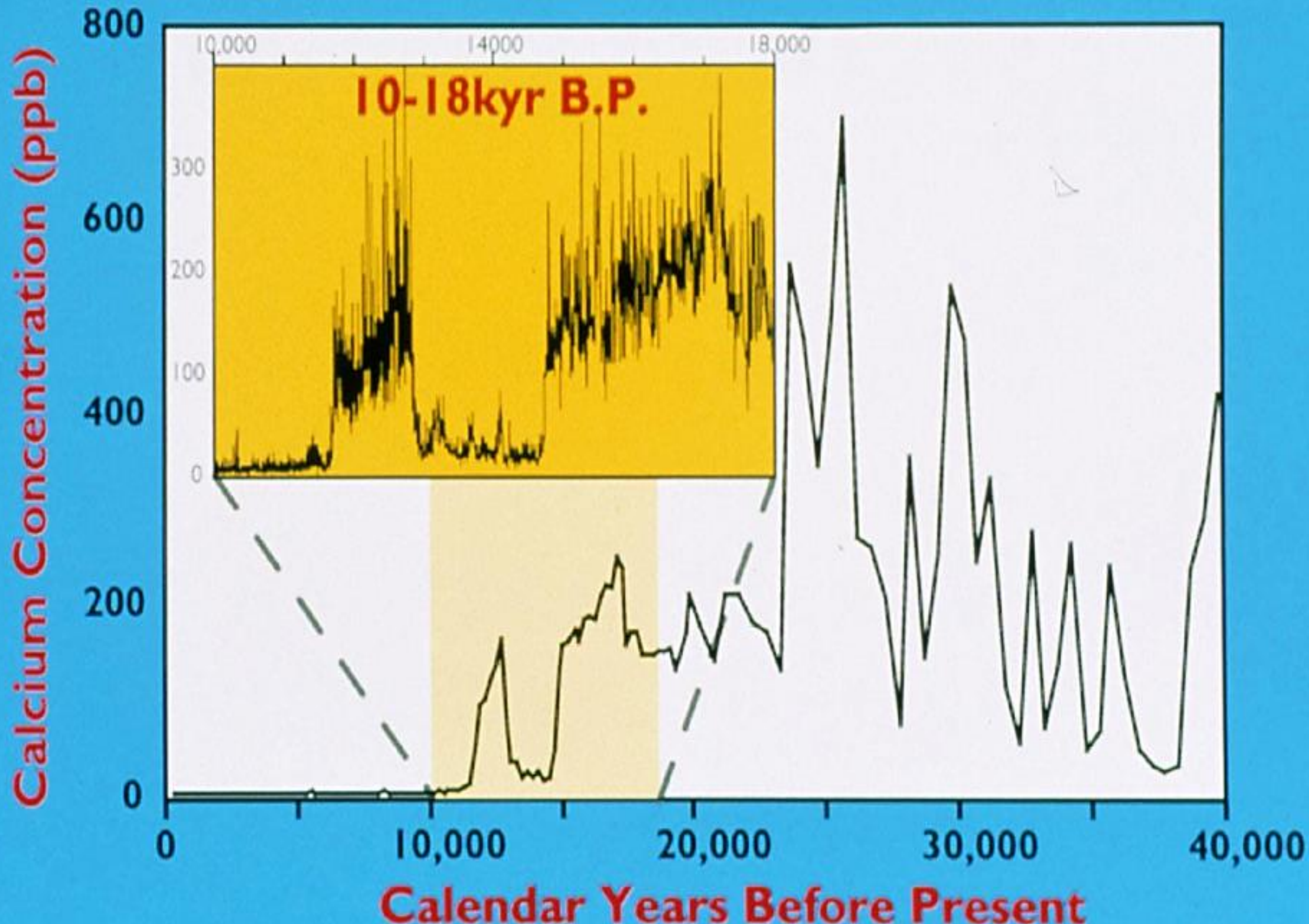

Data from Mayewski et al., University of New Hampshire. Data presented as 200-year averages for 0-20kyr B.P., 500-year averages for 20-40kyr B.P. Data in inset has not been averaged.

DATING METHODS IN THE QUATERNARY STUDIES

ABSOLUTE DATING METHODS

9. Varve-, and dendrochronology

“Absolute” methods or numerical age estimation

10. Non-stable (radioactive) isotopes
    - 10/a Potassium-argon series
        - $^{40}K/^{40}Ar$
        - $^{40}Ar/^{39}Ar$
        - laser fusion $^{40}Ar/^{39}Ar$
    - 10/b Uranium decay series
        - $^{238}U/^{230}Th$
        - $^{234}U/^{230}Th$
        - $^{230}Th/^{231}Pa$ (^{235}U)
    - 10/c Fission-track (^{238}U)
    - 10/d Radiocarbon dating (^{14}C)
11. Luminescence methods
    - -Thermoluminescence (TL)
    - -Optically stimulated luminescence (OSL)
        - InfraRed Stimulated Luminescence (IRSL)
12. Electron-spin resonance (ESR)
13. Cosmogenic isotopes

Varve chronology

varved deposit - any form of repetitive sedimentary rock stratification, either bed or lamination, that was deposited within a one-year time period.
This annual deposit may comprise paired contrasting laminations of alternately finer and coarser silt or clay, reflecting seasonal sedimentation (summer and winter) within the year.

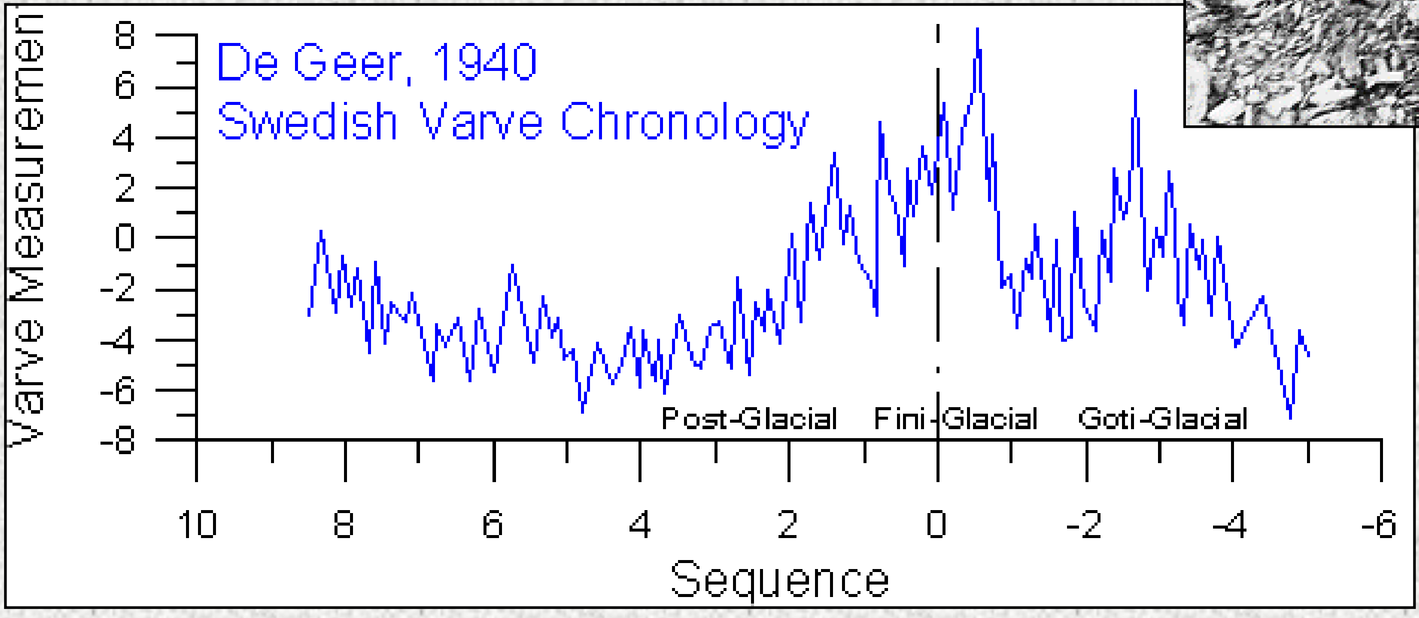

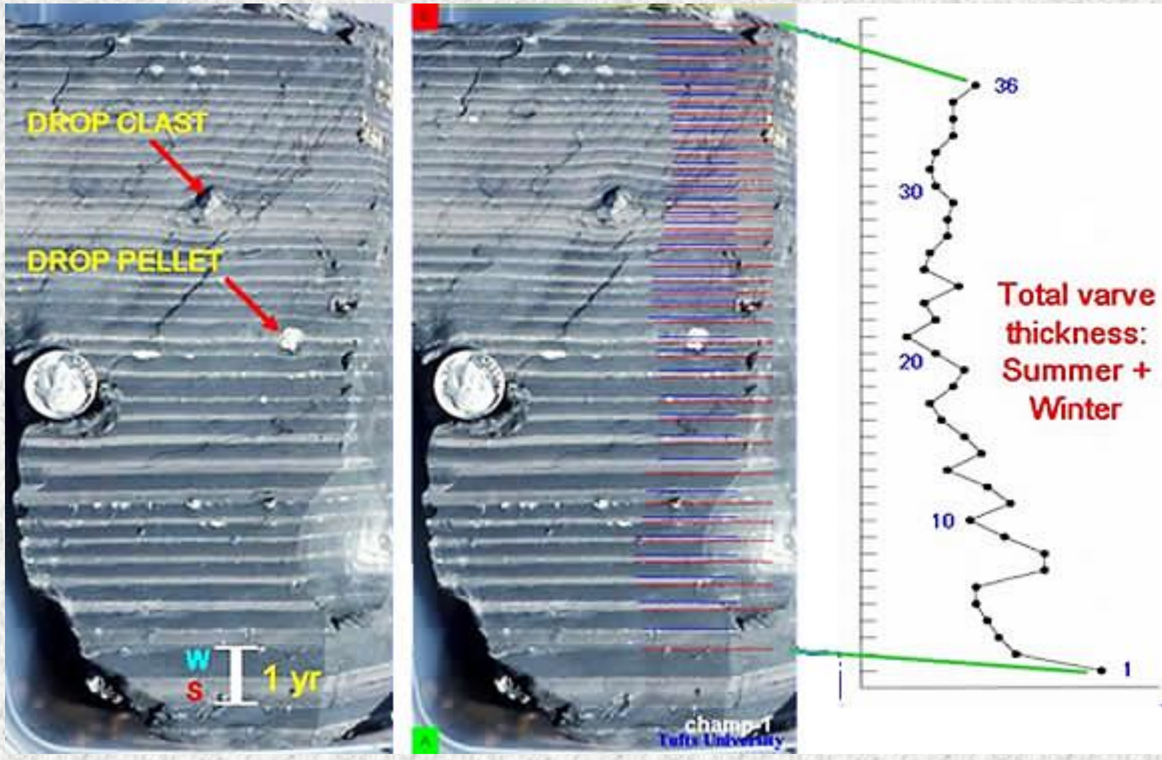

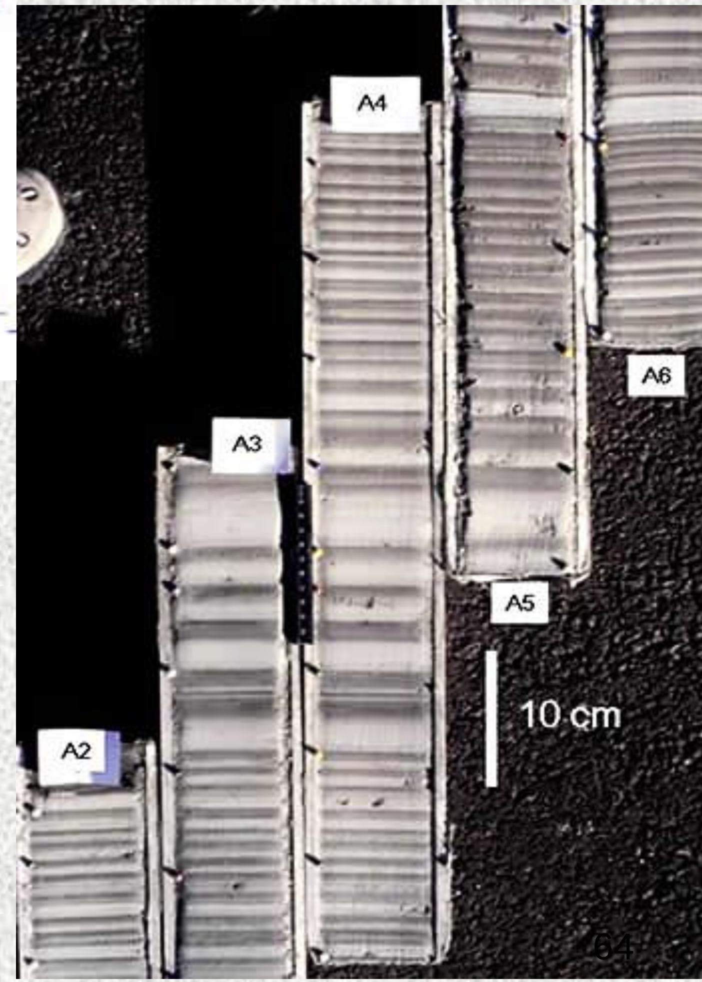

http://eos.tufts.edu/varves/images/varve_chron1.jpg

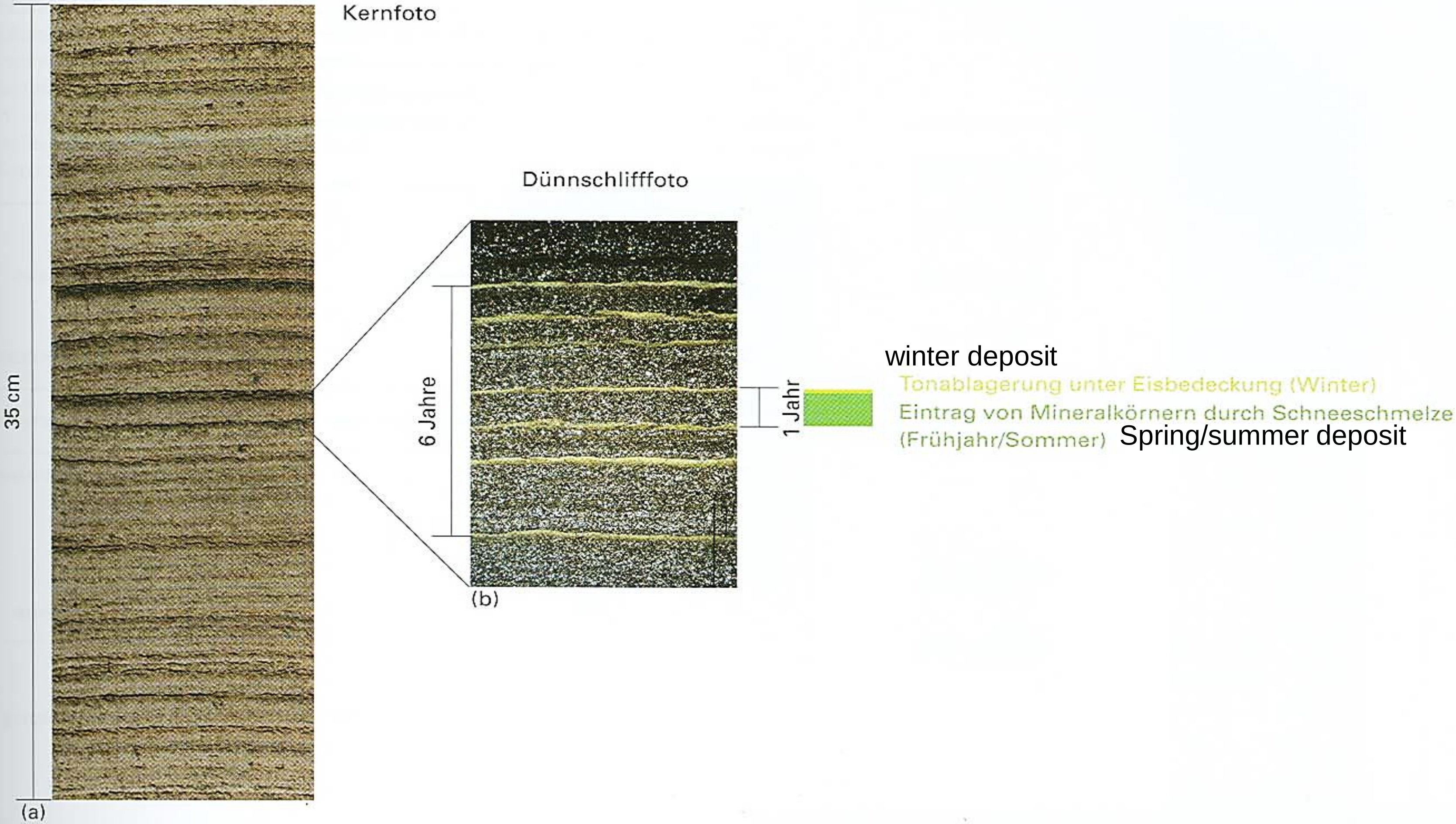

Abb. 10a und b: Ein Bohrkern mit klastischen Warven aus dem Holzmaar, einem Kratersee in der Vulkaneifel; links (a) ein Foto des erbohrten Kerns, rechts (b) ein Dünnschliff unter dem Mikroskop. Gröbere Mineralkörner zeigen die Phase des Schmelzwassereintrags an (Sommerlage). Davon deutlich abgetrennt bildet sich am Ende dieser Ablagerungsphase eine Lage aus feinem Ton, die sich erst unter den Stillwasserbedingungen des wieder zugefrorenen Sees absetzen kann. (Foto: Achim Brauer, GFZ)

Thinsection of a varve sediment

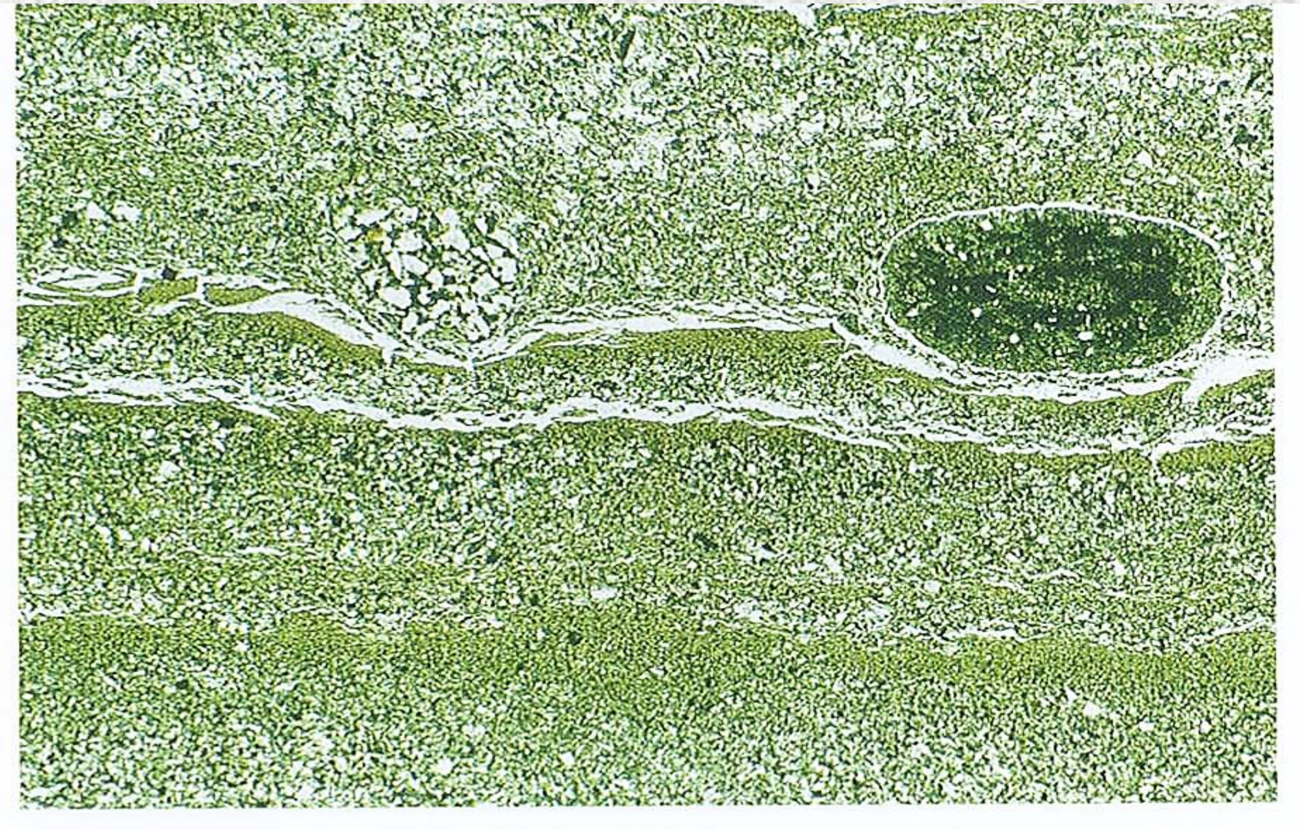

Coarser material transported by ice during spring

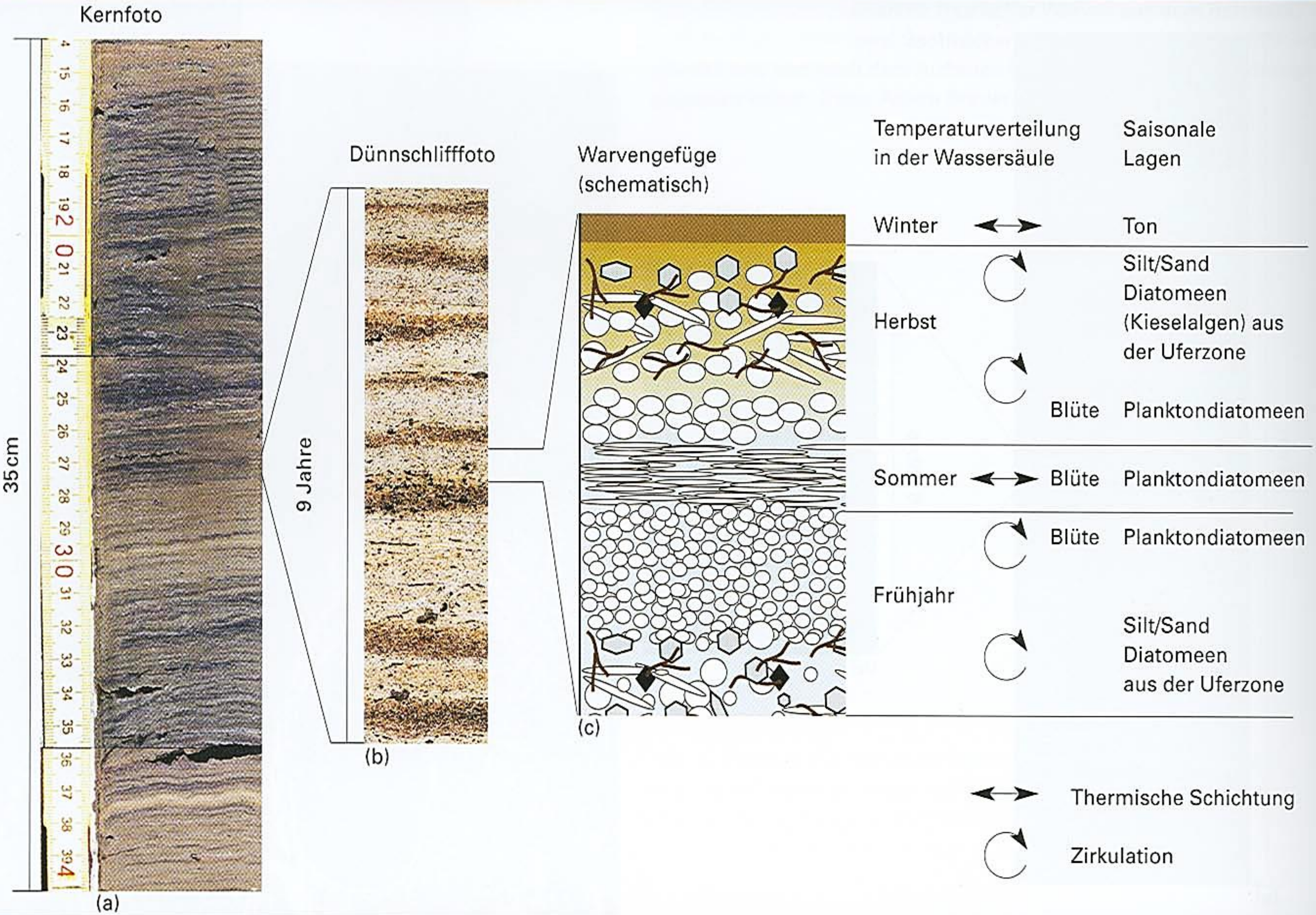

Abb. 12a bis c: Der typische Aufbau biogen-klastischer Warven am Beipiel von Jahreslagen im Holzmaar aus der kleinen Eiszeit; links (a) ein Foto des dem Seegrund entnommenen Sedimentbohrkerns, in der Mitte (b) die Dünnschliffaufnahme unter dem Mikroskop und rechts (c) der schematische Aufbau einer kompletten Jahreslage. (Fotos: Markus Schwab (a), Cathrin Brüchmann (b), Ulrike Krienel (c) GFZ)

Stalagmite-chronology

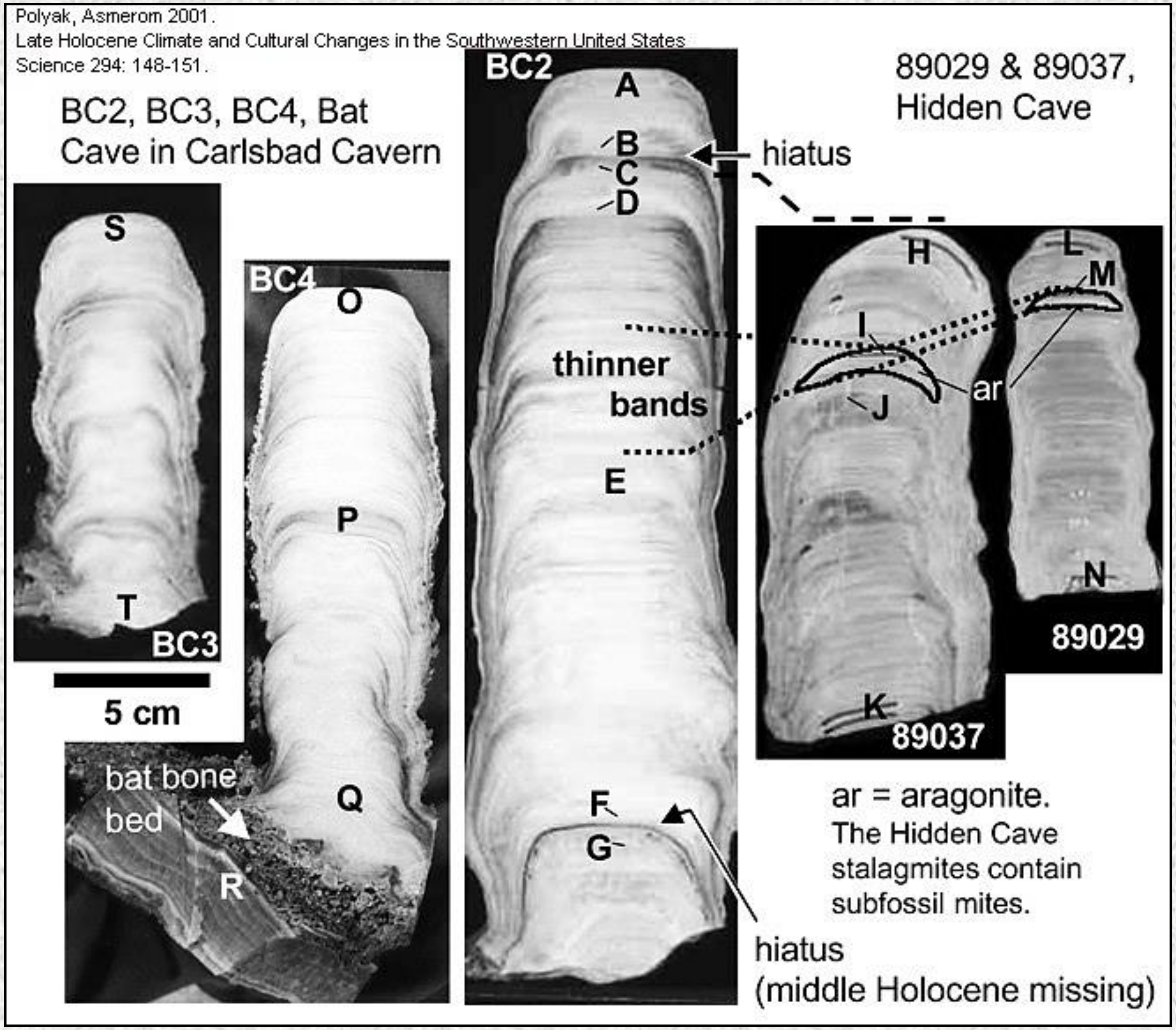

Dendrochronology

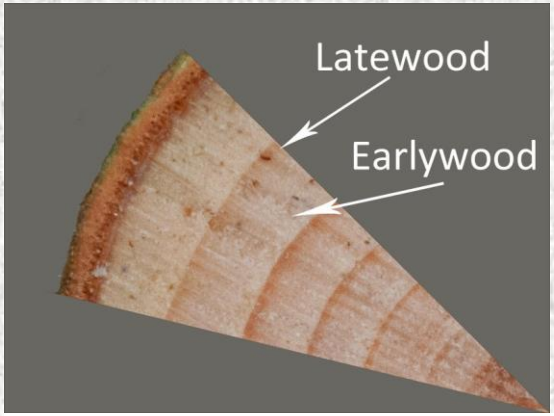

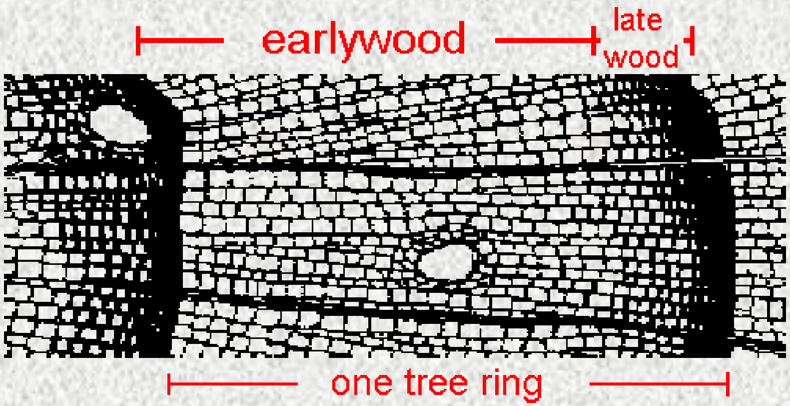

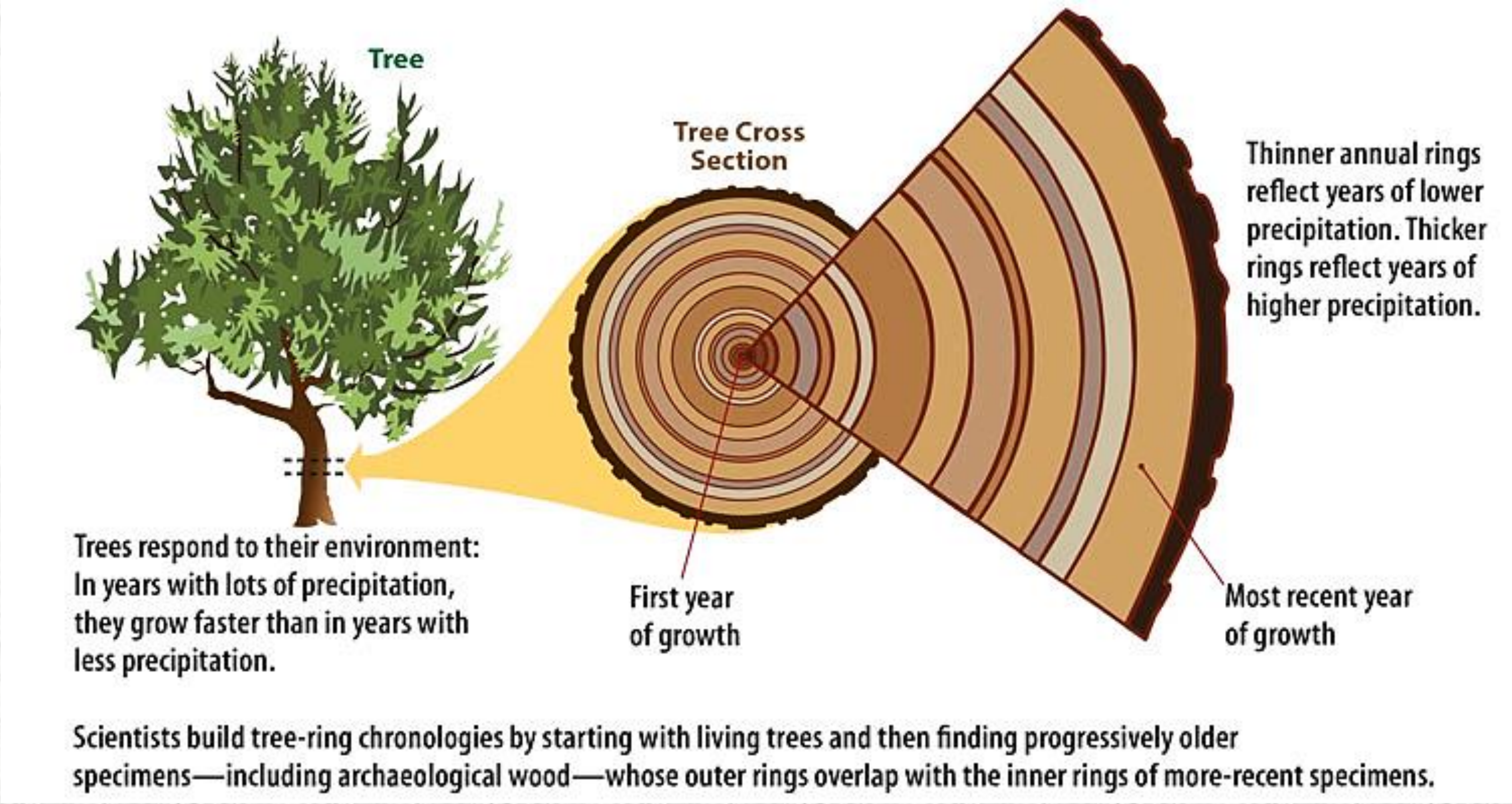

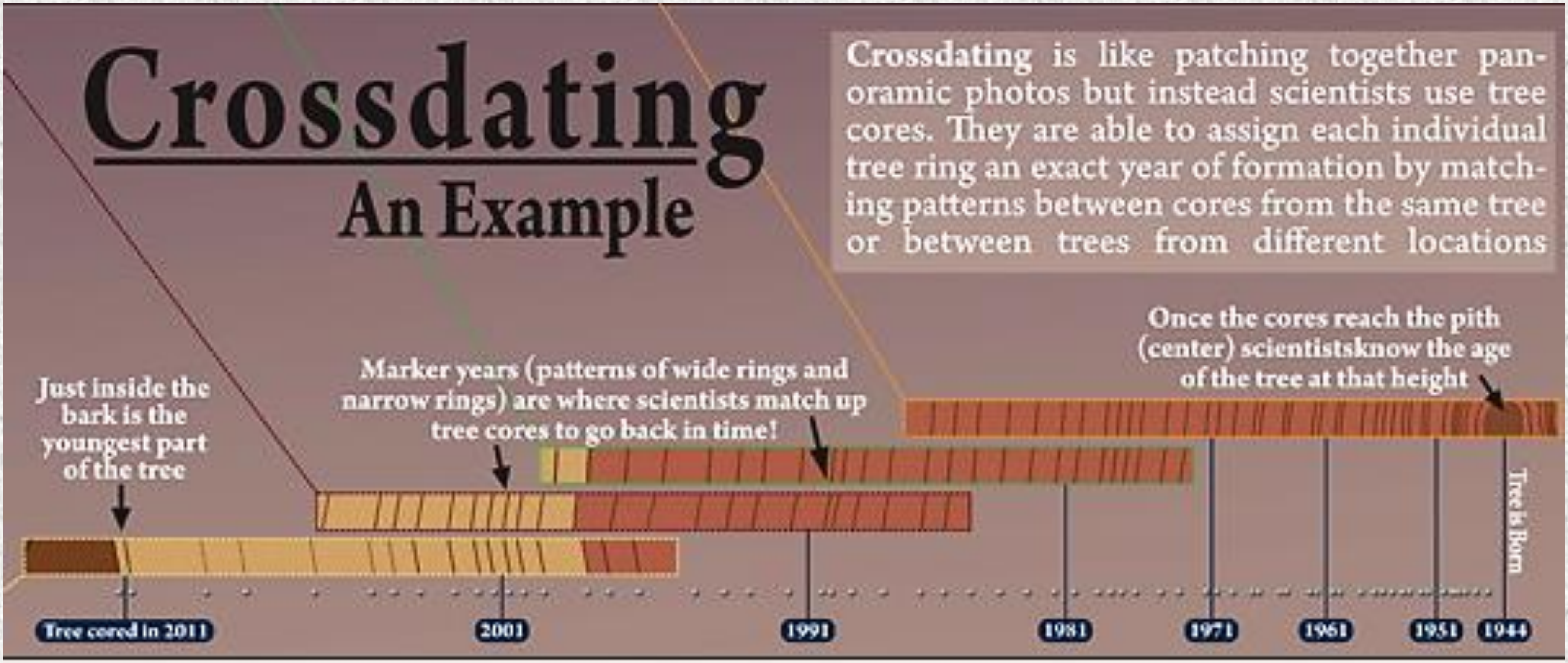
Crossdating
An Example
Crossdating is like patching together panoramic photos but instead scientists use tree cores. They are able to assign each individual tree ring an exact year of formation by matching patterns between cores from the same tree or between trees from different locations
Once the cores reach the pith (center) scientistsknow the age of the tree at that height
Marker years (patterns of wide rings and narrow rings) are where scientists match up tree cores to go back in time!
Just inside the bark is the youngest part of the tree
Tree is Born
Tree cored in 2011
2001
1991
1981
1971
1961
1951
1944

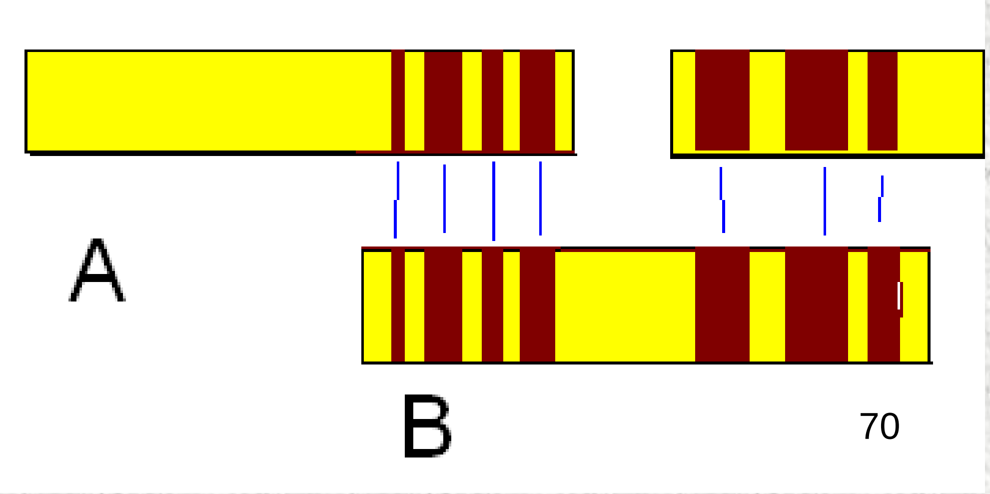
A
B

A case study:
joint application of tree-ring stable carbon and oxygen (δ13C and δ18O) isotopes

Recent European drought extremes beyond Common Era background variability

Ulf Büntgen, Otmar Urban, Paul J. Krusic, Michal Rybníček, Tomáš Kolář, Tomáš Kyncl, Alexander Ač, Eva Koňasová, Josef Čáslavský, Jan Esper, Sebastian Wagner, Matthias Saurer, Willy Tegel, Petr Dobrovolný, Paolo Cherubini, Frederick Reinig & Miroslav Trnka

Nature Geoscience (2021)

https://www.nature.com/articles/s41561-021-00698-0?fbclid=IwAR1HEPRr6TVpjb_WIRJgCXc6U9TXpLikf7FxqTTsGzSonaOm8OKnHmuKP9s

Growth characteristics and temporal coverage of the central European oak stable isotope dataset.

From: Recent European drought extremes beyond Common Era background variabilit

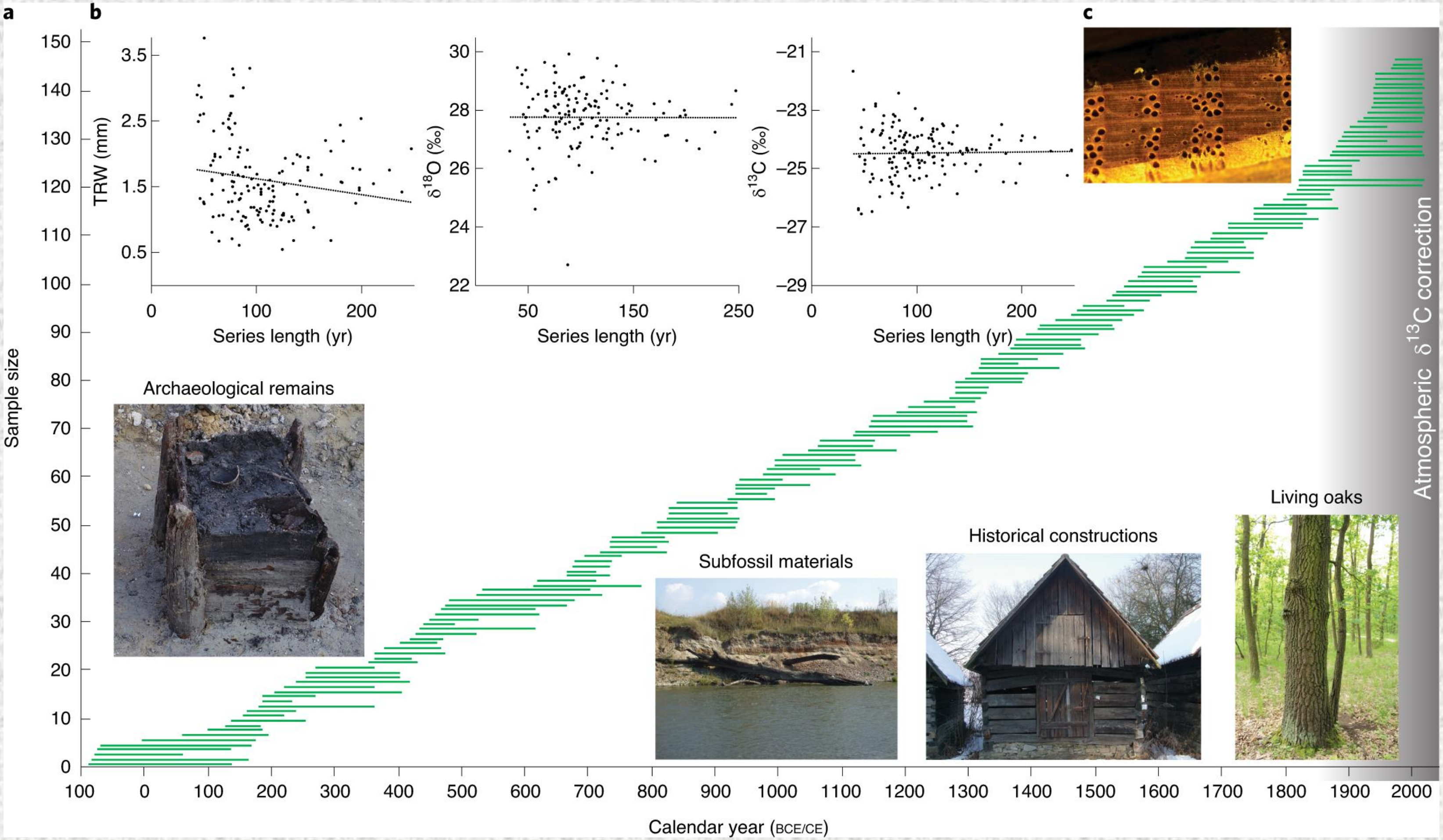

a, Temporal distribution of 147 living, historical, archaeological and subfossil oaks (green bars). The photographs at the bottom show examples of archaeological remains, subfossil materials, historical constructions and living oaks, and the grey shading on the right refers to the industrial period during which anthropogenic fossil fuel emissions affect the isotopic composition of CO_2. **b**, Annually resolved TRW (left), $\delta^{18}O$ (middle) and $\delta^{13}C$ (right) measurement series aligned by their cambial ages (series length). The mean TRW, $\delta^{18}O$ and $\delta^{13}C$ values are 1.6 mm, 27.8‰ and −24.4‰, respectively (Extended Data Fig. 2). **c**, Microscopic amplification of an oak core sample that shows a sequence of well-defined tree rings. Non-pooled TRSI measurements were extracted exclusively from the latewood alpha cellulose

(TRW - tree-ring width; TRSI - tree-ring stable isotope)

Reconstructed central European summer variability over the past 2,110 years.

From: Recent European drought extremes beyond Common Era background variability

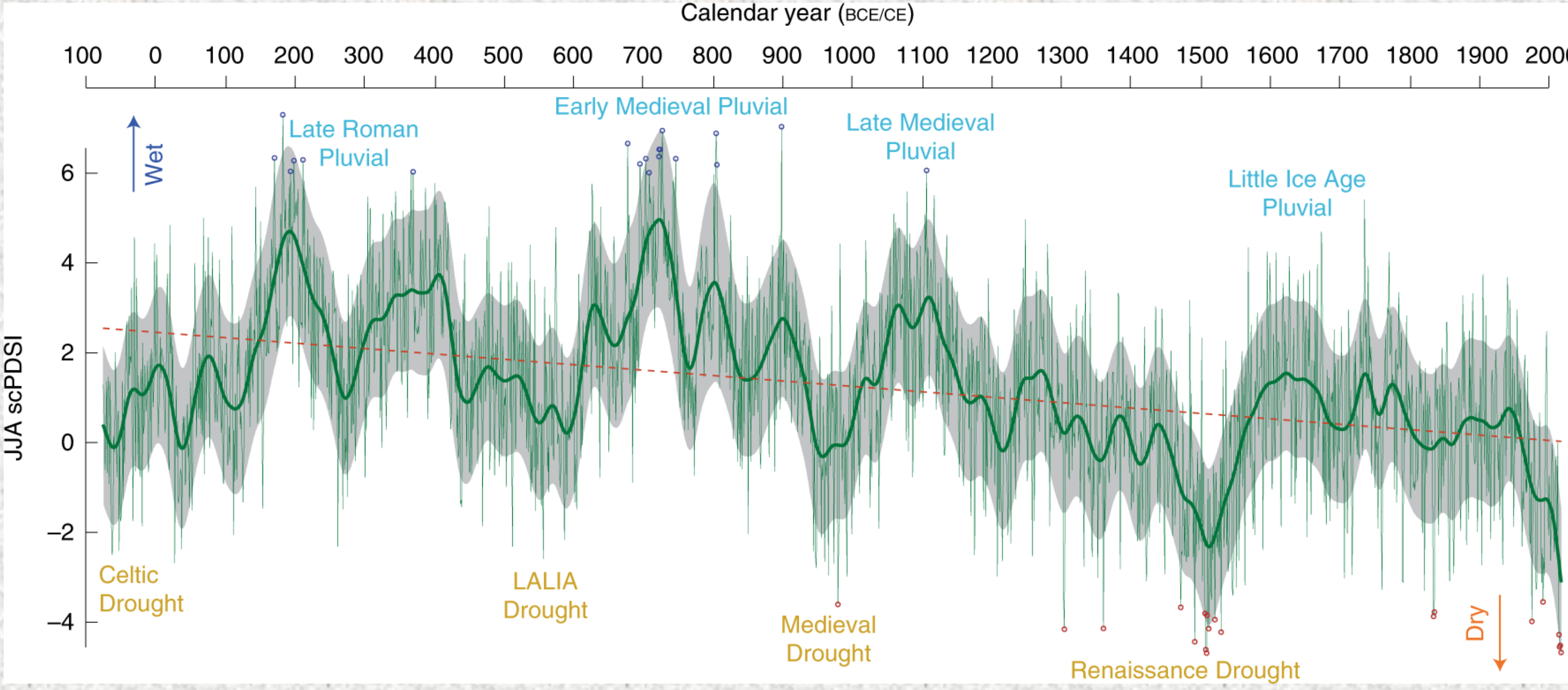

Reconstructed JJA scPDSI from 75 BCE to 2018 CE (Supplementary Data 2). The thick green curve is a 50 yr cubic smoothing spline of the annual values, and the red and blue circles show the 20 lowest and highest reconstructed values, respectively (Extended Data Fig. 6). The grey shading refers to the confidence limits after smoothing, and the dashed line represents the highly significant long-term drying trend ($y = -0.0012x + 2.4561$, $R^2 = 0.1281$).

(PDSI - Palmer Drought Severity Index, based on a supply-and-demand model of soil moisture; scPDSI - self-calibratedPDSI; JJA - June, July and August; LALIA - Late Antique Little Ice Age)

https://www.nature.com/articles/s41561-021-00698-0/figures/4

Temporal and spatial agreement between the oak stable isotopes and European summer drought.

From: Recent European drought extremes beyond Common Era background variability

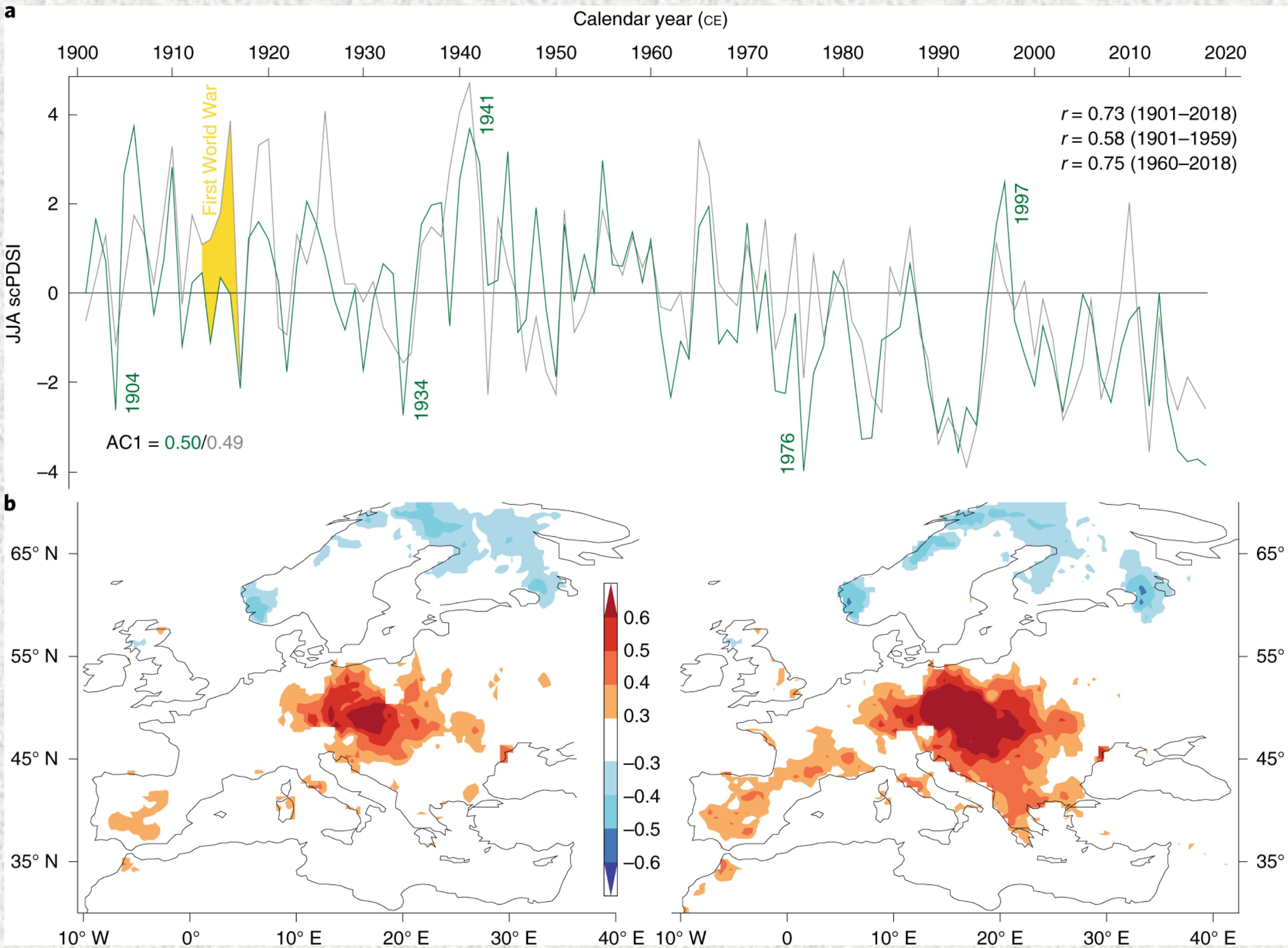

a, Actual (grey; averaged over 49–50° N and 15–18° E) and reconstructed (green; compound TRSI) JJA scPDSI. AC1 of the proxy and target data is provided at bottom left, whereas *r* values between the proxy and target data over the full and two early/late split periods are provided at the top right. **b**, High-resolution, 0.5° spatial correlation coefficients (colour scale) between the TRSI proxy data and the gridded European-wide scPDSI target data (left) and the regional average of the gridded scPDSI target data and European-wide gridded scPDSI target data (right) over the common period 1901–2018 CE.

https://www.nature.com/articles/s41561-021-00698-0?fbclid=IwAR1HFPRr6TVpib_WIRJqCXc6U9TXpLikf7FxqTTsGzSonaQm8QKnHmuKP9s

DATING METHODS IN THE QUATERNARY STUDIES

ABSOLUTE DATING METHODS

9. Varve-, and dendrochronology

“Absolute” methods or numerical age estimation

10. Non-stable (radioactive) isotopes

- 10/a Potassium-argon series
  - $^{40}K/^{40}Ar$
  - $^{40}Ar/^{39}Ar$
  - laser fusion $^{40}Ar/^{39}Ar$
- 10/b Uranium decay series
  - $^{238}U/^{230}Th$
  - $^{234}U/^{230}Th$
  - $^{230}Th/^{231}Pa$ (^{235}U)
- 10/c Fission-track (^{238}U)
- 10/d Radiocarbon dating (^{14}C)

Sir Edward Rutherford:

based on the decay time (half-lives) of radioactive elements, the age of the rocks can be determined

Radioactive decay

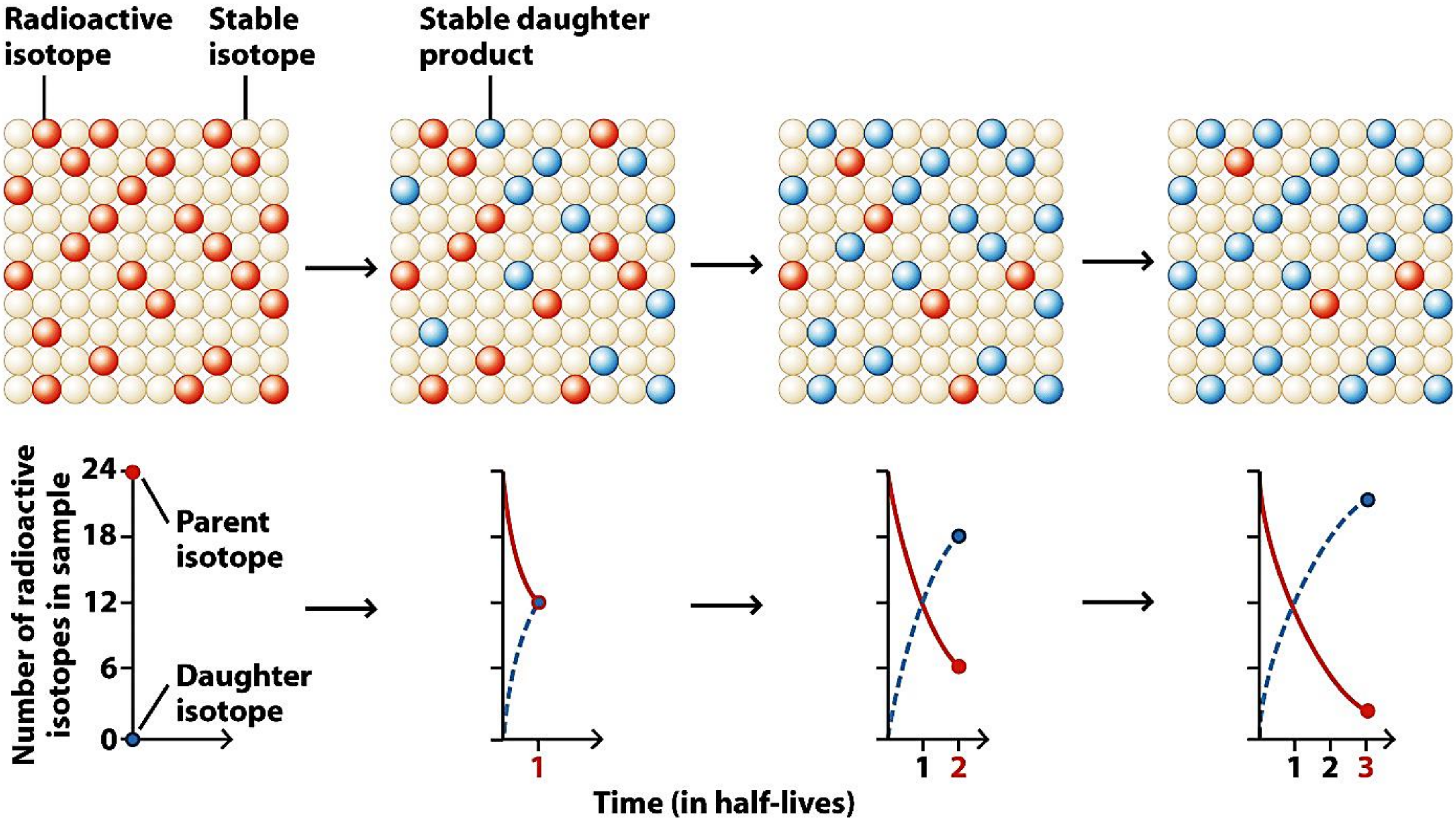

Figure 2-8
Earth's Climate: Past and Future, Second Edition

DATING METHODS IN THE QUATERNARY STUDIES

ABSOLUTE DATING METHODS

9. Varve-, and dendrochronology

“Absolute” methods or numerical age estimation

10. Non-stable (radioactive) isotopes

10/a Potassium-argon series

$^{40}K/^{40}Ar$

$^{40}Ar/^{39}Ar$

laser fusion $^{40}Ar/^{39}Ar$

10/b Uranium decay series

$^{238}U/^{230}Th$

$^{234}U/^{230}Th$

$^{230}Th/^{231}Pa$ (^{235}U)

10/c Fission-track (^{238}U)

10/d Radiocarbon dating (^{14}C)

11. Luminescence methods

-Thermoluminescence (TL)

-Optically stimulated luminescence (OSL)

InfraRed Stimulated Luminescence (IRSL)

12. Electron-spin resonance (ESR)

13. Cosmogenic isotopes

Potassium, Argon, and Calcium Rate Changes

$$^{40}_{19}K + ^{0}_{-1}e \xrightarrow{\text{electron capture}} ^{40}_{18}Ar + ^{0}_{0}\nu$$

$$^{40}_{19}K \xrightarrow{\text{positron decay}} ^{40}_{18}Ar + ^{0}_{+1}e + ^{0}_{0}\nu$$

$$^{40}_{19}K \xrightarrow{\text{beta decay}} ^{40}_{20}Ca + ^{0}_{-1}e + ^{0}_{0}\bar{\nu}$$

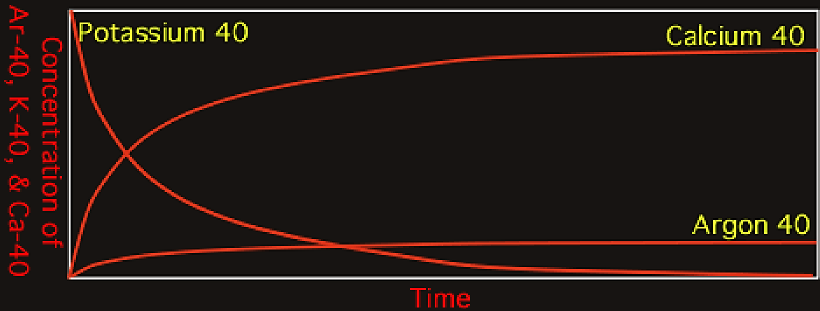

Argon 40 accumulates in the rock. Naturally occuring Ar 40 is assumed to have escaped when the rock was hot. Calcium 40 is produced in the rock but there is no way to make any measurements of the accumulating Ca 40. Naturally occuring Ca 40 would contaminate the measurements. Potassium 40 is used up in the rock. It breaks down into both Ar 40 & Ca 40.

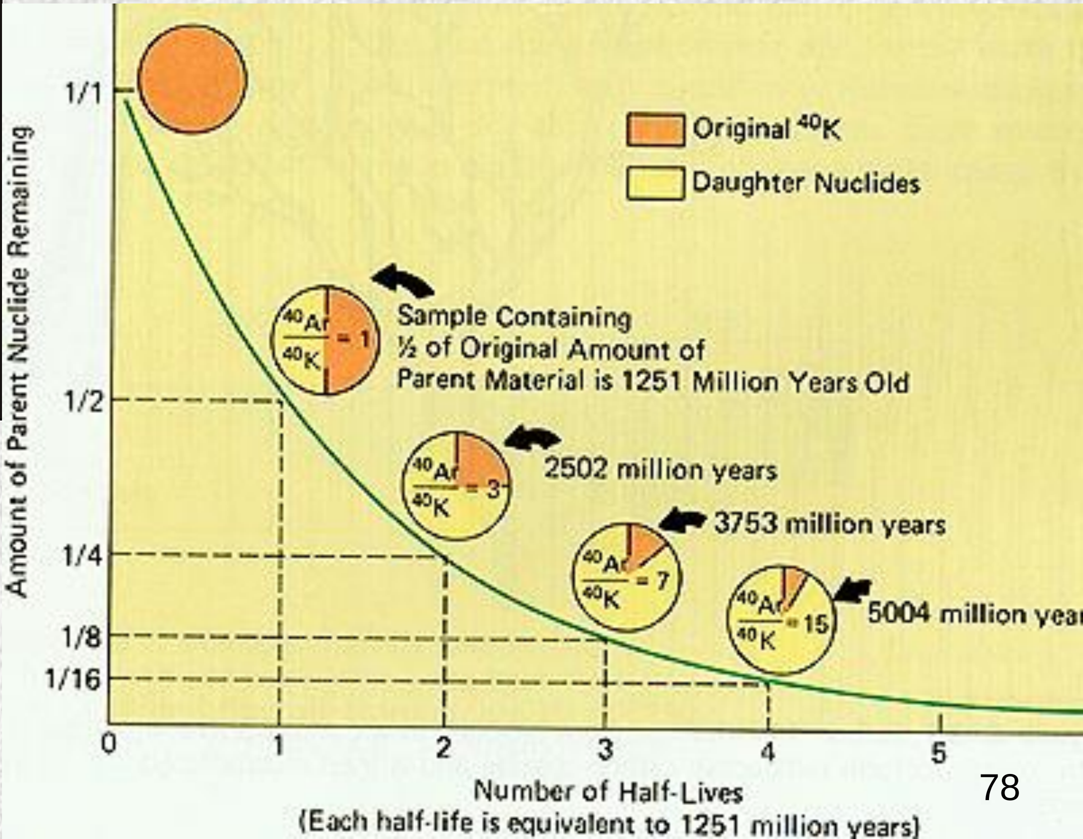

- 10/a Potassium argon series

$^{40}K/^{40}Ar$
$^{40}Ar/^{39}Ar$
laser fusion $^{40}Ar/^{39}Ar$

__* $^{40}K \longrightarrow {}^{40}Ar$ ($T_{1/2}$=1,25 md year, 11,71% $^{40}Ar^*$)
cooling of rock $\longrightarrow$ incorporation of atmospheric $^{40}Ar/^{36}Ar$
$\longrightarrow$ production of $^{40}Ar^*$ radioactive decay (time, K-content)
* $^{40}Ar/^{39}Ar$ (fast neutron irradiation $^{39}Ar \longrightarrow {}^{40}Ar \longrightarrow$
advantage: only Ar measurment
* laser fusion $^{40}Ar/^{39}Ar$

Gradual heating
analytical age
geological age

DATING METHODS IN THE QUATERNARY STUDIES

ABSOLUTE DATING METHODS

9. Varve-, and dendrochronology

"Absolute" methods or numerical age estimation

10. Non-stable (radioactive) isotopes

  10/a Potassium-argon series

    $^{40}K/^{40}Ar$

    $^{40}Ar/^{39}Ar$

    laser fusion $^{40}Ar/^{39}Ar$

  10/b Uranium decay series

    $^{238}U/^{230}Th$

    $^{234}U/^{230}Th$

    $^{230}Th/^{231}Pa$ (^{235}U)

  10/c Fission-track (^{238}U)

  10/d Radiocarbon dating (^{14}C)

11. Luminescence methods

  -Thermoluminescence (TL)

  -Optically stimulated luminescence (OSL)

    InfraRed Stimulated Luminescence (IRSL)

12. Electron-spin resonance (ESR)

13. Cosmogenic isotopes

Uranium-238 decay series

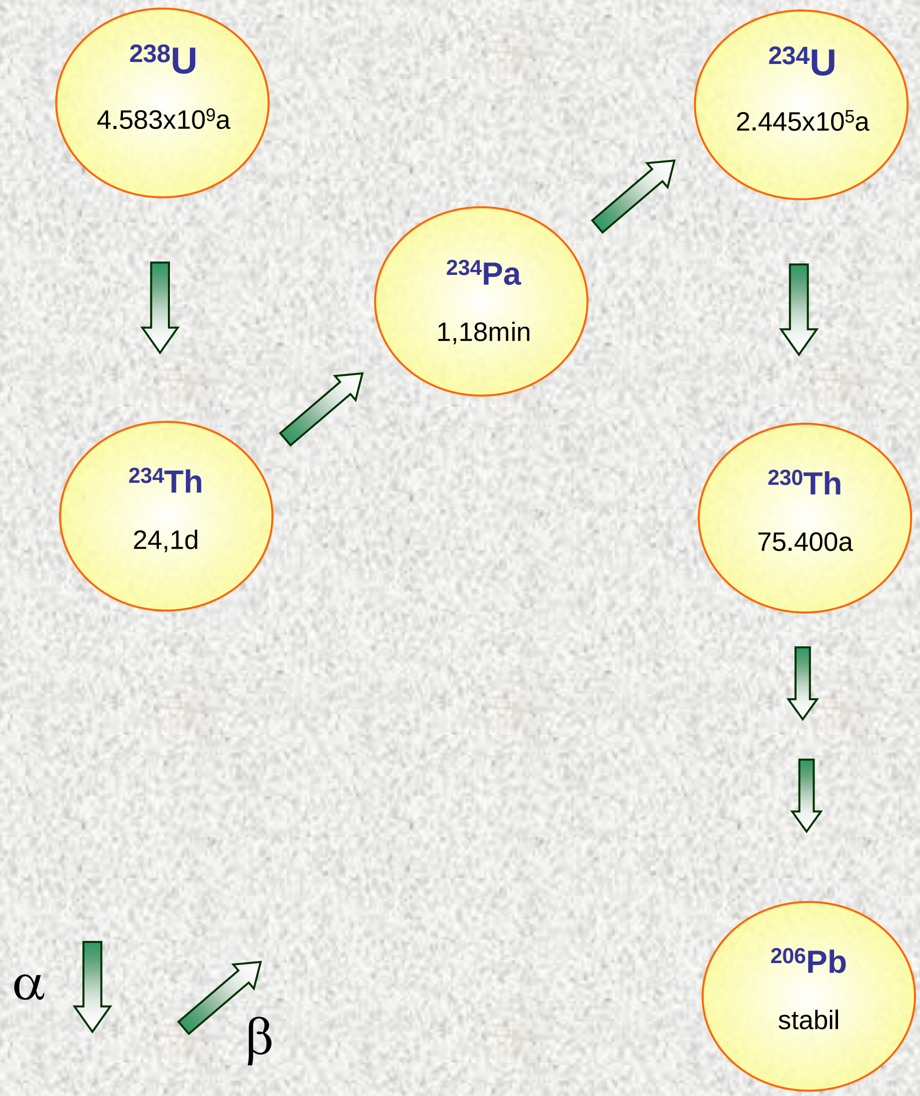

Uranium – thorium $^{234}U/^{230}Th$

- Age range:
  - 0 – 0.5 Ma
- Material:
  - Corals, cave deposits, pit, bone, mollusc's shell, tooth, travertines
- U soluble in water build into carbonate
- Th insoluble--product of decay of U = time
- Measurements: α counting, mass spectrometry

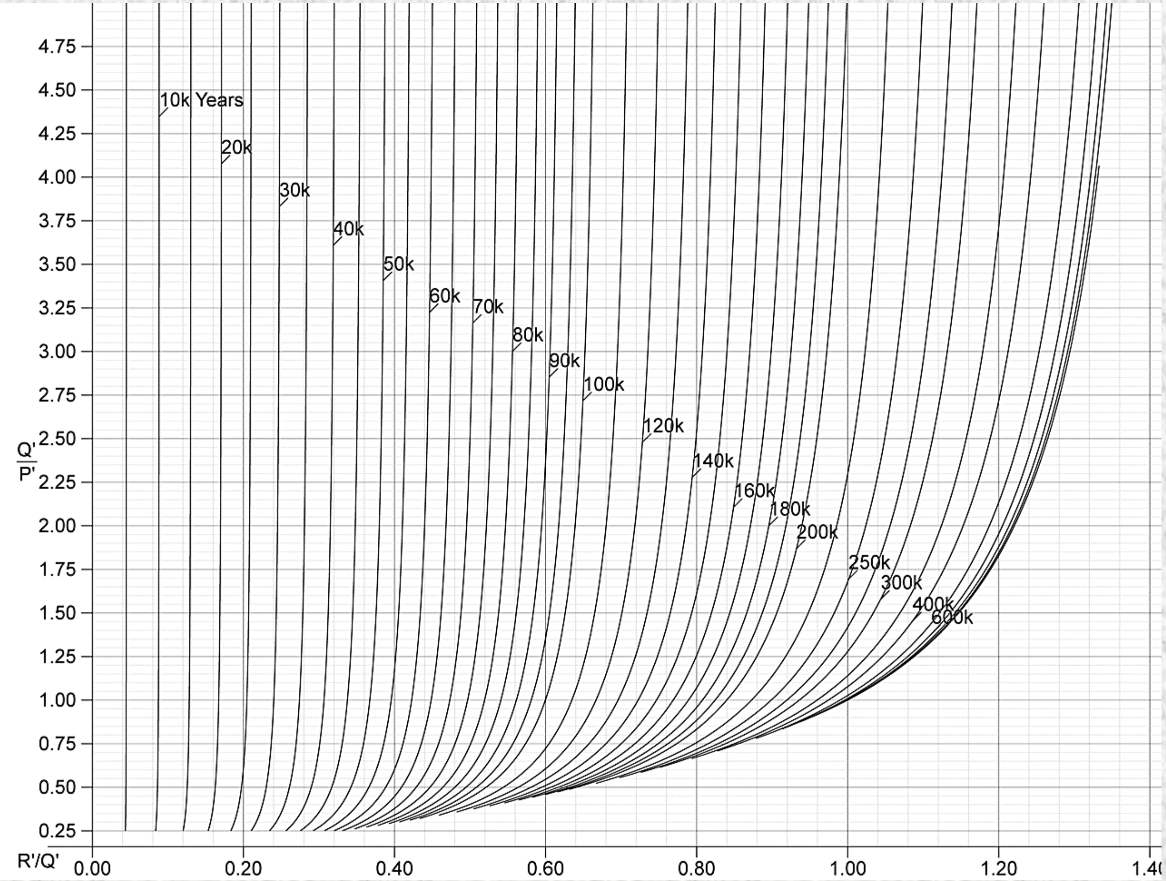

Uranium and Thorium activity ratios vs time. Q'/P' = $^{234}U/^{238}U$, R'/Q' = $^{230}Th/^{234}U$

DATING METHODS IN THE QUATERNARY STUDIES

ABSOLUTE DATING METHODS

9. Varve-, and dendrochronology

"Absolute" methods or numerical age estimation

10. Non-stable (radioactive) isotopes
    - 10/a Potassium-argon series
        - $^{40}K/^{40}Ar$
        - $^{40}Ar/^{39}Ar$
        - laser fusion $^{40}Ar/^{39}Ar$
    - 10/b Uranium decay series
        - $^{238}U/^{230}Th$
        - $^{234}U/^{230}Th$
        - $^{230}Th/^{231}Pa$ (^{235}U)
    - **10/c Fission-track (^{238}U)**
    - 10/d Radiocarbon dating (^{14}C)
11. Luminescence methods
    - -Thermoluminescence (TL)
    - -Optically stimulated luminescence (OSL)
        - InfraRed Stimulated Luminescence (IRSL)
12. Electron-spin resonance (ESR)
13. Cosmogenic isotopes

Fission Tracks:

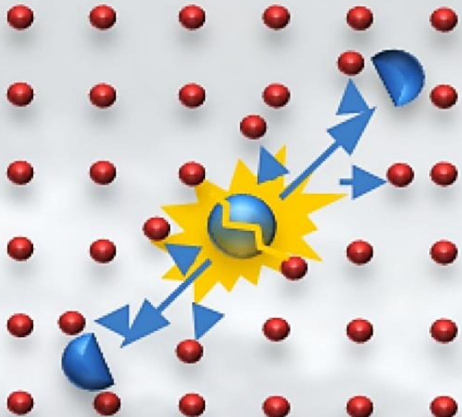

Spontaneous fission of ^{238}U

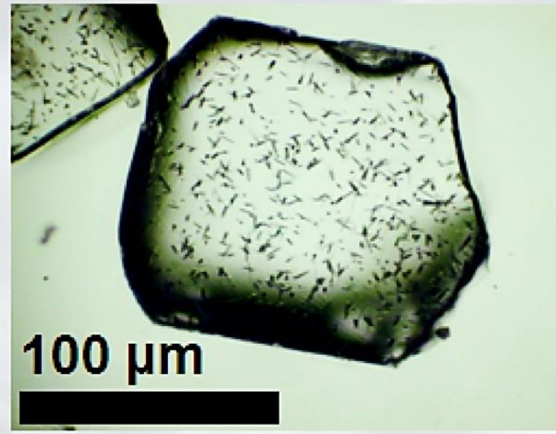

Fission Tracks in crystal

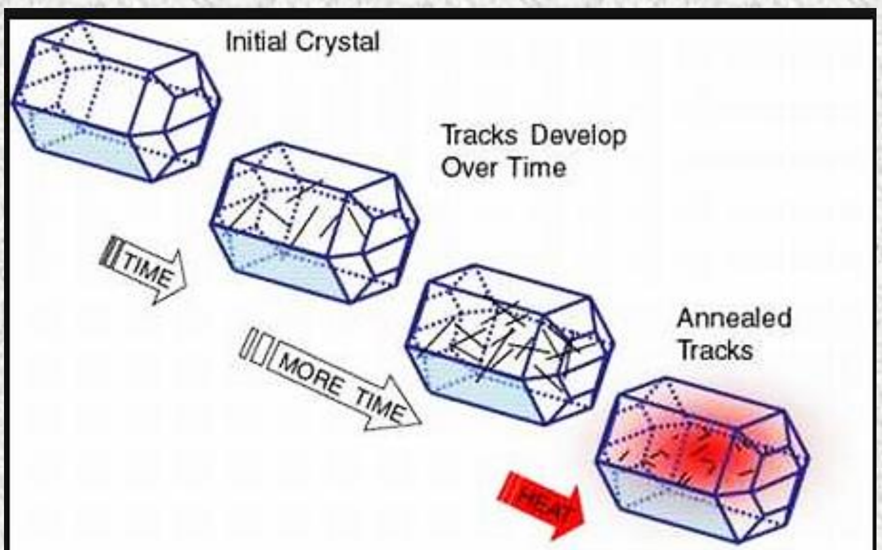

DATING METHODS IN THE QUATERNARY STUDIES

ABSOLUTE DATING METHODS

9. Varve-, and dendrochronology

“Absolute” methods or numerical age estimation

10. Non-stable (radioactive) isotopes

10/a Potassium-argon series

$^{40}K/^{40}Ar$

$^{40}Ar/^{39}Ar$

laser fusion $^{40}Ar/^{39}Ar$

10/b Uranium decay series

$^{238}U/^{230}Th$

$^{234}U/^{230}Th$

$^{230}Th/^{231}Pa$ (^{235}U)

10/c Fission-track (^{238}U)

10/d Radiocarbon dating (^{14}C)

11. Luminescence methods

-Thermoluminescence (TL)

-Optically stimulated luminescence (OSL)

InfraRed Stimulated Luminescence (IRSL)

12. Electron-spin resonance (ESR)

13. Cosmogenic isotopes

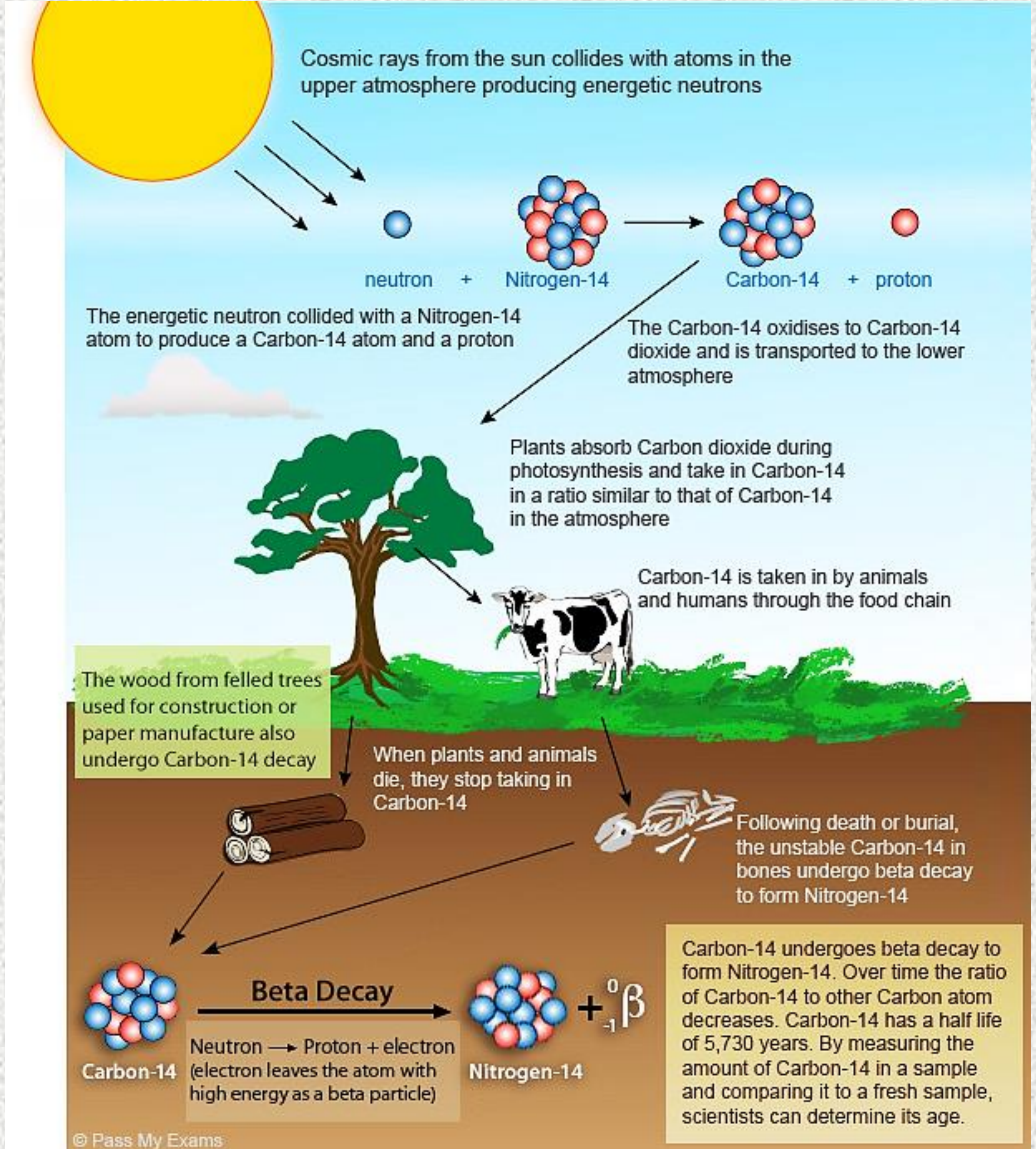

Radiocarbon

^{14}C

Beta-decay

$T_{1/2}$= 5730 year

http://www.passmyexams.co.uk/GCSE/physics/radiocarbon-dating.html

Natural ^{14}C (radiocarbon)

Cosmic ray

↓

neutrons

↓

$^{14}N\,(n,p)\,^{14}C$

^{14}C production

Equilibrium!

51 tonns ^{14}C

Radioactive carbon! $^{14}C \xrightarrow[160\ keV]{\beta^-} {}^{14}N$

$T_{½}$ = 5730 year

^{14}C depletion

$^{14}C \longrightarrow {}^{14}CO_2$

$^{14}CO_2$ will become part of the coal-circle of the Earth!

The ^{14}C-content of the atmospheric carbon reservoir is constant!
(13,6 dpm / g carbon)

^{14}C distribution:

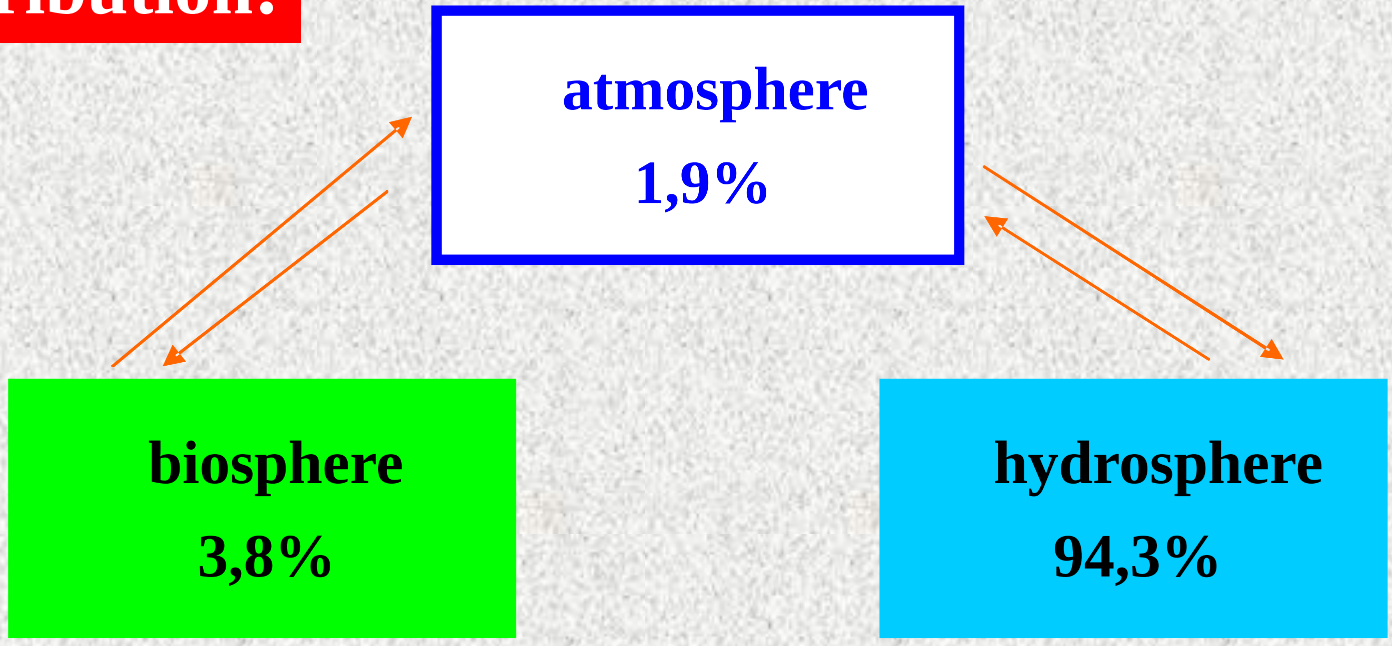

Dating based on the measurment of ^{14}C amount (activity)

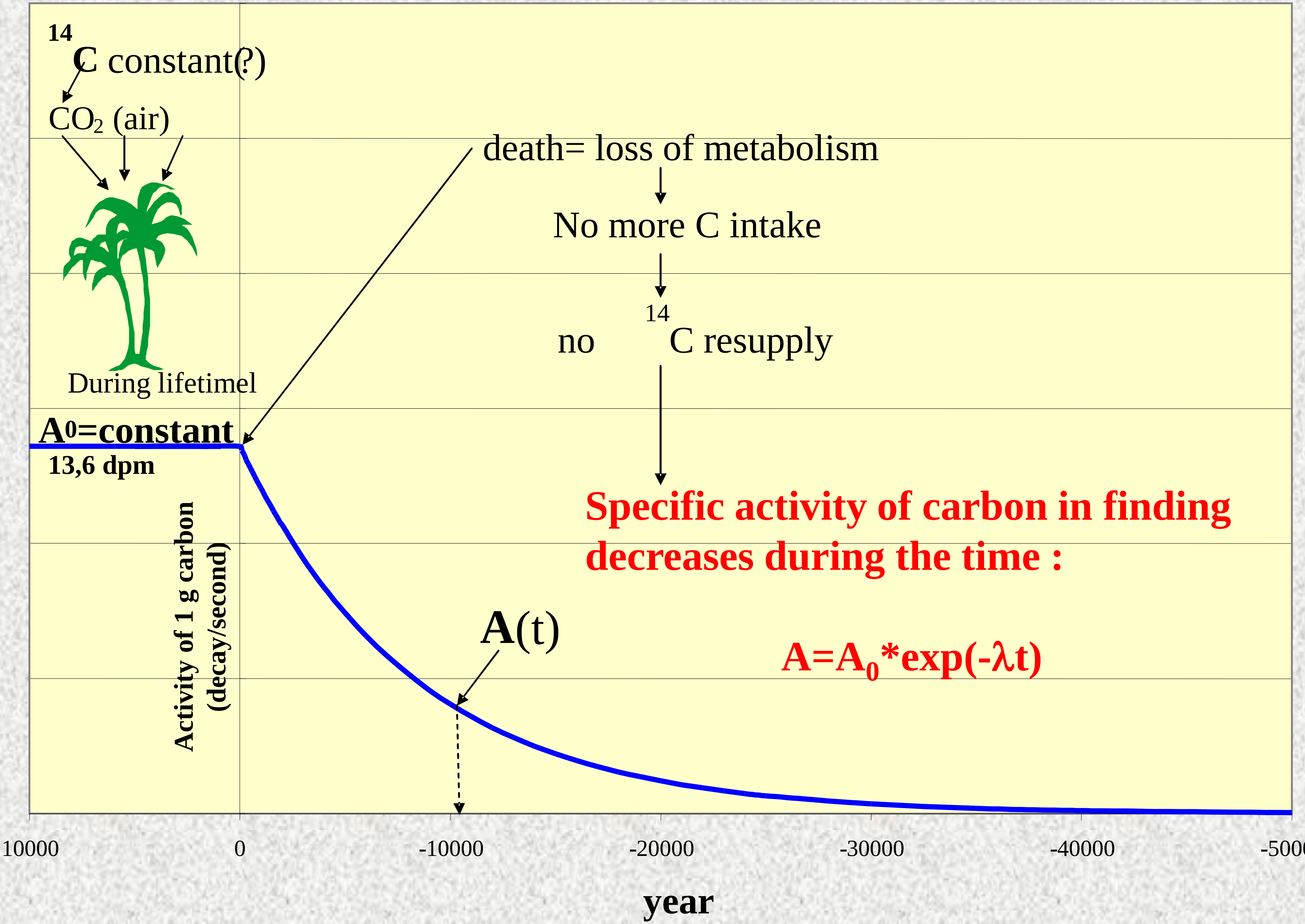

Conventional radiocarbon ages:

$$t(\text{year}) = \frac{5568}{\ln 2} * \ln\left(\frac{A_{\text{begin}}}{A}\right)$$

Most accurate half-lives of ^{14}C (when the theory is created – in 1950):

5568 years

Assumption**:** *A* $_{begin}$ **constant**, atmospheric concentration of ^{14}C did not change during time, the same as it was in 1950.

Agreement: all age is given relative to A.D.1950.
Example:
if the **conventional radiocarbon age** is **2500 years BP** (before present), the calendar time is A.D. 550 years:

1950-2500 = -550, **i.e. A.D. 550 ….**

Materials to date:

Everything containing atmospheric carbon.

Wood, charcoal, seed, leaf, canvas, peat, humus, bone, ivory, cloth, horn, hair, shell, snail, carbonate, stalagtit, soil, organic and inorganic carbon dissolved in water, ice…

Usually not suitable for dating: plaster, mortar, organic material in ceramics

<u>**Suitable with special technique:**</u> *paintings*, *cave paintings*, *carbon in iron tools*.

The amount of sample depends on:

Carbon content, the condition of the organic material, amount of contamination, and the method

Deviation from the BP age because of the different atmospheric radiocarbon content in the past

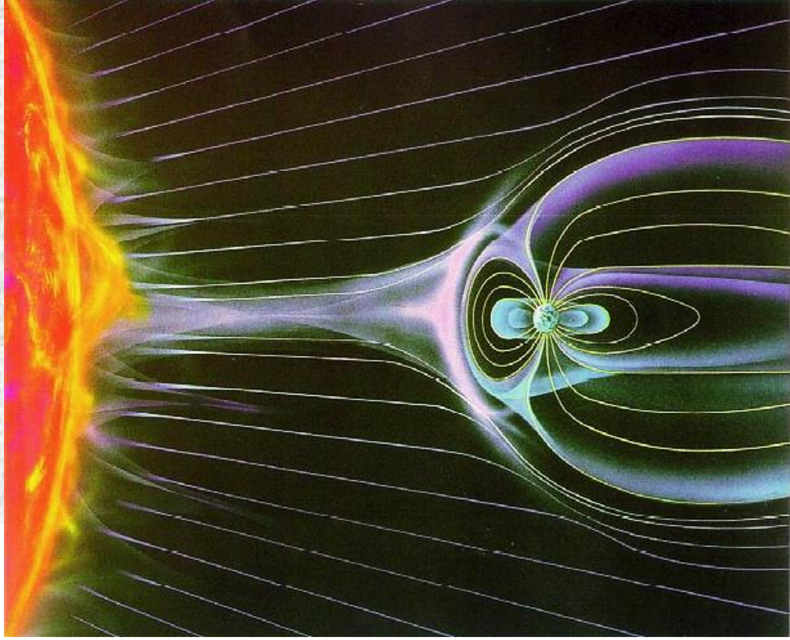

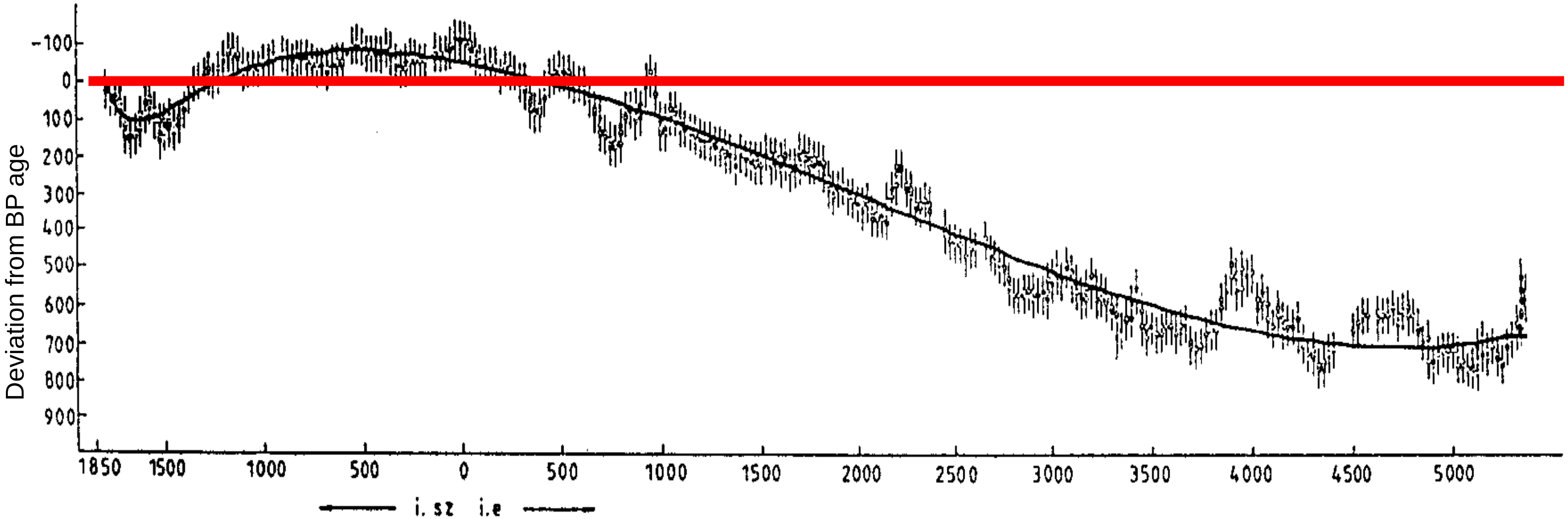

Changes in the ^{14}C concentration due to human impact

Suess-effect: use of the fossil fuel caused the increase of the inactive CO_2 concentration in the atmosphere →

until 1952: 3% decrease of the ^{14}C concentration

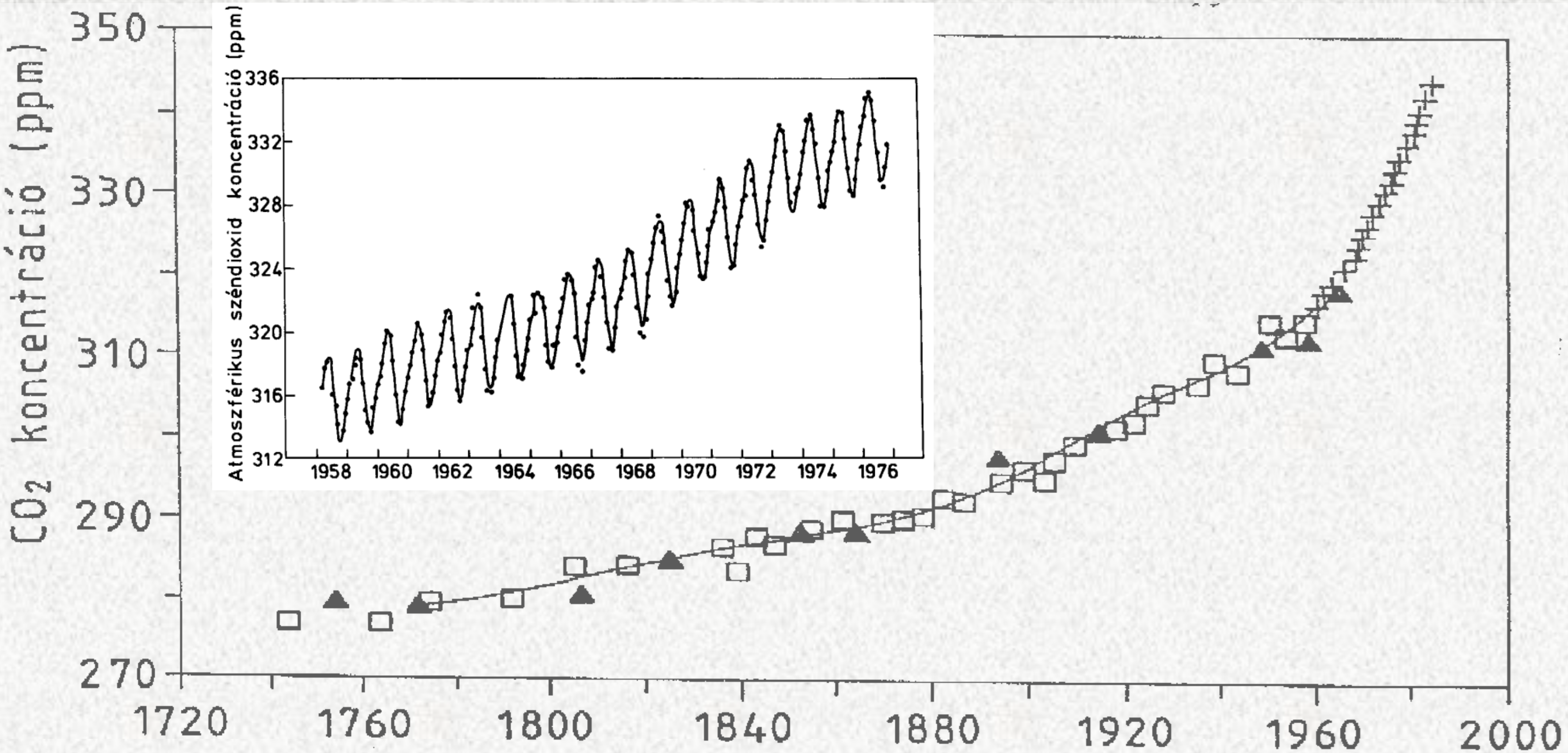

Nuclear weapon tests

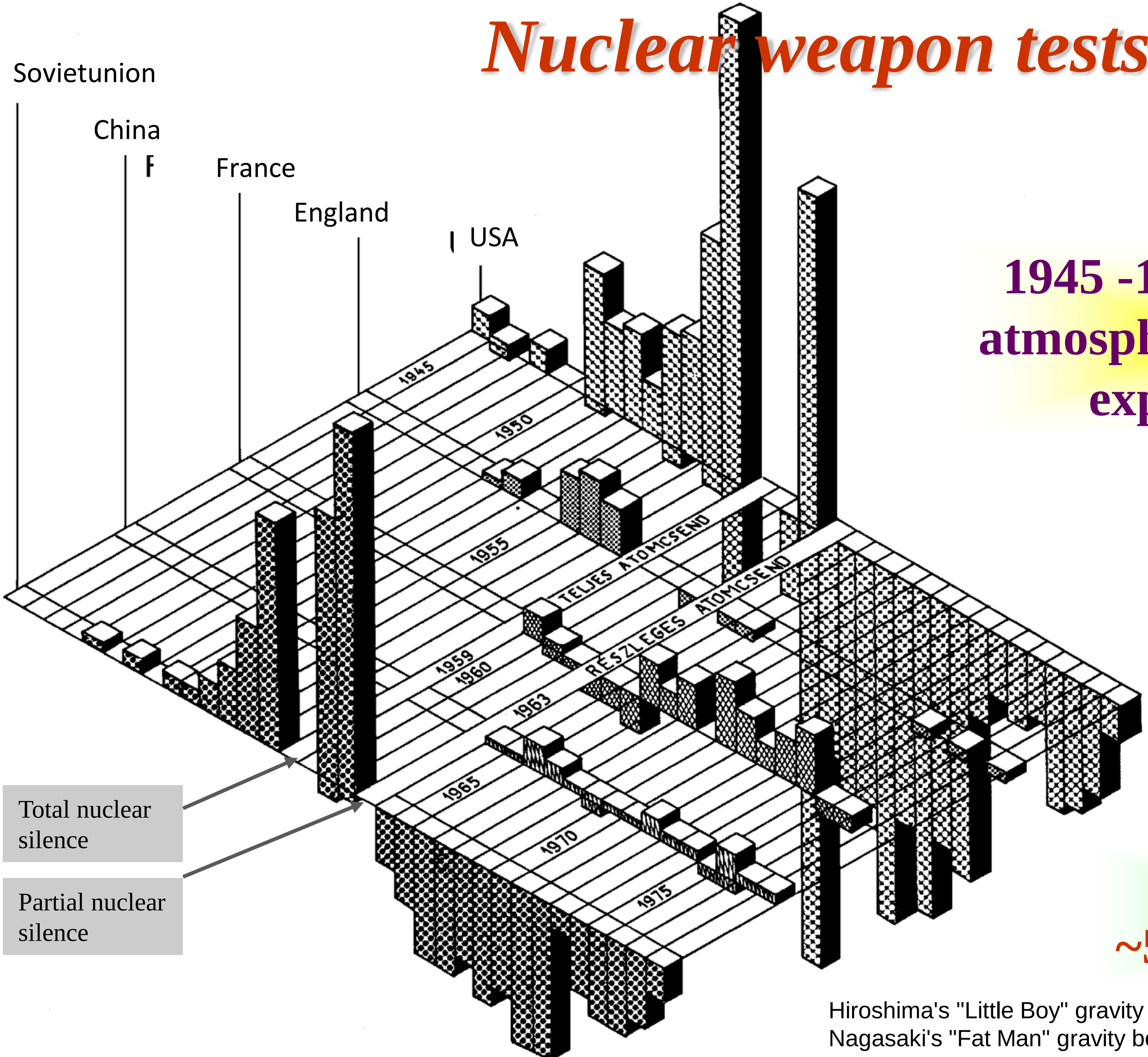

1945 -1962 ca. 400 atmospheric nuclear explosions

All power: ~500 Mt TNT

Hiroshima's "Little Boy" gravity bomb:13–18 kt TNT
Nagasaki's "Fat Man" gravity bomb: 19–23 kt TNT
>1400x!

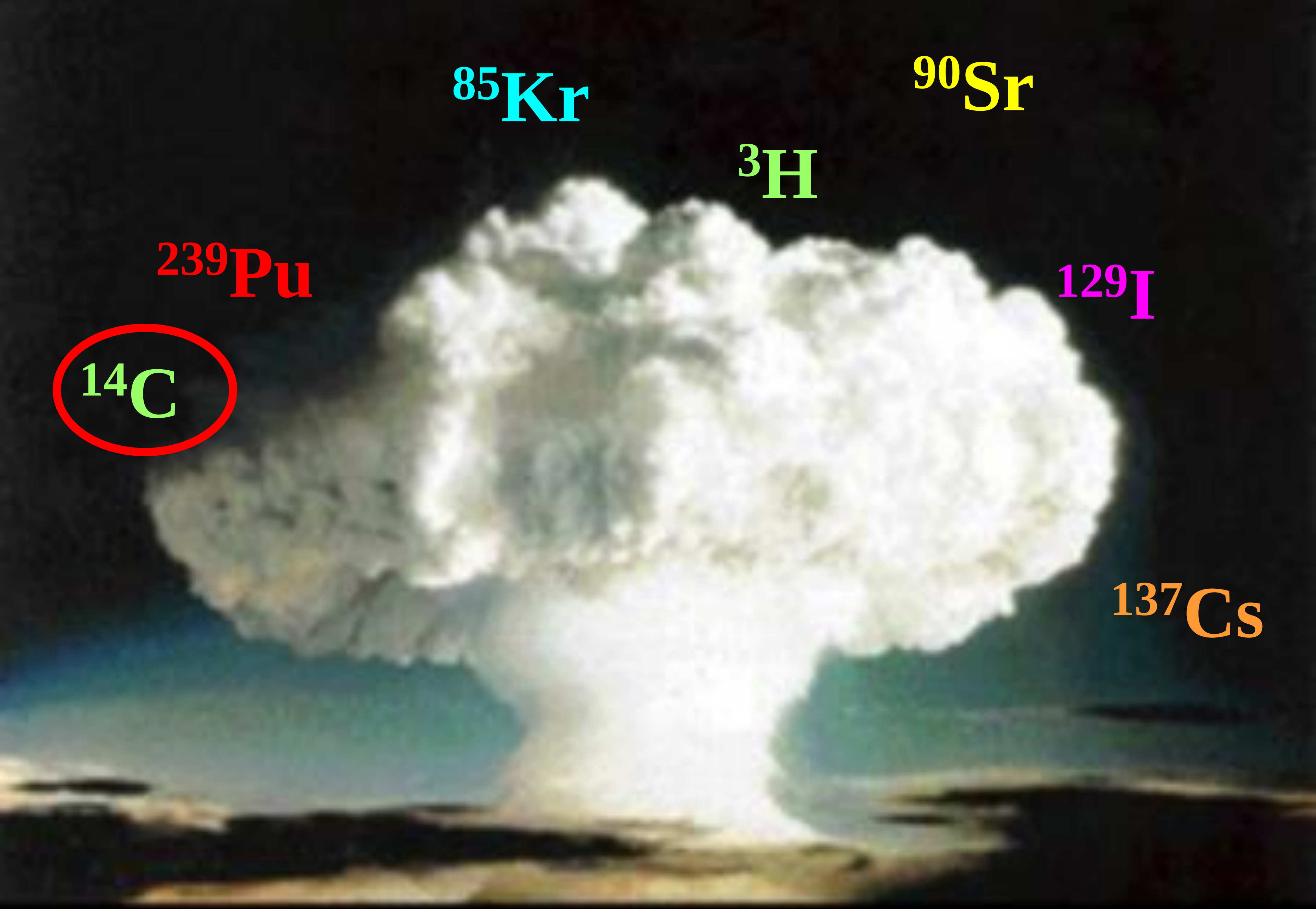
^{85}Kr
^{90}Sr
^{3}H
^{239}Pu
^{129}I
^{14}C
^{137}Cs

Amount of ^{14}C in the atmosphere due to the nuclear tests:

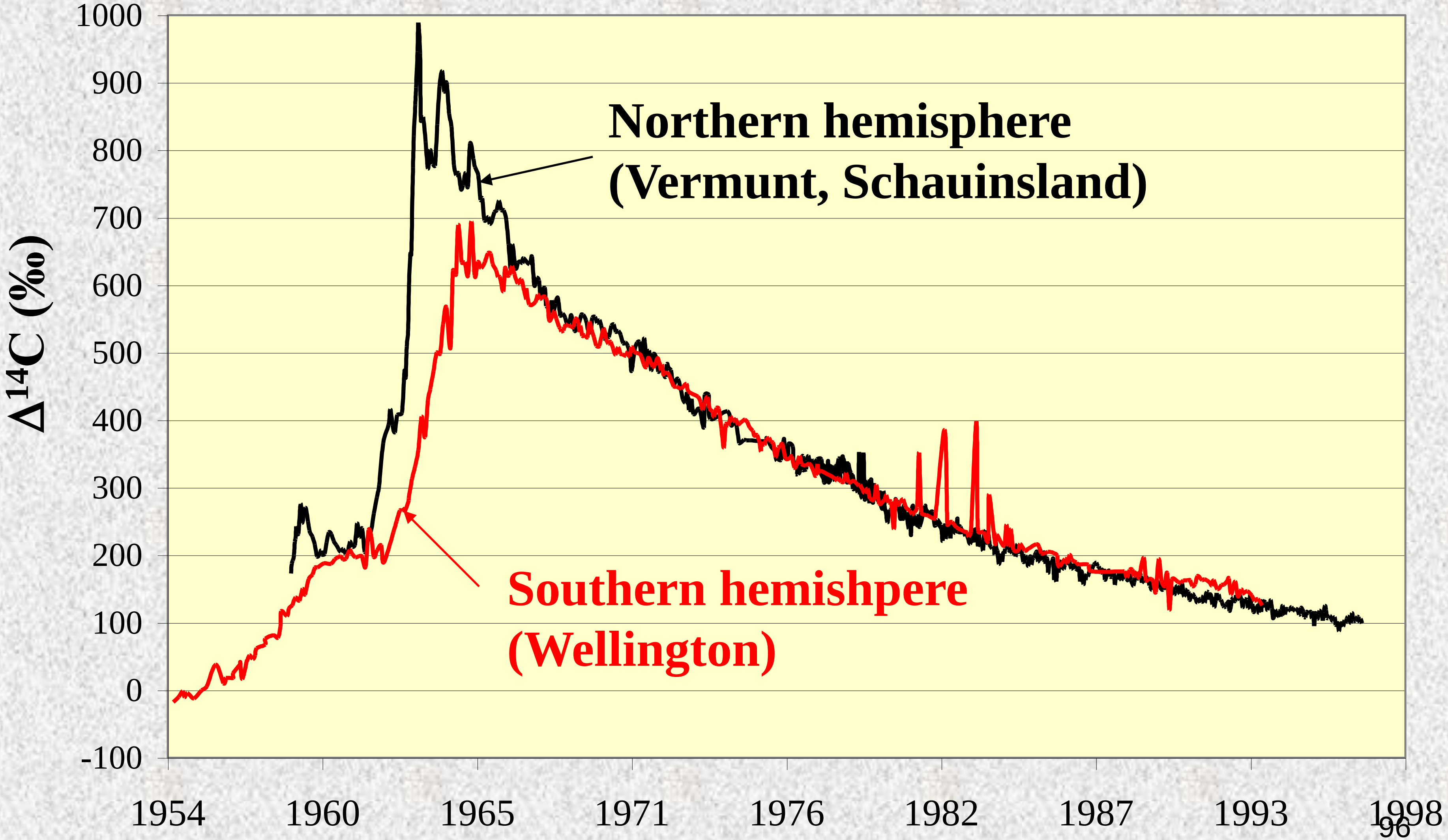

The carbon content of tree ring represents the actual 14C concentration of the atmosphere

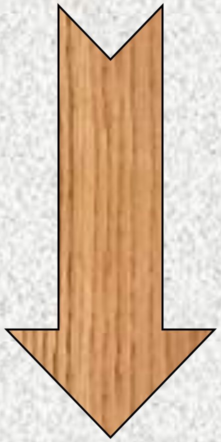

The annual change can be monitored by radiocarbon activity measurement of the annual tree rings

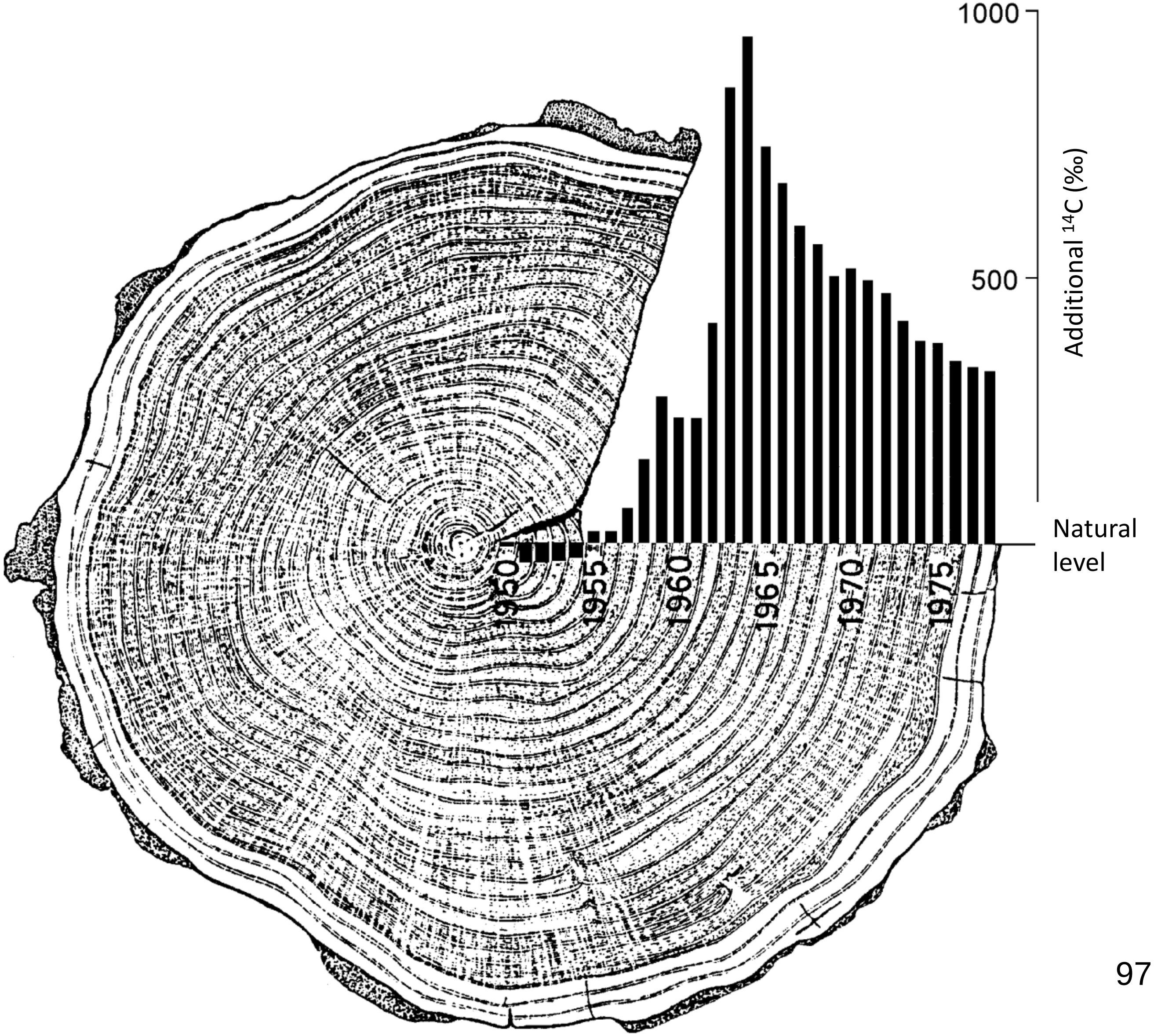

How radiocarbon calibration works

Calibration of radiocarbon determinations is in principle very simple. If you have a radiocarbon measurement on a sample, you can try to find a **tree ring with the same proportion of radiocarbon**. Since the calendar age of the tree rings is known, this then tells you the age of your sample. In practice this is complicated by two factors:

- the measurements on both the tree rings and the samples have a **limited precision** and so there will be a range of possible calendar years
- given the way the atmospheric radiocarbon concentration has varied, there might be several possible ranges

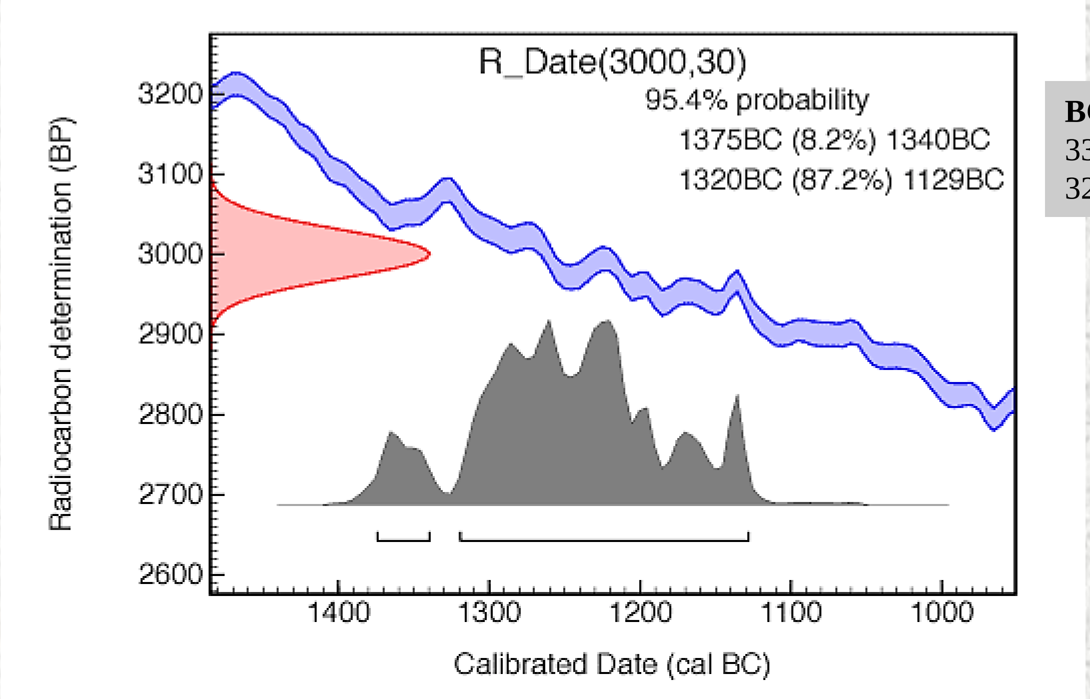

BC converted into cal BP *(BC+1950)*
3325 cal BP (8.2%) 3290 cal BP
3270 cal BP (87.2%) 3076 cal BP

The radiocarbon measurement **3000+-30BP would be calibrated**. The left-hand axis shows *radiocarbon concentration* expressed in years `before present' and the bottom axis shows *calendar years* (derived from the tree ring data). The pair of blue curves show the *radiocarbon measurements on the tree rings* (plus and minus one standard deviation) and the red curve on the left indicates the radiocarbon concentration in the sample. The grey histogram shows possible ages for the sample (the higher the histogram the more likely that age is).

The results of calibration are often given as an age range. In this case, we might say that we could be 95% sure that the sample comes from between 1375 cal BC and 1129 cal BC.

(*https://c14.arch.ox.ac.uk/calibration.html*)

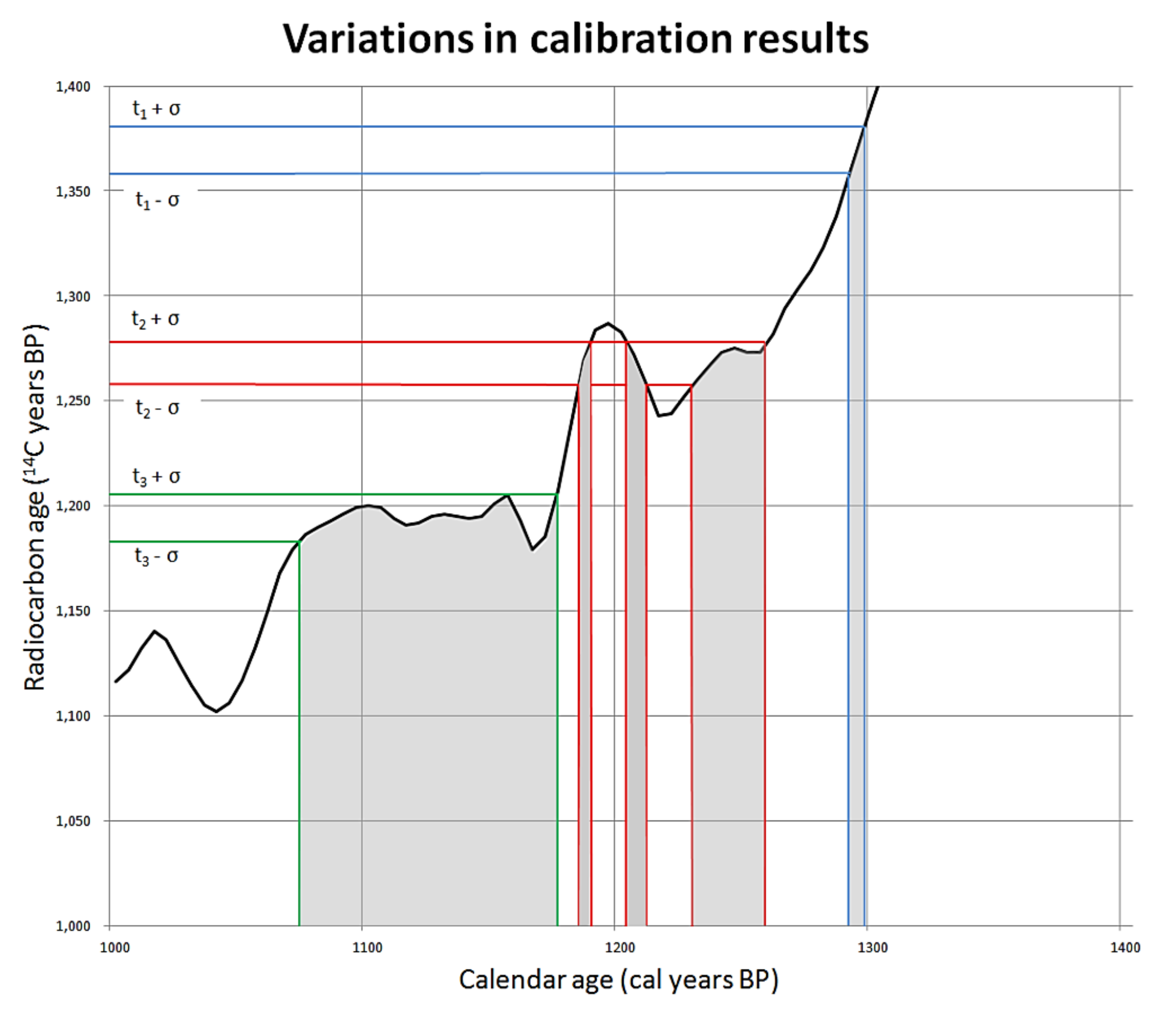

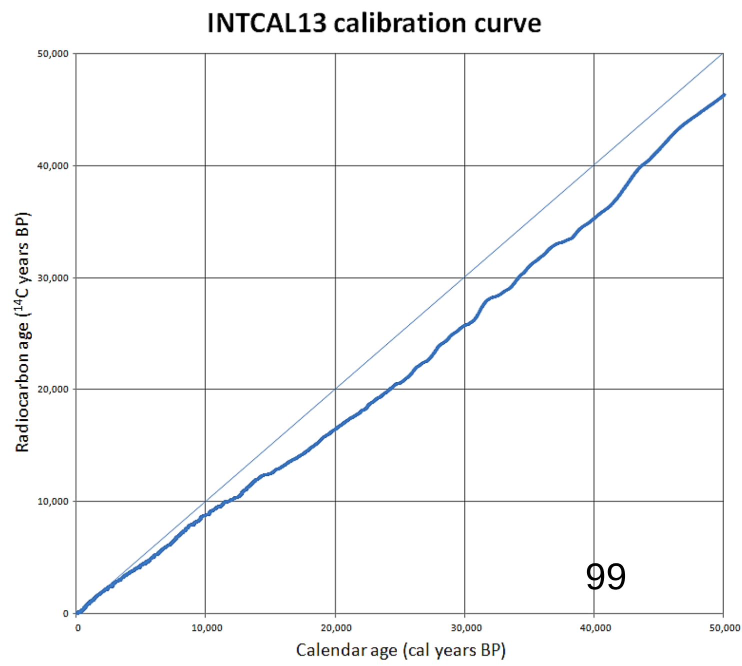

Online calibration of conventional radiocarbon ages:
http://www.calpal-online.de/
https://iosacal.readthedocs.io/en/latest/

DATING METHODS IN THE QUATERNARY STUDIES

ABSOLUTE DATING METHODS

9. Varve-, and dendrochronology

"Absolute" methods or numerical age estimation

10. Non-stable (radioactive) isotopes
    - 10/a Potassium-argon series
        - $^{40}K/^{40}Ar$
        - $^{40}Ar/^{39}Ar$
        - laser fusion $^{40}Ar/^{39}Ar$
    - 10/b Uranium decay series
        - $^{238}U/^{230}Th$
        - $^{234}U/^{230}Th$
        - $^{230}Th/^{231}Pa$ (^{235}U)
    - 10/c Fission-track (^{238}U)
    - 10/d Radiocarbon dating (^{14}C)

11. Luminescence methods
    - -Thermoluminescence (TL)
    - -Optically stimulated luminescence (OSL)
        - InfraRed Stimulated Luminescence (IRSL)

12. Electron-spin resonance (ESR)

13. Cosmogenic isotopes

Luminescence signal

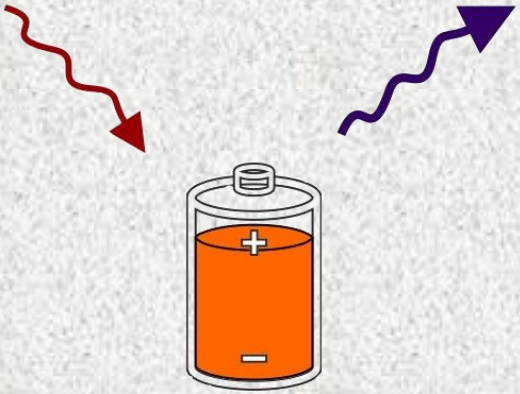

Principle of Optically Stimulated Luminescence (**OSL**)

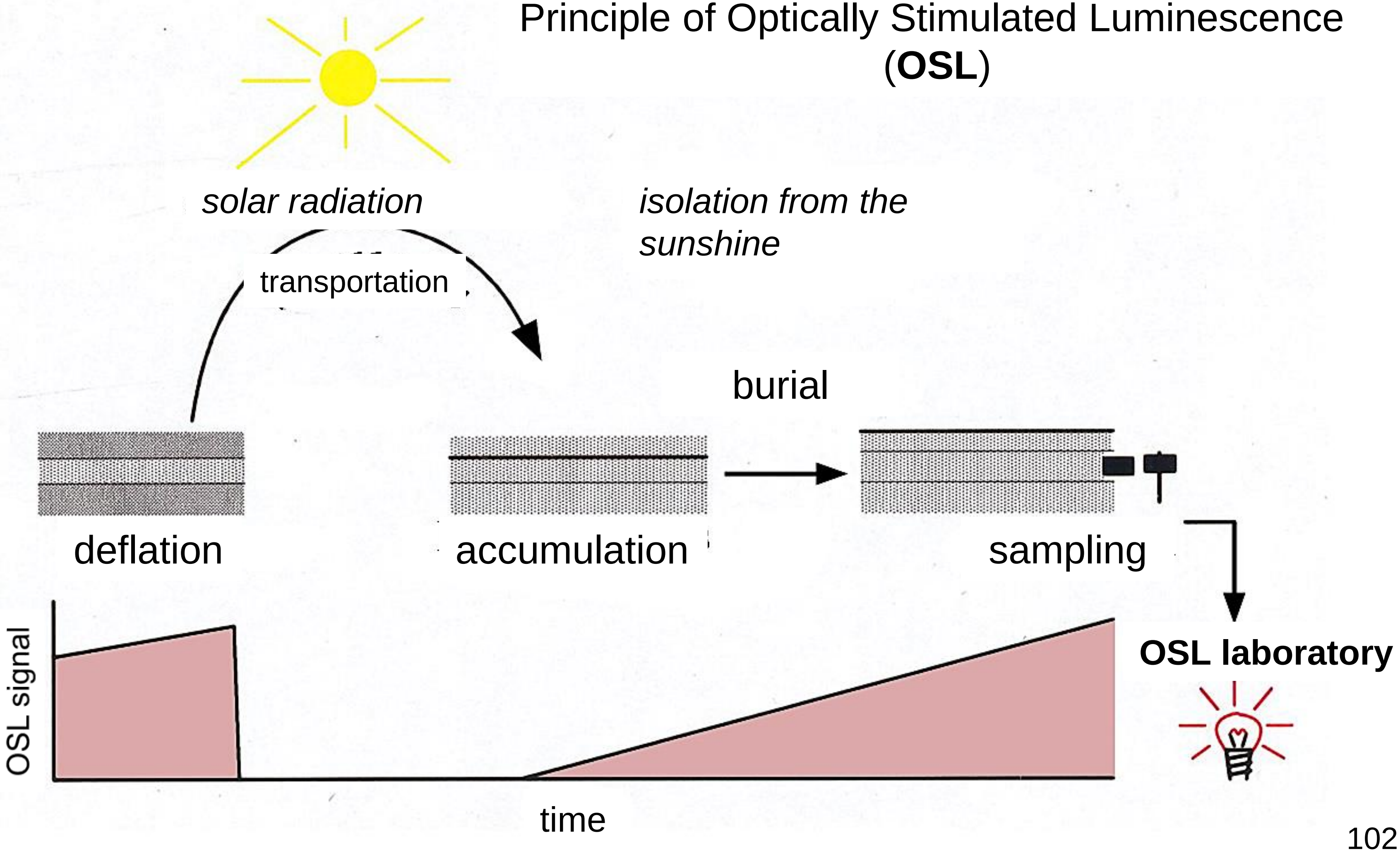

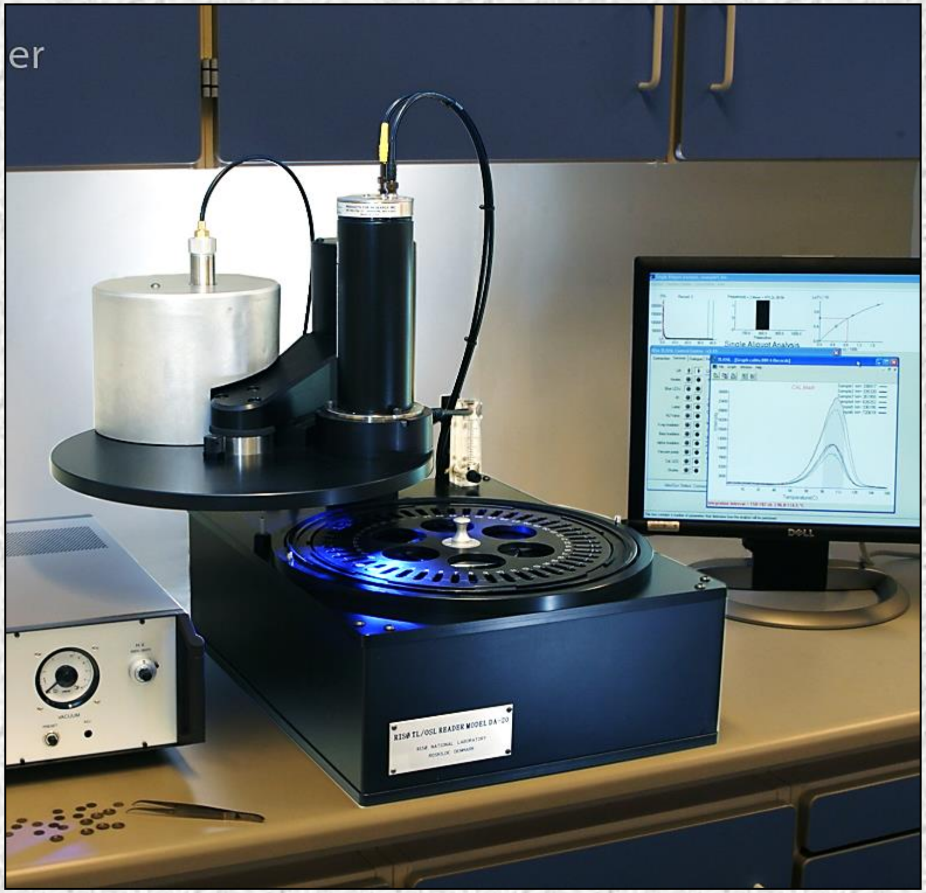

$$\text{Age} = \frac{\text{Equivalent dose}}{\text{Dose rate}} \quad \left(\frac{Gy}{Gy/ka}\right)$$

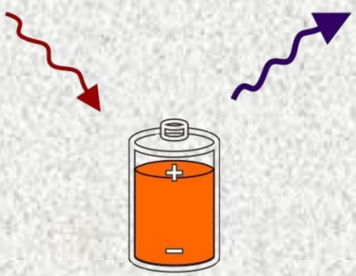

Luminescence dating

Optical luminescence:

•IRSL: Infrared Stimulated Luminescence
feldspar

•BLSL: Blue Light Stimulated Luminescence
quartz

Grain size:

Coarse grain (quartz or K-feldspar): 100-200 µm (sand)

Polymineral (fine grain): 4-11 µm (loess)

Luminescence dating methods

- Thermoluminescence (TL)
- Optically Stimulated Luminescence(OSL)
  - Infrared (IRSL)
  - Red OSL
  - Green OSL
  - Blue OSL
  - Pulsed OSL
  - TT OSL (up to 1 My!)
- Infrared radiofluorescence (IR-RF)

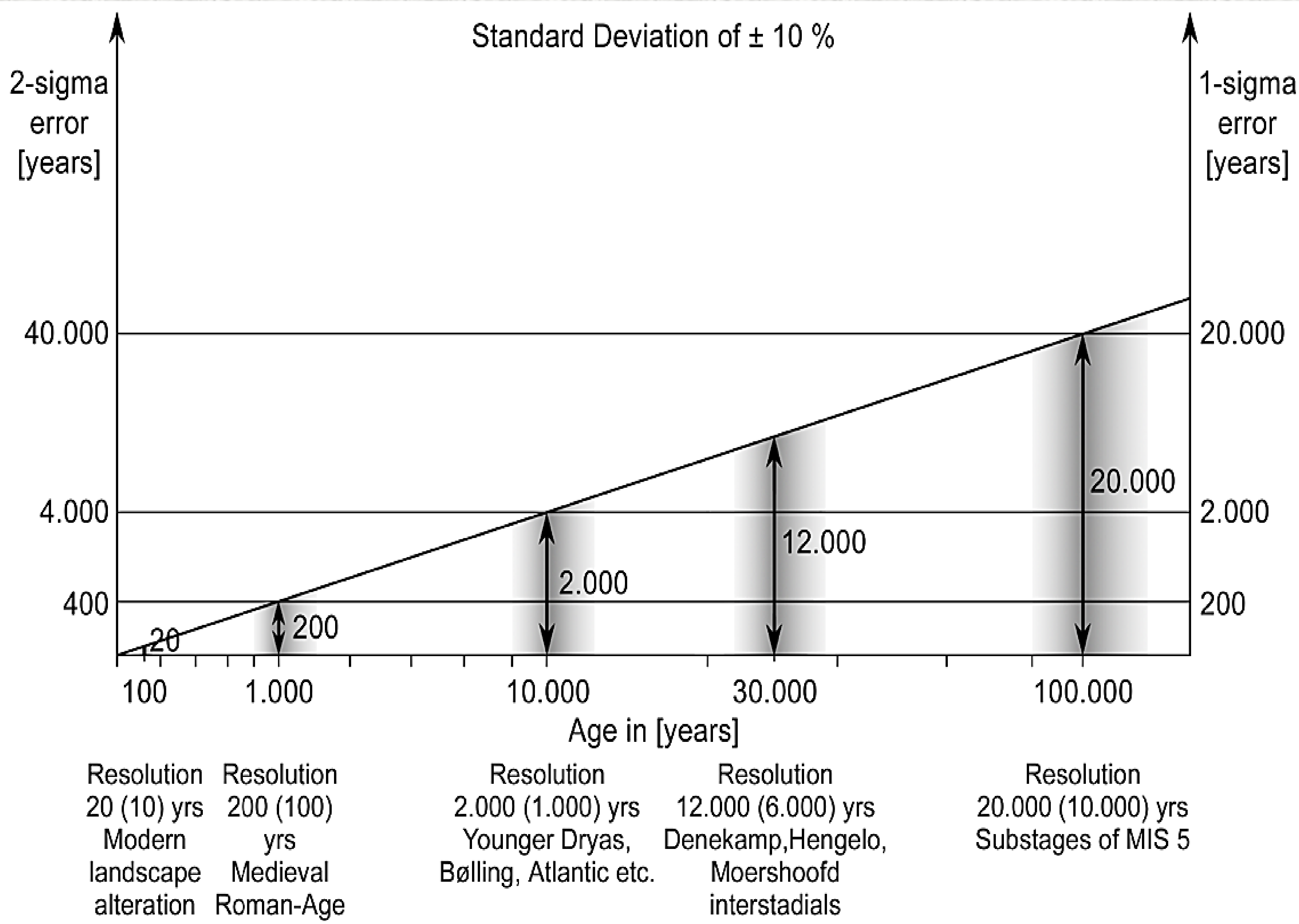
Standard Deviation of ± 10 %
2-sigma error [years]
1-sigma error [years]
40.000
4.000
400
20.000
2.000
200
20
200
2.000
12.000
20.000
100
1.000
10.000
30.000
100.000
Age in [years]
Resolution 20 (10) yrs Modern landscape alteration
Resolution 200 (100) yrs Medieval Roman-Age
Resolution 2.000 (1.000) yrs Younger Dryas, Bølling, Atlantic etc.
Resolution 12.000 (6.000) yrs Denekamp,Hengelo, Moershoofd interstadials
Resolution 20.000 (10.000) yrs Substages of MIS 5

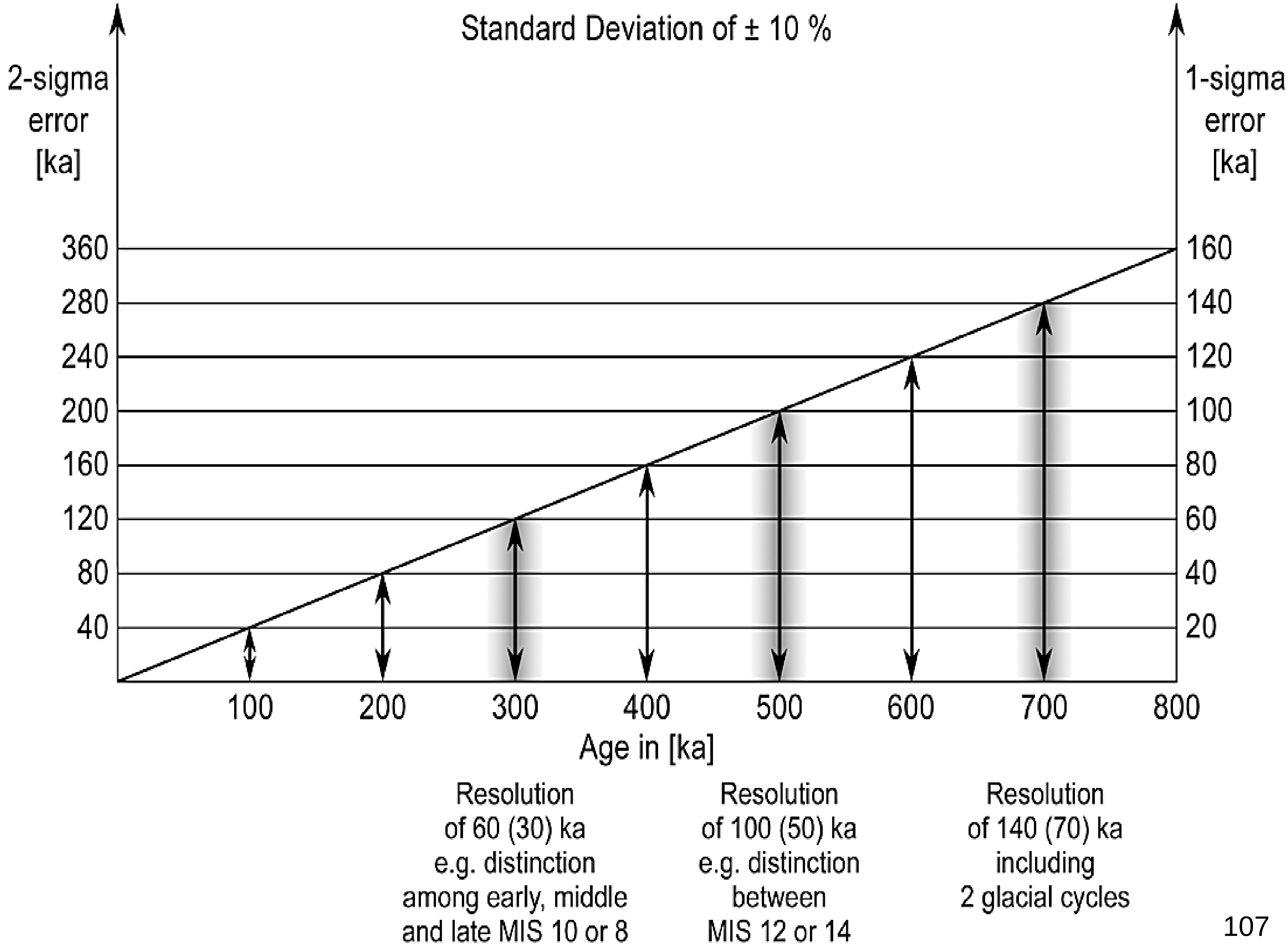
Standard Deviation of ± 10 %
2-sigma error [ka]
1-sigma error [ka]
360
280
240
200
160
120
80
40
160
140
120
100
80
60
40
20
100
200
300
400
500
600
700
800
Age in [ka]
Resolution of 60 (30) ka e.g. distinction among early, middle and late MIS 10 or 8
Resolution of 100 (50) ka e.g. distinction between MIS 12 or 14
Resolution of 140 (70) ka including 2 glacial cycles

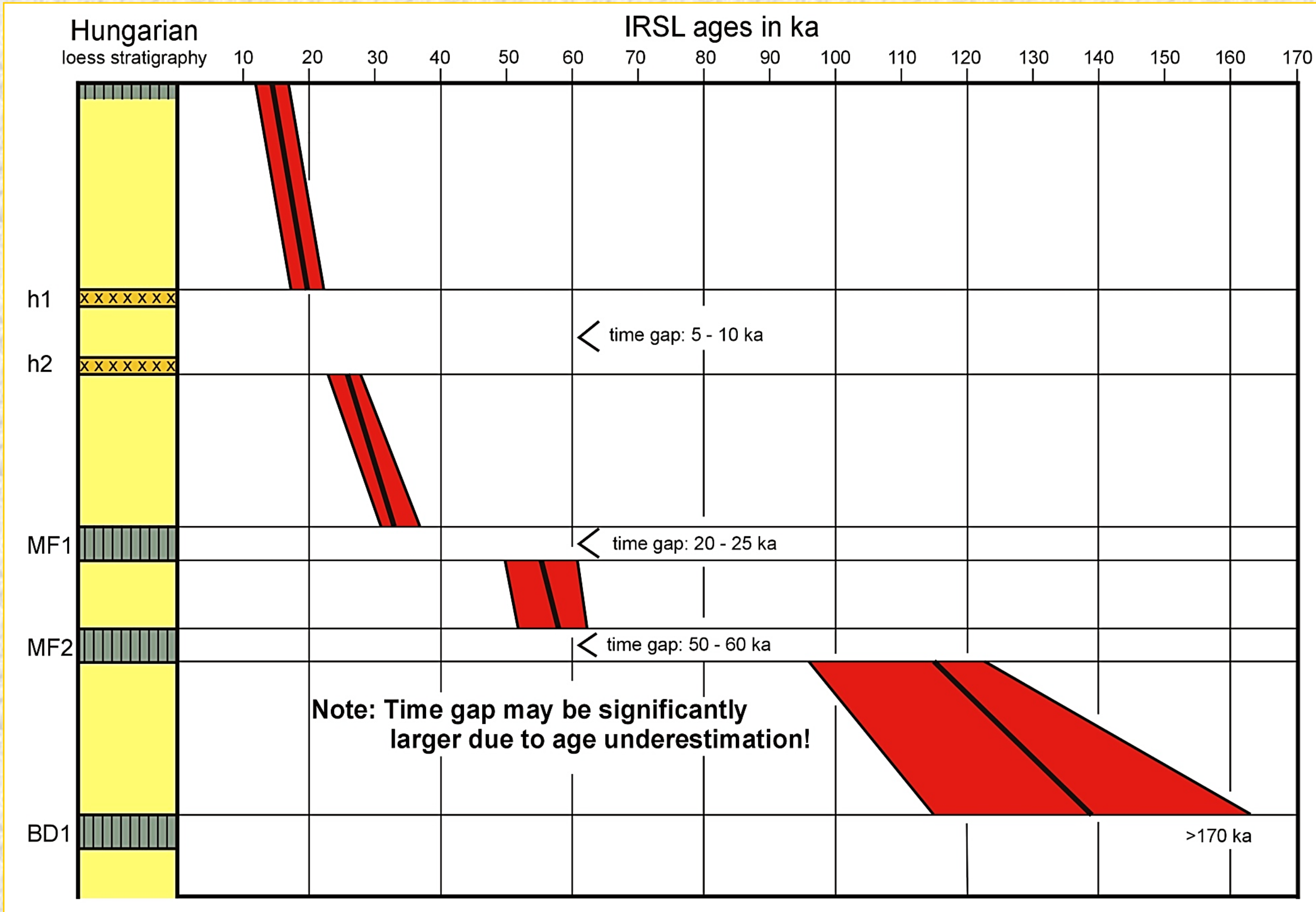

Hungarian
loess stratigraphy
IRSL ages in ka
10
20
30
40
50
60
70
80
90
100
110
120
130
140
150
160
170
h1
h2
MF1
MF2
BD1
time gap: 5 - 10 ka
time gap: 20 - 25 ka
time gap: 50 - 60 ka
Note: Time gap may be significantly larger due to age underestimation!
>170 ka

DATING METHODS IN THE QUATERNARY STUDIES

ABSOLUTE DATING METHODS

9. Varve-, and dendrochronology

“Absolute” methods or numerical age estimation

10. Non-stable (radioactive) isotopes
    - 10/a Potassium-argon series
        - $^{40}K/^{40}Ar$
        - $^{40}Ar/^{39}Ar$
        - laser fusion $^{40}Ar/^{39}Ar$
    - 10/b Uranium decay series
        - $^{238}U/^{230}Th$
        - $^{234}U/^{230}Th$
        - $^{230}Th/^{231}Pa$ (^{235}U)
    - 10/c Fission-track (^{238}U)
    - 10/d Radiocarbon dating (^{14}C)
11. Luminescence methods
    - -Thermoluminescence (TL)
    - -Optically stimulated luminescence (OSL)
        - InfraRed Stimulated Luminescence (IRSL)
12. Electron-spin resonance (ESR)
13. Cosmogenic isotopes

DATING METHODS IN THE QUATERNARY STUDIES

ABSOLUTE DATING METHODS

9. Varve-, and dendrochronology

“Absolute” methods or numerical age estimation

10. Non-stable (radioactive) isotopes
    - 10/a Potassium-argon series
        - $^{40}K/^{40}Ar$
        - $^{40}Ar/^{39}Ar$
        - laser fusion $^{40}Ar/^{39}Ar$
    - 10/b Uranium decay series
        - $^{238}U/^{230}Th$
        - $^{234}U/^{230}Th$
        - $^{230}Th/^{231}Pa$ (^{235}U)
    - 10/c Fission-track (^{238}U)
    - 10/d Radiocarbon dating (^{14}C)
11. Luminescence methods
    - -Thermoluminescence (TL)
    - -Optically stimulated luminescence (OSL)
        - InfraRed Stimulated Luminescence (IRSL)
12. Electron-spin resonance (ESR)
13. Cosmogenic isotopes

Age determination using terrestrial in-situ produced cosmogenic nuclides (TCN)

Exposure age of a rock is the time elapsed since it has been exposed to cosmic irradiation = since it is on the sur

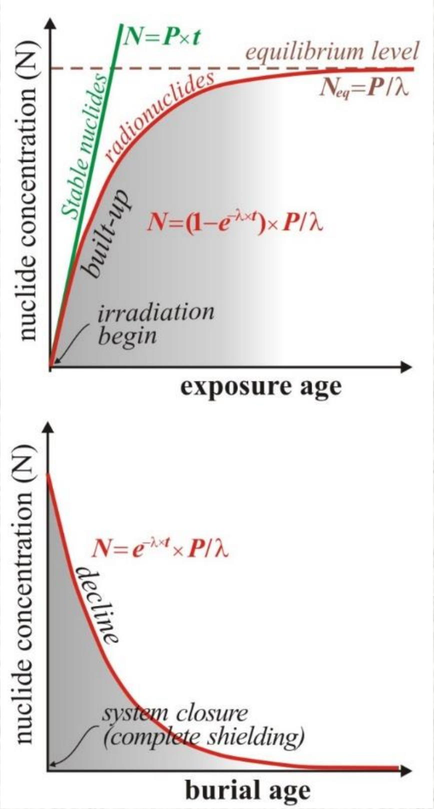

: TCN build-up

- ^{3}He; ^{14}C; ^{10}Be; ^{21}Ne; ^{26}Al; ^{36}Cl

Burial age is the time elapsed since a rock surface or sediment is shielded from cosmic irradiation.

 : decay of radioactive TCN

2 nuclides of different half-lives are neccesary
- $^{26}Al/^{10}Be$; $^{21}Ne/^{10}Be$; $^{14}C/^{10}Be$

Accumulation of cosmogenic nuclides

- **Stable and radioactive (CRN)** nuclides

-**Production rate** scaled to
  - -latitude
  - -altitude

- Selection of nuclide
  1) material
  2) expected age
(datable time range!)

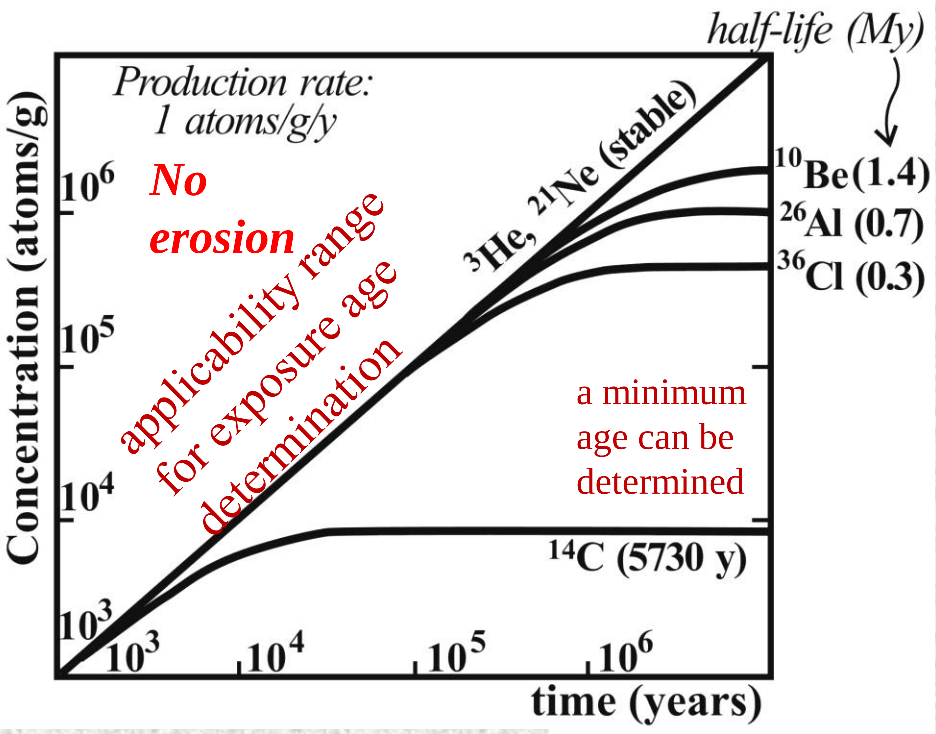

after Cerling and Craig 1994.

Prerequisites of reliable age information:

- Formation of the dated surface is instantaneous
- No erosion and no aggradation since formation (!?)

The effect of erosion or aggradation on the exposure age

Beneath the surface, production of cosmogenic nuclides decreases exponentially.

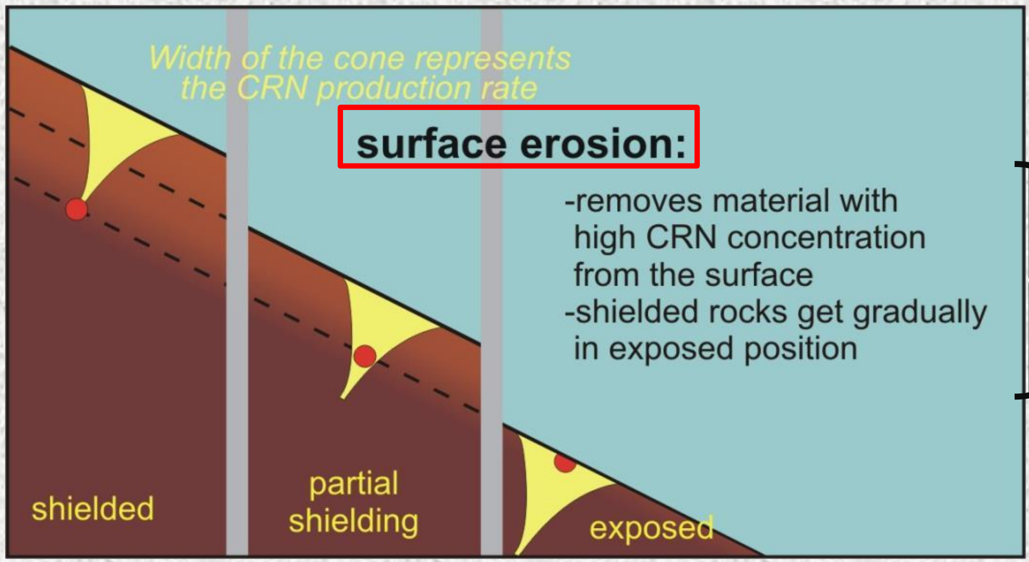

Penetration depth of cosmogenic radiation (if ρ=2.7 g/cm^3)
spallation reactions: 0.6 m (98%) - müon reactions: 16 m

➔ decreased CRN concentration
➔ younger than real apparent ages

Temporal cover (loess, soil, snow) is shielding the surface from cosmic irradiation.

The effect of erosion on TCN concentration in time

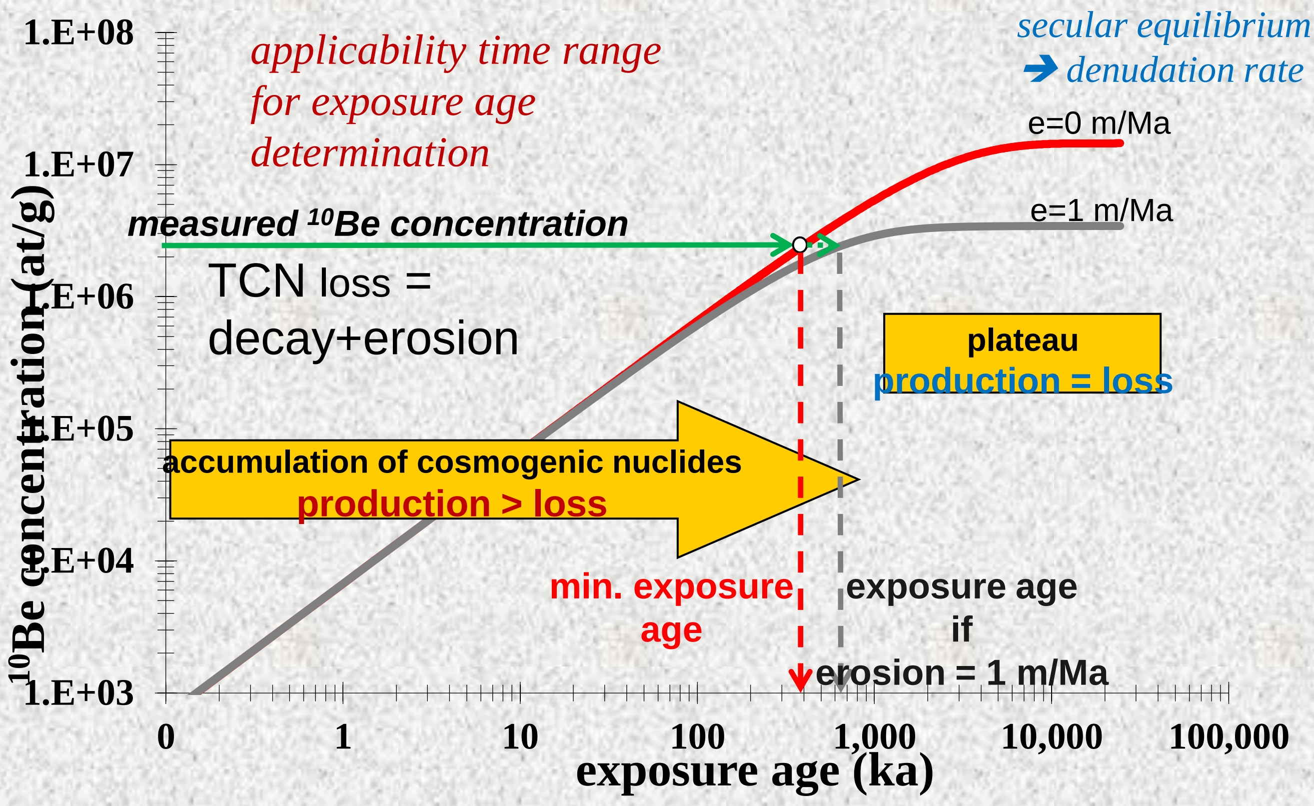

Using surface samples:

minimum exposure age or maximum erosion rate !

Age range of the different dating methods in the Quaternary studies

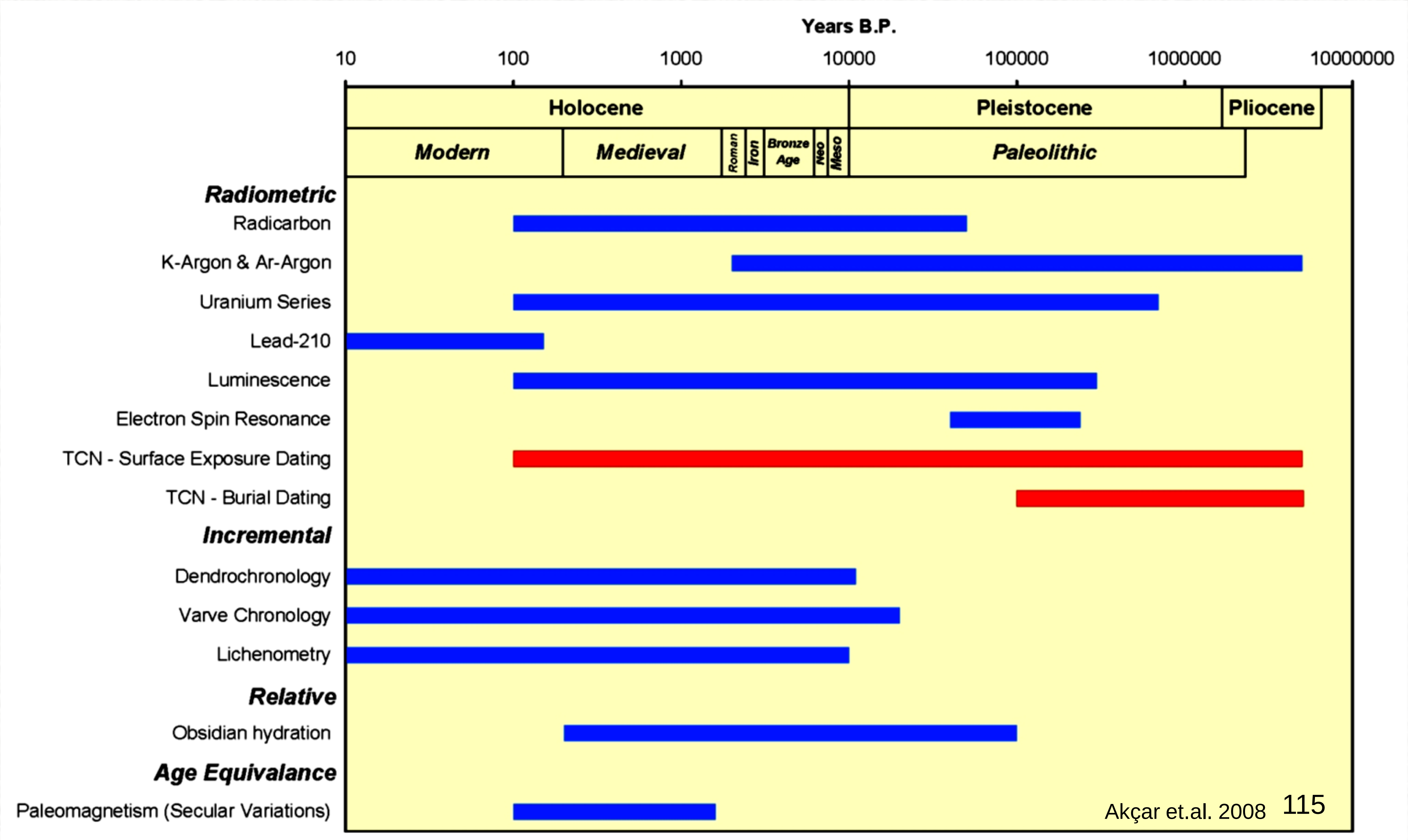

Loess – windows to the Past

A terrestrial climate archive from the Pleistocene

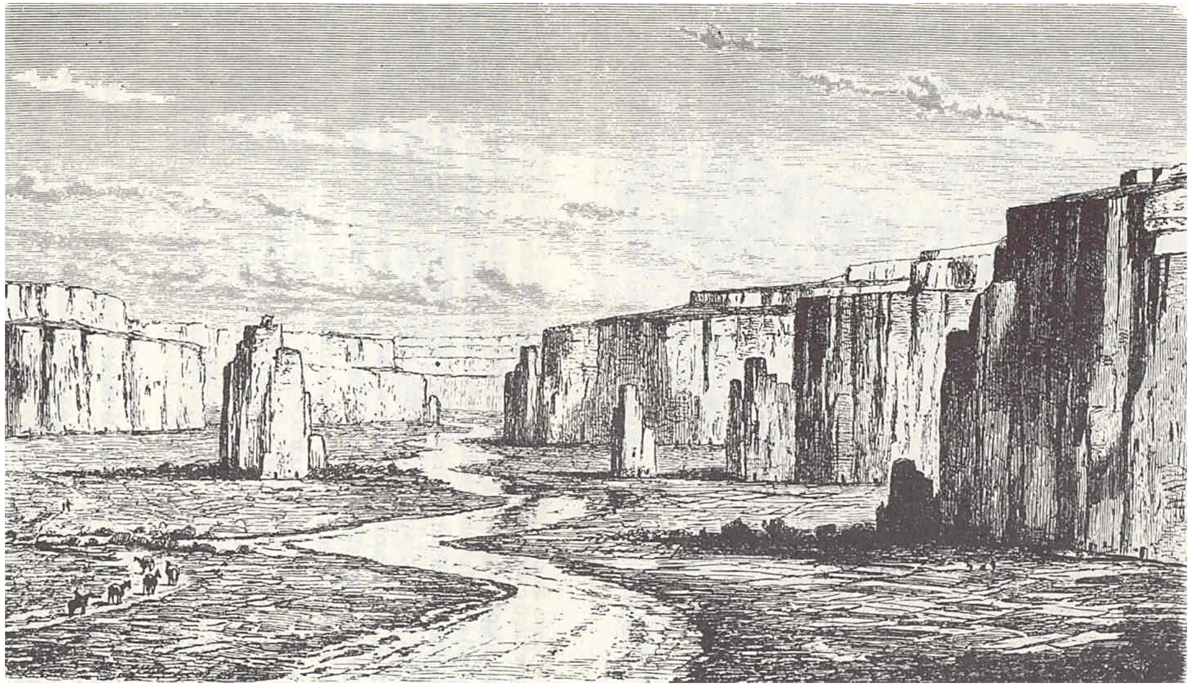

LOESS RESEARCH

- Chinese Loess Plateau by J. Cholnoky

- First description of loess:
- Von Leonhard (Haarlass, near Heilderberg, Germany) 1824

89: Loefs.

Syn. Loesch; Schneckenhäusel-Boden; Mergel (im Badisc
Oberlande); Briz.

STEININGER.

Neue Beiträge zur Geschichte der Rheinischen Vulkane; 51 ff.

Mehrere Notizen, den Löfs betreffend, sind entlehnt aus des H.
Dr Bronn und des Verfassers Manuscript über das Grobkalk-Gebilde
Rheinthale.

Ein lehmiges, unrein gelblichgraues, im Bruc
erdiges Gemenge aus Thon-, Kalk- und Kieselth
len und aus sehr kleinen Glimmer-Blättchen. I
feinstaubigen Theile sind zu einer losen zerreib
chen Masse verbunden.

Im Löfs der Heidelberger Gegend finden sich, auf 2 Th
Thon; ½ Theil kohlensaurer Kalk und ½ Theil quarziger und gli
meriger Sand.

In der Gegend von *Andernach* trifft man, jedoch nur sp
sam, auch Bimsstein- und Schlacken-Stückchen im Löfs.

Eine, über dem Löfs liegende, Schicht von neuerer Ent
hung, untermengt mit Kalk-Geröllen, umschliefst einige A
von *Bulimus* und von *Helix*, welche in der nachbarlichen
gend noch heutiges Tages in gröfster Menge vorkommen.

Schlofsberg bei *Oppenheim*.

Der Löfs enthält versteinte und kalzinirte K
chylien.

Viele sind, vom Tage her, in seine Massen gefl
worden; als ihm mehr eigenthümlich zugehörig, wurden
jezt nur wenige beobachtet, so namentlich einige *Hel.*
und *Lymnaeus*-Arten.

Die gröfsern u. a. bei *Oppenheim* am *Galgenberge*, die kleinern
Weinheim unfern *Alzey*, am *Haarlafs* und bei *Neckargemünd*.

Aus dem Löfs der Gegend von *Andernach* führt STEININGER an: *H*
pomatia, *nemoralis*, *hortensis*, *striata*, *pulchella* und *cristallina*; *L*
naeus pereger und *ovatus*; *Pupa edentula*.

Die Schaalen der Muscheln tragen zum Theil noch i
natürliche Farbe; die meisten sind jedoch weifs und
zerbrechlich.

Auch Stofs- und Mahlzähne vom Mammuth wur
nebst andern, nicht näher bestimmten, meist sehr au
lösten Knochen im Löfs gefunden.

So u. a. unfern *Weinheim* in der *Bergstrafse*.

Auf Veranlassung und durch Vorsorge der Herren v. BABO und Dr. BATT zu
heim, zweier eben so warmen, als einsichtsvollen, Naturfreunde, wurden diese interessa
im Frühlinge 1823 durch Wassergüsse in einem Hohlwege entblöfsten, kolossalen Reste
weiterer Zerstörung geschützt. Sie befinden sich jezt in den Sammlungen der Univers
Heidelberg.

Der Löfs gibt, bei gehöriger Behandlung mit Dünger, ei
zumal für Weinbau, sehr diensamen Boden.

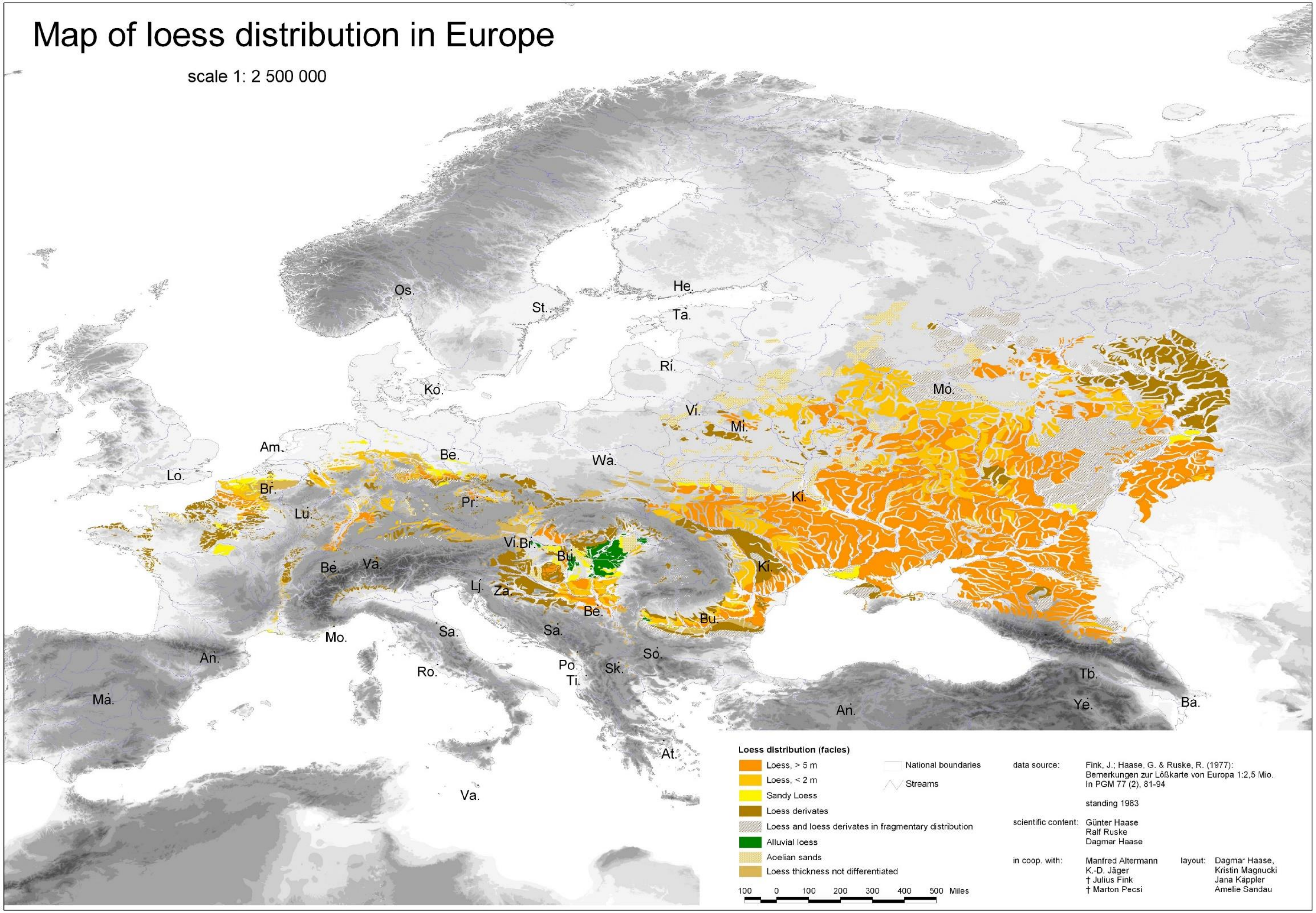
Map of loess distribution in Europe
scale 1: 2 500 000
Os.
St.
He.
Ta.
Ri.
Ko.
Mo.
Vi.
Mi.
Am.
Be.
Wa.
Lo.
Br.
Lu.
Pr.
Ki.
Vi.
Br.
Bu.
Be.
Va.
Lj.
Za.
Ki.
Be.
Bu.
Mo.
Sa.
Sa.
An.
So.
Ro.
Po.
Ti.
Sk.
Ma.
Tb.
An.
Ye.
Ba.
At.
Va.
Loess distribution (facies)
Loess, > 5 m
Loess, < 2 m
Sandy Loess
Loess derivates
Loess and loess derivates in fragmentary distribution
Alluvial loess
Aoelian sands
Loess thickness not differentiated
National boundaries
Streams
100 0 100 200 300 400 500 Miles
data source:
Fink, J.; Haase, G. & Ruske, R. (1977): Bemerkungen zur Lößkarte von Europa 1:2,5 Mio. In PGM 77 (2), 81-94
standing 1983
scientific content:
Günter Haase
Ralf Ruske
Dagmar Haase
in coop. with:
Manfred Altermann
K.-D. Jäger
† Julius Fink
† Marton Pecsi
layout:
Dagmar Haase,
Kristin Magnucki
Jana Käppler
Amelie Sandau

Why loess research is important in Hungary?

- Archive of the Quaternary climate and environmental changes
- Importance of the Carpathian Basin in the West-East loess-transect
- Tradition (thick loess, outcrops, brickyards)
- Big „chaos” in:
  - Number of buried soils
  - Numbering or labeling of paleosoils
  - Position of the last interglacial

History of Loess research in Hungary

- Szabó, J. (1877): *sea or lake sediment*
- Inkey, B. (1878), Halaváts, Gy. (1895), Treitz, P. (1901), Horusitzky, H. (1898, 1903): *subaerial sediment*
- Cholnoky J. (1902): *dust from Inner-Asia*
- Prinz Gy. (1926): *dust from the margin of the Northern-European icesheet*
- Bulla, B. (1934, 1938):
  - *Loess: glacials, loamy horizons (=paleosoils): interglacials (according to Soergel's theory)*
  - *Dust principally from „floodplains of the Hungarian-Basin"*
- Pécsi, M. (1969, 1975):
  - *Poligenetic origin*

    (frost weathering in mountains → mass movement → fluvial transport → accumulation on alluvial fans and floodplains → eolian transport → dust accumulation on river terraces, hilly regions, flat surfaces → diagenesis)

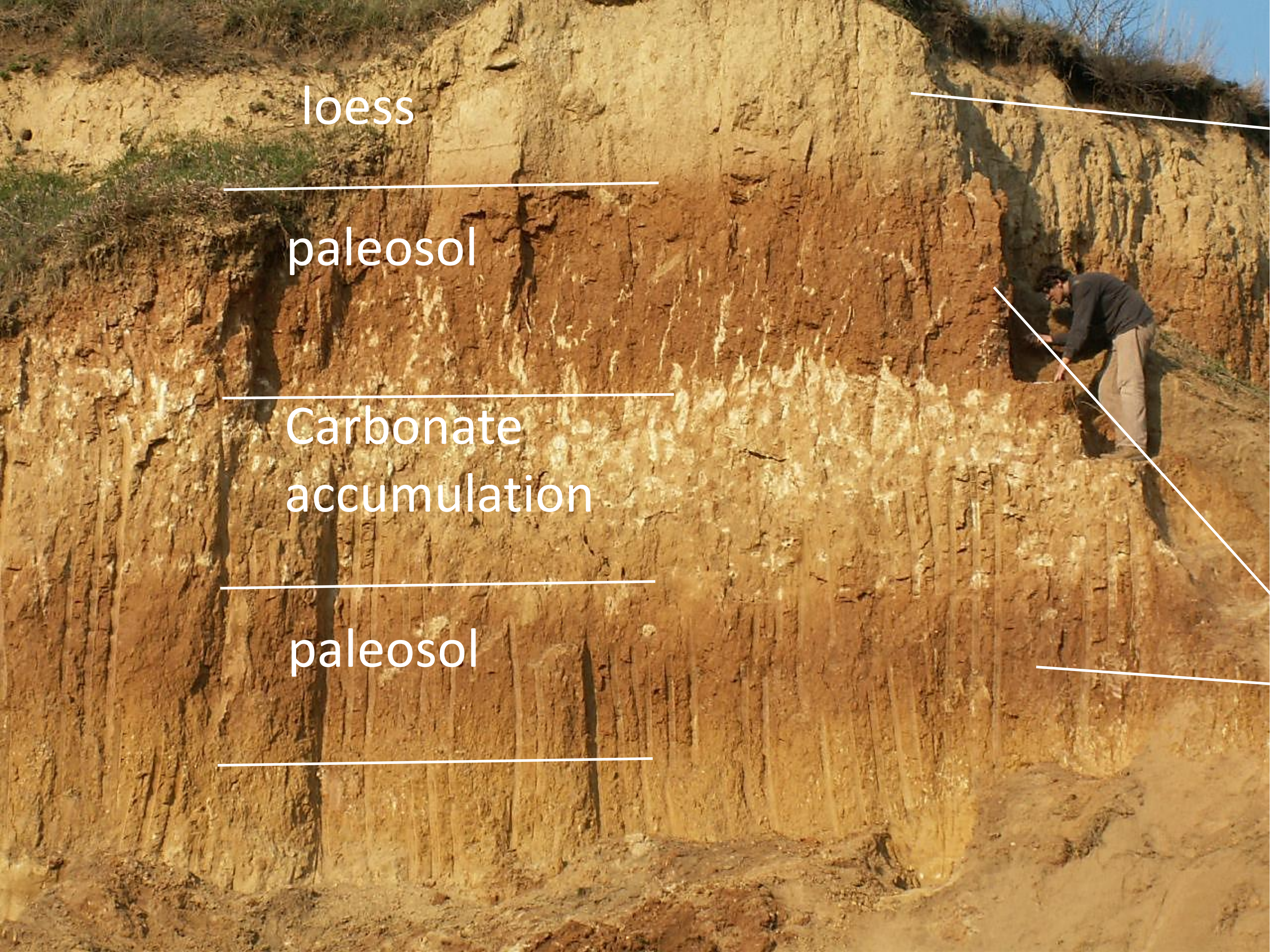

Ice age=glacial, stadial

Warmer period=interglacial, interstadial

Polygenetic theory of loess formation

Glacial periods: peroglacial environment (cold, dry) – **physical weathering**, kolluvium formation

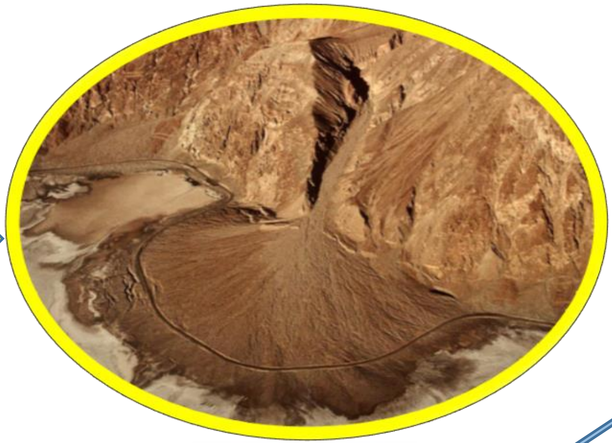

Interglacials: more humid, mild climate, warmer (similar to the recent climate) – **fluvial erosion and accumulation**

Glacial periods: periglacial environment (cold, dry) – wind – dust storms – **dust accumulation**

Interglacials: more humid, mild climate, warmer – **soil development** on loess

$CaCO_3$ in the matrix - the **diagenesis of the loess**

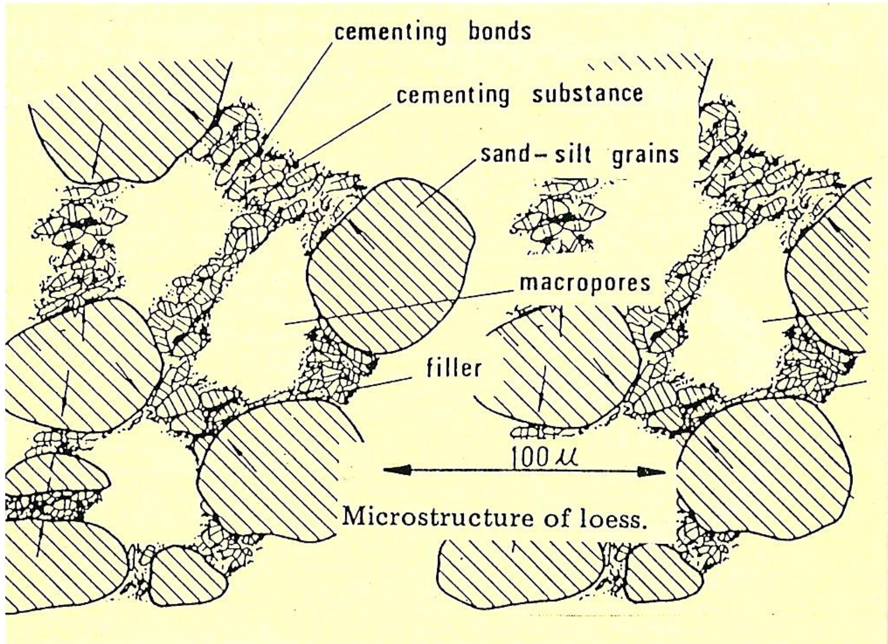

Diagenesis after dust accumulation

(from sediment to loose clastic sedimentary rock)

Loess on terraces in Hungary

Esztergom (Danube; N-Hungary)

Pilismarót (Danube; N-Hungary)

Basaharc (Danube; N-Hungary)

Hévízgyörk (Galga river; Middle-Hungary)

Correlation of the theoretical loess-paleosol sequence (based on the results of different Hungarian loess outcrops) with the marine oxygen isotope stages

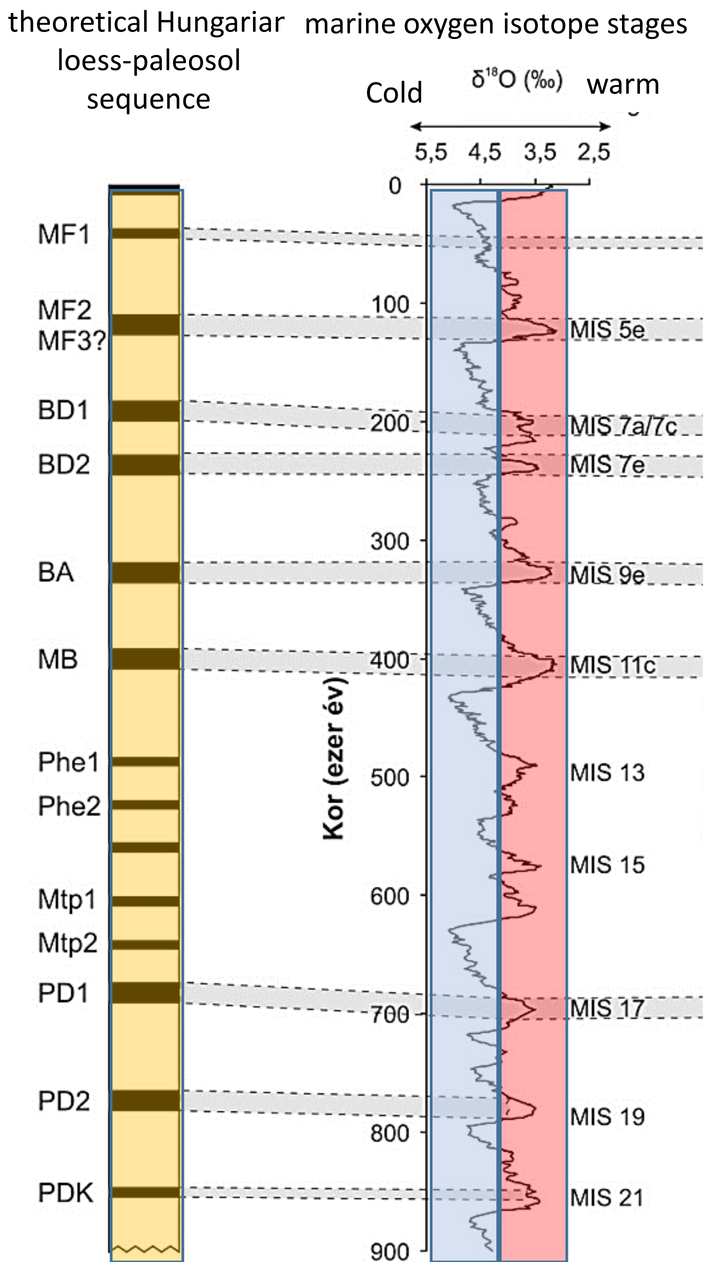

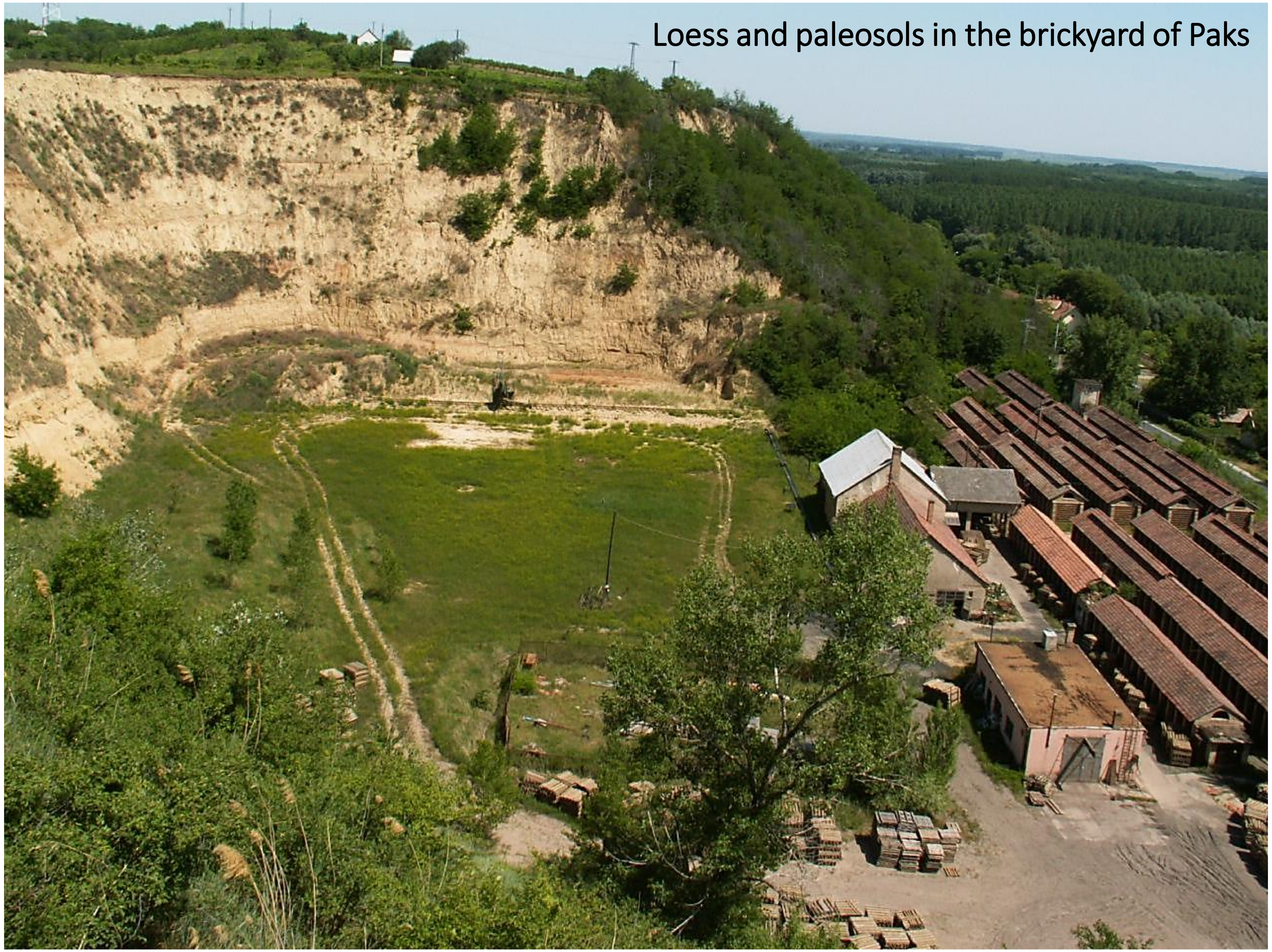

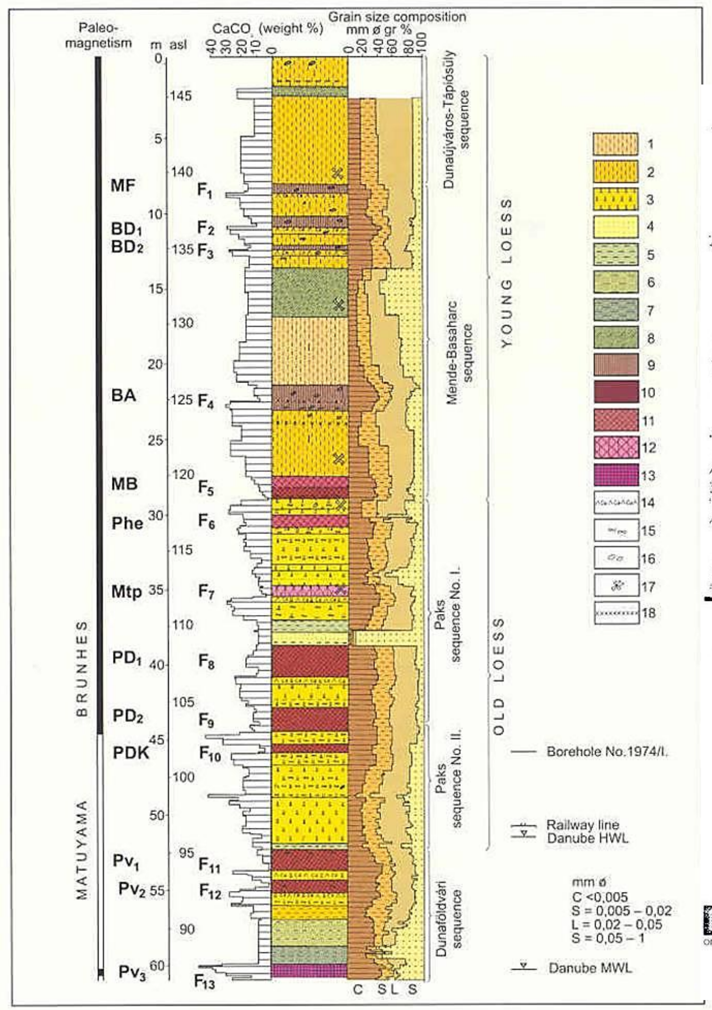

Paks 1977 North profile (PÉCSI, M., SZEBÉNYI, E. *et al.* 1978). – 1 = sandy loess; 2 = stratified loess; 3 = old loess; 4 = fluvial sand; 5 = silt, gleyed silt; 6 = silty sand; 7 = sandy silt; 8 = sandy slope loess; 9 = steppe soil, chernozem, chestnut soil; 10 = lessivated brown forest soil; 11 = reddish brown fossil soil; 12 = hydromorphous soil; 13 = red clay; 14 = $CaCO_3$ accumulation; 15 = loess doll; 16 = krotovina; 17 = microfauna; 18 = tephra

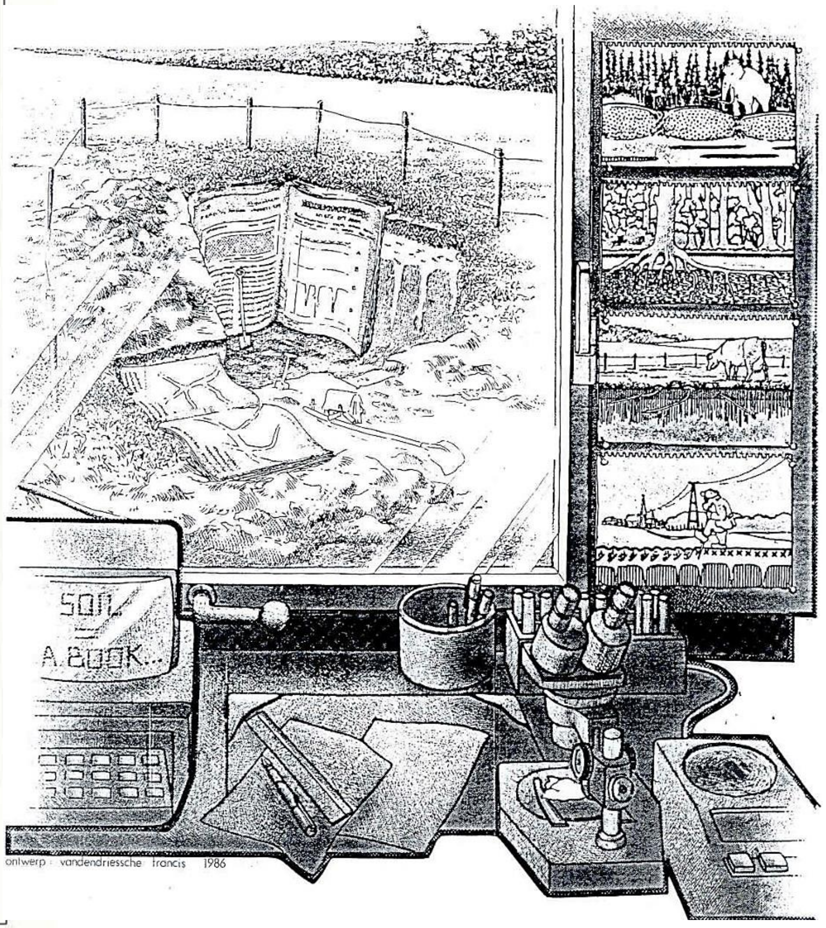


SOIL
A BOOK...
ontwerp : vandendriessche francis 1986

Multiproxy studies

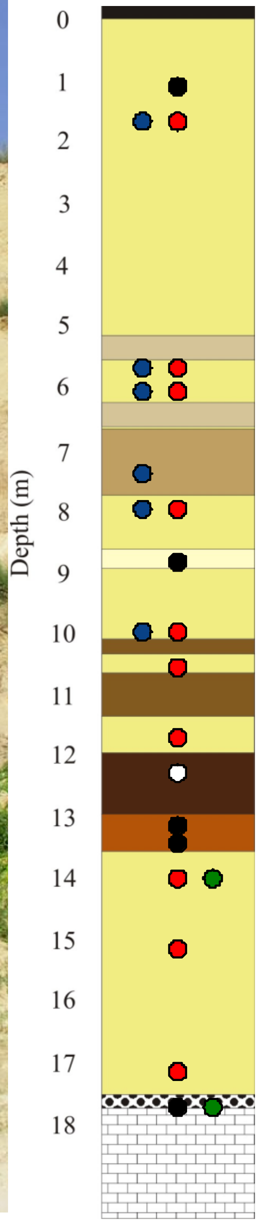

Luminescence dating

^{14}C

AAR

Malakology

Magnetic susceptibility (5cm)

Paleomagnetic investigations (10cm)

Granulometry (2cm)

Stabile isotopes (2cm)

Geochemical investigations (2cm)

Biomarkers (25cm)

Secondary carbonates

Thinsections (selected)

(Novothny et al. 2009, 2011, Barta 2011, Sierralta et al. 2009)

Multiproxy studies 2. (grainsize, magnetic susceptibility

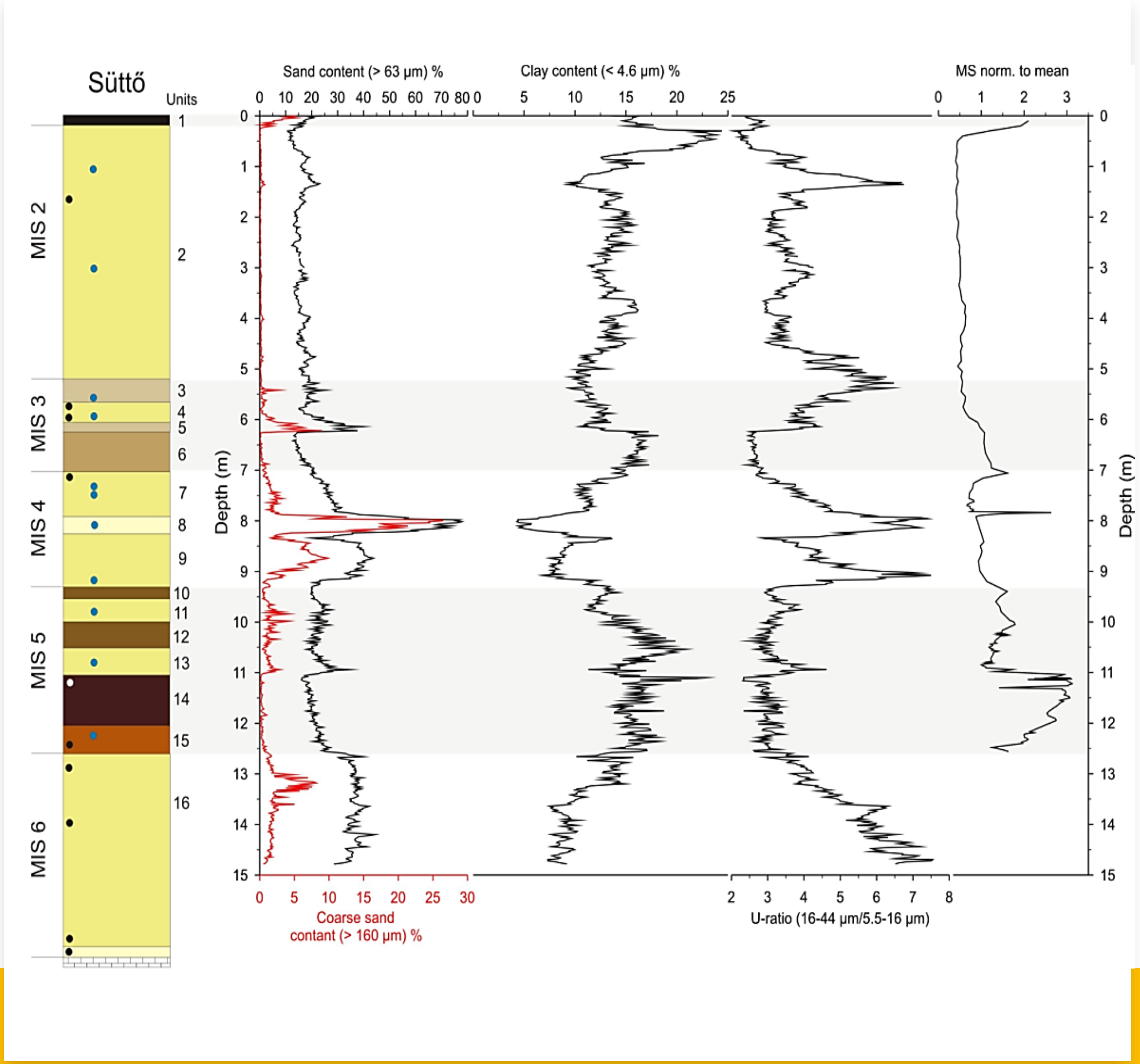

Multiproxy studies 3. ($CaCO_3$)

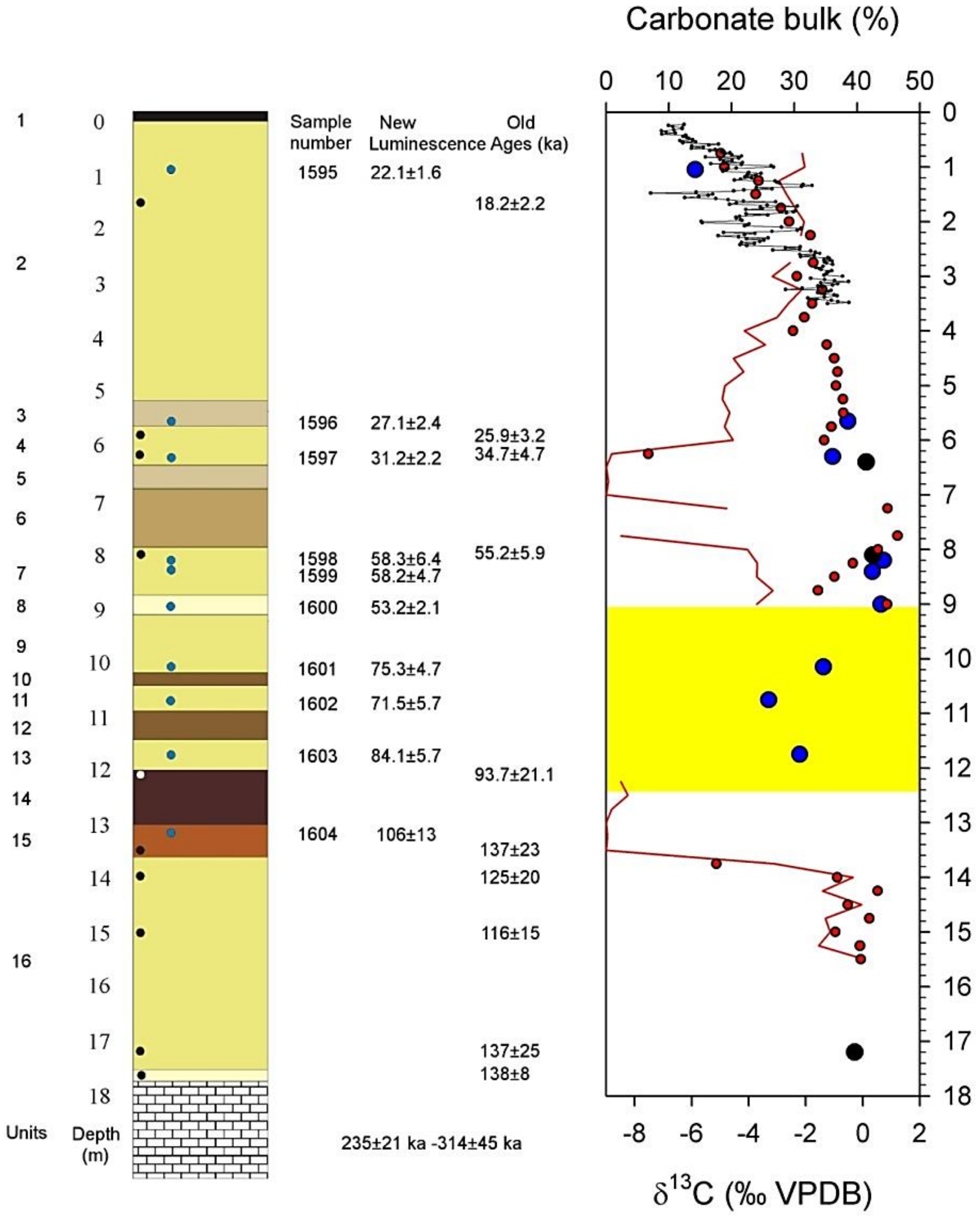

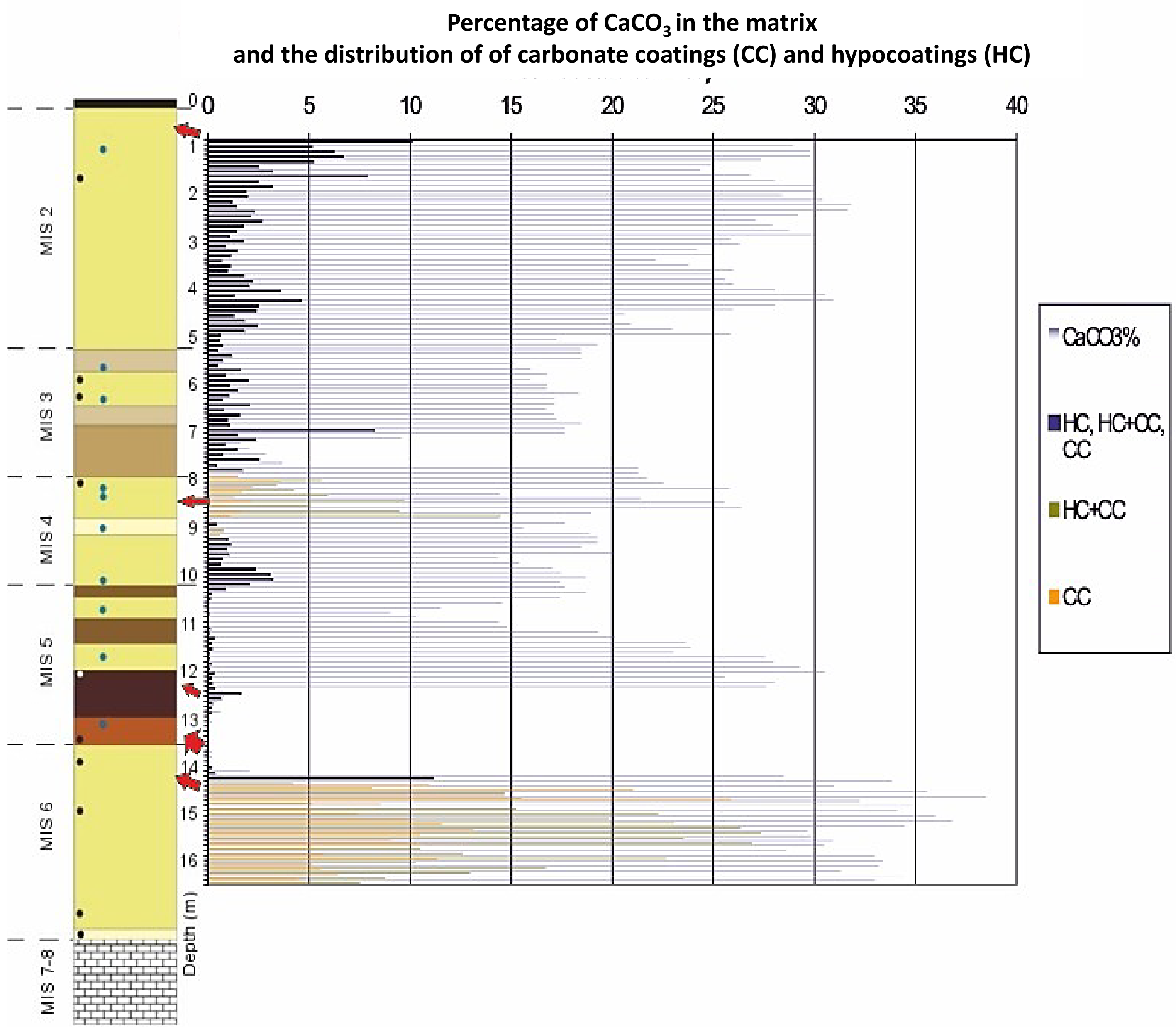

Tephrostratigraphy

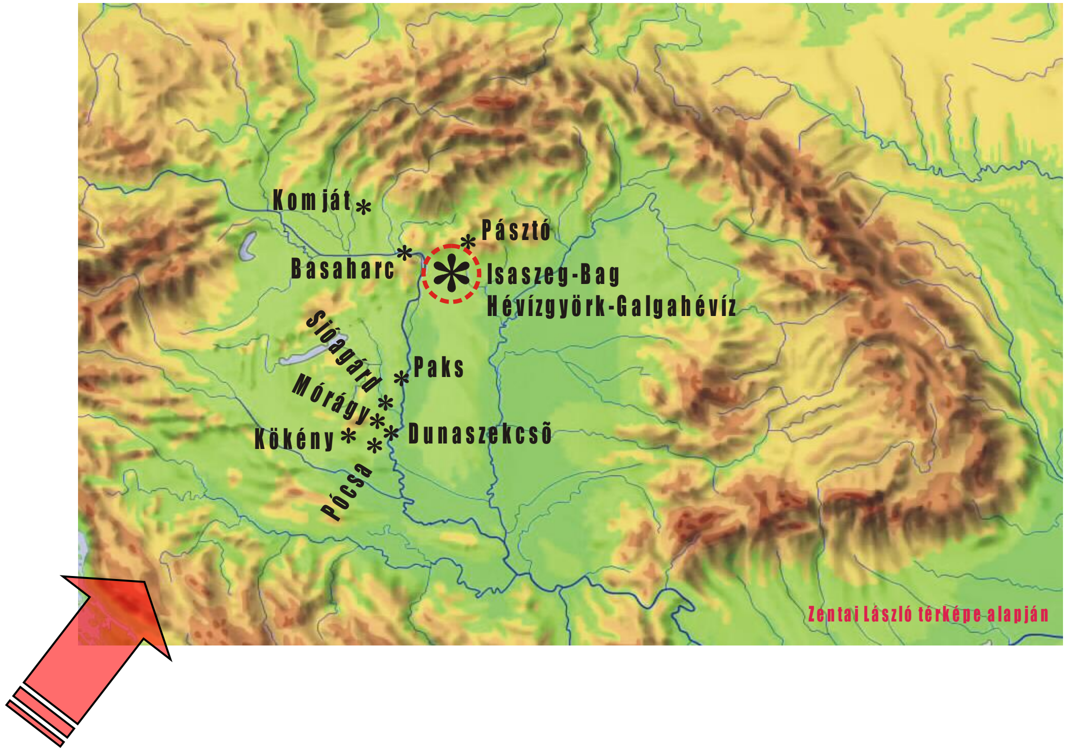

Campanian volcanic field
(Mte Vulture, Italy)

(High potassium content)

Paks Tephra
(≈ 30ka)

Bag Tephra

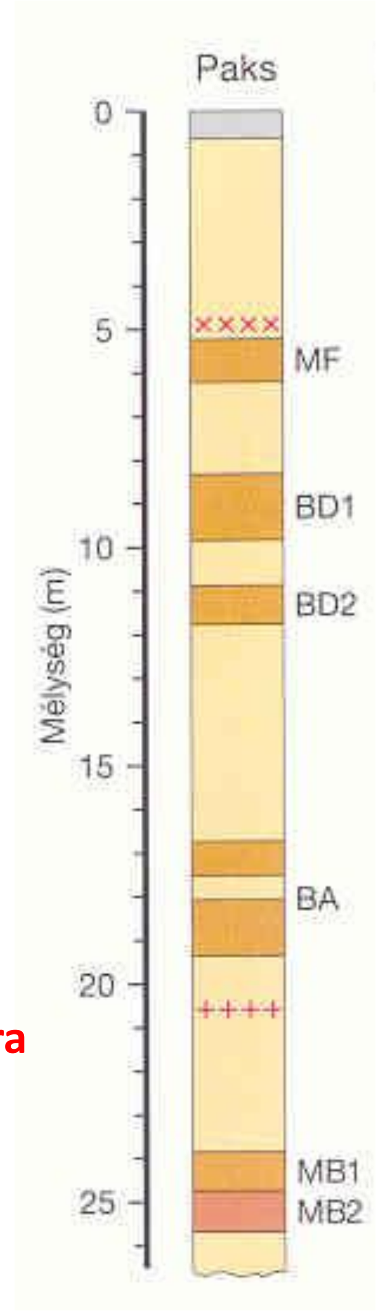

(Horváth 2001, Horváth et al. 2006)

The importance of the marker horizons (here: tephra layer) in Quaternary research in Hungary

- Projection of stratigraphical results from well investigated profiles to less known profiles
- Possibility of correlation with the stratigraphy of neighbouring countries (eg. Bohemian, Slovakian, Croatian)
- Reconstruction of the paleosurface

Loess profiles with Bag Tephra layer in the Carpathian Basin

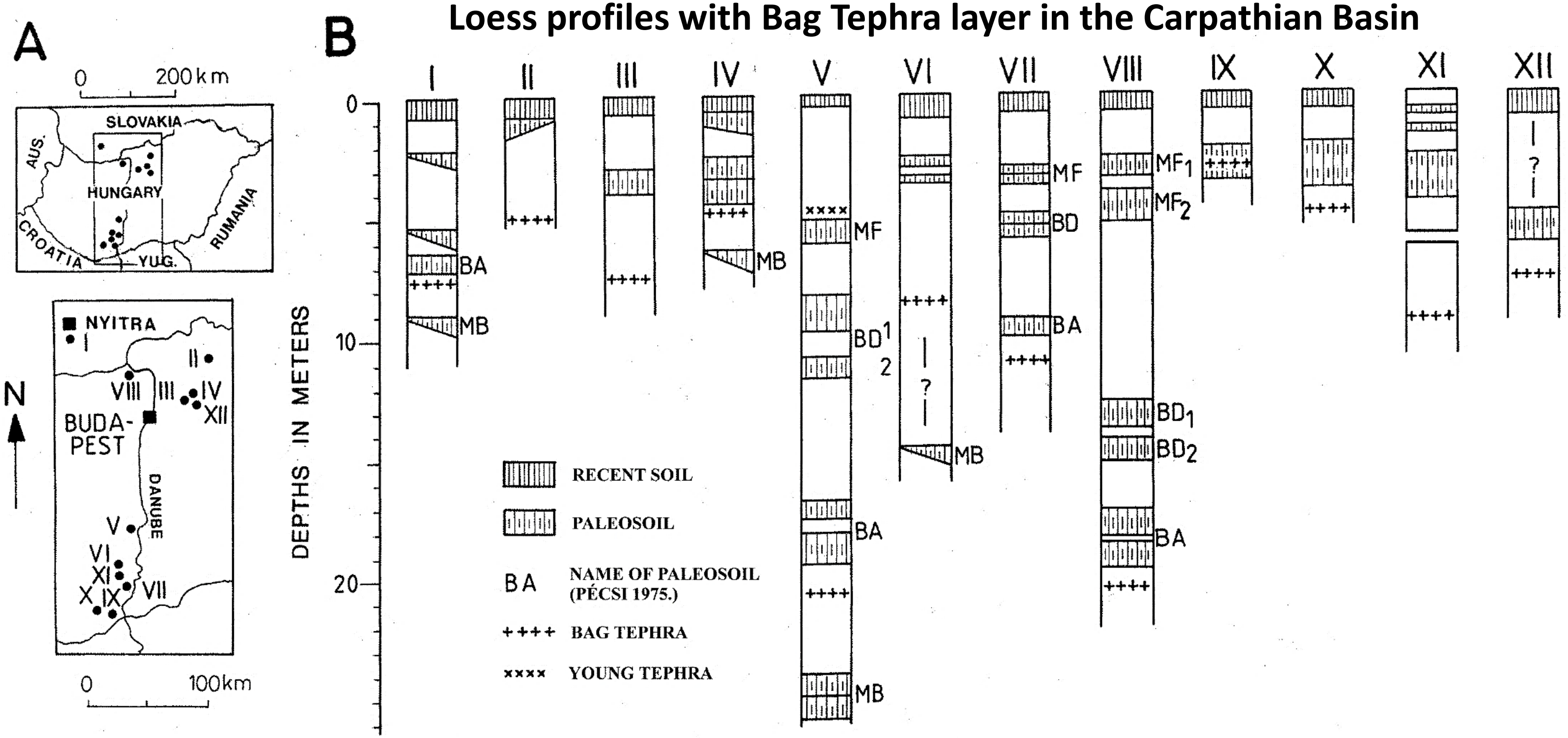

(see more in:Horváth 2001, Horváth et al. 2006)

The Bag Tephra layer in the outcrops and in thinsection

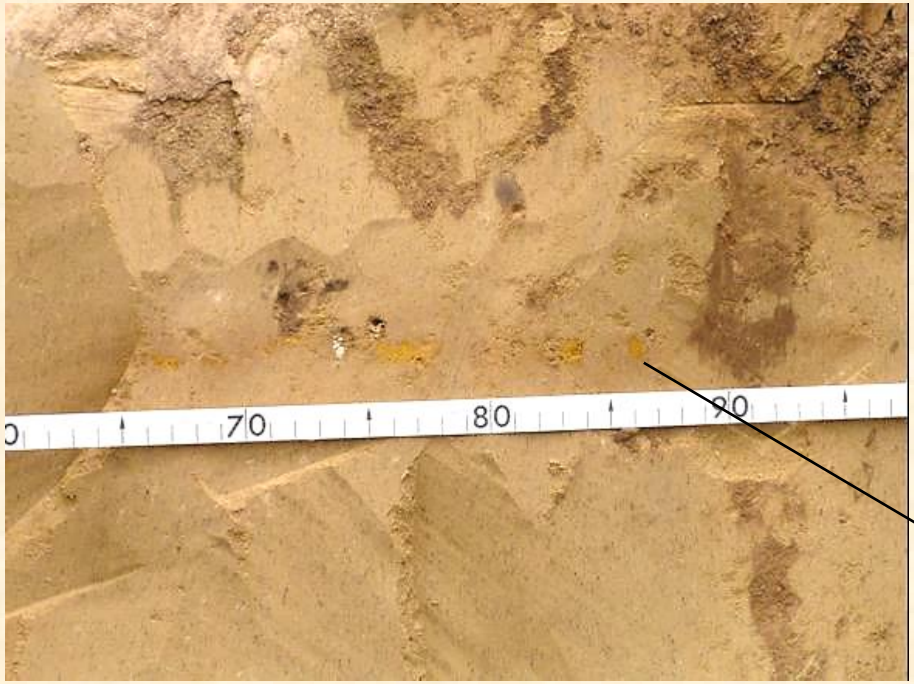

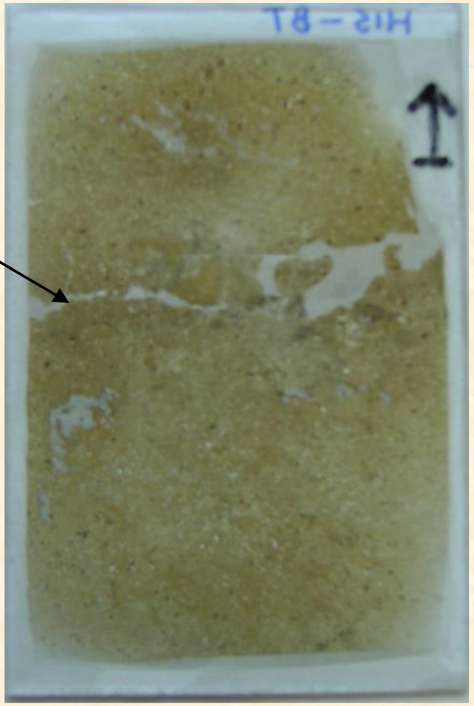

Reconstruction of a paleosurface based on the Bag tephra layer in the outcrop of Isaszeg – an example of the geomorphological inversion

The volcanic ash deposited in a valley

today it is a loessridge between two valleys

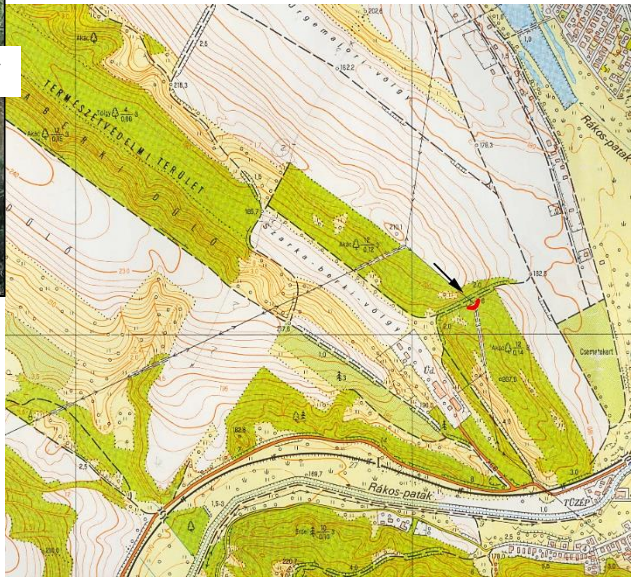

Stratigraphy

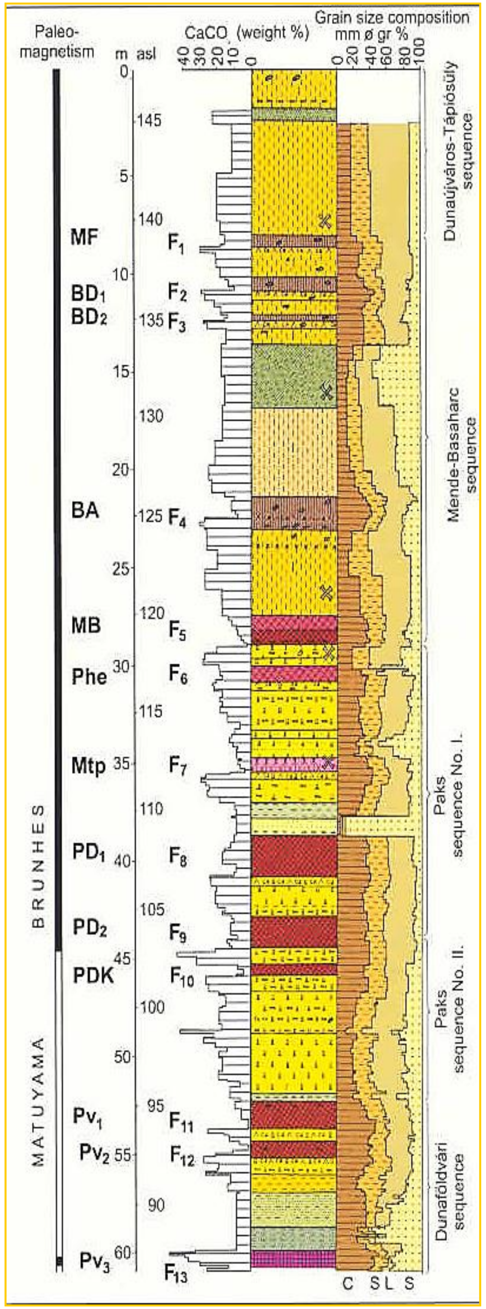

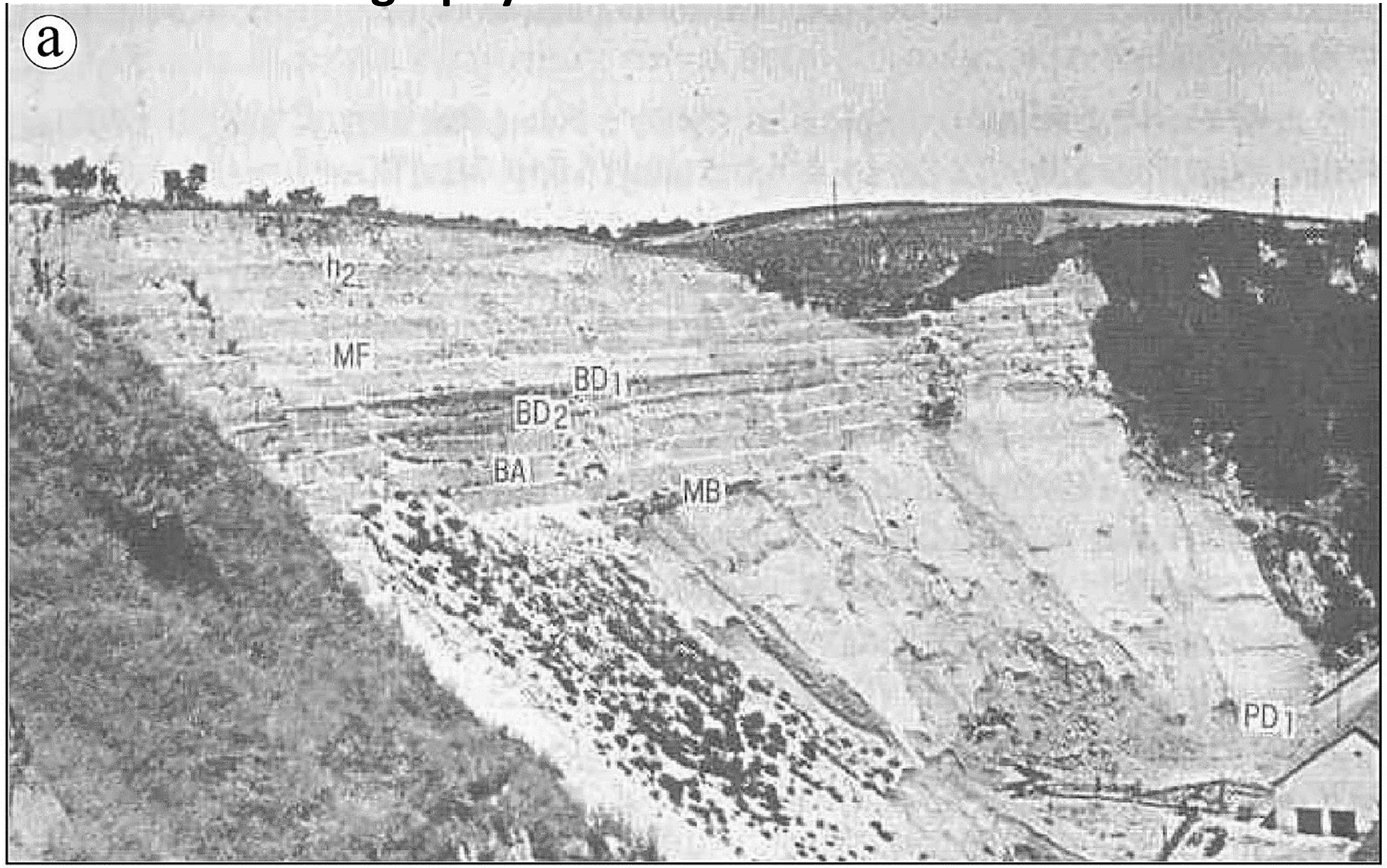

humic horizon 2
Mende Upper
Basaharc Double 1
Basaharc Double 2
Basaharc Lower
Mende Base
Paks Double 1

MIS5e (Frechen et al 1997; Novothny et al 2002)
MIS5e (Pécsi 1995)
MIS5e (Bulla 1938)

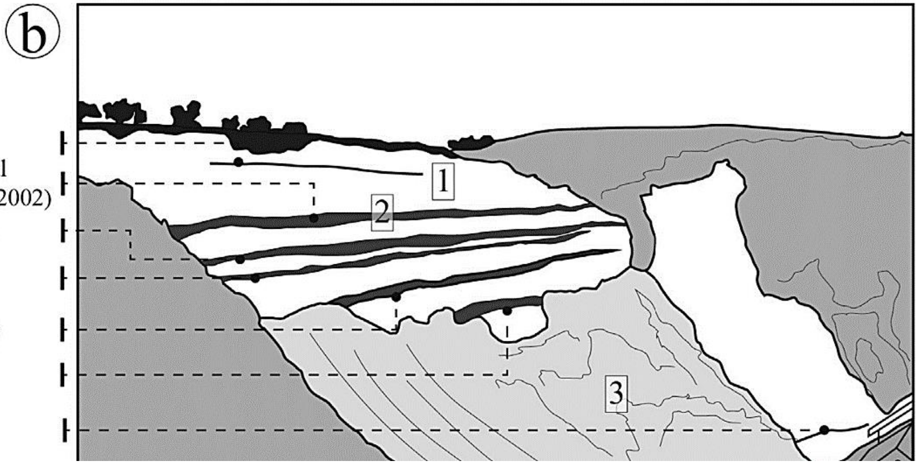

In: Horváth E, Bradák B. Sárga föld, lősz, lösz: short historical overview of loess research and lithostratigraphy in Hungary. QI 319:(1) pp. 1-10. (2014)

Chistory of the chronostratigraphy of the Hungarian loess (ka)

	Bulla, 1938	Kriván, 1955	Pécsi, 1975	Wintle-Packman, 1988	Oches-McCoy, 1995	Pécsi, 1995	Frechen et al., 1997, Novothny et al. 2002
			C^{14}	*TL*	*AAR*	*C^{14}, TL, (estimation)*	*TL+IRSL*
rec. talaj						0-11,3	
l1				15,8±1,3			
l1				17,6±1,4			(13-20)
h1			(16,75 ±0,4)			**W3** (16-17)	
l1				23,2±1,9			
h2			(20-22)			**W2/W3** (27-32)	
l2				24,0±2,0			(25-35)
MF1			(28-29)	20,9±1,7		**W2/W3** (45-60)	
l3				43,4±3,8			(50-60)
MF2			(32)	**R/W** (74,7±6,5)	**MIS 5** (<128 BP)	**W1/W2** (85-105)	**MIS 5** (65±10)
l4		**W2**		**R** (79,2±6,1)			**MIS 6** (>130)
BD1	**W2/W3**	**W2**				**R2/W1** (120-140)	
		W1					
BD2	**W1/W2**				<245 BP	**R2/W1** (150-170)	
l5		**W1**					
BA	**R/W**				<339 BP	**R1/R2** (195-230)	
l6		**R2**					
MB1			**R/W**			**MR3/MR4** (280-310)	
MB2			**R/W**		<423 BP	**MR2/MR3** (320-360)	
L1		**R1**					

(After Horváth 2001)

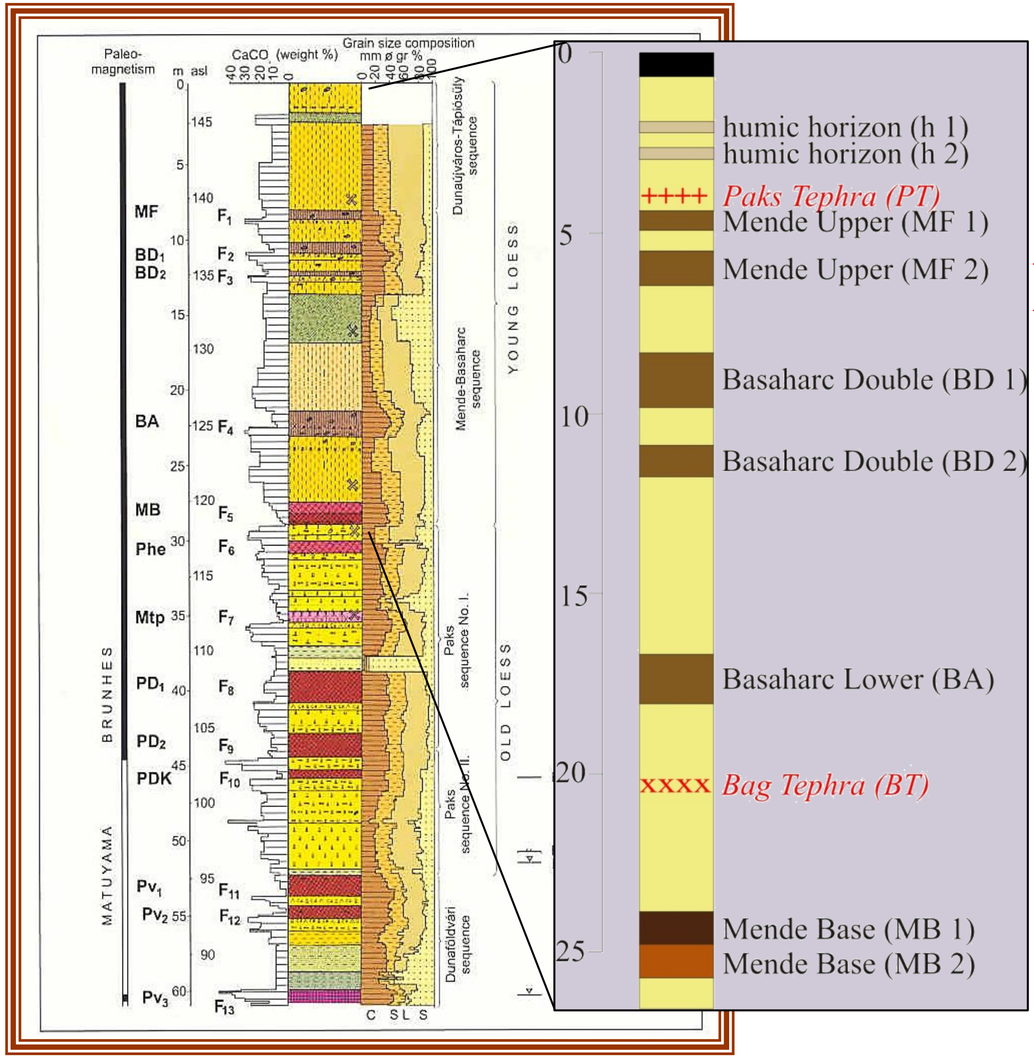

30 ky

MIS 5e ?

MIS6

~~MIS 5e~~ MIS 7

~350 ky

~~MIS 5e~~

Correlation of loess-paleosoils sequences based on MS investigations

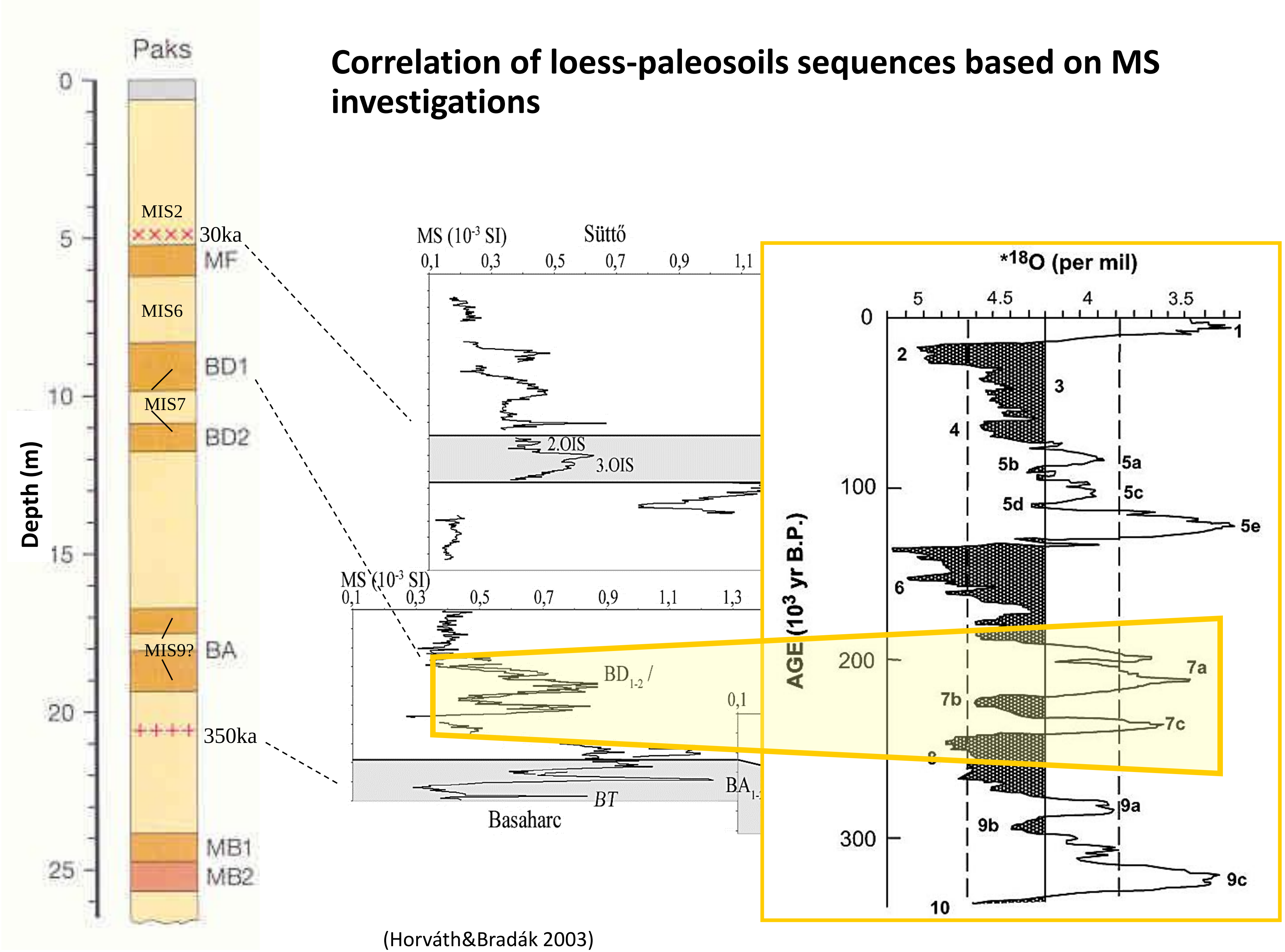

(Horváth&Bradák 2003)

Accumulation of $CaCO_3$ in different forms: Secondary carbonates

$CaCO_3$ Infilling of cracks

Powdery accumulation of $CaCO_3$

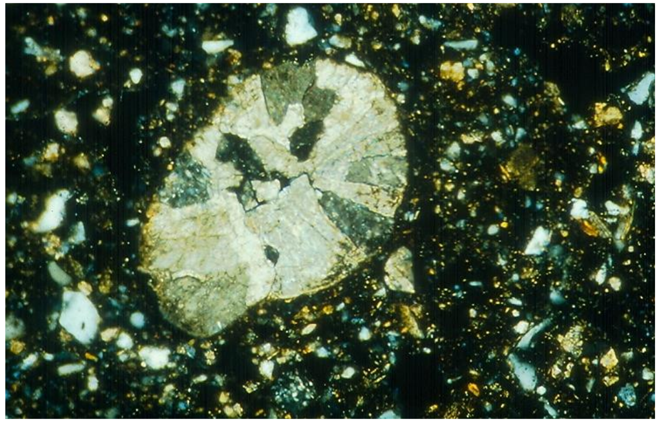

Biospheroid (EBS)

$CaCO_3$ concretion (loessdoll)

Secondary carbonates:

Calcified rootcells

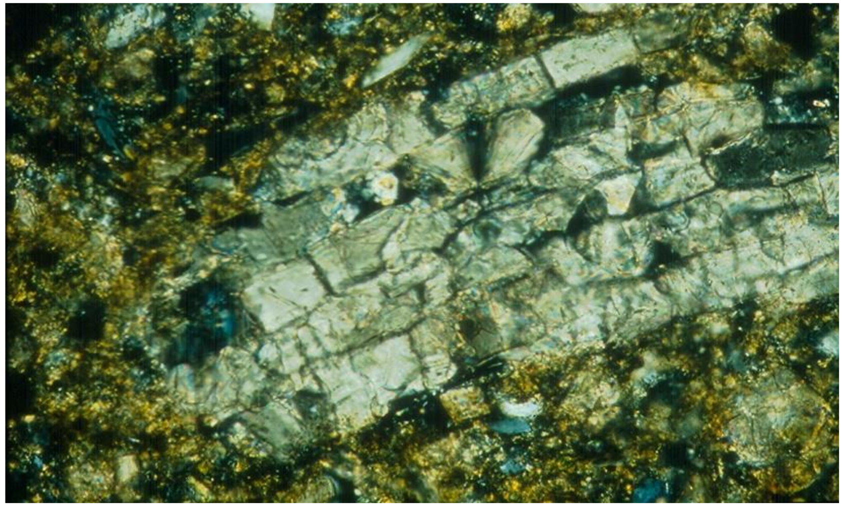

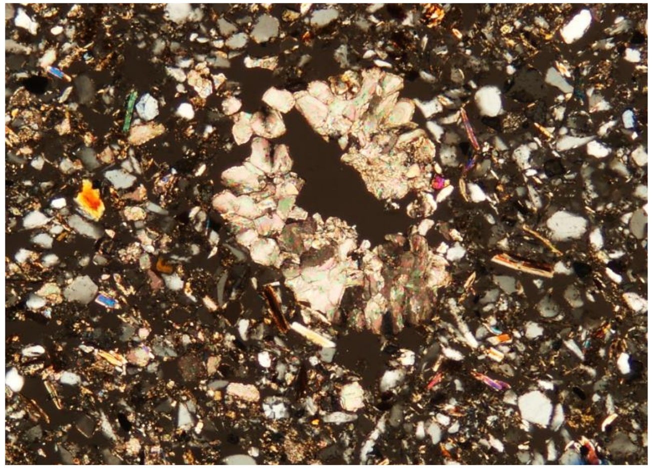

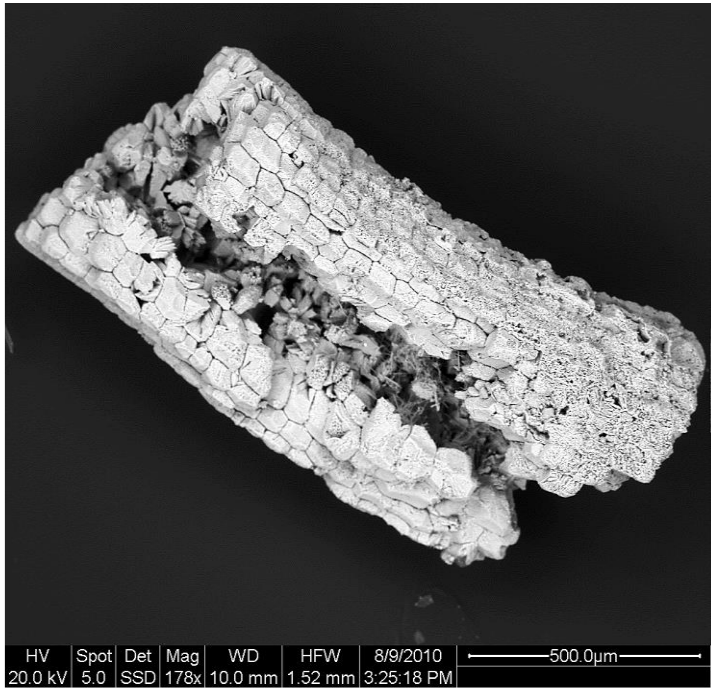

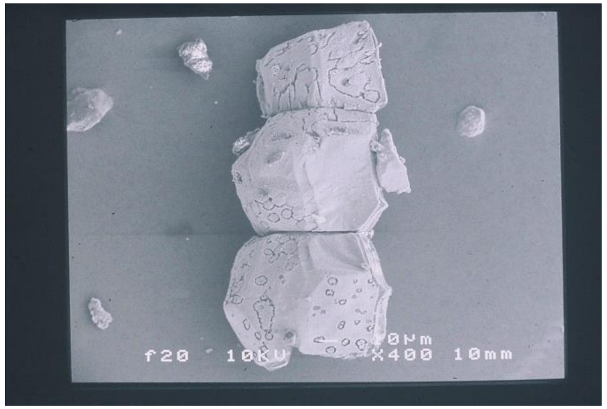

Secondary carbonates:

Calcified rootcells - reworked

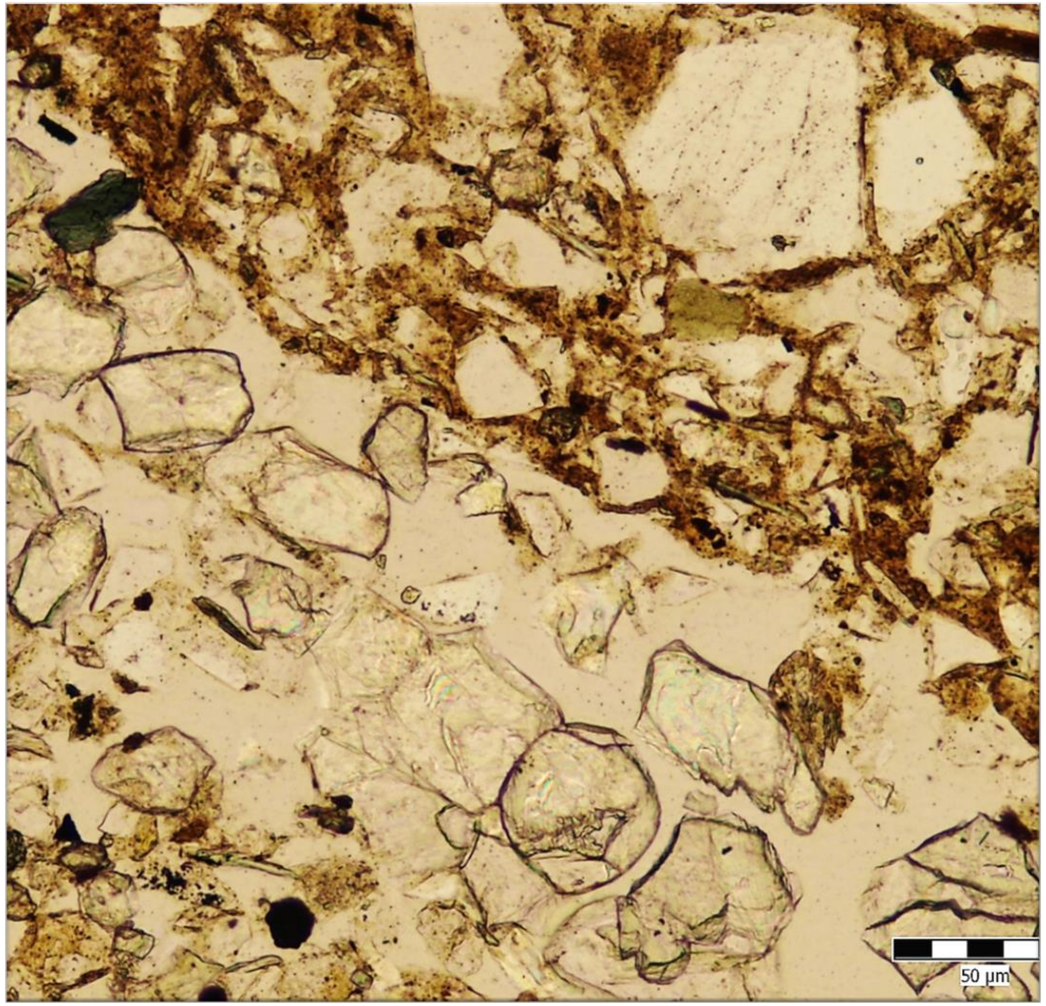

Secondary carbonates

Needle fiber calcite

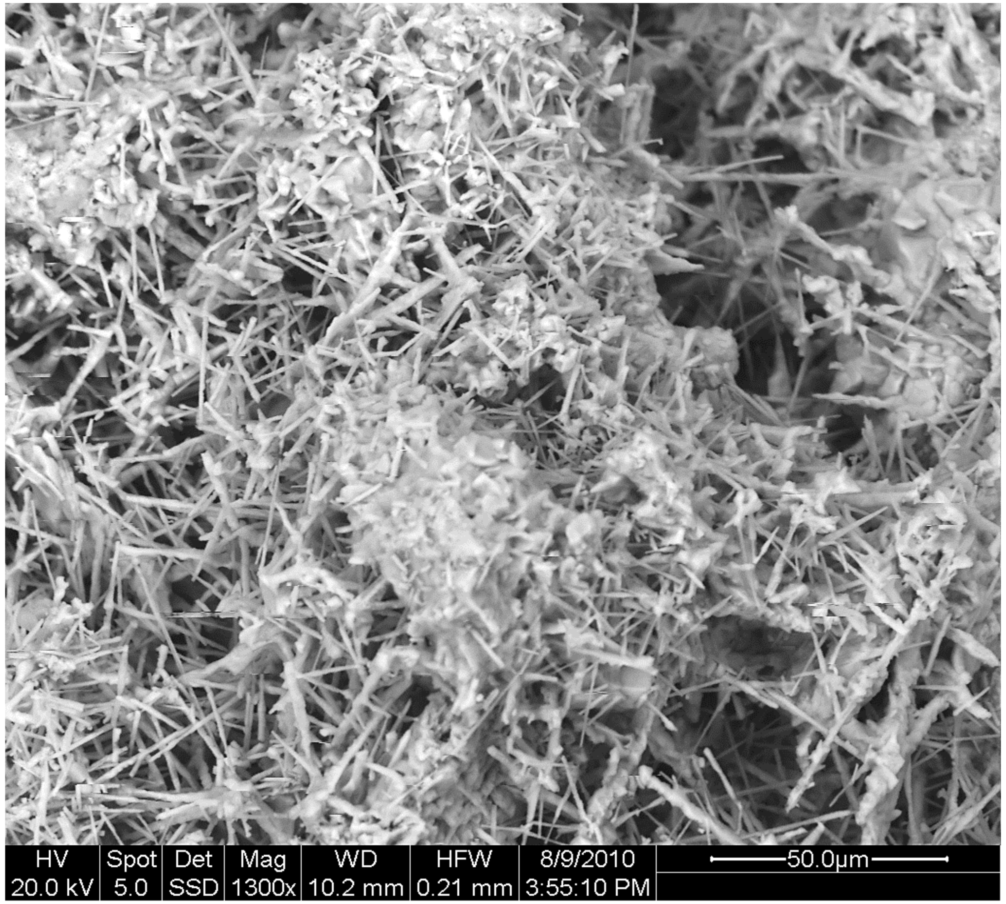

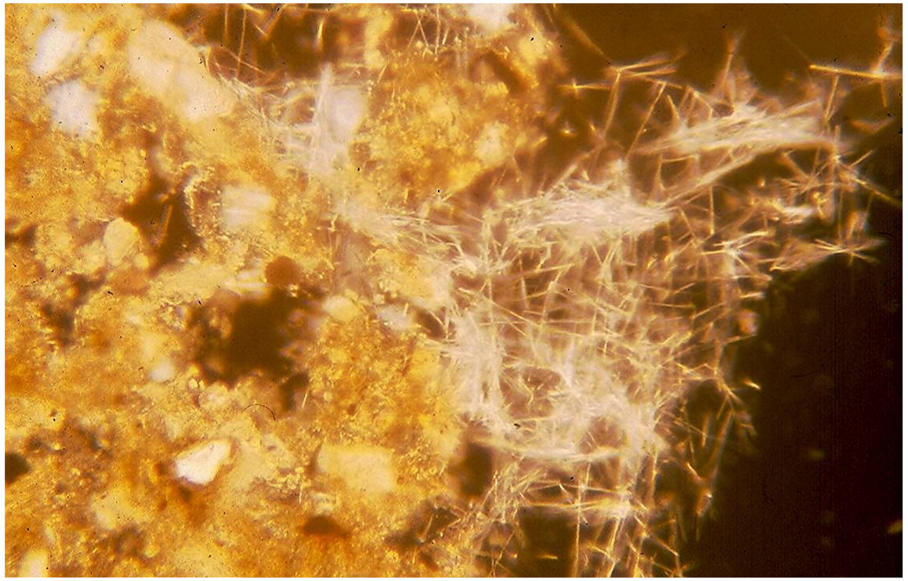

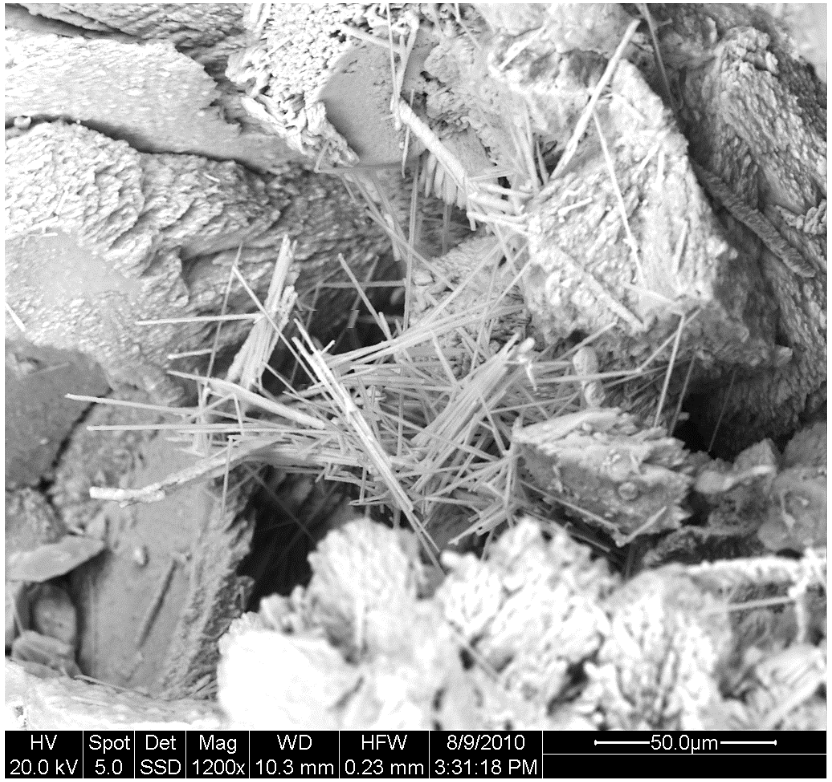

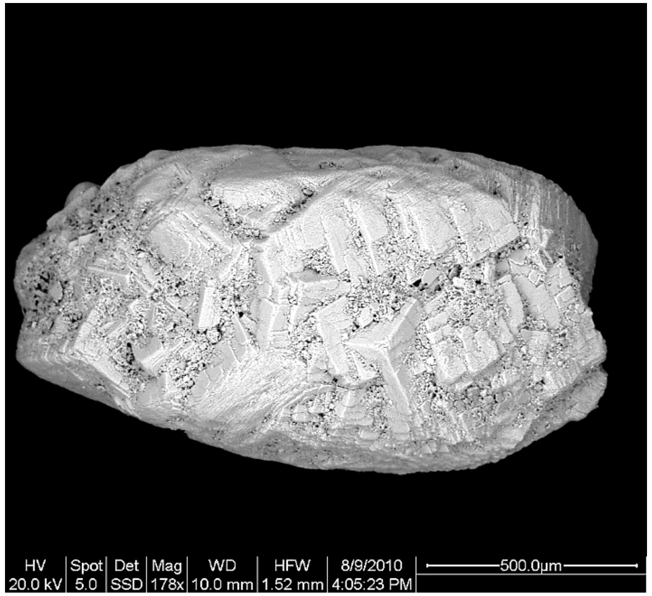

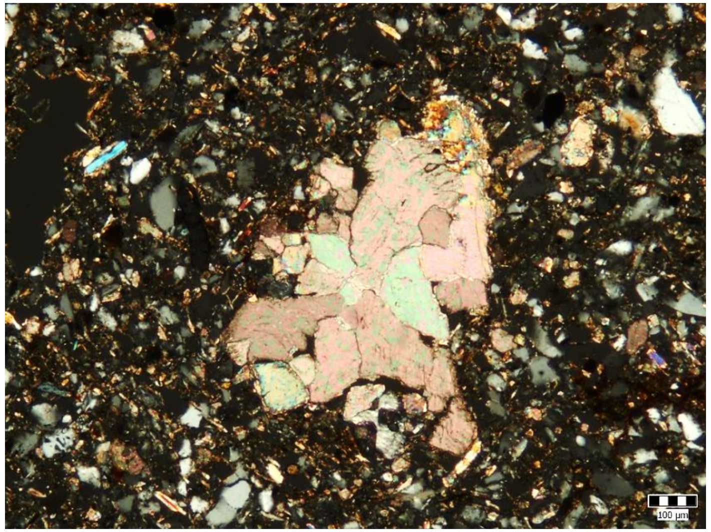

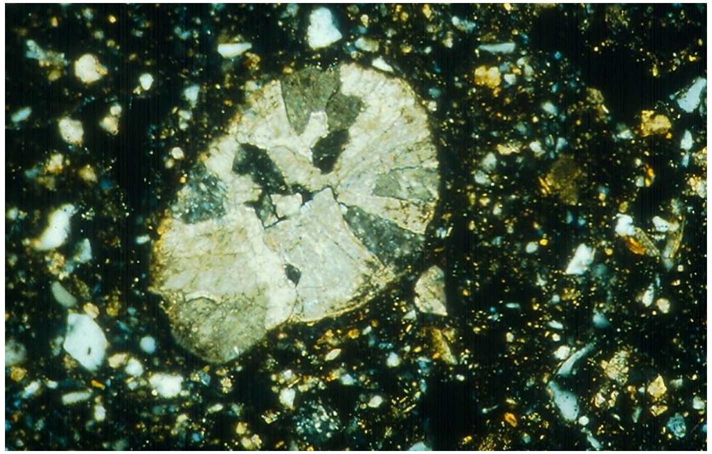

Secondary carbonates:

Earhtworm „calculus”: Biospheroid

- See more about secondary carbonates: **Barta, G.** 2014. Paleoenvironmental reconstruction based on the morphology and distribution of secondary carbonates of the loess-paleosol sequence at Süttő, Hungary. *Quaternary International 319*, pp. 65-75.

Secondary carbonates

HC - Hypocoating

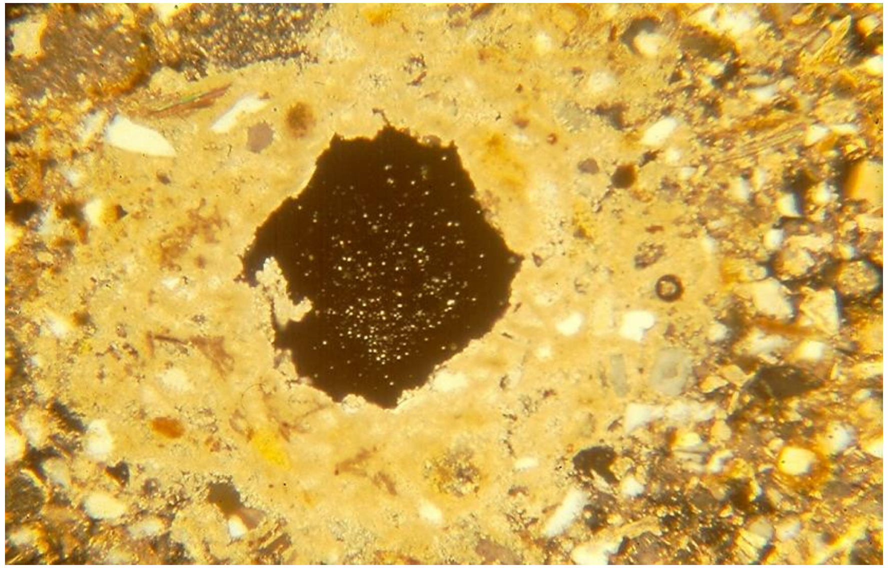

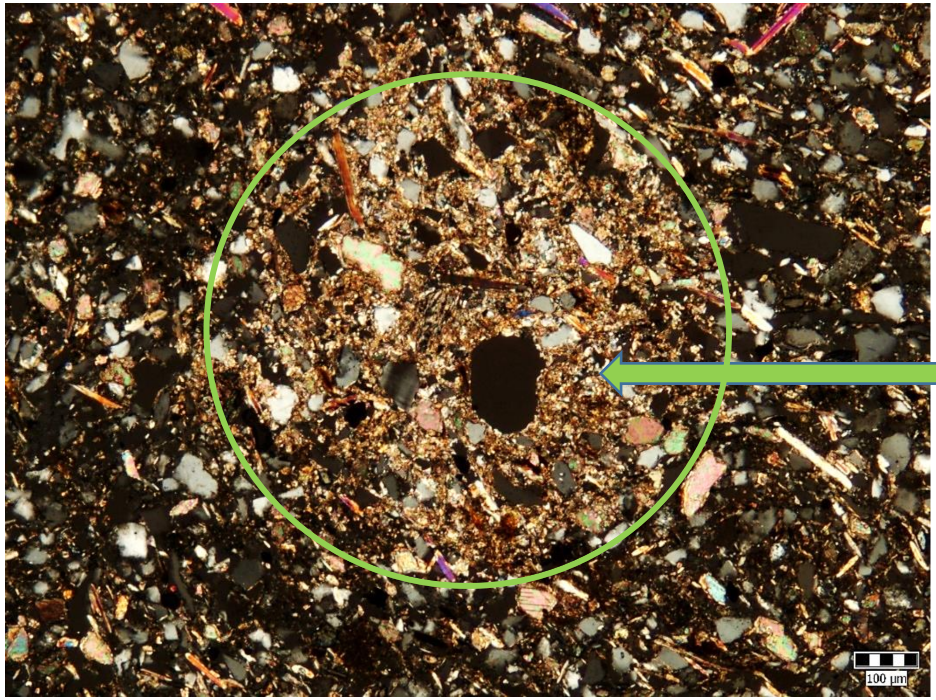

$CaCO_3$ coating (CCo - coating)

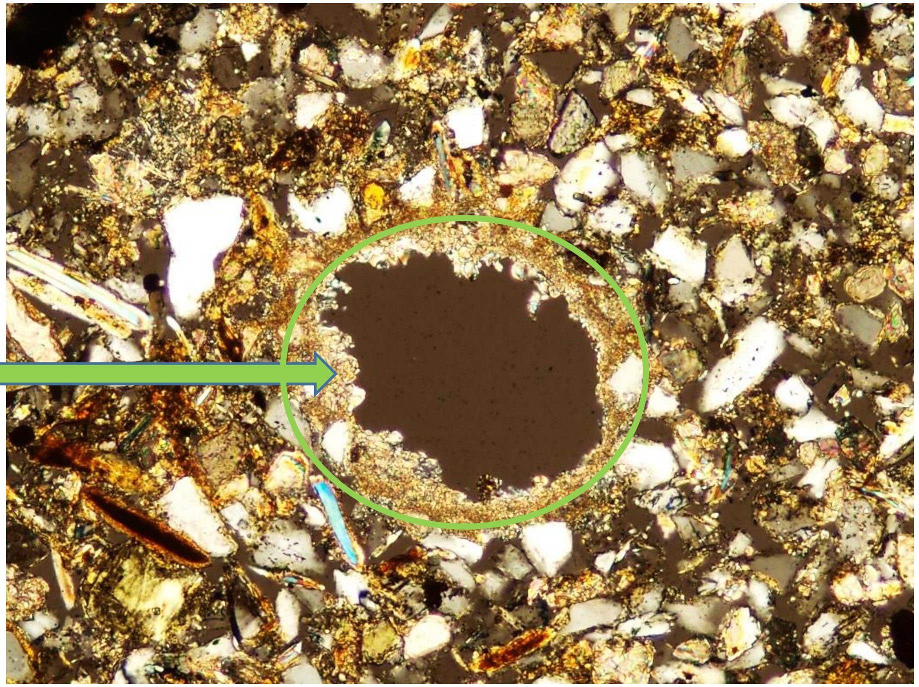

Similar features in different climate: semiarid climate (Iran)

Gypsum instead of $CaCO_3$

Clay coating

Smooth and shiny surfaces, usually on ped surfaces, but also along biogalleries

Clay and Mn coating

Mixed features

Clay coating on $CaCO_3$ coating

Different forms of clay in the loess-paleosol series

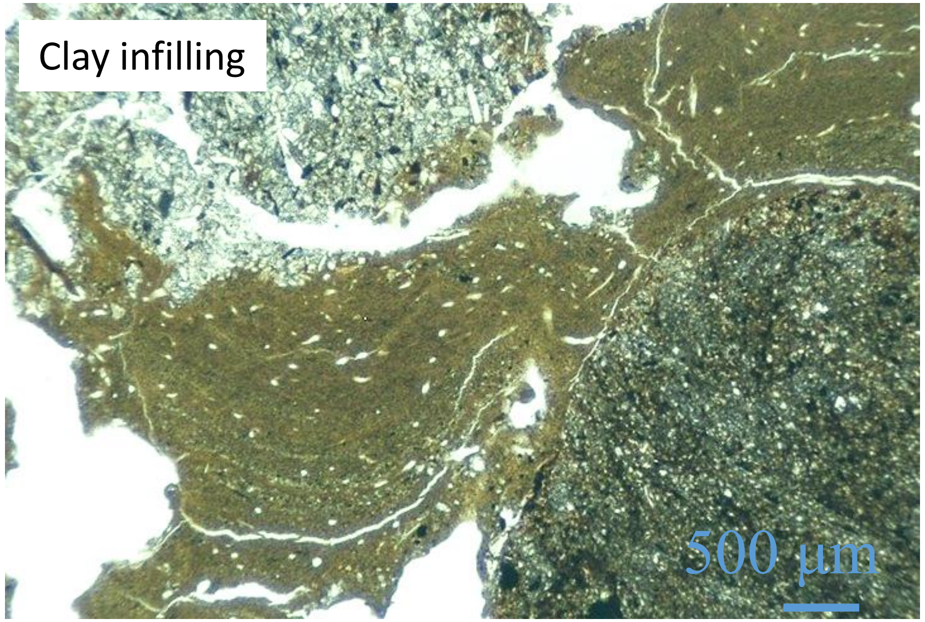

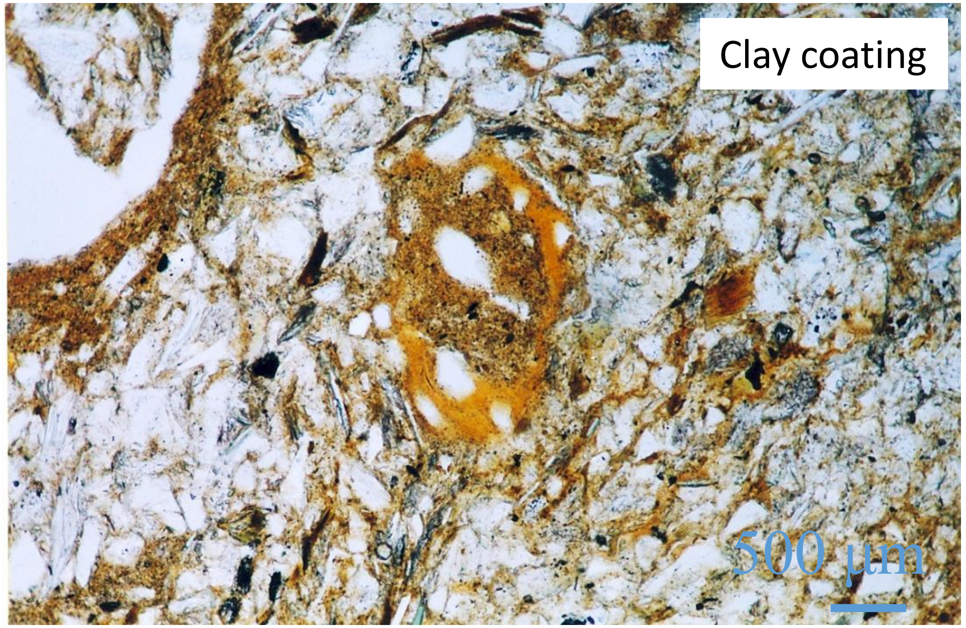

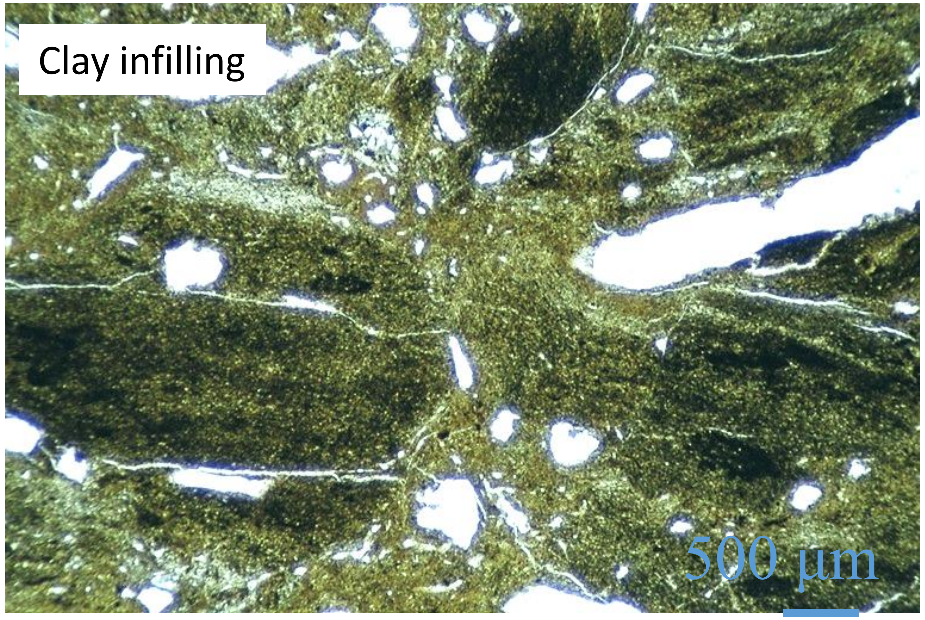

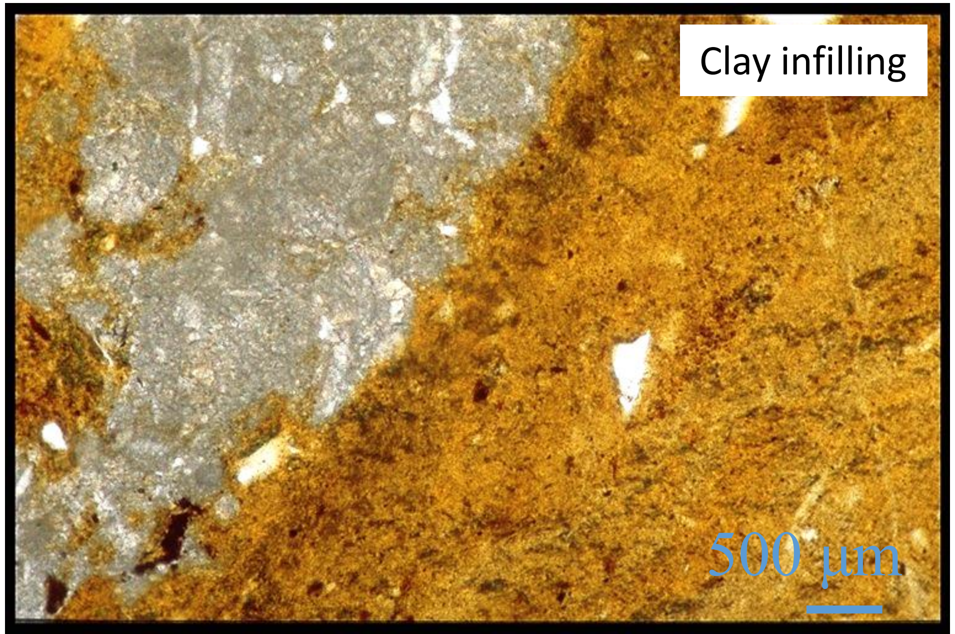

Signs of reworking in loess

(in thin section)

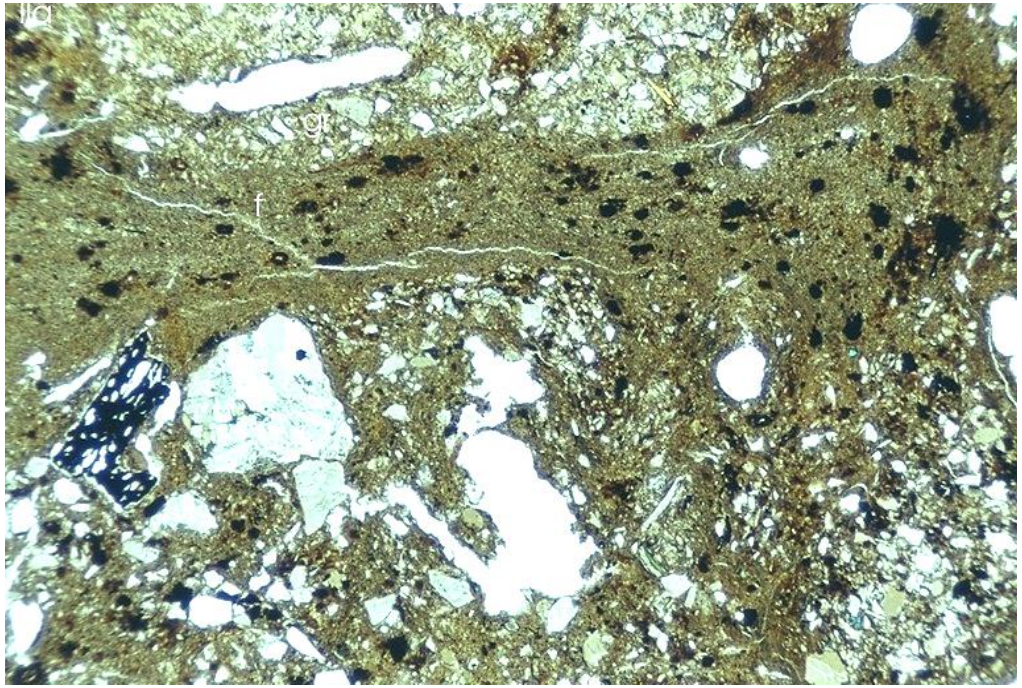

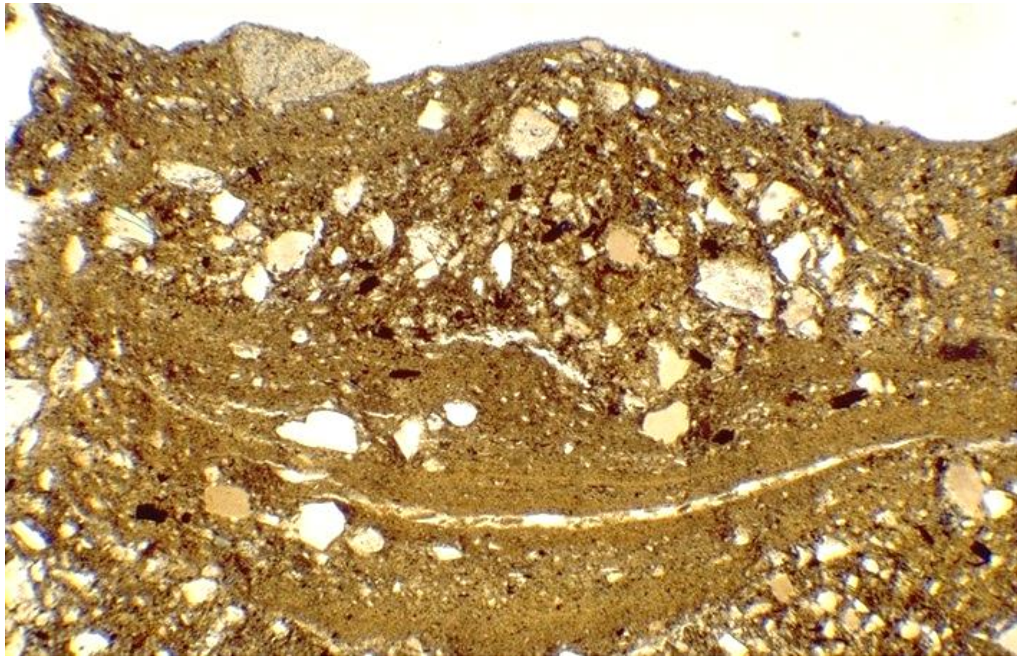

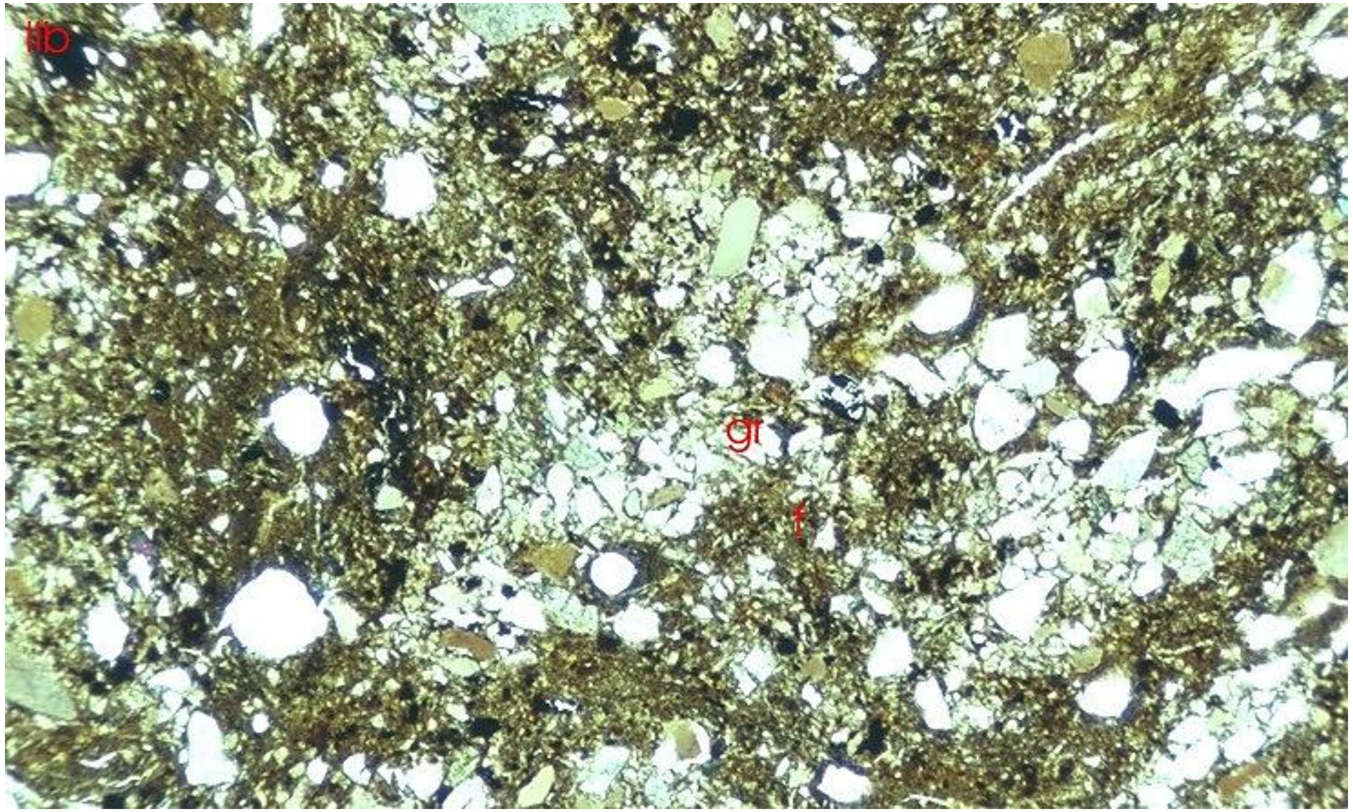

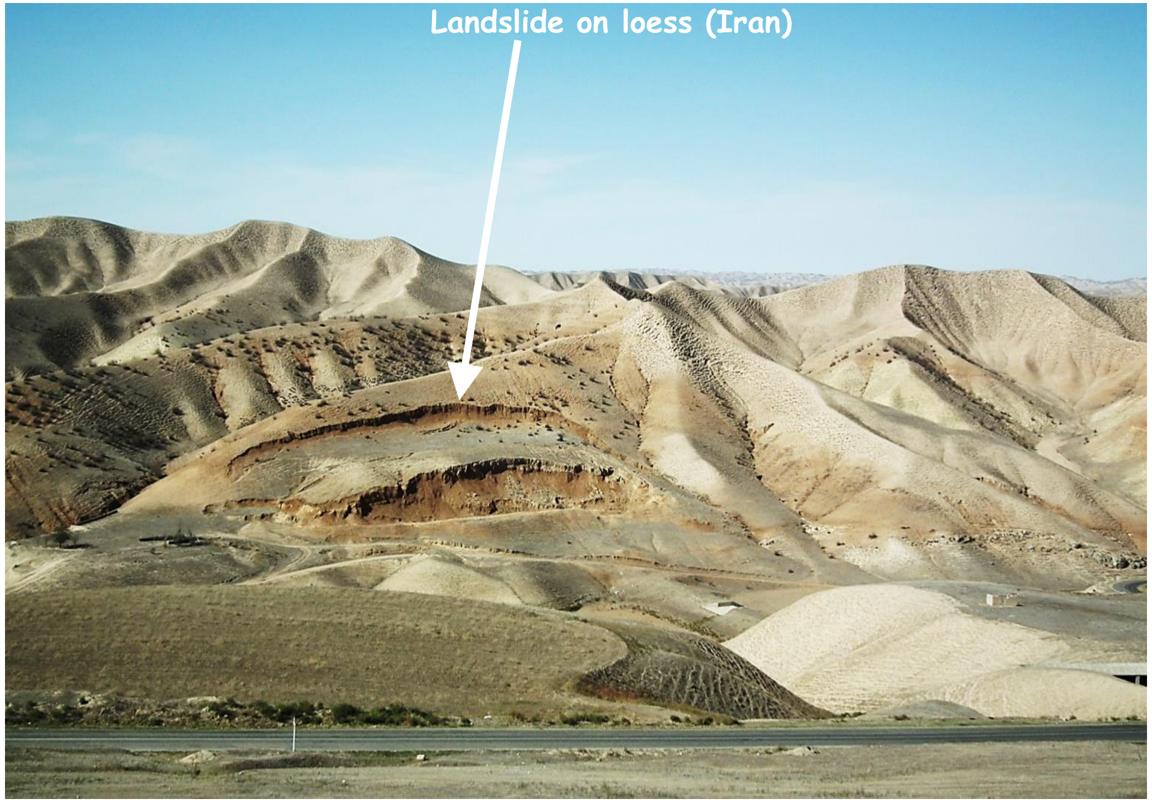

- Reworking by geomorphological processes

Landslide on loess – Dunaszekcső (Hungary)

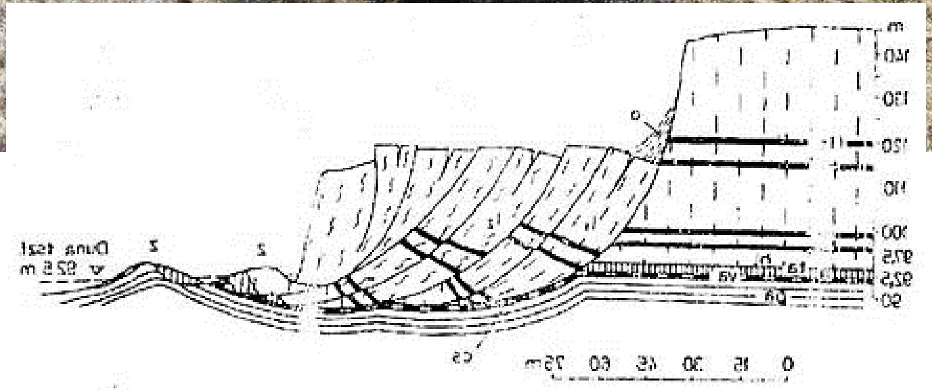

Signs of freezing-thawing

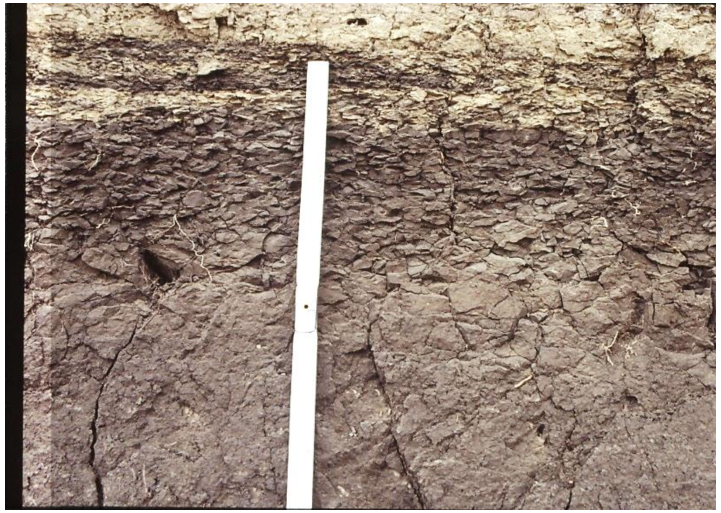

Bioturbation

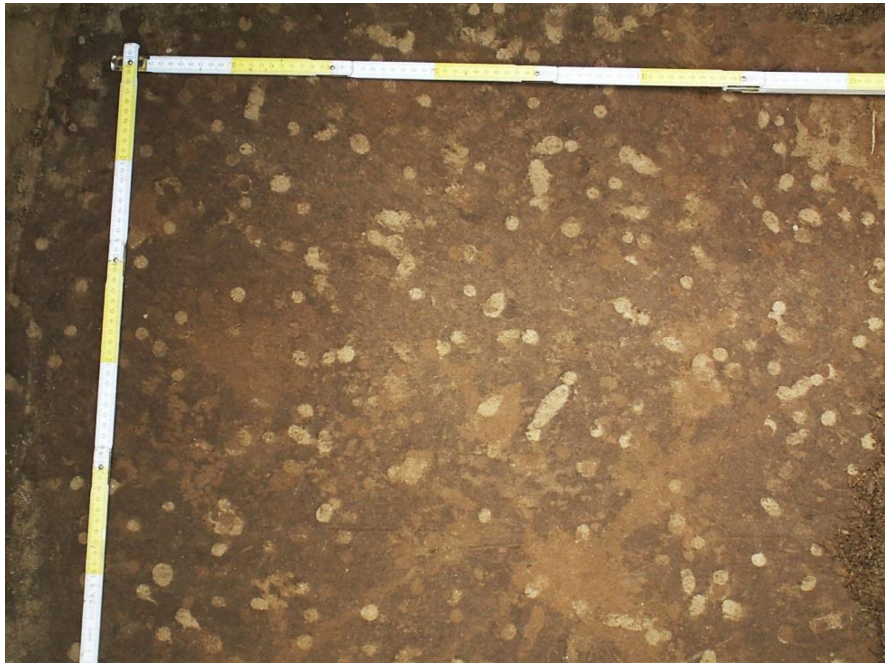

Recent bioturbation

On the surface

Recent bioturbation

ants

anthill

Insects holes in loess

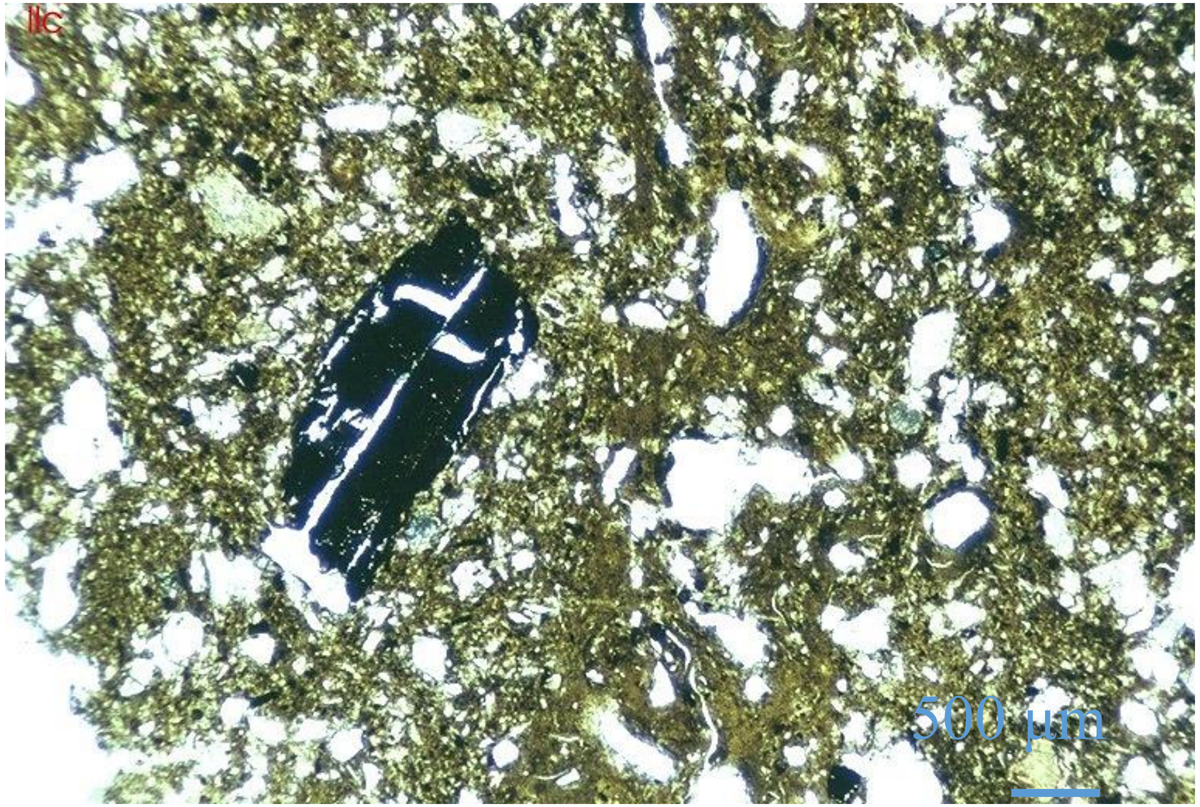

Charcoal in loess

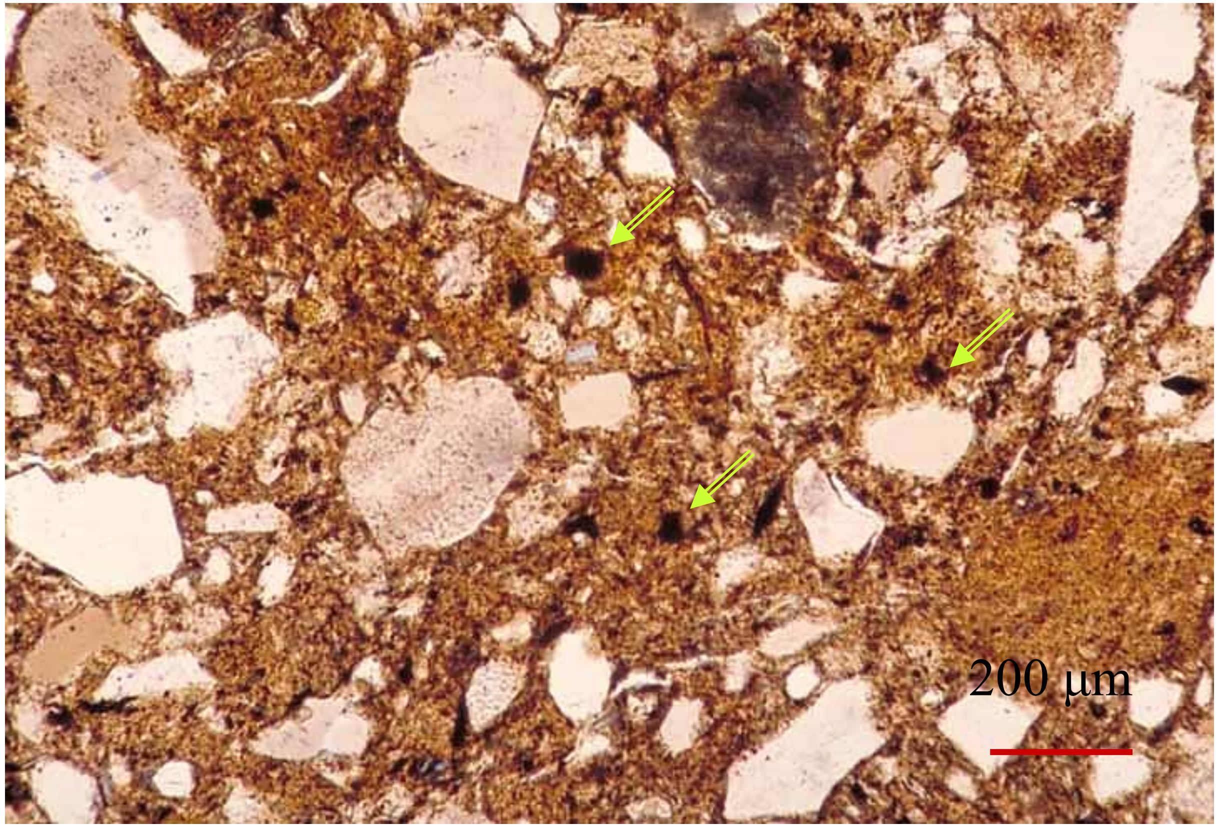

Roots

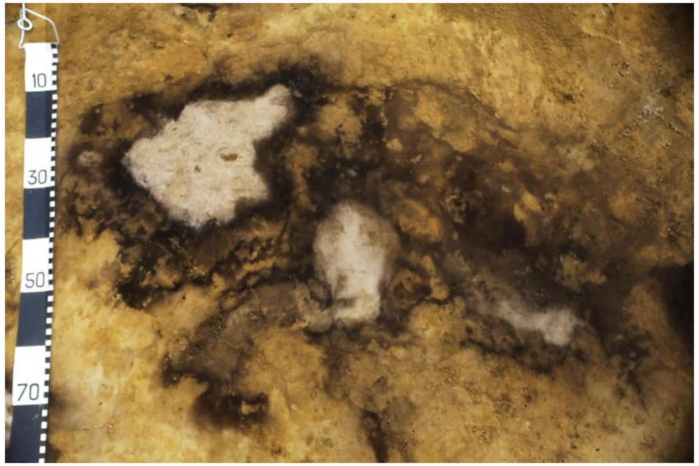

Wetting-drying

Wetting-drying

Hydromorphic features

Mn on clay coating

Mn concretions

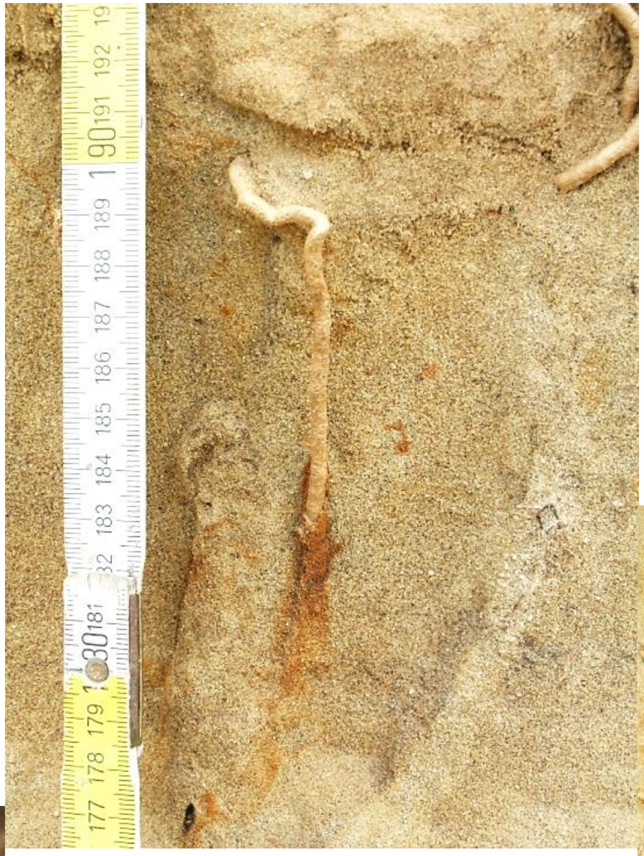

Fe along roots

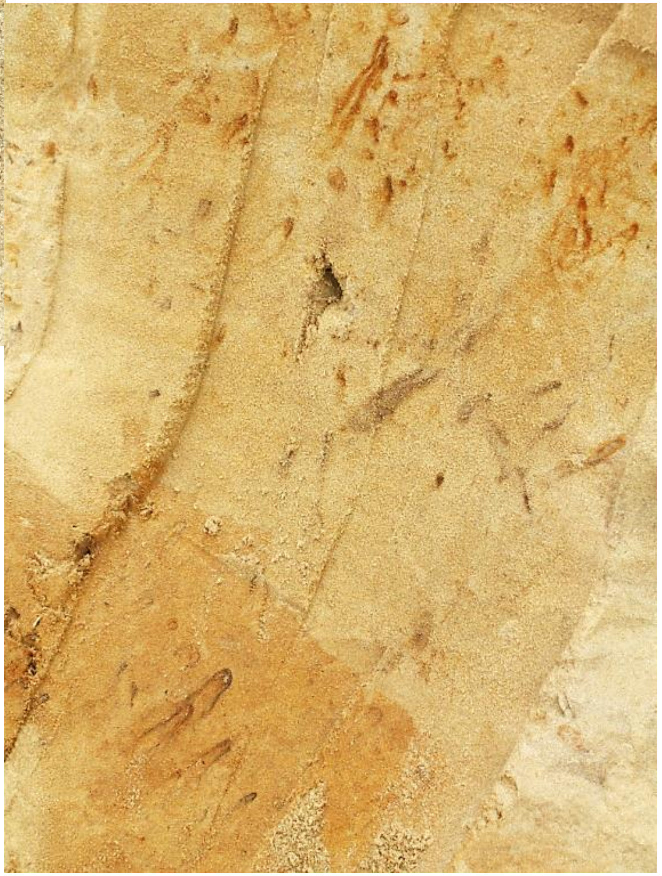

Hydromorphic features

Recent environment (small intermittent lake in sandy area)

Quaternary in the Carpathian Basin

Different environments during the glacials and intergalcials


Svédország
Norvégia
Finnország
Észtország
Lettország
Litvánia
Dánia
Egyesült Királyság
Írország
Hollandia
Belgium
Németország
Lengyelország
Fehéroroszország
Csehország
Szlovákia
Ukrajna
Moldova
Ausztria
Magyarország
Franciaország
Románia
Horvátország
Szerbia
Portugália
Olaszország
Bulgária
Spanyolország
Görögország
Törökország
Grúzia
Azerbajdzsán
Kazahsztán
Kirgizisztán
Üzbegisztán
Türkmenisztán
Afganisztán
Irán
Szíria
Irak
Libanon
Izrael
Jordánia
Egyesült Arab Emírségek
Marokkó
Tunézia
Nyugat-Szahara

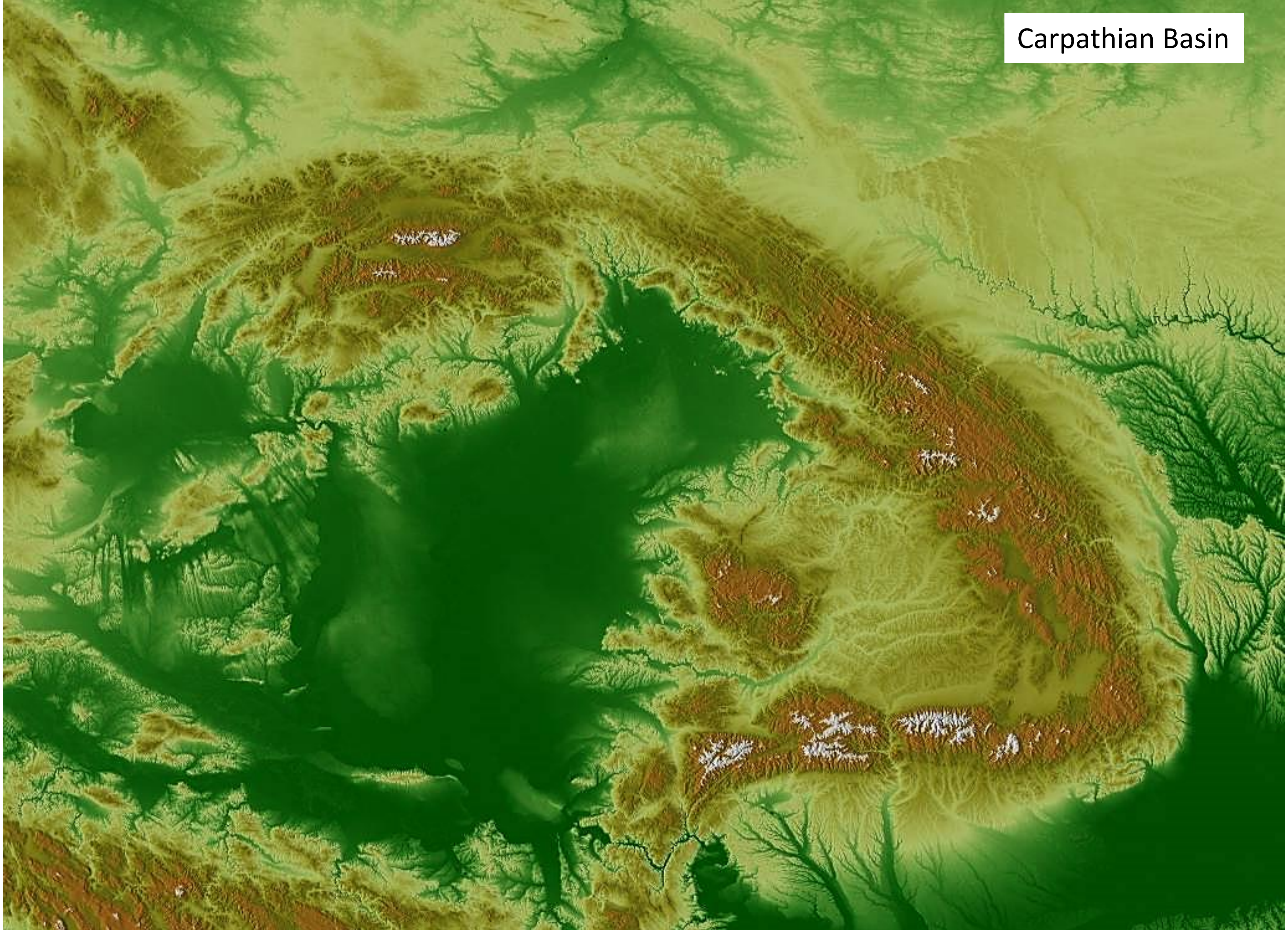
Carpathian Basin

Quaternary in Hungary

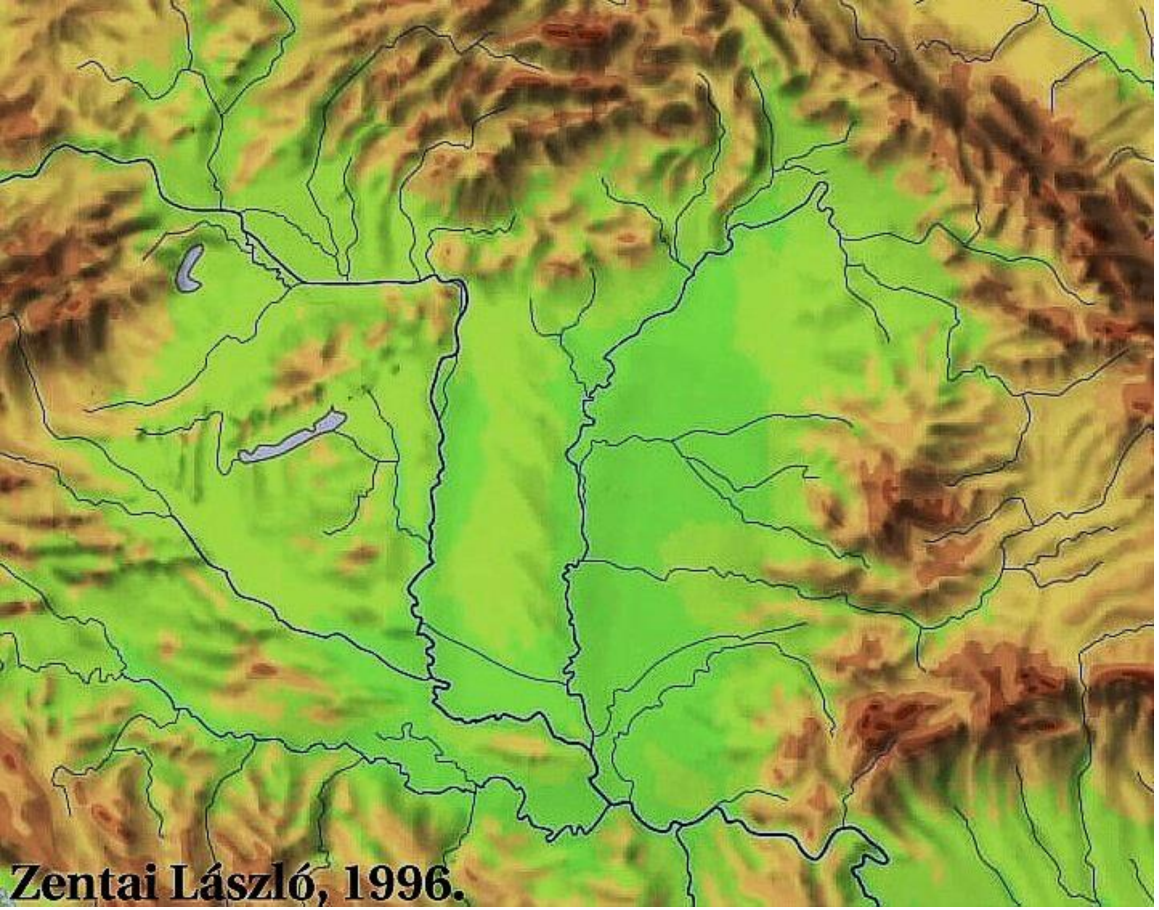

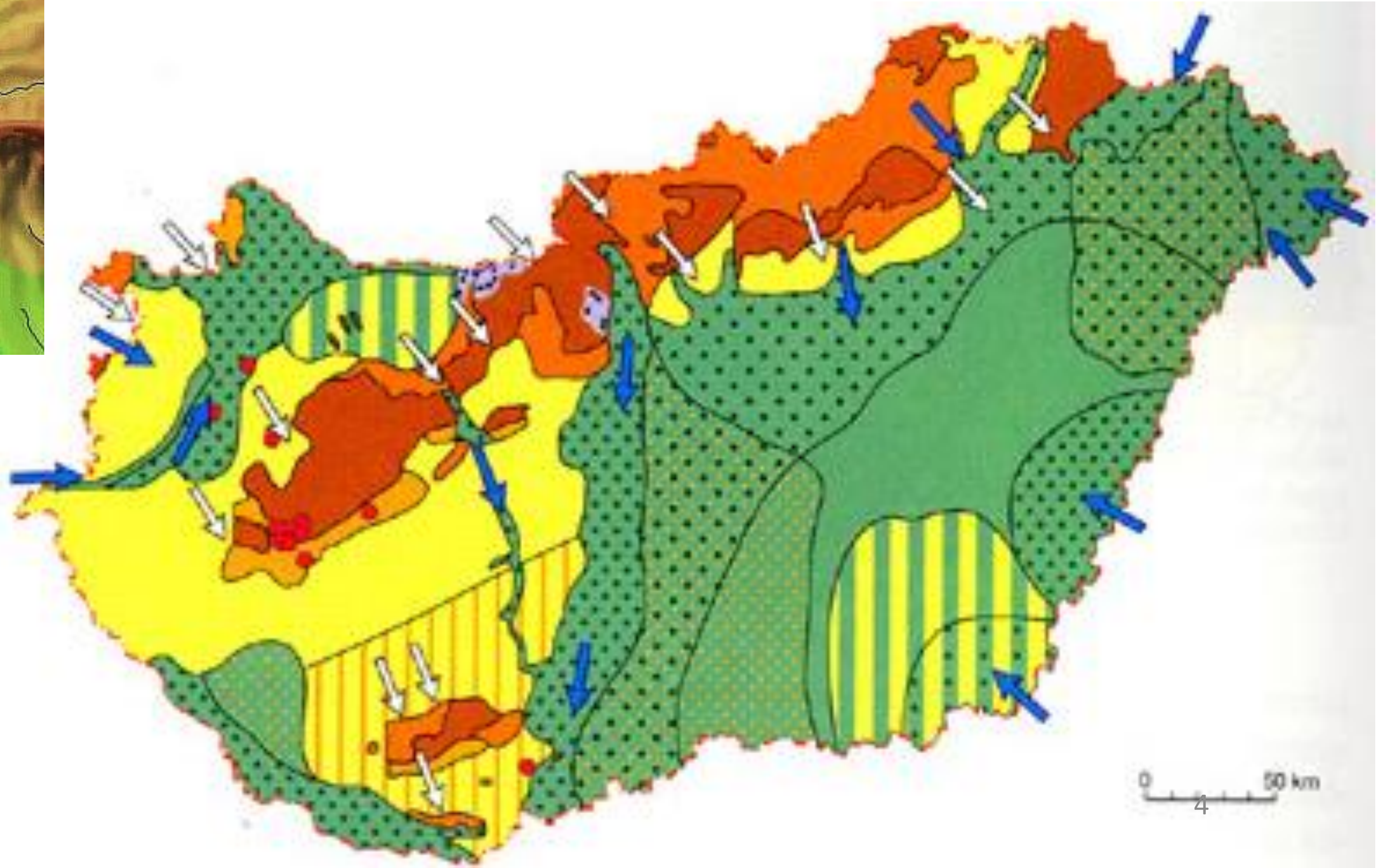

Quaternary surface development in the Carpathian Basin

Periglacial environment (during glacials)

- Annual precipitation: 100 - 300mm
- Annual temperature: -3 - -5°C

Higher surfaces

- Bare surfaces
  - Physical weathering (mainly frost)
  - Mass movements: gelisolifluction, creep, falls (talus)

Lower surfaces

- sedimentation
  - Fluvial
  - Eolian: sand, dust
  - Loess formation

River incision

Environment similar to recent (during interglacials)

- Annual precipitation: 500 - 700mm
- Annual temperature: 10-12°C

Higher surfaces

- Vegetation cover
  - Chemical weathering, soil formation
  - Land slides

Lower surfaces

- sedimentation
  - Fluvial – alluvial fan
- Chemical weathering
  - soil formation

Environments during the glacials*

- High mountains (Alps, Carpathians)
- Lower mountains (in the Carpathian Basin)
- Hilly regions
- Lower part of the basin (floodplains, alluvial fans, subsiding basins)

**The environments during interglacials are similar to the recent environment without anthropogenic impact*

High mountains (Alps, Carpathians):

- Glaciers
- Nivation
- frost weathering

The landscape after the deglaciation

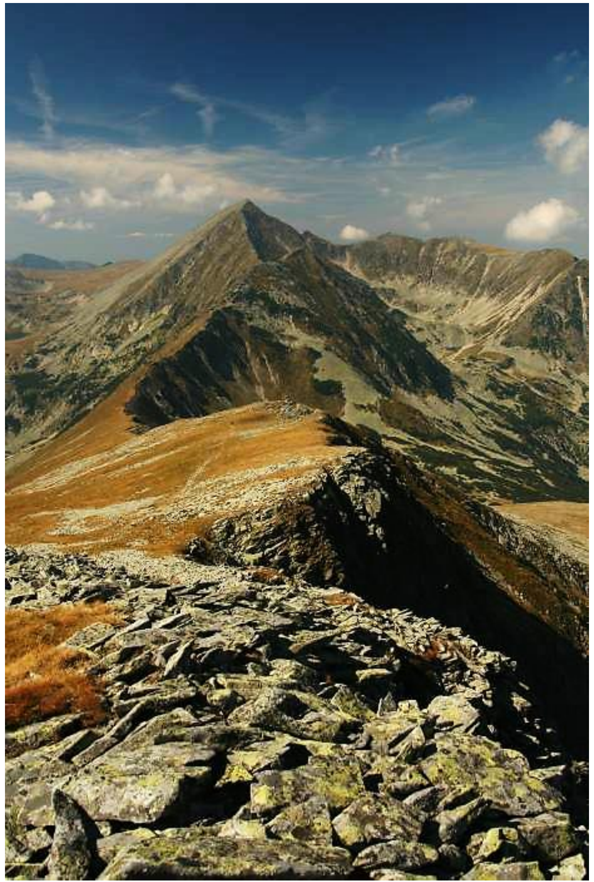

- **Lower mountains (in the Carpathian Basin)**
- frost and insolation weathering
- Rockfalls
- Talus development

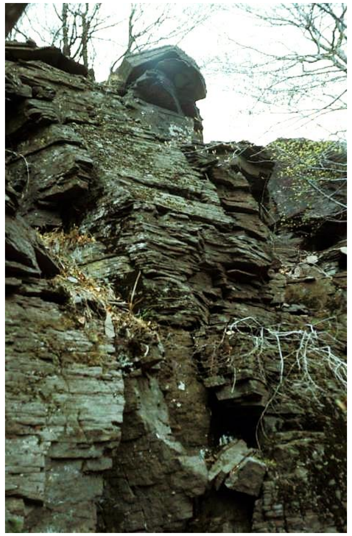

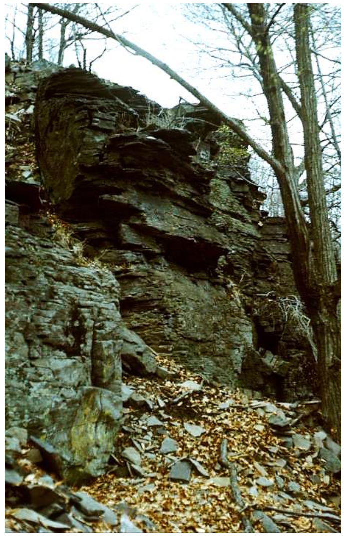

Pediment

Loess on travertine (calc sinter)

9

- **Hilly regions and river terraces (hills and piedmont surfaces)**:
  - Mass movement
  - Pediment formation
  - Dust accumulation and loess formation

Contact point of the mountains and the basin

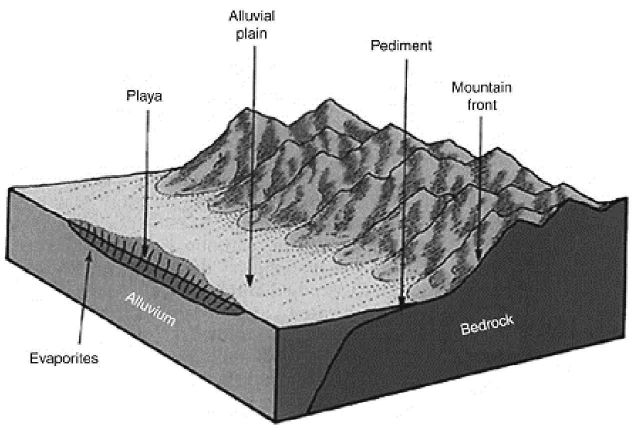

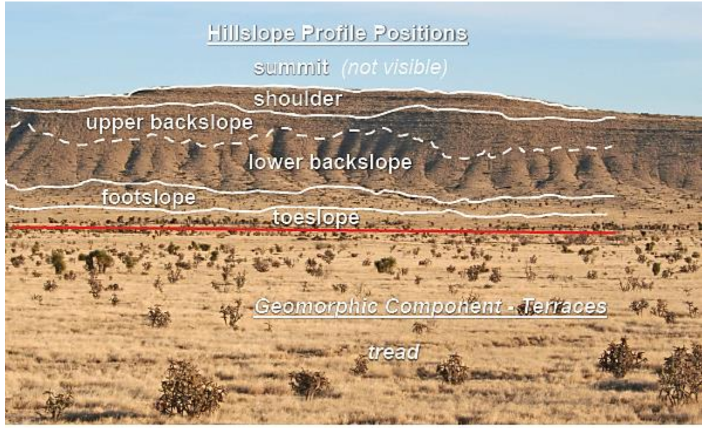

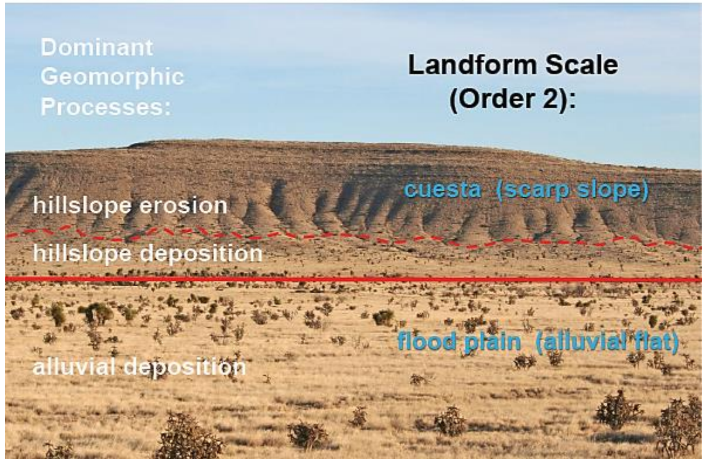


Landslide


Gelisolifluction in loess

Cryoturbation in terrace sediments

Cryoturbation in loose sediments

A sand dune and its cross section

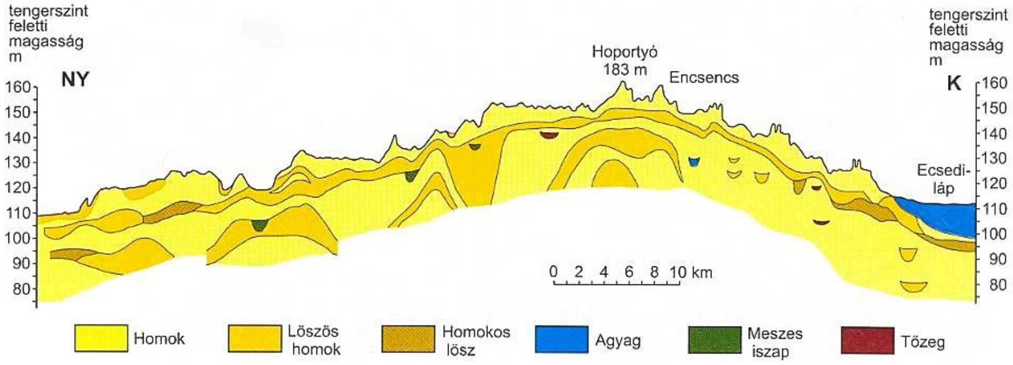

A Nyírség domborzati és földtani keresztszelvénye *(Kuti L. nyomán)*

- **Lower part of the basin (floodplains, alluvial fans, subsiding basins)**:
  - Eolian sand accumulation
  - Accumulation in the riverbed
  - Sediment accumulation in subsiding basins
  - Cryoturbation in sediments
  - Permafrost?

JOHN HOWELL 2002
WWW.BSRG.ORG.UK

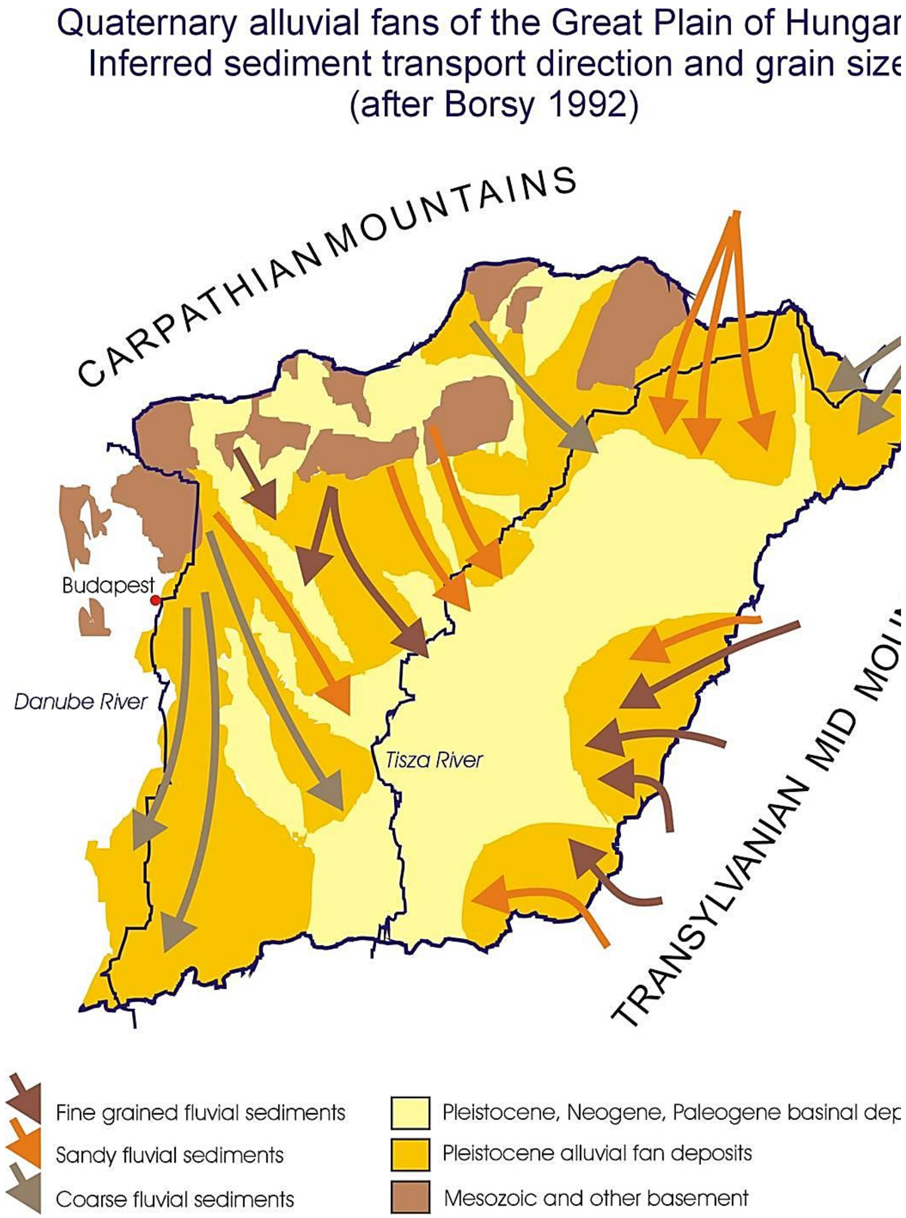

Quaternary alluvial fans of the Great Plain of Hungar
Inferred sediment transport direction and grain size
(after Borsy 1992)
CARPATHIAN MOUNTAINS
Budapest
Danube River
Tisza River
TRANSYLVANIAN MID MOU
Fine grained fluvial sediments
Sandy fluvial sediments
Coarse fluvial sediments
Pleistocene, Neogene, Paleogene basinal dep
Pleistocene alluvial fan deposits
Mesozoic and other basement

High-resolution stratigraphy of a Quaternary fluvial deposit based on magnetic susceptibility variations (Jászság Basin, Hungary)

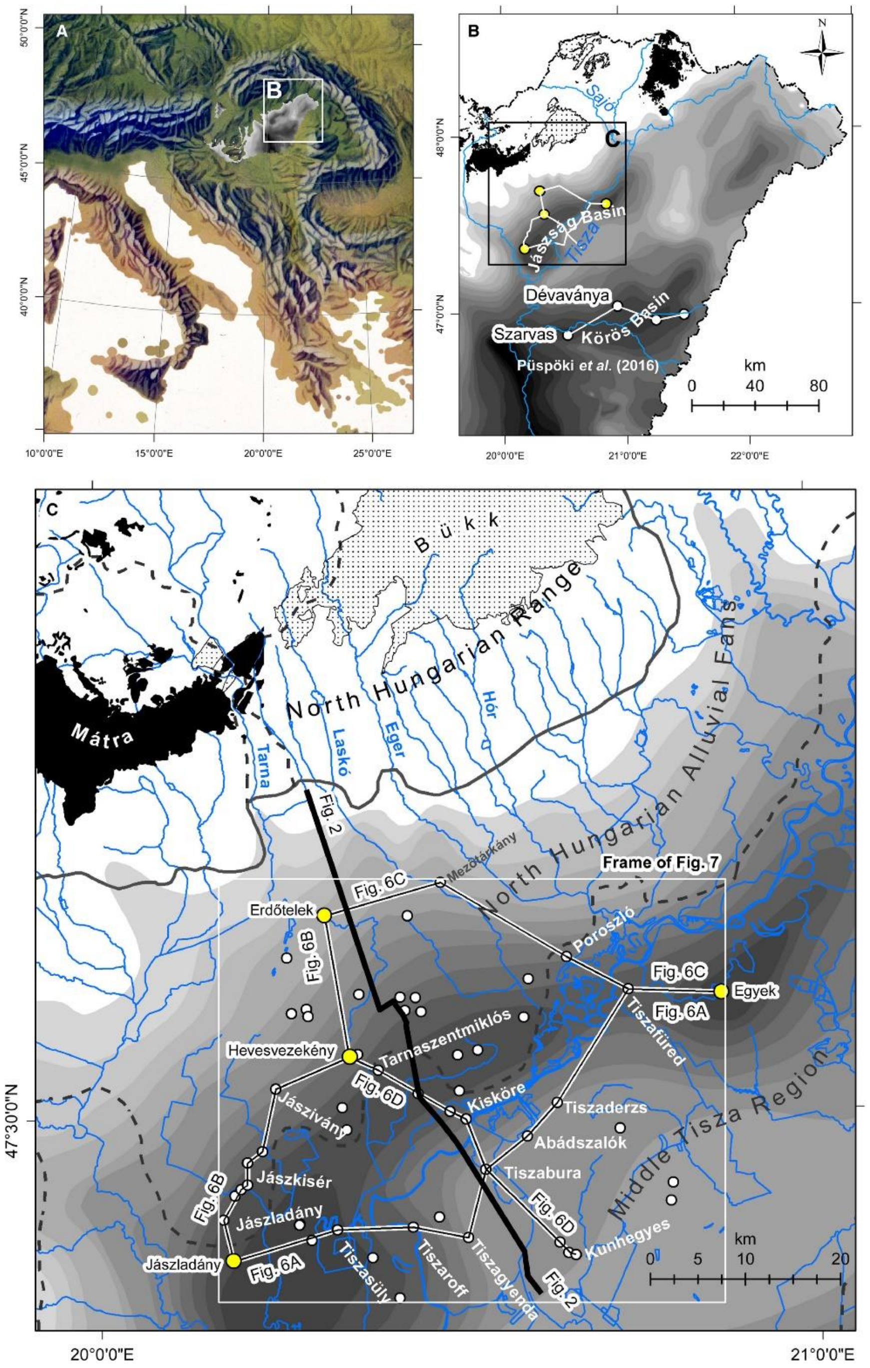

Boreas, Volume: 49, Issue: 1, Pages: 181-199, First published: 27 September 2019, DOI: (10.1111/bor.12412)

High-resolution stratigraphy of a Quaternary fluvial deposit based on magnetic susceptibility variations (Jászság Basin, Hungary)

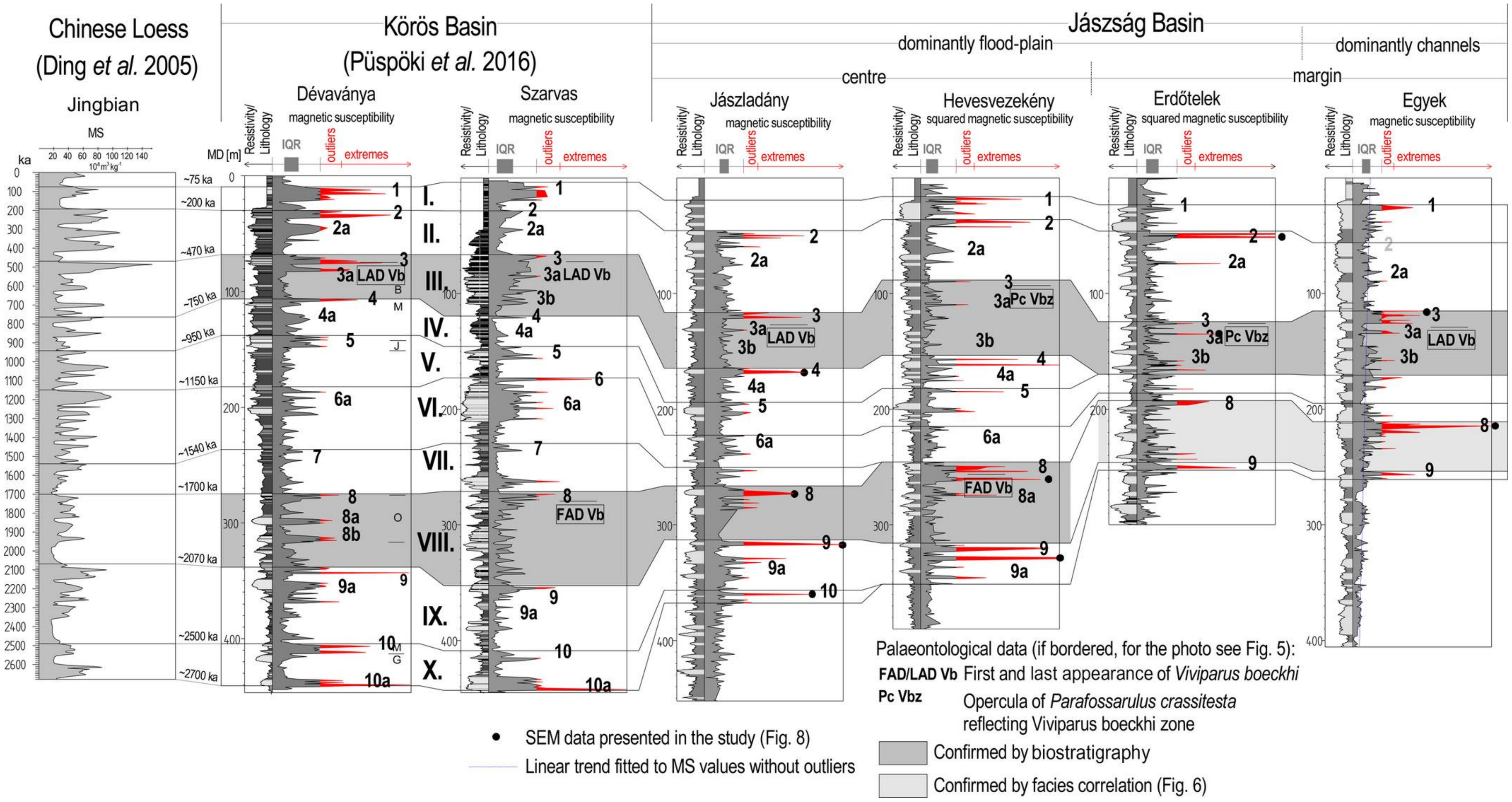

Boreas, Volume: 49, Issue: 1, Pages: 181-199, First published: 27 September 2019, DOI: (10.1111/bor.12412)

High-resolution stratigraphy of a Quaternary fluvial deposit based on magnetic susceptibility variations (Jászság Basin, Hungary)

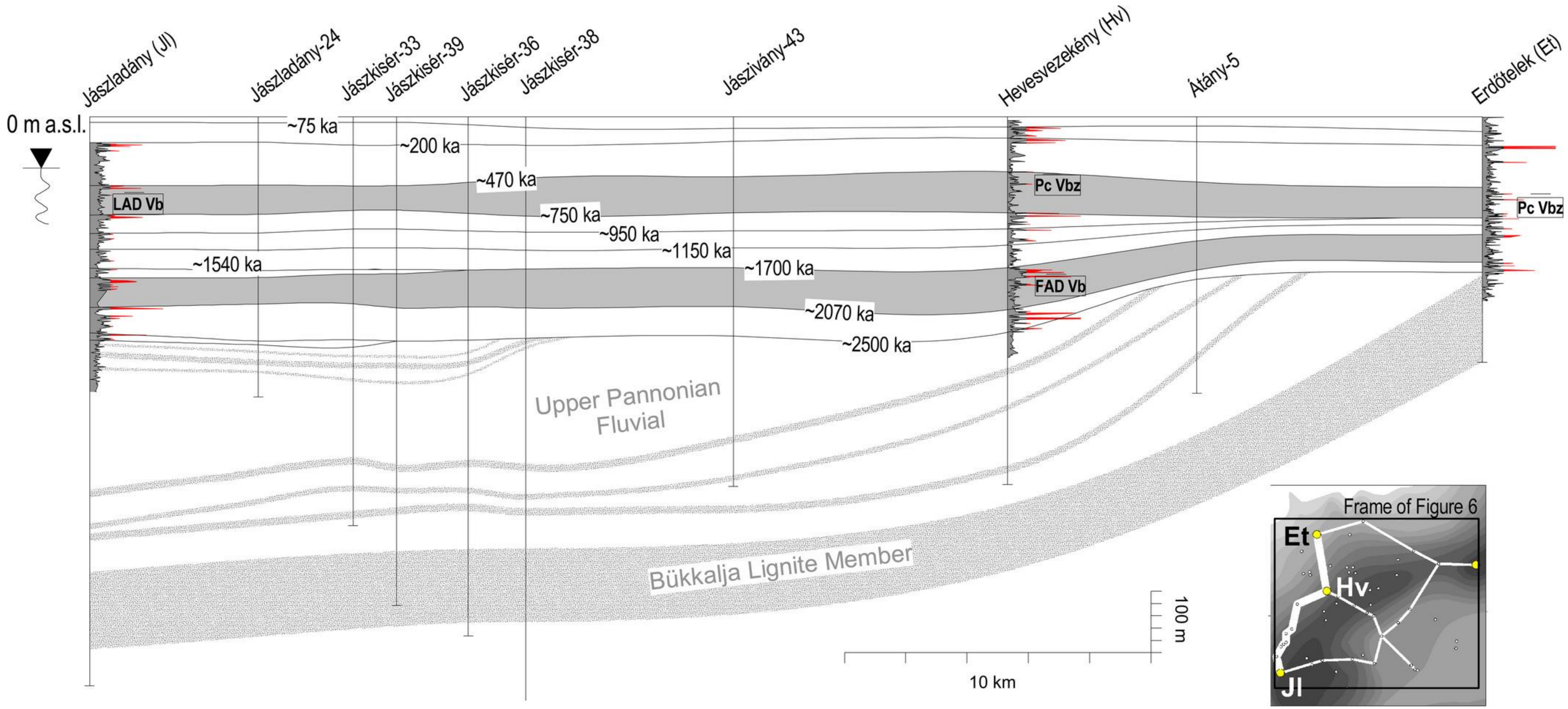

Boreas, Volume: 49, Issue: 1, Pages: 181-199, First published: 27 September 2019, DOI: (10.1111/bor.12412)

River terraces – the results of the consecutive climate changes

Castle Hill, Buda - IV. Terrace of the river Danube

(the river sediment is covered by travertine)

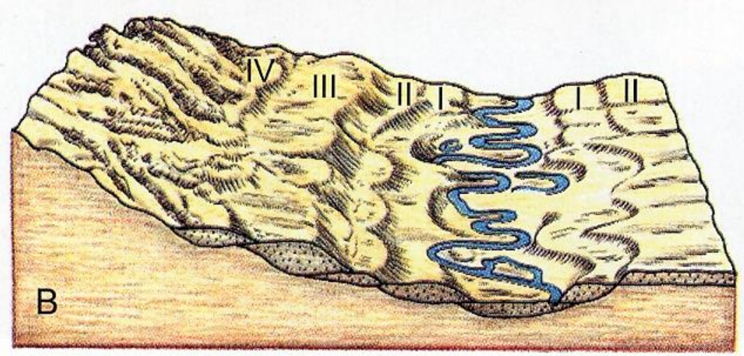

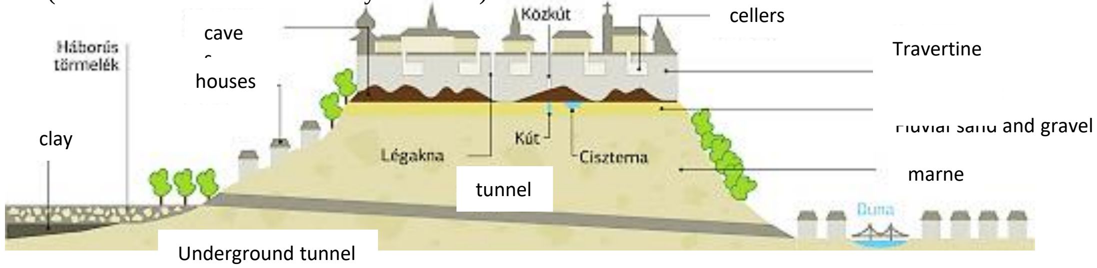

The Hungarian terrace system

- T = termination
- IS = interstadial
- MIS = marine oxygenisotope stadium
- ka = 1000 years

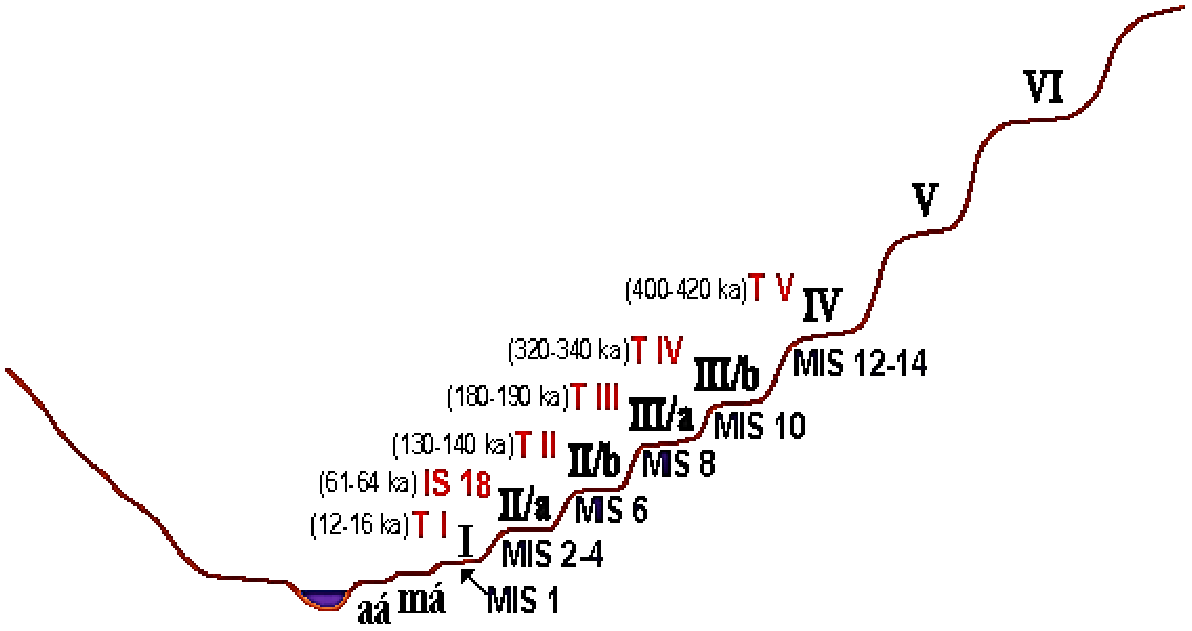

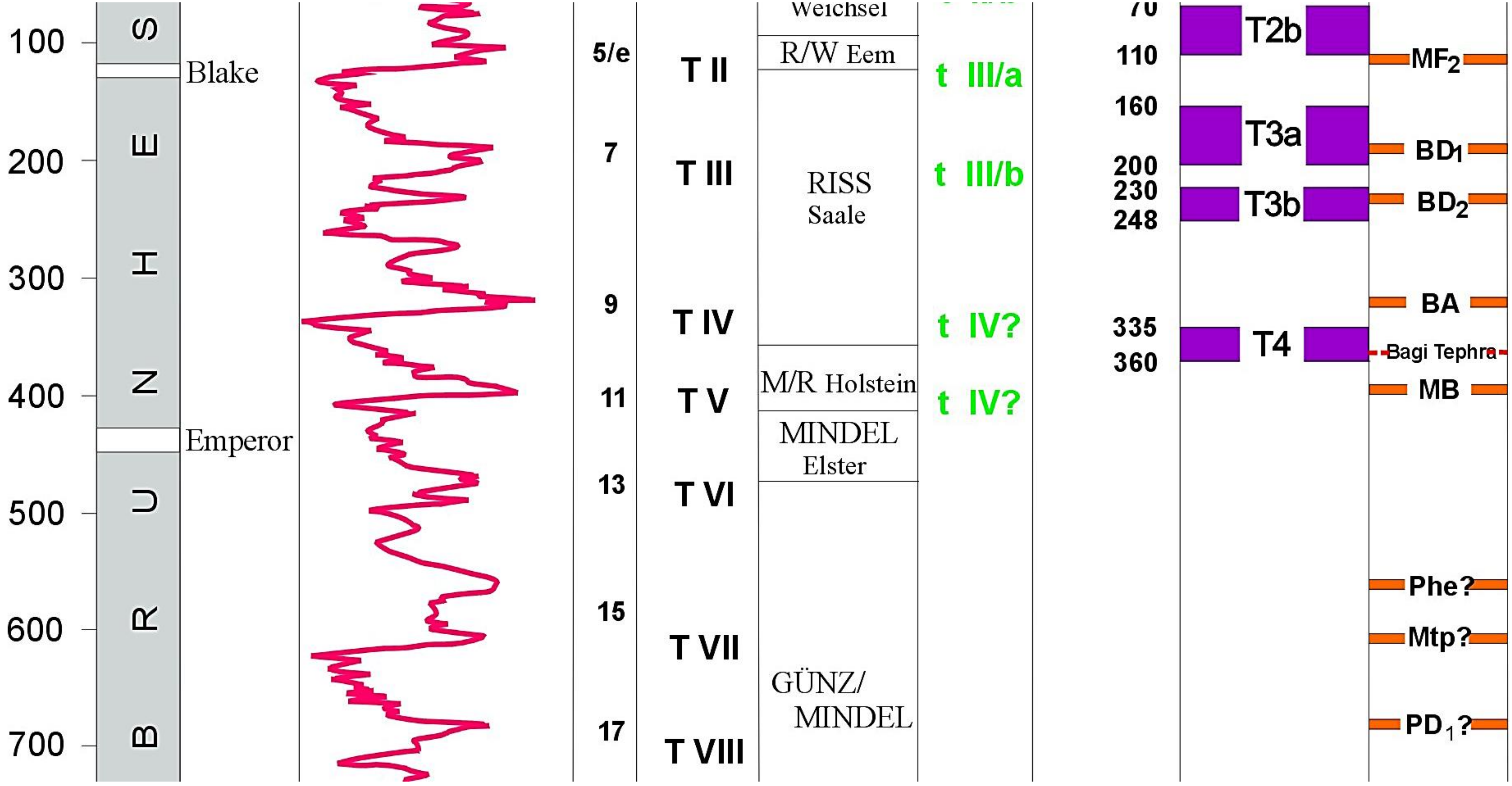
100
200
300
400
500
600
700
B R U N H E S
Blake
Emperor
5/e
7
9
11
13
15
17
T II
T III
T IV
T V
T VI
T VII
T VIII
Weichsel
R/W Eem
RISS
Saale
M/R Holstein
MINDEL
Elster
GÜNZ/
MINDEL
t III/a
t III/b
t IV?
t IV?
70
110
160
200
230
248
335
360
T2b
T3a
T3b
T4
MF2
BD1
BD2
BA
Bagi Tephra
MB
Phe?
Mtp?
PD1?